
Thesis submitted for the degree of
Doctor of Philosophy

# Non-perturbative Techniques in Quantum Field Theory

Joseph Aaron Hayling

Supervisor

Dr Constantinos Papageorgakis

February 14, 2020

Centre for Research in String Theory
School of Physics and Astronomy
Queen Mary University of London

*This thesis is dedicated to my family,*
*for their wonderful humour, unconditional love and continual support.*

*There is a theory which states that if ever anyone discovers exactly what the Universe is for and why it is here, it will instantly disappear and be replaced by something even more bizarre and inexplicable.*

*There is another theory which states that this has already happened.*

– Douglas Adams, *The Restaurant at the End of the Universe*

# Abstract

In this work we study supersymmetric quantum field theories across dimensions by using various non-perturbative techniques. These quantum field theories arise naturally in the context of stacks of branes in string and M-theory.

The first chapter is a brief, non-technical invitation to the topic including some historical background for a wider context.

The second chapter is a lightning quick exposition of the techniques that we will use in the thesis, both directly and indirectly. It includes some background on conformal field theories, the superconformal index, supersymmetric localisation and the refined topological vertex.

The third chapter provides a systematic analysis of the superconformal algebras in 5d and 6d. This includes a level-by-level analysis of the states permitted by the allowed superconformal multiplets and their corresponding superconformal indices. Where possible, we also discuss any definitive statements about the theories that we can make based on a purely algebraic line of reasoning. We also include an introduction to a `python` package that can be used to reproduce all our results as one of the appendices.

The fourth and fifth chapters explore the theme of dimensional deconstruction. That is, we start with lower dimensional supersymmetric theories that dynamically generate an additional circular dimension and test these proposals using some of the exact techniques that were briefly introduced in the earlier chapters. The fourth chapter involves the deconstruction of 6d theories and the fifth chapter includes various supersymmetric defects when going from 3d to 4d.

# Acknowledgements

It is my pleasure to thank my supervisor, Dr Constantinos Papageorgakis. His seemingly infinite patience and enthusiasm helped shape what has been a truly wonderful phase of my life. I could not have asked for a better supervisor during my PhD. It was always comforting to know that I could rely on him for guidance; both as a mentor and as a friend.

I must also thank my fellow PhD students at CRST, past and present. The lively debates, discussions and humour were integral in facilitating both a productive and enjoyable environment to work in. My only regret is not letting them suffer through *more* of my awful jokes. In particular I thank James McGrane, Felix Rudolph, Edward Hughes, Zac Kenton, Paolo Mattioli, Martyna Jones, Emanuele Moscato, Rodolfo Panerai, Arnau Koemans Collado, Zoltán Laczkó, Christopher Lewis–Brown, Ray Otsuki, Luigi Alfonsi, Nadia Bahjat–Abbas, Nejc Čeplak, Linfeng Li, Ricardo Stark–Muchão, Manuel Accettulli Huber, Rashid Alawadhi, Enrico Andriolo, Stefano De Angelis, Marcel Hughes, Gergely Kantor, David Peinador Veiga, Rajath Radhakrishnan, and Shun-Qing Zhang. I would especially like to extend the warmest gratitude to Brenda Penante. Her support, companionship and wonderful weirdness has kept me sane throughout my PhD.

In addition to the students, I also wish to thank the faculty members at QMUL over the years for always being happy to share their wisdom and expertise; or, in many cases, just have a chat over a cup of tea. In particular Matt Buican, Andreas Brandhuber, Sanjaye Ramgoolam, Rodolfo Russo, Steve Thomas, Gabriele Travaglini, Brian Wecht and Christopher White. Special thanks go to David Berman for his instrumental role as my Master's thesis supervisor, and for inspiring me to pursue a PhD in the first place.

Lastly, I would like to thank my friends outside of academia for keeping me tethered to the real world. In particular, thanks to James Daniels and Daniel Lattimer for their great humour and kindness; and thanks to Matthew Harvey for periodically topping up my dose of surreal nonsense and serious philosophical inquiry in simultaneity.

This work was supported by an STFC research studentship.

# Declaration

I, Joseph Aaron Hayling, confirm that the research included within this thesis is my own work or that where it has been carried out in collaboration with, or supported by others, that this is duly acknowledged below and my contribution indicated. Previously published material is also acknowledged below.

I attest that I have exercised reasonable care to ensure that the work is original, and does not to the best of my knowledge break any UK law, infringe any third party's copyright or other Intellectual Property Right, or contain any confidential material.

I accept that the College has the right to use plagiarism detection software to check the electronic version of the thesis.

I confirm that this thesis has not been previously submitted for the award of a degree by this or any other university.

The copyright of this thesis rests with the author and no quotation from it or information derived from it may be published without the prior written consent of the author.

Signature:

Date: February 14, 2020

Details of collaboration and publications:

This thesis describes research carried out with my supervisor Constantinos Papageorgakis, which was published in [1–4]. It also contains some unpublished material. We collaborated with Matthew Buican in [1]; with Elli Pomoni and Diego Rodríguez-Gómez in [2]; with Rodolfo Panerai in [3]; and with Vasilis Niarchos in [4]. Where other sources have been used, they are cited in the bibliography.

# Contents

# Chapter 1

# Introduction

The two crowning achievements of twentieth century theoretical physics are quantum field theory (QFT) and general relativity (GR). Quantum field theory has led to a profound understanding of subatomic particles and eventually developed into the Standard Model (SM) of particle physics. That is, a core set of fundamental particles and rules governing their possible interactions. The SM is very successful and has been probed at extremely high energies in particle accelerators. Indeed the Standard Model is responsible for one of the most accurate predictions in all of science: the anomalous magnetic moment of the electron, which is correct up to a staggering eleven decimal places of accuracy. Put into context, this is akin to measuring the width of the Atlantic ocean and only being wrong by the thickness of a hair.

General relativity, on the other hand, is on the opposite side of the spectrum in terms of the length scales of physics that it describes. It is a set of mathematical laws governing the motion of planets in orbits, galactic formation and the evolution of the cosmos. Like QFT, this theory has been experimentally verified to astounding levels of precision, for example in the recent LIGO experiments for gravitational waves.

However, these theories are not without their shortcomings. For example, quantum field theory in general suffers from divergences arising at very high energies. This manifests itself in the Standard Model as a series of infinities in the calculations that add quantum corrections to the mass of the Higgs Boson due to the top-quark loops. This pathology is due to our incomplete understand of both QFT and the SM. Various extensions to the SM have been proposed, one of which being supersymmetry (SUSY), which postulates that for every bosonic/fermionic particle there is a particle with the same mass and charge but with the opposite spin statistic. This helps to counteract the infinities that appear in the calculations since the contributions of bosonic particles come with an opposite sign to fermionic particles. With all other parameters fixed, this should roughly equate to being able to cancel out each divergence as and when they appear.

There are problems in GR, too. We still lack an understanding of dark matter, dark energy, and our description of nature breaks down entirely when we try to describe black hole spacetime singularities. These core issues with our theories of nature are seemingly distinct but, as we will see, they suffer from the same problem: our models are incomplete.

The notion of a grand theory of everything is a tantalising prospect. It is the idea that, one day, we might be able to write the complete set of laws governing our universe and explain our place in the cosmos simply by evolving a system in time with specified boundary conditions. This holy grail of science would be a phenomenal achievement and would lead to a host of philosophical questions. At the moment this goal is incredibly far away. The reason is that QFT and GR are seemingly incompatible.

The Standard Model of particle physics makes no mention of gravity and general relativity does not pretend to be quantum. Quantum field theory postulates that the fundamental forces in nature are in fact mediated by subatomic particles themselves. For quantum electrodynamics (QED) this is the photon; the nuclear force has the W and Z bosons; and for quantum chromodynamics (QCD) it is the gluon. The logical next step is to do the analogous thing for the gravitational force and introduce the so-called graviton. While nice in principle, it remains incredibly hard to extract meaningful information out this quantum theory of gravity due to the appearance of many (an infinite number of) divergences which one cannot get rid of using standard renormalisation techniques. Moreover, there are an infinite number of vertices that one needs to consider in the interacting theory, so the number of possible Feynman diagrams grows at an alarming rate for each loop order.

Supersymmetry can be combined with gravity to form supergravity (SUGRA) in which the divergences coming from the graviton are countered by its corresponding fermionic partner, the gravitino. However, it seems that the theory is ill-defined at very high energies. Only with such an enormous degree of SUSY do we see promising results. That is, as of today, 4d $\mathcal{N} = 8$ SUGRA has no known UV divergences, though there is no reason *a priori* for this to be the case.

This is a problem because we do not observe supersymmetry in nature. Therefore supersymmetry needs to 'break' at lower energies, so a minimal amount of SUSY is desirable for realistic theories. To circumvent this issue, a supplementary approach can be used which revisits the common lore that particles are points.

String theory postulates that, when one goes to small enough length scales, subatomic particles are actually the result of a one-dimensional string. These strings vibrate at different frequencies, and each vibrational mode corresponds to its own subatomic particle. In this picture we see two types of strings: closed strings, which mediate gravitational interactions, and open strings which mediate the other forces. The reason why string theory is helpful in obtaining a consistent theory of everything

is that strings have an infinite number of vibrational modes which we can excite. This means that, once we reach an energy level where our original description of physics breaks down, the higher energy modes of the string come to the rescue. String theory is exciting because it provides a theory of quantum gravity and particle physics which is seemingly free from UV divergences.

Unfortunately, for string theory to be internally consistent, it needs to exist in ten-dimensional spacetime. A natural question to then ask is how do we recover the four-dimensional spacetime that we observe. One splits spacetime into $\mathcal{M}^{10} = \mathbb{R}^{1,3} \times \mathcal{M}^6$ where $\mathcal{M}^6$ compact six-dimensional manifold. This manifold is then shrunk to zero volume and the geometric data of the shrunken space becomes field theoretic data in the remaining 4d theory. Therefore, for a unified theory of everything, we simply need to find such a space that results in the minimally supersymmetric extension of the standard model coupled to gravity. It turns out that there are approximately $10^{272,000}$ vacua that one can choose from [5]. Indeed it is not even clear if there *should* be a vacuum that reproduces what we desire.

In spite of this impasse string theory remains an intrinsically interesting theory to study. It is very rich mathematically and has led to many interesting discoveries on this front. It has uncovered some hidden symmetries and structures in supersymmetric quantum field theories that have helped further our understanding of QFT as a whole. Notably in the context of strongly coupled gauge theories and strong-weak duality. Moreover it has lead to some new techniques that we can use to probe QFTs, even in the case where they do not posses a Lagrangian description.

This is largely due to the other extended objects that exist in string theory. While a string only has one intrinsic dimension, a "brane" is a higher dimensional analogue upon which strings can end. Strings ending on stacks of these branes have a low energy effective description in terms of supersymmetric quantum field theories. In some cases, the theory is also conformal, like the prototypical 4d $\mathcal{N} = 4$ super Yang-Mills (sYM) which arises as the low energy limit of a stack of D3 branes in type IIB string theory.

Another example closer to the heart of this thesis comes from M-theory, the strong-coupling limit of type IIA string theory. It is defined in eleven dimensions and, instead of strings as the fundamental objects, it has two and five dimensional membranes, respectively denoted as M2 and M5 branes. Both of these stacks of branes lead to superconformal field theories, with the former being related to the three-dimensional ABJM theory [6] and the latter giving the six-dimensional (2,0) theory [7].

M-theory is notoriously difficult to describe due to the fact that it is purely non-perturbative, though it gives rise to all five possible models of string theory when one dimension is compactified [8]. A fruitful avenue to study the inner-workings of M-theory is to study the dynamics of both the M2 and M5 branes. The M2 dynamics are relatively well understood, first through Bagger–Lambert–Gustavsson theory [9,10] and

then through ABJM by Aharony, Bergman, Jafferis and Maldacena [6], leading to a tractable Lagrangian description. No such success has been found, despite an attempt at replicating the Lie 3-algebra technique used in [9] for the (2,0) theory [11].

While we cannot write down an action for the non-Abelian 6d (2,0) theory, we can appeal to other techniques that were developed to probe it. For example, since this theory is conformal, we can use the power of conformal symmetry to infer information about this mysterious entity. A conformal field theory (CFT) does not have any length scale and does not need to make any reference to a Lagrangian. It needs only what is known as the "conformal data" of the theory, which is the set of scaling dimensions and structure constants of the operator product algebra. This is touched upon in Section 2.1. This, alongside the heavy constraints imposed by conformal symmetry and unitarity has lead to the conformal bootstrap program [12], which provides precision calculations for the spectrum of a theory. Notably it has been used to derive bounds on the scaling dimensions of operators in the 3d Ising model at the critical temperature [13] which have been measured in a lab.

A similar procedure was developed for superconformal field theories in [14] for 4d $\mathcal{N} = 4$ sYM. It was later applied precisely to the 6d (2,0) theory in [15] leading to a very non-trivial exploration of the interacting theory and its operator content.

Another approach to tackling mysterious higher dimensional theories is to appeal to their lower dimensional daughter theories. In [16] it was shown that the (2,0) theory reduced on a Riemann surface leads to a 4d $\mathcal{N} = 2$ SCFT whose operator content is specified by the geometric data of the surface. Through studying these (possibly non-Lagrangian) theories we have managed to uncover small pieces of information about their higher dimensional origin; along with a hidden symmetry known as the Alday–Gaiotto–Tachikawa (AGT) conjecture [17]. The idea is that one puts the (2,0) theory on the space $\mathcal{M}_4 \times \Sigma_2$. When one shrinks either the compact manifold $\mathcal{M}_4$ or the Riemann surface $\Sigma_2$ one finds a relationship between observables in the resulting 2d and 4d theories.

This is mostly conjectural and so far lacks any counter example, though it has been proven when $\mathcal{M}_4 = \mathcal{M}_3 \times \mathbb{S}^1$ for a subclass of manifolds [18]. This is because, when defined on a circle, the (2,0) theory can be reduced to 5d $\mathcal{N} = 2$ sYM, where there is a Lagrangian description.

The relationship between the (2,0) theory and 5d $\mathcal{N} = 2$ sYM may yet be even more special than a simple dimensional reduction. It has been conjectured that, once one includes all the instanton contributions to the theory, the 5d $\mathcal{N} = 2$ sYM *is* the (2,0) theory on a circle [19, 20]. An interpretation is that the instanton levels are in one-to-one correspondence with the Kaluza–Klein modes of the (2,0) fields on a circle, with some evidence for this provided in [21].

This notion of a lower dimensional theory being identified as a higher dimensional

one actually pre-dates the above conjecture. In [22] it was shown that a 4d quiver gauge theory in a certain limit of parameters can dynamically generate an additional dimension. Thus the 4d theory becomes five dimensional, albeit with the circular dimension being latticised. The continuum limit for the lattice spacing going to zero was later proposed in [23] for 4d superconformal theories where there is no issue with taking the lattice spacing to zero. There were two 4d theories which ended up dynamically generating two dimensions, giving the 6d (2,0) theory and the 6d (1,1) little string theory (LST). One of the goals of this current work is to study these mysterious higher dimensional theories by appealing to both the high degree of symmetry present and to this idea of dimensional deconstruction.

In Chapter 2 we review the relevant background material that we use liberally throughout the thesis. First we introduce conformal symmetry across various dimensions in Sec. 2.1, along with its implications about how we describe states and operators in these theories. This is then extended to superconformal symmetry, where we discuss the resulting algebras specifically in 5d and 6d. We move on to describing how the states of a conformal theory can be counted in a way that is insensitive to continuous deformations of the theory via the superconformal index in Sec. 2.2, along with an example for 4d $\mathcal{N} = 2$ SQCD.

The superconformal index for an interacting SCFT is not always easy to calculate. One can use a technique known as supersymmetric localisation to compute this quantity; along with various partition functions and observables on compact manifolds for generic theories (supersymmetry permitting). This is covered in Sec. 2.3.1 along with a 3d $\mathcal{N} = 2$ example on an $\mathbb{S}^3$. A complementary, albeit more restricted, technique for extracting partition functions in $d \geq 4$ is known as the refined topological vertex. This is particularly useful when calculating partition functions of non-Lagrangian field theories, and is reviewed in Sec. 2.4, along with an example calculating the partition function of the 4d $\mathcal{N} = 2$ circular quiver theory that we later use.

Equipped with the basics of the superconformal algebra and the superconformal index, we move onto Chapter 3. We perform level-by-level constructions of all unitary multiplets that one can construct in SCFTs with dimension greater than four. The most general superconformal index is provided for the theories with eight supercharges, whereas we only provide a refined limit of the index in the sixteen supercharge case. For the latter to be fully refined, we refer the reader to the accompanying `Mathematica` notebook of the paper upon which this chapter is based [1]. Section 3.4.5 provides some unpublished work with the aim of helping elucidate the multiplet structure of the interacting (2,0) theories. Lastly, we extend the discussion in [24] to the eight supercharge theories and describe the procedure of moving from the supercharacter to the index in Section 3.5.

Chapter 4 revisits the idea of dimensionally deconstructing six dimensional theories

proposed in [23]. Section 4.1 deals with the (2,0) theory which starts with a 4d $\mathcal{N} = 2$ circular quiver theory and then applies a limit of the parameters of the theory to recover the additional dimensions. The proposal is tested using some exact methods such as the Hilbert series, superconformal index and topological strings; where we find agreement between 4d and 6d quantities in the specified limit. The following Section 4.2 focuses on the second proposal for 6d Little String Theory. We start with a 4d $\mathcal{N} = 1$ $\mathbb{S}^4$ partition function which is subsequently generalised from [25] to be on the squashed four-sphere. We then compare the deconstruction limit for the 4d toroidal quiver theory partition function to that of LST, again finding agreement.

The process of dimensional deconstruction is then extended to include defects that couple to the bulk theory in Chapter 5. The aim is to extend the dictionary of observables that we can compute through dimensional deconstruction to lend credibility to the novel predictions we make through it. This chapter is based on [4] and focuses on two cases in that paper. Namely the deconstruction of 4d theories with 2d (2,2) and (4,0) supersymmetric defects.

Since the exact computations require manipulations of special functions, we provide a technical Appendix A that details our conventions for these functions. It also contains various identities that are used liberally throughout the thesis.

The last Appendix B is an introduction to a `python` package that goes alongside Chapter 3. It also contains information about a key technique that we use in that chapter, the Racah–Speiser algorithm and its relation to momentum null states in conformal field theory.

# Chapter 2

# Review

This chapter will review some core concepts that will be central to this thesis. This includes an overview of conformal field theories (CFTs), along with some techniques developed to study these theories. While there is a veritable smorgasbord of methods to choose from, we will focus specifically on the following non-perturbative techniques: the superconformal index, localisation and the refined topological vertex. This survey is mostly for exposition, with a more detailed treatment deferred to later chapters when required.

## 2.1 Conformal Field Theories

A quantum field theory (QFT) is said to be a conformal field theory if it invariant under conformal transformations. That is, the physics is unaffected by the transformations $x \to x'$ such that the metric transforms according to

$$g_{\mu\nu}(x) \to g'_{\mu\nu}(x') = \Omega^2(x) g_{\mu\nu}(x) \ , \tag{2.1}$$

where $\Omega(x)$ is some position dependent scaling factor. The set of these conformal transformations forms a group, whose transformations we will now explore. Consider the infinitesimal transformation $x^\mu \to x'^\mu = x^\mu + \epsilon^\mu(x)$. The metric changes as $g_{\mu\nu} \to g_{\mu\nu} - (\partial_\mu \epsilon_\nu + \partial_\nu \epsilon_\mu)$, which implies that

$$\partial_\mu \epsilon_\nu + \partial_\nu \epsilon_\mu = C(x) g_{\mu\nu} \tag{2.2}$$

It then follows that $C(x) = \frac{2}{d} \partial_\rho \epsilon^\rho$ after taking the trace of both sides. Equation (2.2) can be further manipulated by applying one more derivative and taking a linear combination. We then arrive at

$$2\partial_\mu \partial_\nu \epsilon_\rho = g_{\mu\rho} \partial_\nu C(x) + g_{\nu\rho} \partial_\mu C(x) - g_{\mu\nu} \partial_\rho C(x)$$

$$\implies (2-D)\partial_\mu\partial_\nu C(x) = g_{\mu\nu}\partial^2 C(x)\ . \tag{2.3}$$

Note that a further contraction with the metric leads to

$$(d-1)\partial^2 C(x) = 0\ . \tag{2.4}$$

These equations have some interesting implications for the explicit form of conformal transformations in $d$ dimensions.

- $d = 1$: Equation (2.4) does not impose any constraint on the function $C(x)$; hence any smooth transformation in one dimension is a conformal one. Intuitively this makes sense since a conformal transformation can be thought of as one that preserves the angle between two arbitrary curves. Given that there are no angles in one dimension, it follows that there should be no restriction on $C(x)$.

- $d = 2$: Equation (2.2) in two dimensions tells us that

$$\partial_1\epsilon_1 = \partial_2\epsilon_2\ , \qquad \partial_1\epsilon_2 = -\partial_2\epsilon_1\ . \tag{2.5}$$

  Once we rewrite these constraints in complex coordinates $\epsilon(z) = \epsilon_1(z) + i\epsilon_2(z)$ with $z = x^1 + ix^2$, then the aforementioned constraints are simply the Cauchy-Riemann equations. Consequently $\epsilon$ can be any analytic function of $z$. Another way to phrase this is that the conformal field theory in $2d$ is invariant under

$$z \to f(z)\ , \qquad \bar{z} \to \bar{f}(\bar{z})\ . \tag{2.6}$$

  The local algebra described by these transformations is infinite dimensional, see *e.g.* [12].

- $d > 2$: In other dimensions, the constraints imply that $\partial_\mu\partial_\nu C(x) = 0$, which is simply the statement that $C(x)$ is linear in $x$ at most. This then implies that the most general form for $\epsilon_\mu$ is

$$\epsilon_\mu = a_\mu + b_{\mu\nu}x^\nu + c_{\mu\nu\rho}x^\nu x^\rho\ . \tag{2.7}$$

  After some algebra, one discovers that the finite transformations to the above are:

$$\begin{aligned}
\text{Translations:}\quad & x'^\mu = a^\mu + x^\mu\ , \\
\text{Rotations:}\quad & x'^\mu = M^\mu{}_\nu x^\nu\ , \\
\text{Dilations:}\quad & x'^\mu = \lambda x^\mu\ , \\
\text{Special Conformal:}\quad & x'^\mu = \frac{x^\mu - b^\mu x^2}{1 - 2b_\nu x^\nu + b_\nu b^\nu x_\rho x^\rho}\ .
\end{aligned} \tag{2.8}$$

Crucially, this algebra is finite dimensional. This is the set of transformations that is most relevant for this thesis.

### 2.1.1 The Conformal Group

In dimensions greater than two, we observe the familiar subgroups. The first two transformations form the Poincaré group, while the third is simply a scaling transformation. The fourth is slightly more subtle, but in essence it is three transformations: an inversion $x^\mu \to \frac{x^\mu}{x^2}$, followed by a translation $b^\mu$, followed by another inversion.

The generators of these transformations can be represented in the following way:

$$\begin{aligned} \text{Translations: } & P_\mu = -i\partial_\mu \ , \\ \text{Rotations: } & L_{\mu\nu} = -i(x_\mu\partial_\nu - x_\nu\partial_\mu) \ , \\ \text{Dilations: } & D = x^\mu\partial_\mu \ , \\ \text{Special Conformal: } & K_\mu = i(2x_\mu x^\nu\partial_\nu - x^2\partial_\mu) \ , \end{aligned} \tag{2.9}$$

with the commutation relations

$$\begin{aligned} [D, P_\mu] &= P_\mu \ , \\ [D, K_\mu] &= -K_\mu \ , \\ [K_\mu, P_\nu] &= 2(\delta_{\mu\nu}D - iL_{\mu\nu}) \ , \\ [K_\rho, L_{\mu\nu}] &= i(\delta_{\rho\nu}K_\mu - \delta_{\rho\mu}K_\nu) \ , \\ [P_\rho, L_{\mu\nu}] &= i(\delta_{\rho\nu}P_\mu - \delta_{\rho\mu}P_\nu) \ , \\ [L_{\mu\nu}, L_{\rho\sigma}] &= i(\delta_{\mu\rho}L_{\nu\sigma} + \delta_{\nu\sigma}L_{\mu\rho} - \delta_{\nu\rho}L_{\mu\sigma} - \delta_{\mu\sigma}L_{\nu\rho}) \ . \end{aligned} \tag{2.10}$$

The scaling dimension of an operator $\mathcal{O}$ is defined as the eigenvalue of the dilation operator: $D\mathcal{O} = \Delta\mathcal{O}$. This has two immediate implications for the operators $K_\mu$ and $P_\mu$

$$\begin{aligned} DK_\mu\mathcal{O} &= ([D, K_\mu] + K_\mu D)\mathcal{O} = (\Delta - 1)K_\mu\mathcal{O} \ , \\ DP_\mu\mathcal{O} &= ([D, P_\mu] + P_\mu D)\mathcal{O} \ = (\Delta + 1)P_\mu\mathcal{O} \ . \end{aligned} \tag{2.11}$$

These have a very natural interpretation in terms of the radial quantisation picture. This is discussed at length in [26, 27] so we will only summarise it here.

In QFT we canonically foliate spacetime with equal-time slices of $\mathbb{R}^{1,d-1}$, that is, for each $x_0$ we have a unique $\mathbb{R}^{d-1}$, upon which we define the space of states. We then impose equal-time canonical commutation relations to quantise the theory. The states that are characterised by representations of the Poincaré group can then be unitarily evolved in time. Instead of doing this for the operators of the CFT, we foliate

spacetime with $(d-1)$-dimensional spheres around the origin of $\mathbb{R}^d$, each specified by some constant-radius slice. The states defined on these spheres are characterised by their $\mathrm{SO}(d) \times \mathrm{SO}(2)$ quantum numbers. The $D$ operator then plays the role of a Hamiltonian with the eigenvalues $\Delta$ being the energies. Eigenstates of $D$ are then in one-to-one correspondence with local operators in the CFT inserted at the origin of the sphere

$$|\Delta; \vec{\ell}\,\rangle = \mathcal{O}_{\Delta,\vec{\ell}}(0)\,|0\rangle \implies D\,|\Delta; \vec{\ell}\,\rangle = \Delta\,|\Delta; \vec{\ell}\,\rangle \ , \tag{2.12}$$

where $\vec{\ell}$ represents an arbitrary label of a representation of $\mathrm{SO}(d)$. The dilation operator acts by scaling the radius of the sphere, with the $P_\mu$ operators progressing us from one distinct slice to the next in a discrete jump. Likewise the $K_\mu$ operator moves us one slice backwards. It therefore follows that, when we are at the origin:

$$K_\mu \mathcal{O}(0) = 0 \ , \tag{2.13}$$

which we denote as a primary operator. Operators of higher dimension can be obtained from primaries by acting with the 'raising' operators for dimension

$$\mathcal{O}(0) \to P_{\mu_1} \cdots P_{\mu_n} \mathcal{O}(0) \ , \tag{2.14}$$

with $\Delta \to \Delta + n$. These operators are called descendant operators. It then follows that $\mathcal{O}(x) = e^{x \cdot P}\mathcal{O}(0)$ is a linear combination of one primary operator and an infinite number of conformal descendants. It is through this definition of states defined on $\mathbb{S}^{d-1}$ that we can define some notion of a norm of a state, along side positivity for said norms. This will be a central theme in the upcoming Chapter 3.

Lastly, one can show that there is an isomorphism between the conformal group in $d$ dimensions and $\mathrm{SO}(d,2)$ with the following redefinitions:

$$\begin{aligned} M_{\mu\nu} &= L_{\mu\nu} \ , & M_{-1,\mu} &= -\frac{i}{2}(P_\mu - K_\mu) \ , \\ M_{-1,0} &= D \ , & M_{0,\mu} &= \frac{1}{2}(P_\mu + K_\mu) \ , \end{aligned} \tag{2.15}$$

which now obey the $\mathrm{SO}(d,2)$ commutation relations

$$[M_{IJ}, M_{KL}] = i(\delta_{IK} M_{JL} + \eta_{JL} M_{IK} - \eta_{JK} M_{IL} - \eta_{IL} M_{JK}) \ , \tag{2.16}$$

with $I = -1, 0, \ldots, d$ and $\eta_{IJ} = \mathrm{diag}(-1, -1, 1, \ldots, 1)$.

### 2.1.2 Superconformal Symmetry

Extending the conformal algebra to include supersymmetry is achieved by adding the generators of supertranslations $\mathcal{Q}$ and superconformal translations $\mathcal{S}$ to our existing set of conformal generators. This is collectively known as the superconformal algebra (SCA). An additional global symmetry is present, known as the R-symmetry, which is an additional symmetry that rotates the supercharges.

Superconformal field theories (SCFTs) exhibit such a high degree of symmetry that they are somewhat simpler arenas in which we can test and understand general ideas in quantum field theory; such as duality [16, 28–32] or emergent symmetry [33].

In his pioneering work, Nahm showed that these algebras admit a simple classification [34]. These are

$$
\begin{aligned}
&d = 3 \quad \mathfrak{osp}(\mathcal{N}|4) \supset \mathfrak{so}(3,2) \times \mathfrak{so}(\mathcal{N})_R \,, \\
&d = 4 \quad \begin{cases} \mathfrak{su}(2,2|\mathcal{N}) \supset \mathfrak{so}(4,2) \times \mathfrak{u}(\mathcal{N})_R \,, & \mathcal{N} \neq 4 \,, \\ \mathfrak{psu}(2,2|4) \supset \mathfrak{so}(4,2) \times \mathfrak{su}(4)_R \,, \end{cases} \\
&d = 5 \quad \mathfrak{f}(4) \supset \mathfrak{so}(5,2) \times \mathfrak{su}(2)_R \,, \quad \mathcal{N} = 1 \,, \\
&d = 6 \quad \mathfrak{osp}(8^*|\mathcal{N}) \supset \mathfrak{so}(6,2) \times \mathfrak{sp}(2\mathcal{N})_R \,,
\end{aligned}
\tag{2.17}
$$

where we have indicated the splitting of the SCA into the conformal algebra and the R-symmetry piece. Consequently, all states in an SCFT can be classified by their quantum numbers $|\Delta\,;\vec{\ell}\,;\vec{r}\,\rangle$.

Note that, with the exception of five dimensions, we have a parameter $\mathcal{N}$ through which we can dictate the level of supersymmetry present. It was shown in [35] that interacting SCFTs can only exist for $\mathcal{N} \leq 8, 4, 2$ in $d = 3, 4, 6$ respectively.

Since each dimension needs to be treated differently, we will focus on the two dimensions that are pertinent for this thesis. Namely, five and six dimensions. For detailed accounts of three and four dimensions we refer the reader to [36–38].

#### Five dimensions

Extending the 5d conformal algebra to include supersymmetry is achieved by adding to our existing set (now with $d = 5$) the generators of supertranslations $\mathcal{Q}_{\mathbf{A}a}$ and superconformal translations $\mathcal{S}_{\mathbf{A}a}$. These are equipped with a Lorentz spinor index $a = 1, \ldots, 4$ and an $\mathfrak{su}(2)_R$ index $\mathbf{A} = 1, 2$. Their associated Clifford algebras are generated by $\Gamma_\mu$ and $\tilde{\Gamma}_\mu$, respectively. The collection of bosonic and fermionic generators build

the $\mathfrak{f}(4)$ superconformal algebra, the bosonic part of which is $\mathfrak{so}(5,2) \oplus \mathfrak{su}(2)_R$.

First, it will be useful to relate $L_{\mu\nu}$ to the Lorentz raising (lowering) operators $\mathcal{M}_i^{\pm}$, associated with the positive (negative) simple roots, and the Cartans $\mathcal{H}_i$ (the eigenvalues of which are $l_i$), where $i = 1, 2$. We do so using the relations

$$\begin{aligned} \mathcal{M}_1^{\pm} &= L_{13} \pm iL_{23} \mp iL_{14} + L_{24} \ , \\ \mathcal{M}_2^{\pm} &= L_{35} \pm iL_{45} \ , \\ \mathcal{H}_i &= L_{2i-1\,2i} \ , \qquad \text{such that } [\mathcal{H}_i, \mathcal{H}_j] = 0 \ . \end{aligned} \tag{2.18}$$

The algebra is now extended to include the following commutation relations— see e.g. [36]:

$$\begin{aligned} &[L_{\mu\nu}, \mathcal{Q}_{\mathbf{A}a}] = \frac{i}{4}[\Gamma_\mu, \Gamma_\nu]_a{}^b \mathcal{Q}_{\mathbf{A}b} \ , && [L_{\mu\nu}, \mathcal{S}_{\mathbf{A}a}] = \frac{i}{4}[\tilde{\Gamma}_\mu, \tilde{\Gamma}_\nu]_a{}^b \mathcal{S}_{\mathbf{A}b} \ , \\ &[D, \mathcal{Q}_{\mathbf{A}a}] = \frac{1}{2}\mathcal{Q}_{\mathbf{A}a} \ , && [D, \mathcal{S}_{\mathbf{A}a}] = -\frac{1}{2}\mathcal{S}_{\mathbf{A}a} \ , \\ &[P_\mu, \mathcal{Q}_{\mathbf{A}a}] = 0 \ , && [P_\mu, \mathcal{S}_{\mathbf{A}a}] = i(\tilde{\Gamma}_\mu \tilde{\Gamma}_5)_a{}^b \mathcal{Q}_{\mathbf{A}b} \ , \\ &[K_\mu, \mathcal{Q}_{\mathbf{A}a}] = i(\Gamma_\mu \Gamma_5)_a{}^b \mathcal{S}_{\mathbf{A}b} \ , && [K_\mu, \mathcal{S}_{\mathbf{A}a}] = 0 \ . \end{aligned} \tag{2.19}$$

The generators of the $\mathfrak{su}(2)_R$ algebra are denoted $T_m$ for $m = 1, 2, 3$. They act on the supercharges according to

$$\begin{aligned} [T_m, \mathcal{Q}_{\mathbf{A}a}] &= \left(\frac{\sigma_m}{2}\right)_{\mathbf{A}}{}^{\mathbf{B}} \mathcal{Q}_{\mathbf{B}a} \ , \\ [T_m, \mathcal{S}_{\mathbf{A}a}] &= \left(\frac{\sigma_m}{2}\right)_{\mathbf{A}}{}^{\mathbf{B}} \mathcal{S}_{\mathbf{B}a} \ , \end{aligned} \tag{2.20}$$

where $\sigma_m$ are the Pauli matrices. In fact we may compactly write these $R$-symmetry generators as

$$[R_{\mathbf{A}}{}^{\mathbf{B}}] = \left[(T^m \sigma_m)_{\mathbf{A}}{}^{\mathbf{B}}\right] = \begin{pmatrix} \hat{\mathcal{R}} & \mathcal{R}^+ \\ \mathcal{R}^- & -\hat{\mathcal{R}} \end{pmatrix} \ , \tag{2.21}$$

with the algebra

$$[R_{\mathbf{A}}{}^{\mathbf{B}}, R_{\mathbf{C}}{}^{\mathbf{D}}] = \delta_{\mathbf{C}}^{\mathbf{B}} R_{\mathbf{A}}{}^{\mathbf{D}} - \delta_{\mathbf{A}}^{\mathbf{D}} R_{\mathbf{C}}{}^{\mathbf{B}} \ . \tag{2.22}$$

From the above, we may infer that

$$\begin{aligned} &[\mathcal{R}^+, \mathcal{Q}_{\mathbf{1}a}] = 0 \ , \quad [\mathcal{R}^-, \mathcal{Q}_{\mathbf{1}a}] = \mathcal{Q}_{\mathbf{2}a} \ , \quad [\hat{\mathcal{R}}, \mathcal{Q}_{\mathbf{1}a}] = \frac{1}{2}\mathcal{Q}_{\mathbf{1}a} \ , \\ &[\mathcal{R}^+, \mathcal{S}_{\mathbf{1}a}] = 0 \ , \quad [\mathcal{R}^-, \mathcal{S}_{\mathbf{1}a}] = \mathcal{S}_{\mathbf{2}a} \ , \quad [\hat{\mathcal{R}}, \mathcal{S}_{\mathbf{1}a}] = \frac{1}{2}\mathcal{S}_{\mathbf{1}a} \ . \end{aligned} \tag{2.23}$$

We denote the eigenvalue of $\hat{\mathcal{R}}$ in the orthogonal basis to be $k$. The odd elements of the 5d superconformal algebra satisfy

$$\begin{aligned}
\{\mathcal{Q}_{\mathbf{A}a}, \mathcal{Q}_{\mathbf{B}b}\} &= (\Gamma^\mu P_\mu C)_{ab}\epsilon_{\mathbf{AB}} \,, \\
\{\mathcal{S}_{\mathbf{A}a}, \mathcal{S}_{\mathbf{B}b}\} &= (\tilde{\Gamma}^\mu K_\mu C)_{ab}\epsilon_{\mathbf{AB}} \,, \\
\{\mathcal{Q}_{\mathbf{A}a}, \mathcal{S}_{\mathbf{C}c}\} &= \left[\delta^{\mathbf{B}}_{\mathbf{A}} L_a{}^b + \delta^{\mathbf{B}}_{\mathbf{A}}\delta^b_a D - 3R_{\mathbf{A}}{}^{\mathbf{B}}\delta^b_a\right](i\epsilon_{\mathbf{BC}}\Gamma^5 C)_{bc} \,,
\end{aligned} \tag{2.24}$$

where $C$ is the charge-conjugation matrix and $\epsilon_{\mathbf{AB}}$ is the antisymmetric $2\times 2$ matrix such that $\epsilon_{\mathbf{12}} = 1$. It is straightforward to check that these matrices are given by

$$\begin{aligned}
\left[(\Gamma^\mu P_\mu C)_{ab}\right] &= \begin{pmatrix} 0 & P_1 & iP_2 & -P_3 \\ -P_1 & 0 & -P_3 & iP_4 \\ -iP_2 & P_3 & 0 & P_5 \\ P_3 & -iP_4 & -P_5 & 0 \end{pmatrix} \,, \\
\left[(\tilde{\Gamma}^\mu K_\mu C)_{ab}\right] &= \begin{pmatrix} 0 & K_1 & iK_2 & K_3 \\ -K_1 & 0 & K_3 & iK_4 \\ -iK_2 & -K_3 & 0 & K_5 \\ -K_3 & -iK_4 & -K_5 & 0 \end{pmatrix} \,.
\end{aligned} \tag{2.25}$$

We have also used the matrix $L_a{}^b$, which is defined by

$$\begin{aligned}
[L_a{}^b] &= \frac{i}{4}[\Gamma^\mu, \Gamma^\nu]_a{}^b L_{\mu\nu} \\
&= \begin{pmatrix} \mathcal{H}_1 + \mathcal{H}_2 & \mathcal{M}_2^+ & -\frac{1}{2}[\mathcal{M}_1^+, \mathcal{M}_2^+] & -\frac{1}{2}[[\mathcal{M}_1^+, \mathcal{M}_2^+], \mathcal{M}_2^+] \\ \mathcal{M}_2^- & \mathcal{H}_1 - \mathcal{H}_2 & \mathcal{M}_1^+ & \frac{1}{2}[\mathcal{M}_1^+, \mathcal{M}_2^+] \\ \frac{1}{2}[\mathcal{M}_1^-, \mathcal{M}_2^-] & \mathcal{M}_1^- & -\mathcal{H}_1 + \mathcal{H}_2 & \mathcal{M}_2^+ \\ -\frac{1}{2}[[\mathcal{M}_1^-, \mathcal{M}_2^-], \mathcal{M}_2^-] & -\frac{1}{2}[\mathcal{M}_1^-, \mathcal{M}_2^-] & \mathcal{M}_2^- & -\mathcal{H}_1 - \mathcal{H}_2 \end{pmatrix} .
\end{aligned} \tag{2.26}$$

The supercharges have the following conjugation relations [36]

$$\mathcal{Q}_{\mathbf{A}a} = i\epsilon_{\mathbf{AB}}(C\Gamma_5^T)_{ab}\mathcal{S}^{\dagger\mathbf{B}b} \,, \quad \mathcal{S}_{\mathbf{A}a} = -i\epsilon_{\mathbf{AB}}(C\tilde{\Gamma}_5^T)_{ab}\mathcal{Q}^{\dagger\mathbf{B}b} \,, \tag{2.27}$$

which allows us to rewrite the $\{\mathcal{Q}, \mathcal{S}\}$ anticommutator as

$$\{\mathcal{Q}_{\mathbf{A}a}, \mathcal{Q}^{\dagger\mathbf{B}b}\} = \delta^{\mathbf{B}}_{\mathbf{A}} L_a{}^b + \delta^{\mathbf{B}}_{\mathbf{A}}\delta_a{}^b D - 3R_{\mathbf{A}}{}^{\mathbf{B}}\delta_a{}^b \,. \tag{2.28}$$

Our Gamma matrix conventions in five dimensions are

$$\Gamma^1 = \begin{pmatrix} 0 & \mathbb{I}_{2\times 2} \\ \mathbb{I}_{2\times 2} & 0 \end{pmatrix} \,, \quad \Gamma^2 = \begin{pmatrix} 0 & i\,\mathbb{I}_{2\times 2} \\ -i\,\mathbb{I}_{2\times 2} & 0 \end{pmatrix} \,, \quad \Gamma^3 = \begin{pmatrix} \sigma_2 & 0 \\ 0 & -\sigma_2 \end{pmatrix} \,,$$

$$\Gamma^4 = \begin{pmatrix} \sigma_1 & 0 \\ 0 & -\sigma_1 \end{pmatrix} , \quad \Gamma^5 = \begin{pmatrix} -\sigma_3 & 0 \\ 0 & \sigma_3 \end{pmatrix} . \tag{2.29}$$

These are supplemented by the charge conjugation matrix

$$C = \begin{pmatrix} 0 & i\sigma_2 \\ i\sigma_2 & 0 \end{pmatrix} . \tag{2.30}$$

Note that $\tilde{\Gamma}^{1,2,3,4} = \Gamma^{1,2,3,4}$, while $\tilde{\Gamma}^5 = -\Gamma^5$. Each set generates the Euclidean Clifford algebra in five dimensions, that is they satisfy the relations

$$\{\Gamma^\mu, \Gamma^\nu\} = 2\delta^{\mu\nu} , \ \ (\Gamma^\mu)^\dagger = \Gamma^\mu , \ \ \Gamma^1\Gamma^2\ \Gamma^3\Gamma^4\Gamma^5 = \mathbb{I}_{4\times 4} , \ \ (C\Gamma^\mu)^T = -C\Gamma^\mu \tag{2.31}$$

and similarly for the $\tilde{\Gamma}$ matrices.

### Six dimensions

The superconformal algebra in 6d is $\mathfrak{osp}(8^*|2\mathcal{N})$, the bosonic part of which is $\mathfrak{so}(6,2) \oplus \mathfrak{sp}(\mathcal{N})_R$. The set of conformal generators is extended to include the generators of supersymmetry $\mathcal{Q}_{\mathbf{A}a}$ and superconformal translations $\mathcal{S}_{\mathbf{A}\dot{a}}$. The Lorentz spinor index ranges from $a, \dot{a} = 1, \ldots, 4$ (the dotted spinor index refers to the fact that it is in a conjugate spinor representation), while the $\mathfrak{sp}(\mathcal{N})_R$ index ranges from $\mathbf{A} = 1, \ldots, 2\mathcal{N}$. Their associated Clifford algebras are generated by $\Gamma_\mu$ and $\tilde{\Gamma}_\mu$ respectively, which will be provided later on.

Since their algebras are very similar, we first list the features that are shared by both $\mathcal{N} = 1$ and $\mathcal{N} = 2$ cases. Due to the fact that spinors in 6d are pseudo-real, they satisfy the reality conditions

$$\mathcal{Q}_{\mathbf{A}a} = i\Omega_{\mathbf{AB}}(C\Gamma_6^T)_{a\dot{b}}\mathcal{S}^{\dagger\mathbf{B}\dot{b}} , \quad \mathcal{S}_{\mathbf{A}\dot{a}} = -i\Omega_{\mathbf{AB}}(C\tilde{\Gamma}_6^T)_{\dot{a}b}\mathcal{Q}^{\dagger\mathbf{B}b} , \tag{2.32}$$

where $\Omega_{\mathbf{AB}}$ is the appropriate antisymmetric matrix in $2\mathcal{N}$ dimensions.[1] The commutation relations of the $\mathcal{Q}$ and $\mathcal{S}$ with the 6d conformal algebra are given by

$$\begin{aligned}
&[L_{\mu\nu}, \mathcal{Q}_{\mathbf{A}a}] = \frac{i}{4}[\Gamma_\mu, \Gamma_\nu]_a{}^b\mathcal{Q}_{\mathbf{A}b} , && [L_{\mu\nu}, \mathcal{S}_{\mathbf{A}\dot{a}}] = \frac{i}{4}[\tilde{\Gamma}_\mu, \tilde{\Gamma}_\nu]_{\dot{a}}{}^{\dot{b}}\mathcal{S}_{\mathbf{A}\dot{b}} , \\
&[D, \mathcal{Q}_{\mathbf{A}a}] = \frac{1}{2}\mathcal{Q}_{\mathbf{A}a} , && [D, \mathcal{S}_{\mathbf{A}\dot{a}}] = -\frac{1}{2}\mathcal{S}_{\mathbf{A}\dot{a}} , \\
&[P_\mu, \mathcal{Q}_{\mathbf{A}a}] = 0 , && [P_\mu, \mathcal{S}_{\mathbf{A}\dot{a}}] = i(\tilde{\Gamma}_\mu\tilde{\Gamma}_6)_{\dot{a}}{}^b\mathcal{Q}_{\mathbf{A}b} , \\
&[K_\mu, \mathcal{Q}_{\mathbf{A}a}] = i(\Gamma_\mu\Gamma_6)_a{}^{\dot{b}}\mathcal{S}_{\mathbf{A}\dot{b}} , && [K_\mu, \mathcal{S}_{\mathbf{A}\dot{a}}] = 0 .
\end{aligned} \tag{2.33}$$

[1] For $\mathcal{N} = 1$ one has $\Omega_{\mathbf{AB}} = \epsilon_{\mathbf{AB}}$, the 2d antisymmetric matrix. For $\mathcal{N} = 2$, $\Omega_{\mathbf{AB}}$ is the 4d symplectic matrix with $\Omega_{\mathbf{14}} = -\Omega_{\mathbf{41}} = \Omega_{\mathbf{23}} = -\Omega_{\mathbf{32}} = 1$ and all other components vanishing.

It is helpful to define the Lorentz raising/lowering operators $\mathcal{M}_i^{\pm}$ and Cartans $\mathcal{H}_i$—the eigenvalues of which are $h_i$ in the orthogonal basis of $\mathfrak{so}(6)$—in terms of $L_{\mu\nu}$. The relations are provided below:

$$\begin{aligned}
\mathcal{M}_1^{\pm} &= L_{13} \pm iL_{23} \mp iL_{14} + L_{24} \ , \\
\mathcal{M}_2^{\pm} &= L_{35} \pm iL_{45} \mp iL_{36} + L_{46} \ , \\
\mathcal{M}_3^{\pm} &= L_{35} \pm iL_{45} \pm iL_{36} - L_{46} \ , \\
\mathcal{H}_i &= L_{2i-1\,2i} \ , \qquad \text{such that } [\mathcal{H}_i, \mathcal{H}_j] = 0 \ .
\end{aligned} \tag{2.34}$$

For a superconformal algebra in six dimensions, all supercharges must have the same chirality [36], which we choose to be positive. Therefore we define the projector $\mathcal{P}_+ = \frac{1}{2}(1+\Gamma_7)$ and have that

$$\begin{aligned}
\{\mathcal{Q}_{\mathbf{A}a}, \mathcal{Q}_{\mathbf{B}b}\} &= (\mathcal{P}_+ \Gamma^\mu P_\mu C)_{ab} \Omega_{\mathbf{AB}} \ , \\
\left\{\mathcal{S}_{\mathbf{A}\dot{a}}, \mathcal{S}_{\mathbf{B}\dot{b}}\right\} &= (\mathcal{P}_+ \tilde{\Gamma}^\mu K_\mu C)_{\dot{a}\dot{b}} \Omega_{\mathbf{AB}} \ .
\end{aligned} \tag{2.35}$$

We may also use the projector $\mathcal{P}_+$ to define $M_a{}^b$ as

$$\begin{aligned}
[L_a{}^b] &= -\frac{i}{4}(\mathcal{P}_+)_a{}^c \Gamma^\mu, \Gamma^\nu]_c{}^b L_{\mu\nu} \\
&= \begin{pmatrix}
\mathcal{H}_1 + \mathcal{H}_2 + \mathcal{H}_3 & i\mathcal{M}_3^- & -\frac{1}{2}[\mathcal{M}_1^-, \mathcal{M}_3^-] & \frac{1}{4}[\mathcal{M}_1^-, [\mathcal{M}_2^-, \mathcal{M}_3^-]] \\
-i\mathcal{M}_3^+ & \mathcal{H}_1 - \mathcal{H}_2 - \mathcal{H}_3 & i\mathcal{M}_1^- & \frac{1}{2}[\mathcal{M}_1^-, \mathcal{M}_2^-] \\
\frac{1}{2}[\mathcal{M}_1^+, \mathcal{M}_3^+] & -i\mathcal{M}_1^+ & -\mathcal{H}_1 + \mathcal{H}_2 - \mathcal{H}_3 & i\mathcal{M}_2^- \\
\frac{1}{4}[\mathcal{M}_1^+, [\mathcal{M}_2^+, \mathcal{M}_3^+]] & -\frac{1}{2}[\mathcal{M}_1^+, \mathcal{M}_2^+] & -i\mathcal{M}_2^+ & -\mathcal{H}_1 - \mathcal{H}_2 + \mathcal{H}_3
\end{pmatrix} .
\end{aligned} \tag{2.36}$$

$\mathcal{N} = 1$

For this case, the $R$-symmetry algebra is $\mathfrak{sp}(1)_R \simeq \mathfrak{su}(2)_R$. Conveniently, all the information we require about $\mathfrak{su}(2)_R$ has already been provided in the 5d $\mathcal{N} = 1$ discussion, specifically (2.20) onwards. We may therefore use the previously-defined $R_{\mathbf{AB}}$ and write the $\{\mathcal{Q}, \mathcal{Q}^\dagger\}$ anticommutator as

$$\{\mathcal{Q}_{\mathbf{A}a}, \mathcal{Q}^{\dagger \mathbf{B}b}\} = \delta_{\mathbf{A}}^{\mathbf{B}} L_a{}^b + \delta_{\mathbf{A}}^{\mathbf{B}} (\mathcal{P}_+)_a{}^b D - 4R_{\mathbf{A}}{}^{\mathbf{B}} (\mathcal{P}_+)_a{}^b \ . \tag{2.37}$$

$\mathcal{N} = 2$

For this case, the $R$-symmetry algebra is $\mathfrak{sp}(2)_R \simeq \mathfrak{so}(5)_R$. The matrix $R_{\mathbf{A}}{}^{\mathbf{B}}$ for $\mathfrak{so}(5)_R$ is

$$[R_{\mathbf{A}}{}^{\mathbf{B}}] = \begin{pmatrix} \mathcal{J}_1 + \mathcal{J}_2 & \mathcal{R}_2^+ & -\frac{1}{2}[\mathcal{R}_1^+, \mathcal{R}_2^+] & -\frac{1}{2}[[\mathcal{R}_1^+, \mathcal{R}_2^+], \mathcal{R}_2^+] \\ \mathcal{R}_2^- & \mathcal{J}_1 - \mathcal{J}_2 & \mathcal{R}_1^+ & \frac{1}{2}[\mathcal{R}_1^+, \mathcal{R}_2^+] \\ \frac{1}{2}[\mathcal{R}_1^-, \mathcal{R}_2^-] & \mathcal{R}_1^- & -\mathcal{J}_1 + \mathcal{J}_2 & \mathcal{R}_2^+ \\ -\frac{1}{2}[[\mathcal{R}_1^-, \mathcal{R}_2^-], \mathcal{R}_2^-] & -\frac{1}{2}[\mathcal{R}_1^-, \mathcal{R}_2^-] & \mathcal{R}_2^- & -\mathcal{J}_1 - \mathcal{J}_2 \end{pmatrix} , \tag{2.38}$$

where the $\mathcal{J}_i$ are the Cartans of $\mathfrak{so}(5)_R$—the eigenvalues of which are $j_i$—and $\mathcal{R}_i^\pm$ are the raising/lowering operators. This allows the $\{\mathcal{Q}, \mathcal{Q}^\dagger\}$ anticommutator to be written as [36]

$$\{\mathcal{Q}_{\mathbf{A}a}, \mathcal{Q}^{\dagger \mathbf{B}b}\} = \delta_{\mathbf{A}}^{\mathbf{B}} L_a{}^b + \delta_{\mathbf{A}}^{\mathbf{B}} (\mathcal{P}_+)_a{}^b D - 2R_{\mathbf{A}}{}^{\mathbf{B}} (\mathcal{P}_+)_a{}^b \, . \tag{2.39}$$

Finally we collect our gamma-matrix conventions. For Euclidean $\mathfrak{so}(6)$ spinors we have

$$\begin{aligned} &\Gamma^1 = \sigma_1 \otimes \mathbb{I}_{2\times 2} \otimes \mathbb{I}_{2\times 2} \, , \quad \Gamma^2 = \sigma_2 \otimes \mathbb{I}_{2\times 2} \otimes \mathbb{I}_{2\times 2} \, , \quad \Gamma^3 = \sigma_3 \otimes \sigma_1 \otimes \mathbb{I}_{2\times 2} \, , \\ &\Gamma^4 = \sigma_3 \otimes \sigma_2 \otimes \mathbb{I}_{2\times 2} \, , \quad \Gamma^5 = \sigma_3 \otimes \sigma_3 \otimes \sigma_1 \, , \quad \Gamma^6 = \sigma_3 \otimes \sigma_3 \otimes \sigma_2 \, . \end{aligned} \tag{2.40}$$

We also have $\Gamma^7 = i\Gamma^1\Gamma^2\Gamma^3\Gamma^4\Gamma^5\Gamma^6$, which can be equivalently defined as

$$\Gamma^7 = \sigma_3 \otimes \sigma_3 \otimes \sigma_3 \, . \tag{2.41}$$

Since we are in even dimensions, we have a choice between which charge conjugation matrices to use, $C_{(\pm)}$. These have the properties $C_{(\pm)}^T = \mp C_{(\pm)}$ and $C_{(\pm)}^2 = \mp 1$. We choose $C_{(-)}$, but to lighten the notation, we will omit the subscript. We define our $C_{(-)} = C$ as

$$C = (-i\sigma_2) \otimes \sigma_1 \otimes (-i\sigma_2) \, , \tag{2.42}$$

Note that $\Gamma^{1,2,3,4,5} = \tilde{\Gamma}^{1,2,3,4,5}$, while $\tilde{\Gamma}^6 = -\Gamma^6$. They each generate the Euclidean Clifford algebra in six dimensions. The $\Gamma$s satisfy the relations

$$\{\Gamma^\mu, \Gamma^\nu\} = 2\delta^{\mu\nu} \, , \quad (\Gamma^\mu)^\dagger = \Gamma^\mu \, , \quad C(\Gamma^\mu)^T C^{-1} = -\Gamma^\mu \, . \tag{2.43}$$

and similarly for the $\tilde{\Gamma}$ matrices.

## 2.2 The Superconformal Index

The superconformal index was introduced as a way to count the protected operator spectrum of a given SCFT [39, 40]. It is insensitive to contributions from short multiplets that recombine into long multiplets under continuous changes in parameters, and thus remains invariant along an RG flow. This is important as it allows one to conduct non-trivial checks of certain dualities [41]. The index can be defined purely algebraically as in [42], which will be explored in Chapter 3; and can also be used as a calculational tool to extract information about a theory as in Chapters 4 and 5.

The index is defined through the trace formula

$$\mathcal{I}(\mu_i) = \mathrm{Tr}(-1)^F e^{-\beta\delta} \prod_i x_i^{\mu_i} \,, \tag{2.44}$$

where $\delta = \{\mathcal{Q}^\dagger, \mathcal{Q}\}$ is the Hamiltonian and $\mu_i$ is the set of mutually commuting charges (which also commute with the chosen Poincaré supercharge $\mathcal{Q}$ and its conjugate) and $F$ is the fermion number. The trace is taken over the Hilbert space of the radially quantised theory on $\mathbb{S}^{d-1}$.

This index decomposes into the set of states where $\delta = 0$ and where $\delta \neq 0$. The latter set of states can be constructed using the basis $(\phi, \mathcal{Q}\phi)$, and have the same charges under $\{\mu_i\}$ but with the opposite sign. Thus this set of states cancel each other out, along the lines of [43].[2] The only states that are counted are when $\delta = 0$, namely those that are annihilated by both $\mathcal{Q}$ and $\mathcal{Q}^\dagger$. One can also see that the index is free from the coupling $\beta$, and only receives contributions from states that are annihilated by some fraction of supersymmetry (i.e. those that are in short multiplets).

Another definition of the index is as a partition function on $\mathbb{S}^{d-1} \times \mathbb{S}^1$ with twisted boundary conditions on the $\mathbb{S}^1$. This has the advantage of being able to be generalised to non-conformal theories, although care must be taken when putting the desired theory on this background *à la* [44]. One can calculate these partition functions via the technique of localisation (for an example in 4d one has *e.g.* [45]) which we explore in the next section, or by exploiting the free field realisation. That is, one can use the fact that the index is independent of the coupling on this background to flow to free fixed point in which one simply needs to use Gaussian integration; *cf.* [46, 47].

### 2.2.1 The 4d $\mathcal{N} = 2$ Index

As a concrete example, we will study the superconformal index for general Lagrangian 4d $\mathcal{N} = 2$ theories. These indices will feature in Chapter 5 in the context of defect contributions to the bulk 4d index. There are many introductions and applications to

[2] Indeed this is essentially just a version of the Witten index but refined to carry more information and regulate the infinite tower of states.

| $\delta = 0$ Operator | $E$ | $j_1$ | $j_2$ | $R$ | $r$ | $\mathcal{I}(\mathfrak{p}, \mathfrak{q}, \mathfrak{t})$ |
|---|---|---|---|---|---|---|
| $\phi$ | 1 | 0 | 0 | 0 | $-1$ | $\mathfrak{pq}/\mathfrak{t}$ |
| $\lambda_{1\pm}$ | 3/2 | $\pm$ 1/2 | 0 | 1/2 | $-1/2$ | $-\mathfrak{p}$, $-\mathfrak{q}$ |
| $\bar{\lambda}_{1\dot{+}}$ | 3/2 | 0 | 1/2 | 1/2 | 1/2 | $-\mathfrak{t}$ |
| $\bar{F}_{\dot{+}\dot{+}}$ | 2 | 0 | 1 | 0 | 0 | $\mathfrak{pq}$ |
| $\partial_{-\dot{+}}\lambda_{1+} + \partial_{+\dot{+}}\lambda_{1-} = 0$ | 5/2 | 0 | 1/2 | 1/2 | $-1/2$ | $\mathfrak{pq}$ |
| $q$ | 1 | 0 | 0 | 1/2 | 0 | $\sqrt{\mathfrak{t}}$ |
| $\bar{\psi}_{\dot{+}}$ | 3/2 | 0 | 1/2 | 0 | $-1/2$ | $-\mathfrak{pq}/\sqrt{\mathfrak{t}}$ |
| $\partial_{\pm\dot{+}}$ | 1 | $\pm$1/2 | 1/2 | 0 | 0 | $\mathfrak{p}$, $\mathfrak{q}$ |

**Table 1:** The $\delta = 0$ operators for the 4d $\mathcal{N} = 2$ vector multiplet and $\mathcal{N} = 2$ half-hyper multiplet. The contributions from derivatives is also included in the bottom line.

this topic, with the most relevant being [48], as it also introduces various limits and hidden structures within the index.

The superconformal algebra for a 4d $\mathcal{N} = 2$ SCFT is $\mathrm{SU}(2,2|2)$ whose maximally compact bosonic subalgebra is $\mathrm{SU}(2)_1 \times \mathrm{SU}(2)_2 \times \mathrm{SU}(2)_R \times \mathrm{U}(1)_r$, with charges $j_1$, $j_2$, $R$ and $r$ respectively. We define the index with respect to $\widetilde{\mathcal{Q}}_{1\dot{-}}$ with charges $j_1 = 0$, $j_2 = -1/2$, $R = 1/2$, $r = -1/2$, which gives

$$\delta = \{\widetilde{\mathcal{Q}}^{\dagger}_{1\dot{-}}, \widetilde{\mathcal{Q}}_{1\dot{-}}\} = E - 2j_2 - 2R + r \ , \tag{2.45}$$

defining the index

$$\mathcal{I}(\mathfrak{p}, \mathfrak{q}, \mathfrak{t}) = \mathrm{Tr}_{\delta=0}(-1)^F \mathfrak{p}^{j_2 - j_1 - r} \mathfrak{q}^{j_2 + j_1 - r} \mathfrak{t}^{R+r} \ . \tag{2.46}$$

To get the single letter indices for the 4d $\mathcal{N} = 2$ multiplets, one simply goes through the operators in the multiplet and counts the ones with $\delta = 0$. These states are given in Table 1. Note the inclusion of the equations of motion constraint. This is because we count an infinite tower of derivatives, so we will eventually encounter an equation of motion which should be subtracted from the index (providing one is counting the right operators that constitute the equation of motion).

The derivatives contribute

$$\sum_{i=0}^{\infty} \sum_{j=0}^{\infty} \mathfrak{p}^i \mathfrak{q}^j = \frac{1}{(1-\mathfrak{p})(1-\mathfrak{q})} \tag{2.47}$$

to the index.

Putting everything together, the so-called single letter contributions to the index

are then

$$i_{\frac{1}{2}-\text{hyp}}(\mathfrak{p},\mathfrak{q},\mathfrak{t}) = \frac{\sqrt{t}-\frac{\mathfrak{pq}}{\sqrt{\mathfrak{t}}}}{(1-\mathfrak{p})(1-\mathfrak{q})} ,$$
$$i_{\text{vec}}(\mathfrak{p},\mathfrak{q},\mathfrak{t}) = -\frac{\mathfrak{p}}{1-\mathfrak{p}} - \frac{\mathfrak{q}}{1-\mathfrak{q}} + \frac{\frac{\mathfrak{pq}}{\mathfrak{t}}-\mathfrak{t}}{(1-\mathfrak{p})(1-\mathfrak{q})} . \tag{2.48}$$

The index for a free half-hypermultiplet would simply be the Plethystic exponential of the single-letter index, given by

$$\mathcal{I}_{\frac{1}{2}-\text{hyp}}(\mathfrak{p},\mathfrak{q},\mathfrak{t}) = \text{P.E.}\left[i_{\frac{1}{2}-\text{hyp}}(\mathfrak{p},\mathfrak{q},\mathfrak{t})\right] = \exp\left[\sum_{n=1}^{\infty}\frac{1}{n}i_{\frac{1}{2}-\text{hyp}}(\mathfrak{p}^n,\mathfrak{q}^n,\mathfrak{t}^n)\right]$$
$$= \Gamma_e\left(\sqrt{\mathfrak{t}}\,|\mathfrak{p},\mathfrak{q}\right) , \tag{2.49}$$

with the elliptic gamma function defined as

$$\Gamma_e(z|\mathfrak{p},\mathfrak{q}) = \prod_{\ell_1,\ell_2\geq 0}\frac{1-z^{-1}\mathfrak{p}^{\ell_1+1}\mathfrak{q}^{\ell_2+1}}{1-z\mathfrak{p}^{\ell_1}\mathfrak{q}^{\ell_2}} . \tag{2.50}$$

The motivation for such an operation can be found in Section A.3. One can obtain the $\mathcal{N}=1$ superconformal index simply with the limit $\mathfrak{t}\to\sqrt{\mathfrak{pq}}$

One can also refine the index to include data about global and gauge symmetries not associated with the superconformal algebra. In this case it would look something like

$$\mathcal{I}(\mathfrak{p},\mathfrak{q},\mathfrak{t}) = \text{Tr}_{\delta=0}(-1)^F\mathfrak{p}^{j_2-j_1-r}\mathfrak{q}^{j_2+j_1-r}\mathfrak{t}^{R+r}\prod_i\mathfrak{u}_i^{c_i}\prod_a\mathfrak{v}_a^{d_a} , \tag{2.51}$$

where $\mathfrak{u}_i$ is a fugacity associated with the charge $c_i$ under the gauge group, and $\mathfrak{v}_a$ is a fugacity associated with a charge $d_a$ under the set of global symmetries. For example, a vector multiplet for an SU(2) gauge theory would have the contribution

$$\left[-\frac{\mathfrak{p}}{1-\mathfrak{p}} - \frac{\mathfrak{q}}{1-\mathfrak{q}} + \frac{\frac{\mathfrak{pq}}{\mathfrak{t}}-\mathfrak{t}}{(1-\mathfrak{p})(1-\mathfrak{q})}\right](\mathfrak{u}^2+1+\mathfrak{u}^{-2}) , \tag{2.52}$$

where the second part is simply the adjoint character of SU(2) in terms of the fugacity $\mathfrak{u}$. Indeed more generally if the $j^{th}$ multiplet has representations $\mathcal{R}_j$ under a gauge and $\widetilde{\mathcal{R}}_j$ under a flavour group, with characters $\chi_{\mathcal{R}_j}(U)$ and $\chi_{\widetilde{\mathcal{R}}_j}(V)$ respectively, then their single letter contribution to the index is given by

$$i_j(\mathfrak{p},\mathfrak{q},\mathfrak{t};U,V) = i_j(\mathfrak{p},\mathfrak{q},\mathfrak{t})\chi_{\mathcal{R}_j}(U)\chi_{\widetilde{\mathcal{R}}_j}(V) , \tag{2.53}$$

where $j$ can represent a half-hypermultiplet or a vector multiplet; and $U$ and $V$ are the

set of gauge and global symmetry fugacities respectively.

For theories with a weakly-coupled description admit one can simply integrate the entire interacting index (that is, take the Plethystic exponential of the single letter components) over the gauge group fugacities with the Haar measure in order to project onto the space of gauge invariant operators. Hence

$$\mathcal{I}(\mathfrak{p},\mathfrak{q},\mathfrak{t};V)=\int[\mathrm{d}U]\,\mathrm{P.E.}\left[\sum_j i_j(\mathfrak{p},\mathfrak{q},\mathfrak{t};U,V)\right]\,, \tag{2.54}$$

where the sum is over all the multiplet content of the theory and $[\mathrm{d}U]$ is the Haar measure of the gauge group.

As a concrete example, let us take 4d $\mathcal{N}=2$ SU($N$) SQCD with $N_f=2N$ flavours. The index is given by

$$\begin{aligned}\mathcal{I}(\mathfrak{p},\mathfrak{q},\mathfrak{t};V)=\int[\mathrm{d}U]\,\mathrm{P.E.}\Big[i_{\frac{1}{2}-\mathrm{hyp}}\left(\chi_{\square}(U)\chi_{\overline{\square}}(V)+\chi_{\overline{\square}}(U)\chi_{\square}(V)\right)\\ +i_{\mathrm{vec}}(\mathfrak{p},\mathfrak{q},\mathfrak{t})\chi_{\mathrm{Adj}}(U)\Big]\,,\end{aligned} \tag{2.55}$$

We note that, for SU($N$), the Haar measure is

$$[\mathrm{d}U]=\prod_{j=1}^{N}\frac{\mathrm{d}\mathfrak{u}_j}{2\pi i\mathfrak{u}_j}\prod_{j\neq k}\left(1-\frac{\mathfrak{u}_j}{\mathfrak{u}_k}\right)=\prod_{j=1}^{N}\frac{\mathrm{d}\mathfrak{u}_j}{2\pi i\mathfrak{u}_j}\,\mathrm{P.E.}\left[\sum_{j\neq k}-\frac{\mathfrak{u}_j}{\mathfrak{u}_k}\right]\,, \tag{2.56}$$

with the constraint $\prod_{j=1}^{N}\mathfrak{u}_j=1$. The adjoint character of SU($N$) is given by

$$\chi_{\mathrm{Adj}}(U)=-1+\sum_{j,k=1}^{N}\frac{\mathfrak{u}_j}{\mathfrak{u}_k}\,. \tag{2.57}$$

Focusing on the off-diagonal part of the SU($N$) contribution from the vector multiplet, we can combine it with the Haar measure as

$$\begin{aligned}&\mathrm{P.E.}\left[\sum_{j\neq k}-\frac{\mathfrak{u}_j}{\mathfrak{u}_k}\right]\times\mathrm{P.E.}\left[\sum_{j\neq k}\left(-\frac{\mathfrak{p}}{1-\mathfrak{p}}-\frac{\mathfrak{q}}{1-\mathfrak{q}}\right)\frac{\mathfrak{u}_j}{\mathfrak{u}_k}\right]=\\ &\prod_{j\neq k}\mathrm{P.E.}\left[\left(-1-\frac{\mathfrak{p}}{1-\mathfrak{p}}-\frac{\mathfrak{q}}{1-\mathfrak{q}}\right)\frac{\mathfrak{u}_j}{\mathfrak{u}_k}\right]=\prod_{j\neq k}\mathrm{P.E.}\left[-\frac{1-\mathfrak{p}\mathfrak{q}}{(1-\mathfrak{p})(1-\mathfrak{q})}\frac{\mathfrak{u}_j}{\mathfrak{u}_k}\right]\,,\end{aligned} \tag{2.58}$$

where we can use the (A.49) to write this as

$$\prod_{j\neq k}\Gamma_e(\mathfrak{u}_j\mathfrak{u}_k^{-1}|\mathfrak{p},\mathfrak{q})^{-1}\,. \tag{2.59}$$

since $j \leftrightarrow k$ is symmetric under the product. So we see that the Haar measure has been absorbed into the definition of special function. All in all our full index is then

$$\mathcal{I}(\mathfrak{p},\mathfrak{q},\mathfrak{t};V) = \left(\frac{(\mathfrak{p};\mathfrak{p})(\mathfrak{q};\mathfrak{q})}{\Gamma_e(\mathfrak{t}|\mathfrak{p},\mathfrak{q})}\right)^{N-1} \int \prod_{j=1}^{N} \frac{\mathrm{d}\mathfrak{u}_j}{2\pi i \mathfrak{u}_j} \prod_{j\neq k} \frac{\Gamma_e\left(\frac{\mathfrak{p}\mathfrak{q}}{\mathfrak{t}}\mathfrak{u}_j\mathfrak{u}_k^{-1}|\mathfrak{p},\mathfrak{q}\right)}{\Gamma_e(\mathfrak{u}_j\mathfrak{u}_k^{-1}|\mathfrak{p},\mathfrak{q})} \times \prod_{j=1}^{N}\prod_{b=1}^{2N} \Gamma_e\left(\sqrt{\mathfrak{t}}\,\mathfrak{u}_j\mathfrak{v}_b^{-1}|\mathfrak{p},\mathfrak{q}\right)\Gamma_e\left(\sqrt{\mathfrak{t}}\,\mathfrak{u}_j^{-1}\mathfrak{v}_b|\mathfrak{p},\mathfrak{q}\right) , \tag{2.60}$$

where the contour integral can be calculated by considering residues inside $|\mathfrak{u}_i| < 1$.

Note that this approach only works here since one has a weakly-coupled description. When one does not have this, for example in dimensions higher than four, while one can describe the index algebraically as in [42], one has to get creative in how one calculates the full interacting index. This will often involve techniques such as localisation or the refined topological vertex which are covered in the following sections.

Another fruitful avenue is to appeal to various symmetries and hidden structures present in the theory. For example, one can exploit the AGT correspondence [17] to use 2d sYM correlators to calculate 4d indices [49] for non-Lagrangian theories by appealing to their higher dimensional origin (the (2,0) theory).

Through this relationship one can use tools of topological quantum field theory to recover unrefined limits of the 4d index as in [48]. There are a whole host of techniques, especially in 4d, for computing the superconformal index. For a comprehensive review the reader should consult [50] and the references therein.

## 2.3 Localisation

As previously mentioned, there exists an extremely powerful technique for calculating exact forms of protected quantities such as partition functions and Wilson loops on compact manifolds known as localisation. It was initially used in the context of cohomological and topological field theories [51], and notably in [52] on the so-called $\Omega$ background. It was applied to more realistic 4d theories on the $\mathbb{S}^4$ with at least $\mathcal{N} = 2$ SUSY in the seminal paper by Pestun [53],[3] subsequently followed by the $\mathbb{S}^3$ version in [55]. By now there are too many papers on this topic to do justice to this subfield, so we will simply reference those that are particularly pertinent to this thesis. For a complete review and survey of this area we refer the reader to the tome-like [56] and the contained references.

[3]Note that it is thought to be impossible to perform localisation for minimally supersymmetry theories on the $\mathbb{S}^4$, but certain techniques are available to circumvent this as in [25]. Note that this is not the same as declaring that partition functions on $\mathbb{S}^4$ cannot exist, thought they may be completely scheme dependent [54].

The schematic process will be presented in abstract, followed by an example in [55]. Suppose we have a fermionic symmetry of the action $\mathcal{Q}$ such that

$$\mathcal{Q}S = 0 \,. \tag{2.61}$$

We deform the path integral with some additional $\mathcal{Q}$-exact term, parametrised by $t$

$$Z(t) = \int \mathcal{D}\varphi e^{-S[\varphi]-t\mathcal{Q}V[\varphi]} \,. \tag{2.62}$$

We require $\mathcal{Q}^2 V[\varphi]$ to be zero, which can be achieved either with $\mathcal{Q}^2 = 0$ or $\mathcal{Q}^2 = \delta_B$, where $\delta_B$ is a bosonic symmetry,[4] when acting on $V[\varphi]$.

It is straightforward to show that, if the measure $\mathcal{D}\varphi$ is invariant under $\mathcal{Q}$, then

$$\frac{\partial Z(t)}{\partial t} = 0 \,, \tag{2.63}$$

which can be extended to include all operators $\mathcal{O}[\varphi]$ that are also $\mathcal{Q}$-invariant. This has led to a host of results for computing correlators via localisation as in [58–65] Since the deformed path integral is independent of $t$, the result at $t = 0$ (the undeformed theory) should be equivalent to the result for generic $t$. Therefore as long as $\mathcal{Q}V[\varphi] \geq 0$ along the chosen contour, all field configurations for which $\mathcal{Q}V[\varphi]$ are infinitely suppressed.

This is where the moniker 'localisation' comes from, in the sense that the deformed path integral localises to the space of bosonic zeros of $\mathcal{Q}V[\varphi]$. Suppose we have found a zero $\varphi_0$, we then expand our field around this saddle point

$$\varphi \to \varphi_0 + \frac{\varphi}{\sqrt{t}} \,, \tag{2.64}$$

and after Taylor expanding for large $t$ we have

$$S + t\mathcal{Q}V[\varphi] = S[\varphi_0] + (\mathcal{Q}V)^{(2)}[\varphi] + \mathcal{O}(t^{-1/2}) \,. \tag{2.65}$$

What this tells us is that the only important parts are the on-shell action evaluated at $\varphi_0$ and the quadratic fluctuations of $\mathcal{Q}V[\varphi]$ around that fixed point. These are colloquially known as "classical" and the "one-loop" piece of the partition function respectively.[5]

Given that the expansion around $t$ suppresses all dynamic field configurations with power greater than two, the one-loop piece is usually able to be computed exactly either by simple Gaussian integration or by the use of index theorem methods from

[4] Typically this can be a combination of Lorentz, scale and $R$-symmetry transformations. See [57] for a nice discussion. This would require that $V[\varphi]$ be a scalar under these symmetries.

[5] Note that we can also have non-perturbative contributions to the partition function that one should make sure are accounted for.

cohomology.

Our deformed path integral is then able to be written as

$$Z(t) = \int \mathcal{D}\varphi_0 e^{-S[\varphi_0]} \frac{1}{\text{SDet}\left(\mathcal{Q}V\right)^{(2)}|_{\varphi_0}} , \tag{2.66}$$

where the superdeterminant is the ratio of of bosonic and fermionic determinants.

Note that there is a somewhat canonical choice for the deformation term in Eq. (2.62). It is normally given by

$$V[\varphi] = \sum_{\psi} \left(\mathcal{Q}\psi\right)^{\dagger} \psi , \tag{2.67}$$

where the sum is over all fermions in the theory. If this bosonic part of $\mathcal{Q}V[\varphi]$ is positive-semi-definite along the contour and $\delta_B V[\varphi] = 0$ then the fixed points are simply when $\mathcal{Q}\psi = 0$.

### 2.3.1 Localisation in 3d

We now proceed with an explicit demonstration of this principle. Specifically we will derive the partition function for a 3d $\mathcal{N} = 2$ vector multiplet on the round $\mathbb{S}^3$ with unit radius in pure Chern-Simons theory, following [55].

The action is given by

$$S = \int \mathrm{d}^3x\sqrt{g}\ \text{Tr}\left[\epsilon^{\mu\nu\rho}\left(A_\mu\partial_\nu A_\rho + \frac{2i}{3}A_\mu A_\nu A_\rho\right) - \lambda^\dagger\lambda + 2D\sigma\right] , \tag{2.68}$$

and is invariant under the supersymmetry transformations

$$\begin{aligned}
\delta A_\mu &= \frac{i}{2}(\eta^\dagger\gamma_\mu\lambda - \lambda^\dagger\gamma_\mu\epsilon) , \\
\delta\sigma &= -\frac{1}{2}(\eta^\dagger\lambda + \lambda^\dagger\epsilon) , \\
\delta D &= \frac{i}{2}(\eta^\dagger\gamma^\mu(\mathrm{D}_\mu\lambda) - (\mathrm{D}_\mu\lambda^\dagger)\gamma^\mu\epsilon) - \frac{i}{2}(\eta^\dagger[\lambda,\sigma] - [\lambda^\dagger,\sigma]\epsilon) \\
&\qquad + \frac{i}{6}(\nabla_\mu\eta^\dagger\gamma^\mu\lambda - \lambda^\dagger\gamma^\mu\nabla_\mu\epsilon) , \\
\delta\lambda &= (-\frac{1}{2}\gamma^{\mu\nu}F_{\mu\nu} - D + i\gamma^\mu\mathrm{D}_\mu\sigma)\epsilon + \frac{2i}{3}\sigma\gamma^\mu\nabla_\mu\epsilon , \\
\delta\lambda^\dagger &= \eta^\dagger(\frac{1}{2}\gamma^{\mu\nu}F_{\mu\nu} - D - i\gamma^\mu\mathrm{D}_\mu\sigma) - \frac{2i}{3}\sigma\nabla_\mu\eta^\dagger\gamma^\mu ,
\end{aligned} \tag{2.69}$$

where $\eta$ and $\epsilon$ are Killing spinors satisfying

$$\nabla_\mu\epsilon = \frac{i}{2}\gamma_\mu\epsilon . \tag{2.70}$$

We now specify the fermionic symmetry that we wish to localise with respect to. It is beneficial to choose the simplest symmetry possible while still constraining all fields in the deformed action. This can be achieved by simply setting $\eta = 0$.

The new supersymmetry variations are

$$\begin{aligned}
\mathcal{Q}A_\mu &= -\lambda^\dagger \gamma_\mu \epsilon \,, \\
\mathcal{Q}\sigma &= -\frac{1}{2}\lambda^\dagger \epsilon \,, \\
\mathcal{Q}D &= -\frac{i}{2}(\mathrm{D}_\mu \lambda^\dagger)\gamma^\mu \epsilon + \frac{i}{2}[\lambda^\dagger, \sigma]\epsilon - \frac{i}{6}\lambda^\dagger \gamma^\mu \nabla_\mu \epsilon \,, \\
\mathcal{Q}\lambda &= (-\frac{1}{2}\gamma^{\mu\nu}F_{\mu\nu} - D + i\gamma^\mu \mathrm{D}_\mu \sigma)\epsilon + \frac{2i}{3}\sigma\gamma^\mu \nabla_\mu \epsilon \,, \\
\mathcal{Q}\lambda^\dagger &= 0 \,.
\end{aligned} \tag{2.71}$$

It is clear that $\mathcal{Q}^2 = 0$ on all the bosonic fields, as required.

Given that we only have one fermion, our deformation is simply

$$V = \mathrm{Tr}'(\mathcal{Q}\lambda)^\dagger \lambda \,, \tag{2.72}$$

where the prime is to distinguish it from initial trace. After considerable algebra one can show that the bosonic and fermionic parts of $\mathcal{Q}V$ are

$$\begin{aligned}
\mathcal{Q}V\big|_{\mathrm{bos}} &= \mathrm{Tr}'(\mathcal{Q}\lambda)^\dagger \mathcal{Q}\lambda = \mathrm{Tr}'\left[\frac{1}{2}F_{\mu\nu}F^{\mu\nu} + \mathrm{D}^\mu \sigma \mathrm{D}_\mu \sigma + (D+\sigma)^2\right] \,, \\
\mathcal{Q}V\big|_{\mathrm{fer}} &= \mathrm{Tr}'\left(\mathcal{Q}(\mathcal{Q}\lambda)^\dagger\right)\lambda = \mathrm{Tr}'\left[i\lambda^\dagger \gamma^\mu \mathrm{D}_\mu \lambda + i[\lambda^\dagger, \sigma]\lambda - \frac{1}{2}\lambda^\dagger \lambda\right] \,.
\end{aligned} \tag{2.73}$$

Finding the saddle point amounts to finding the configuration where $\mathcal{Q}\lambda = 0$, and can be worked out to be

$$F_{\mu\nu} = 0 \,, \qquad \sigma = \sigma_0 = -D \,. \tag{2.74}$$

Therefore our classical part in (2.66) is calculated using

$$\begin{aligned}
S_{\mathrm{cl}}[\sigma_0] &= -2\int \mathrm{d}^3x\sqrt{g}\ \mathrm{Tr}(\sigma_0)^2 \\
&= -4\pi^2 \mathrm{Tr}(\sigma_0)^2 \,,
\end{aligned} \tag{2.75}$$

therefore

$$Z_{\mathrm{cl}}[\sigma_0] = e^{4\pi^2 \mathrm{Tr}(\sigma_0)^2} \,. \tag{2.76}$$

Note that one still needs to perform the integral over $\sigma_0$. Next we focus on the one-loop

determinant part. We expand the fields around their VEVs

$$\sigma = \sigma_0 + \frac{\sigma}{\sqrt{t}} \,, \quad D = -\sigma_0 + \frac{D}{\sqrt{t}} \,, \quad X = \frac{X}{\sqrt{t}} \,, \tag{2.77}$$

where $X$ represents all fields without VEVs. An interesting observation is that, once we do this, the kinetic term for the gauge field becomes effectively abelianised since in this expansion

$$F_{\mu\nu}F^{\mu\nu} = \frac{1}{t}(\partial^\mu A^\nu - \partial^\nu A^\mu)(\partial_\mu A_\nu - \partial_\nu A_\mu) + \mathcal{O}(t^{-3/2}) \,. \tag{2.78}$$

This breaks the gauge group to $\mathrm{U}(1)^{\mathrm{rank}}$, hence the colloquial term "Coulomb branch localisation". We will denote this diagonalised field strength as $F^{A\mu\nu}$.

Repeating this for all fields and keeping the leading terms in the $t \to \infty$ limit gives us the deformed action

$$\begin{aligned}
S_{\mathrm{bos}} &= \int \mathrm{d}^3x\sqrt{g}\ \mathrm{Tr}'\left[\frac{1}{2}F^{A\mu\nu}F^{A}{}_{\mu\nu} + \partial^\mu\sigma\partial_\mu\sigma + (D+\sigma)^2 - [A_\mu,\sigma_0][A^\mu,\sigma_0]\right] \,, \\
S_{\mathrm{fer}} &= \int \mathrm{d}^3x\sqrt{g}\ \mathrm{Tr}'\left[i\lambda^\dagger\gamma^\mu\nabla_\mu\lambda + i[\lambda^\dagger,\sigma_0]\lambda - \frac{1}{2}\lambda^\dagger\lambda\right] \,, \\
S_{\mathrm{gf}} &= \int \mathrm{d}^3x\sqrt{g}\ \mathrm{Tr}'\left[\partial^\mu\bar{c}\partial_\mu c + b\nabla^\mu A_\mu\right] \,,
\end{aligned} \tag{2.79}$$

where the last expression is simply a gauge fixing contribution. Since $D$ and $b$ only appear algebraically in the action we can integrate them out. When $\nabla^\mu A_\mu = 0$ it is possible to write $F^{A\mu\nu}F^{A}{}_{\mu\nu} = -2A^\mu\Delta A_\mu$ after integrating by parts, with $\Delta$ being the Laplacian on the $\mathbb{S}^3$.

The $\sigma$ and $c$ fields can be integrated out to give factors of $\det(-\Delta)^{-1/2}$ and $\det(-\Delta)$ respectively. To deal with the gauge field we need to split it into a divergenceless piece and a pure divergence piece $A_\mu = B_\mu + \partial_\mu\phi$; now $\nabla^\mu B_\mu = 0$ and the Lorenz condition becomes $\delta(\Delta\phi)$. This splits the measure into $[\mathcal{D}A_\mu] = [\mathcal{D}\partial_\mu\phi][\mathcal{D}B_\mu]$, and the kinetic term is easily shown to be $-A^\mu\Delta A_\mu = -B^\mu\Delta B_\mu - \partial^\mu\phi\Delta\partial_\mu\phi$.

A vector field that is pure divergence has a mode expansion on a $\mathbb{S}^3$ that is simply proportional to that of a scalar, specifically integrating out $\partial_\mu\phi$ contributes another factor of const $\times \det(-\Delta)^{-1/2}$ which cancels all other determinant factors.

What we are now left with is

$$S = \int \mathrm{d}^3x\sqrt{g}\ \mathrm{Tr}'\left[-B^\mu\Delta B_\mu - [B_\mu,\sigma_0]^2 + i\lambda^\dagger\gamma^\mu\nabla_\mu\lambda + i[\lambda^\dagger,\sigma_0]\lambda - \frac{1}{2}\lambda^\dagger\lambda\right] \,, \tag{2.80}$$

to evaluate

$$Z_{1-\mathrm{loop}}[\sigma_0] = \int [\mathcal{D}B_\mu][\mathcal{D}\lambda]e^{-S} \,. \tag{2.81}$$

Since we still have some gauge structure, we can decompose all fields using their representations under the adjoint. Namely, for any field $X$ we write it as $X = X^\alpha T_\alpha$,[6] where $\alpha$ runs over the roots and $T_\alpha$ is its corresponding generator. This also means that a commutator is $[X, \sigma_0] = \sum_\alpha \langle \alpha, \sigma_0 \rangle X^\alpha T_\alpha$, with $\langle \alpha, \sigma_0 \rangle$ the inner product in root space. The generators are normalised such that $\mathrm{Tr}'(X_\alpha X_\beta) = \delta_{\alpha+\beta}$. Using results from [66] one can trade the integral over all $[\mathcal{D}\sigma_0]$ to just the integral over components of $\sigma_0$ aligned with the Cartan sub-algebra, providing one introduces a Haar measure. Therefore

$$Z = \frac{1}{|W(\mathfrak{g})|} \int [\mathrm{d}\sigma_0] \left( \prod_\alpha \langle \alpha, \sigma_0 \rangle \right) Z_{\mathrm{cl}}[\sigma_0] Z_{1-\mathrm{loop}}[\sigma_0] \,, \tag{2.82}$$

with $[\mathrm{d}\sigma_0] = \prod_{a=1}^{\mathrm{rank}} \mathrm{d}\sigma_0^a$, $W(\mathfrak{g})$ the Weyl subalgebra and, for example in SU($N$)

$$\prod_\alpha \langle \alpha, \sigma_0 \rangle = \prod_{a \neq b} (\sigma_0^a - \sigma_0^b) \,. \tag{2.83}$$

With all this in mind, we have that

$$\begin{aligned} S = \int \mathrm{d}^3x \sqrt{g} \sum_\alpha \Big[ & B^{-\alpha\mu} \left( -\Delta + \langle \alpha, \sigma_0 \rangle^2 \right) B^\alpha{}_\mu \\ & + \lambda^\dagger_{-\alpha} \left( i\gamma^\mu \nabla_\mu + i\langle \alpha, \sigma_0 \rangle - \frac{1}{2} \right) \lambda_\alpha \Big] \,. \end{aligned} \tag{2.84}$$

On the round $\mathbb{S}^3$, the eigenvalues of the Laplacian acting on a divergenceless vector are $(\ell + 1)$ with degeneracy $2\ell(\ell + 2)$, and for the fermion it is $\pm(\ell + 1/2)$ with the same degeneracy. Here $\ell \in \mathbb{Z}_+$. Therefore

$$\begin{aligned} \det(\text{bosons}) &= \prod_\alpha \prod_{\ell=1}^\infty ((\ell+1)^2 + \langle \alpha, \sigma_0 \rangle^2) \,, \\ \det(\text{fermions}) &= \prod_\alpha \prod_{\ell=1}^\infty \left( \pm \left( \ell + \frac{1}{2} \right) + i\langle \alpha, \sigma_0 \rangle + \frac{1}{2} \right) \,. \end{aligned} \tag{2.85}$$

After some creative relabelling of indices and algebraic manipulation, one can finally write

$$Z_{1-\mathrm{loop}}[\sigma_0] = \prod_\alpha \frac{2 \sinh \pi \langle \alpha, \sigma_0 \rangle}{\langle \alpha, \sigma_0 \rangle} \,, \tag{2.86}$$

[6] Note that this decomposition does not include the alignment with the Cartan subalgebra, for which the root vector is zero. To get the correct Cartan factors, one should carefully put them back in.

through the identity

$$\sinh(\pi z) = \pi z \prod_{\ell=1}^{\infty} \left(1 + \frac{z^2}{\ell^2}\right) \ . \tag{2.87}$$

Therefore all in all we have

$$Z = \frac{1}{|W(\mathfrak{g})|} \int \left( \prod_{a=1}^{\text{rank}} \mathrm{d}\sigma_0^a \, e^{-4\pi^2(\sigma_0^a)^2} \right) \prod_{\alpha} 2\sinh \pi \langle \alpha, \sigma_0 \rangle \ . \tag{2.88}$$

Note that, if we had started with 3d sYM as the kinetic term, there would be no classical contribution since the saddle point for the original action is zero.

These calculations were repeated for the squashed $\mathbb{S}^3$ in [57, 67] for the vector multiplet and chiral multiplet. The results are

$$\begin{aligned} Z_{\text{vec}}^{\mathcal{N}=2}(\lambda) &= \prod_{\alpha \in \text{Adj}} \widehat{\Gamma}_h \left( \langle \alpha, \sigma_0 \rangle | \omega_1, \omega_2 \right)^{-1} \\ &= \widehat{\Gamma}_h \left( 0 | \omega_1, \omega_2 \right)^{-\text{rank}(\mathfrak{g})} \prod_{\alpha \in \Delta} \widehat{\Gamma}_h \left( \langle \alpha, \sigma_0 \rangle | \omega_1, \omega_2 \right)^{-1} \ , \\ Z_{\text{chi}}^{\mathcal{N}=2}(\lambda, r) &= \prod_{\alpha \in \mathcal{R}} \Gamma_h \left( r\omega_+ - \langle \alpha, \sigma_0 \rangle | \omega_1, \omega_2 \right) \ , \end{aligned} \tag{2.89}$$

where $\Delta$ are the roots and $\Gamma_h$ is defined in Appendix A with the squashing parameters $\omega_1$ and $\omega_2$ of the $\mathbb{S}^3$. These functions will be important in Chapter 5, and thus we will discuss them there.

## 2.4 The Refined Topological Vertex

Another particularly useful tool for computing partition functions of theories in four and above dimensions is the refined topological vertex formalism [68]. Strictly speaking, the result that one obtains with this method is a partition function on the $\Omega$-background, as defined in [52, 69]. Namely, on the manifold $\mathbb{R}^4_{\epsilon_1,\epsilon_2} \times \mathbb{S}^1_\beta$; with the option to combine copies of this partition function to obtain ones on $\mathbb{S}^4_{\epsilon_1,\epsilon_2} \times \mathbb{S}^1_\beta$ and $\mathbb{CP}^2 \times \mathbb{S}^1_\beta$; *cf.* [70, 71]

While this technique might seem inherently restrictive in its choice of manifolds, it is advantageous in other respects. Firstly, it produces the perturbative and non-perturbative parts of a partition function. Secondly, one can obtain partition functions for theories that lack a Lagrangian description, see for example [72–77]. One simply needs to identify the $(p, q)$ 5-brane configuration whose low energy limit yields the field theory that we desire, then one maps the configuration to the dual toric diagram. From there all that is needed is to follow the algorithmic process of the refined topological vertex, which we enumerate here.

For a comprehensive review of the theory behind the refined topological vertex, we

refer the reader to the previously cited references, in particular [72]; here we simply focus on its application as a means for computing partition functions.

The $\Omega$-background parameters $\mathfrak{q}$ and $\mathfrak{t}$ by

$$\mathfrak{q} = e^{-\beta\epsilon_1} , \qquad \mathfrak{t} = e^{\beta\epsilon_2} , \tag{2.90}$$

where the $\beta$ is the radius of the circle $\mathbb{S}_\beta$. Other Greek letters are reserved for partitions of natural numbers, e.g. $\lambda$ with $\lambda_1 \geq \lambda_2 \geq \ldots \geq \lambda_{l(\lambda)} > 0$, where $l(\lambda)$ denotes the length of the partition. Each partition can be represented as a Young diagram, with the coordinates $(i, j)$ identifying a box in a given diagram. We have that $(i, j) \in \{(i, j)|i = 1, \ldots, l(\lambda); j = 1, \ldots, \lambda_i\}$, so the number of boxes in the $i^{\text{th}}$ column is $\lambda_i$. It is also useful to define the following quantities

$$|\lambda| = \sum_{(i,j)\in\lambda}^{l(\lambda)} 1 = \sum_{i=1}^{l(\lambda)} \lambda_i , \qquad \|\lambda\|^2 = \sum_{(i,j)\in\lambda} \lambda_i = \sum_{i=1}^{l(\lambda)} \lambda_i^2 , \tag{2.91}$$

as well as the transposed Young diagram $\lambda^t$. These are to be used as data that label the refined topological vertex.

Each refined topological vertex consists of three directed edges emanating from the same point. The edges either all point outwards or inwards, forming two-vectors $\vec{v}_{1,2,3}$ which satisfy $\sum_{i=1}^3 \vec{v}_i = 0$ and $\vec{v}_i \wedge \vec{v}_{i+1} := v_i^1 v_{i+1}^2 - v_i^2 v_{i+1}^1 = -1$. Upon picking a "preferred direction"—this will be indicated in our diagrams by a double red line—the basic vertices can be glued together in a unique fashion (outgoing to incoming edges and vice-versa) to form a dual-toric diagram. A chain of dualities relates this geometry to a IIB 5-brane web represented by the same diagram. To every connected edge one associates a partition: $\lambda$ when the arrow points out of a vertex and $\lambda^t$ when the arrow points into a vertex. External edges are assigned an empty partition, $\emptyset$.

The dual-toric diagram can be converted into a closed topological string amplitude (which in turn yields a 5d partition function on $\mathbb{R}^4_{\epsilon_1,\epsilon_2} \times \mathbb{S}^1_\beta$ in the field-theory limit) based on the following rules: To each vertex with outgoing edges we assign the vertex factor

$$C_{\lambda\mu\nu}(\mathfrak{t}, \mathfrak{q}) = \mathfrak{q}^{\frac{\|\mu\|^2+\|\nu\|^2}{2}} \mathfrak{t}^{-\frac{\|\mu^t\|}{2}} \tilde{Z}_\nu(\mathfrak{t}, \mathfrak{q}) \sum_\eta \left(\frac{\mathfrak{q}}{\mathfrak{t}}\right)^{\frac{|\eta|+|\lambda|-|\mu|}{2}} S_{\lambda^t/\eta}(\mathfrak{t}^{-\rho}\mathfrak{q}^{-\nu}) \times S_{\mu/\eta}(\mathfrak{q}^{-\rho}\mathfrak{t}^{-\nu^t}) , \tag{2.92}$$

such that $\nu$ is the partition associated with the edge vector aligned with the "preferred direction". If the edges are incoming then the partitions are simply replaced by their transposes. The $\widetilde{Z}$ functions are a specialisation of the MacDonald polynomials

$P_\nu(\mathbf{x};\mathfrak{t},\mathfrak{q})$ given by

$$\widetilde{Z}_\nu(\mathfrak{t},\mathfrak{q}) = \mathfrak{t}^{-\frac{\|\nu^t\|^2}{2}} P_\nu(\mathfrak{t}^{-\rho};\mathfrak{q},\mathfrak{t}) = \prod_{(i,j)\in\nu} \left(1-\mathfrak{t}^{\nu_j^t-i+1}\mathfrak{q}^{\nu_i-j}\right)^{-1} , \tag{2.93}$$

while the $S_{\lambda/\mu}(\mathbf{x})$ are the skew-Schur functions for the vector $\mathbf{x}=(x_1,\ldots)$. These have the properties that

$$S_{\mu/\emptyset}(\mathbf{x}) = S_\mu(\mathbf{x}) , \qquad S_{\emptyset/\mu}(\mathbf{x}) = \delta_{\mu,\emptyset} , \qquad S_{\emptyset/\emptyset}(\mathbf{x}) = 1 . \tag{2.94}$$

For a partition $\nu$, the vector $\mathfrak{t}^{-\rho}\mathfrak{q}^{-\nu}$ is

$$\mathfrak{t}^{-\rho}\mathfrak{q}^{-\nu} = (\mathfrak{t}^{\frac{1}{2}}\mathfrak{q}^{-\nu_1}, \mathfrak{t}^{\frac{3}{2}}\mathfrak{q}^{-\nu_2}, \mathfrak{t}^{\frac{5}{2}}\mathfrak{q}^{-\nu_3}, \ldots). \tag{2.95}$$

Internal edges in the dual-toric diagram correspond to Kähler moduli in the geometry, generically denoted by $Q$. More precisely, each internal edge is assigned an "edge factor" given by

$$\text{edge factor} = (-Q)^{|\lambda|} \times \text{framing factor} . \tag{2.96}$$

The "framing factor" is determined as follows: After glueing two vertices together, one can assign to each connected edge vector $\vec{v}$ an incoming and outgoing external vector $\vec{v}_{in,out}$, such that $\vec{v}_{in}\cdot\vec{v}_{out} > 0$. External-edge vectors with $\vec{v}_{in}\wedge\vec{v}_{out}\neq 0$ will have non-trivial 'framing factors'. Since we do not deal with framing factors in this thesis, we defer this discussion to [72].

Equipped with the above definitions, we can finally write the Topological string partition function with $M$ internal edges as

$$Z = \sum_{\lambda^1,\ldots,\lambda^M} \prod_{\text{edges}} \text{edge factor} \prod_{\text{vertices}} \text{vertex factor} . \tag{2.97}$$

### 2.4.1 Deriving the 4d Partition Function

In this part we review the computation of the topological amplitude for the basic building block of our Coulomb-branch partition functions, the "strip geometry". We then use this to derive the relevant 4d results that we need later in Chapter 4. Specifically, we will derive the partition function for the 4d $\mathrm{U}(k)^N$ circular quiver theory. The dual toric diagram for the circular quiver theory that we will use in that chapter can be built using the blocks depicted in Fig. 1.

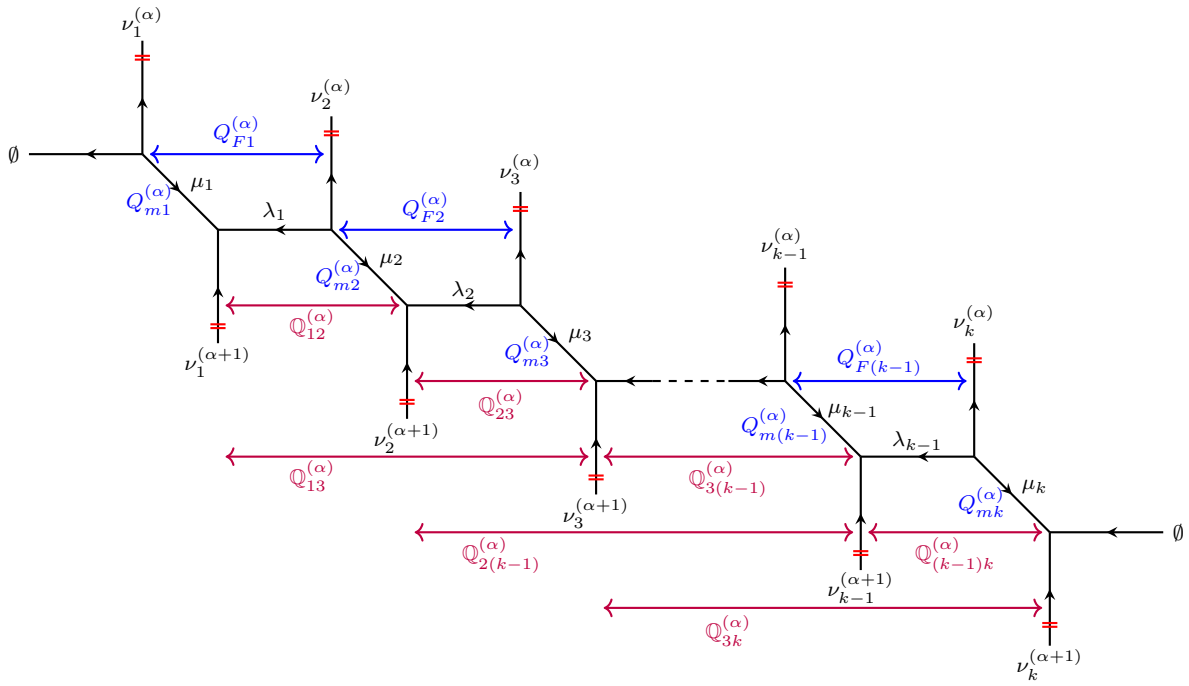


**Figure 1:** The "strip geometry" for the $\mathrm{U}(k)^N$ theory. The preferred direction is highlighted in red. There are no non-trivial framing factors.

### Derivation of the strip-geometry amplitude

The partition functions that we will be deriving in this thesis can all be constructed from a single building block, the "strip geometry". In view of using this for the $\mathrm{SU}(k)^N$ circular-quiver gauge theory, we assign Kähler moduli to each edge: For each vertical edge a $Q_g^{(\alpha)}$, each diagonal edge a $Q_{mb}^{(\alpha)}$ and each horizontal edge a $Q_{fb}^{(\alpha)}$, as well as associated partitions $\nu_b^{(\alpha)}$, $\mu_b^{(\alpha)}$ and $\lambda_b^{(\alpha)}$ respectively. The indices are $\alpha = \lfloor -\frac{N}{2} \rfloor + 1, \ldots, \lfloor \frac{N}{2} \rfloor$ with $N$ the number of nodes for the quiver and $b = 1, \ldots, k$ where $k$ is the rank of $\mathrm{U}(k)$.

The contribution to the partition function from this building block is given by

$$\mathcal{W}_k^{(\alpha)}\left(\nu^{(\alpha)}, \nu^{(\alpha+1)}\right) = \sum_{\vec{\mu},\vec{\lambda}} \prod_{b=1}^{k} \left(-Q_{mb}^{(\alpha)}\right)^{|\mu_b|} \left(-Q_{fb}^{(\alpha)}\right)^{|\lambda_b|} C_{\mu_b \lambda_{b-1} \nu_{(b,\alpha)}}(\mathfrak{t},\mathfrak{q}) C_{\mu_b^{\mathfrak{t}} \lambda_b^t \nu^t_{(b,\alpha+1)}}(\mathfrak{q},\mathfrak{t}) \,, \tag{2.98}$$

where we have denoted $\nu^{(\alpha)} = \{\nu_b^{(\alpha)}\}$ for a fixed $\alpha$ and $\lambda_0 = \lambda_k = \emptyset$. The corresponding dual-toric diagram is given in Fig. 1. Using the definitions (2.92), as well as the identity

$Q^{|\mu|-|\nu|}S_{\mu/\nu}(x) = S_{\mu/\nu}(Qx)$, we then have that

$$\begin{aligned}\mathcal{W}_k^{(\alpha)}(\nu^{(\alpha)},\nu^{(\alpha+1)}) &= \prod_{b=1}^{k}\mathfrak{q}^{\frac{\|\nu_b^{(\alpha)}\|^2}{2}}\widetilde{Z}_{\nu_b^{(\alpha)}}(\mathfrak{t},\mathfrak{q})\mathfrak{t}^{\frac{\|\nu_b^{(\alpha+1)t}\|^2}{2}}\widetilde{Z}_{\nu_b^{(\alpha+1)t}}(\mathfrak{q},\mathfrak{t})\\ &\times\sum_{\substack{\vec{\mu},\vec{\lambda}\\ \vec{\eta},\vec{\xi}}} S_{\mu_b^t/\eta_b}\left(-\frac{Q_{mb}^{(\alpha)}}{\widetilde{Q}_b^{(\alpha)}}\mathfrak{t}^{-\rho}\mathfrak{q}^{-\nu_b^{(\alpha)}}\right)S_{\lambda_{b-1}/\eta_b}\left(-\frac{\widetilde{Q}_b^{(\alpha)}}{Q_{mb}^{(\alpha)}}\mathfrak{q}^{-\rho-\frac{1}{2}}\mathfrak{t}^{-\nu_b^{(\alpha)t}+\frac{1}{2}}\right)\\ &\times S_{\mu_b/\xi_b}\left(-\widetilde{Q}_b^{(\alpha)}\mathfrak{q}^{-\rho}\mathfrak{t}^{-\nu_b^{(\alpha+1)}t}\right)S_{\lambda_b^t/\xi_b}\left(-(\widetilde{Q}_b^{(\alpha)})^{-1}\mathfrak{t}^{-\rho-\frac{1}{2}}\mathfrak{q}^{-\nu_b^{(\alpha+1)}+\frac{1}{2}}\right)\ ,\end{aligned}\tag{2.99}$$

with $\widetilde{Q}_b^{(\alpha)} := \prod_{k=1}^{b-1}Q_{mb}^{(\alpha)}Q_{fk}^{(\alpha)}$. The sum can be computed exactly with the help of the Cauchy relations

$$\begin{aligned}\sum_\lambda Q^{|\lambda|}S_{\lambda/\mu_1}(x)S_{\lambda^t/\mu_2}(y) &= \prod_{i,j=1}^{\infty}(1+Qx_iy_j)\sum_\lambda Q^{|\mu_1|+|\mu_2|-|\lambda|}S_{\mu_2^t/\lambda}(x)S_{\mu_1^t/\lambda^t}(y)\ ,\\ \sum_\lambda Q^{|\lambda|}S_{\lambda/\mu_1}(x)S_{\lambda/\mu_2}(y) &= \prod_{i,j=1}^{\infty}(1-Qx_iy_j)^{-1}\sum_\lambda Q^{|\mu_1|+|\mu_2|-|\lambda|}S_{\mu_2/\lambda}(x)S_{\mu_1/\lambda}(y)\ ,\end{aligned}\tag{2.100}$$

to obtain:

$$\begin{aligned}\mathcal{W}_k^{(\alpha)}\left(\nu^{(\alpha)},\nu^{(\alpha+1)}\right) &= \prod_{b=1}^{k}\mathfrak{q}^{\frac{\|\nu_b^{(\alpha)}\|^2}{2}}\widetilde{Z}_{\nu_b^{(\alpha)}}(\mathfrak{t},\mathfrak{q})\mathfrak{t}^{\frac{\|\nu_b^{(\alpha+1)t}\|^2}{2}}\widetilde{Z}_{\nu_b^{(\alpha+1)t}}(\mathfrak{q},\mathfrak{t})\\ &\times\prod_{i,j=1}^{\infty}\frac{\prod_{1\le b\le c\le k}\left(1-\mathbb{Q}_{bc}^{(\alpha)}Q_{mc}^{(\alpha)}\mathfrak{q}^{j-\frac{1}{2}-\nu_{b,i}^{(\alpha)}}\mathfrak{t}^{i-\frac{1}{2}-\nu_{c,j}^{(\alpha+1)t}}\right)}{\prod_{1\le b<c\le k}\left(1-\mathbb{Q}_{bc}^{(\alpha)}\mathfrak{q}^{i-1-\nu_{b,j}^{(\alpha)}}\mathfrak{t}^{j-\nu_{c,i}^{(\alpha)t}}\right)}\\ &\times\prod_{i,j=1}^{\infty}\frac{\prod_{1\le b<c\le k}\left(1-(Q_{mb}^{(\alpha)})^{-1}\mathbb{Q}_{bc}^{(\alpha)}\mathfrak{q}^{j-\frac{1}{2}-\nu_{b,i}^{(\alpha+1)}}\mathfrak{t}^{i-\frac{1}{2}-\nu_{c,j}^{(\alpha)t}}\right)}{\prod_{1\le b<c\le k}\left(1-(Q_{mb}^{(\alpha)})^{-1}\mathbb{Q}_{bc}^{(\alpha)}Q_{mc}^{(\alpha)}\mathfrak{q}^{i-\nu_{b,j}^{(\alpha+1)}}\mathfrak{t}^{j-1-\nu_{c,i}^{(\alpha+1)t}}\right)}\ ,\end{aligned}\tag{2.101}$$

where we have defined

$$\mathbb{Q}_{bc}^{(\alpha)} := \prod_{l=b}^{c-1}Q_{ml}^{(\alpha)}Q_{fl}^{(\alpha)} =: \prod_{l=b}^{c-1}Q_{Fl}^{(\alpha)}\ .\tag{2.102}$$

This is the refined version of the strip geometry found in [78,79]. Additionally, we need to normalise the building block using the MacMahon function

$$\mathcal{M}(Q;\mathfrak{t},\mathfrak{q}) = \prod_{i,j=1}^{\infty}(1-Q\mathfrak{t}^{i-1}\mathfrak{q}^j)^{-1}\ ,\qquad M(\mathfrak{t},\mathfrak{q}) = \mathcal{M}(1;\mathfrak{t},\mathfrak{q})\ ,\tag{2.103}$$

to give

$$\widehat{\mathcal{W}}_k^{(\alpha)}\left(\nu^{(\alpha)},\nu^{(\alpha+1)}\right)=\mathcal{M}(1;\mathfrak{t},\mathfrak{q})^k\mathcal{W}_k^{(\alpha)}\left(\nu^{(\alpha)},\nu^{(\alpha+1)}\right)\ . \tag{2.104}$$

This is a convention developed in [80] for correctly recovering the Cartan factors in the amplitude by adding one such factor for each closed face of the dual toric diagram.

### The 5d circular quiver

The Coulomb-branch partition function for the 5d uplift of theory depicted in Fig. 2 can be obtained by fusing the building blocks $\widehat{\mathcal{W}}_k^{(\alpha)}$ with the help of the glueing parameters $\sum_{\nu^{(\alpha)}}(-Q_g^{(\alpha)})^{\sum_{b=1}^k|\nu_b^{(\alpha)}|}$ and the cyclic identification of partitions $\nu_b^{(\lfloor N/2\rfloor+1)}=\nu_b^{(\lfloor -N/2\rfloor+1)}$.

Before we proceed, it is helpful to split the building block into one-loop and non-perturbative pieces. We define the former as $\widehat{\mathcal{W}}_k^{(\alpha)}(\emptyset,\emptyset)$. The latter is defined as

$$\mathcal{D}_k^{(\alpha)}\left(\nu^{(\alpha)},\nu^{(\alpha+1)}\right)=\frac{\widehat{\mathcal{W}}_k^{(\alpha)}\left(\nu^{(\alpha)},\nu^{(\alpha+1)}\right)}{\widehat{\mathcal{W}}_k^{(\alpha)}(\emptyset,\emptyset)}\ . \tag{2.105}$$

An additional simplification is afforded to us, since in both examples of interest we will be identifying the top and bottom vertical edges of the dual-toric diagram. For instance, for an $N$-noded circular quiver we identify the indices $\alpha=\lfloor -\frac{N}{2}\rfloor+1$ with $\alpha=\lfloor\frac{N}{2}\rfloor$. We can use this cyclicity alongside the identity

$$\tilde{Z}_\nu(\mathfrak{t},\mathfrak{q})\tilde{Z}_{\nu^t}(\mathfrak{q},\mathfrak{t})=\left(-\sqrt{\frac{\mathfrak{q}}{\mathfrak{t}}}\right)^{|\nu|}\mathfrak{t}^{-\frac{\|\nu^t\|^2}{2}}\mathfrak{q}^{-\frac{\|\nu\|^2}{2}}\mathcal{N}_{\nu\nu}(1;\mathfrak{t},\mathfrak{q})^{-1}\ , \tag{2.106}$$

to write the non-perturbative piece of the building block as

$$\begin{aligned}\mathcal{D}_k^{(\alpha)}&\left(\nu^{(\alpha)},\nu^{(\alpha+1)}\right)=\\&\left(-\sqrt{\frac{\mathfrak{q}}{\mathfrak{t}}}\right)^{\sum_{b=1}^k|\nu_b^{(\alpha)}|}\prod_{1\le b\le c\le k}\frac{\mathcal{N}_{\nu_c^{(\alpha+1)}\nu_b^{(\alpha)}}\left(\mathbb{Q}_{bc}^{(\alpha)}Q_{mc}^{(\alpha)}\sqrt{\frac{\mathfrak{t}}{\mathfrak{q}}}\right)}{\mathcal{N}_{\nu_c^{(\alpha+1)}\nu_b^{(\alpha+1)}}\left((Q_{mb}^{(\alpha)})^{-1}\mathbb{Q}_{bc}^{(\alpha)}Q_{mc}^{(\alpha)}\right)}\\&\times\prod_{1\le b<c\le k}\frac{\mathcal{N}_{\nu_c^{(\alpha)}\nu_b^{(\alpha+1)}}\left((Q_{mb}^{(\alpha)})^{-1}\mathbb{Q}_{bc}^{(\alpha)}\sqrt{\frac{\mathfrak{t}}{\mathfrak{q}}}\right)}{\mathcal{N}_{\nu_c^{(\alpha)}\nu_b^{(\alpha)}}\left(\mathbb{Q}_{bc}^{(\alpha)}\frac{\mathfrak{t}}{\mathfrak{q}}\right)}\ .\end{aligned} \tag{2.107}$$

In the above we have defined the function

$$\mathcal{N}_{\lambda\mu}(Q;\mathfrak{t},\mathfrak{q})=\prod_{i,j=1}^{\infty}\frac{1-Q\mathfrak{t}^{i-1-\lambda_j^t}\mathfrak{q}^{j-\mu_i}}{1-Q\mathfrak{t}^{i-1}\mathfrak{q}^j}$$

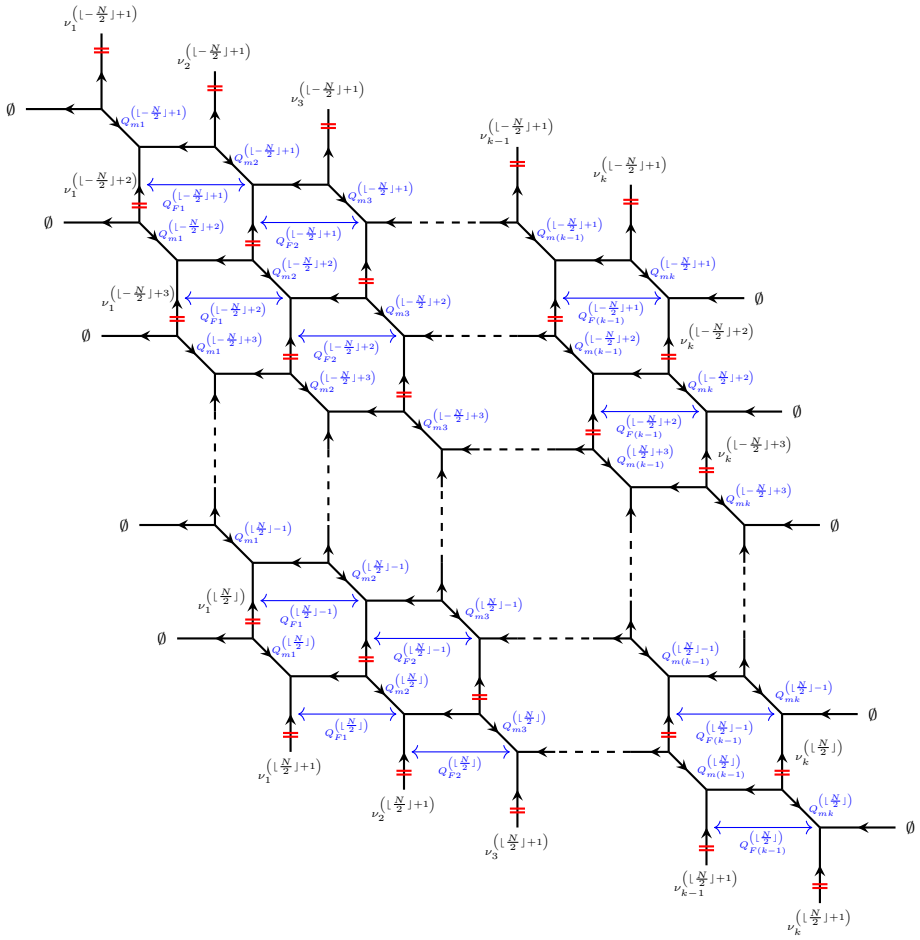

**Figure 2:** The dual-toric diagram for the $\mathrm{U}(k)^N$ theory. The preferred direction is along the compactified circle and is highlighted in red. There are no non-trivial framing factors. We close the quiver by identifying the partitions $\nu_b^{(\lfloor \frac{N}{2} \rfloor+1)} = \nu_b^{(\lfloor -\frac{N}{2} \rfloor+1)}$.

$$= \prod_{(i,j)\in\lambda} (1 - Q\mathfrak{q}^{\lambda_i - j+1}\mathfrak{t}^{\mu_j^t - i}) \prod_{(i,j)\in\mu} (1 - Q\mathfrak{q}^{-\mu_i + j}\mathfrak{t}^{-\lambda_j^t + i - 1}) \,. \quad (2.108)$$

whose properties can be found in App. A. We also adopt the shorthand $\mathcal{N}_{\lambda\mu}(Q) = \mathcal{N}_{\lambda\mu}(Q;\mathfrak{t},\mathfrak{q})$ since the second two arguments will always appear in that order.

The normalised one-loop piece is simply

$$\widehat{\mathcal{W}}_k^{(\alpha)}(\emptyset,\emptyset) = \prod_{1\le b\le c\le k} \frac{\mathcal{M}\left((Q_{mb}^{(\alpha)})^{-1}\mathbb{Q}_{bc}^{(\alpha)}Q_{mc}^{(\alpha)}\right)}{\mathcal{M}\left(\mathbb{Q}_{bc}^{(\alpha)}Q_{mc}^{(\alpha)}\sqrt{\frac{\mathfrak{t}}{\mathfrak{q}}}\right)} \prod_{1\le b<c\le k} \frac{\mathcal{M}\left(\mathbb{Q}_{bc}^{(\alpha)}\frac{\mathfrak{t}}{\mathfrak{q}}\right)}{\mathcal{M}\left((Q_{mb}^{(\alpha)})^{-1}\mathbb{Q}_{bc}^{(\alpha)}\sqrt{\frac{\mathfrak{t}}{\mathfrak{q}}}\right)} \,, \quad (2.109)$$

again with the shorthand $\mathcal{M}(Q) = \mathcal{M}(Q;\mathfrak{t},\mathfrak{q})$.

This results in the partition function

$$Z_{\text{5D}}^{\text{U}(k)^N} = \sum_{\nu} \prod_{\alpha=\lfloor -\frac{N}{2} \rfloor+1}^{\lfloor \frac{N}{2} \rfloor} \widehat{\mathcal{W}}_k^{(\alpha)}\left(\emptyset,\emptyset\right) (-Q_g^{(\alpha)})^{\sum_{b=1}^k |\nu_b^{(\alpha)}|} \mathcal{D}_k^{(\alpha)}\left(\nu^{(\alpha)}, \nu^{(\alpha+1)}\right) , \tag{2.110}$$

where $\nu = \{\nu_b^{(\alpha)}\}$. At this stage we can define the "physical parameters" (where $\beta$ is the radius of the $\mathbb{S}^1$)

$$\mathbf{q}_{(\alpha)} = Q_{gb}^{(\alpha)} \sqrt{Q_{mb}^{(\alpha)} Q_{mb}^{(\alpha+1)}} \quad \forall\, b\,, \quad Q_{Fb}^{(\alpha)} = Q_{fb}^{(\alpha)} Q_{mb}^{(\alpha)}, \quad \mathbb{Q}_{bc}^{(\alpha)} = \prod_{l=b}^{c-1} Q_{Fl}^{(\alpha)}\,, \tag{2.111}$$

which can be motivated by looking at distances between branes in the $(p,q)$ web depicted in Fig 2 and rephrasing them in terms of the Kähler parameters. The $\mathbf{q}_{(\alpha)}$ is interesting because it is independent of $\beta$, and is given by

$$\mathbf{q}_{(\alpha)} = e^{2\pi i \tau^{(\alpha)}}\,, \qquad \tau^{(\alpha)} = \frac{4\pi i}{g_{(\alpha)}^2} + \frac{\theta^{(\alpha)}}{8\pi^2}\,, \tag{2.112}$$

with $\tau^{(\alpha)}$ being the complexified coupling of the $\alpha^{th}$ gauge node.

We may explicitly write:

$$Z_{\text{5d}}^{\text{U}(k)^N} = Z_{\text{5d,1-loop}}^{\text{U}(k)^N} Z_{\text{5d,inst}}^{\text{U}(k)^N}\,, \tag{2.113}$$

with

$$\begin{aligned} Z_{\text{5d,inst}}^{\text{U}(k)^N} &= \sum_{\nu} \prod_{\alpha=\lfloor -\frac{N}{2} \rfloor+1}^{\lfloor \frac{N}{2} \rfloor} (-Q_g^{(\alpha)})^{\sum_{b=1}^k |\nu_b^{(\alpha)}|} \mathcal{D}_k^{(\alpha)}\left(\nu^{(\alpha)}, \nu^{(\alpha+1)}\right) \\ &= \sum_{\nu} \prod_{\alpha=\lfloor -\frac{N}{2} \rfloor+1}^{\lfloor \frac{N}{2} \rfloor} \left(\mathbf{q}_{(\alpha)} \left(Q_{mb}^{(\alpha)} Q_{mb}^{(\alpha+1)}\right)^{-\frac{1}{2}} \sqrt{\frac{\mathfrak{q}}{\mathfrak{t}}}\right)^{\sum_{b=1}^k |\nu_b^{(\alpha)}|} \\ &\quad \times \prod_{1\le b\le c\le k} \frac{\mathcal{N}_{\nu_c^{(\alpha+1)} \nu_b^{(\alpha)}}\left(\mathbb{Q}_{bc}^{(\alpha)} Q_{mc}^{(\alpha)} \sqrt{\frac{\mathfrak{t}}{\mathfrak{q}}}\right)}{\mathcal{N}_{\nu_c^{(\alpha+1)} \nu_b^{(\alpha+1)}}\left((Q_{mb}^{(\alpha)})^{-1} \mathbb{Q}_{bc}^{(\alpha)} Q_{mc}^{(\alpha)}\right)} \\ &\quad \times \prod_{1\le b< c\le k} \frac{\mathcal{N}_{\nu_c^{(\alpha)} \nu_b^{(\alpha+1)}}\left((Q_{mb}^{(\alpha)})^{-1} \mathbb{Q}_{bc}^{(\alpha)} \sqrt{\frac{\mathfrak{t}}{\mathfrak{q}}}\right)}{\mathcal{N}_{\nu_c^{(\alpha)} \nu_b^{(\alpha)}}\left(\mathbb{Q}_{bc}^{(\alpha)} \frac{\mathfrak{t}}{\mathfrak{q}}\right)}\,, \end{aligned} \tag{2.114}$$

and

$$\begin{aligned} Z^{\mathrm{U}(k)^N}_{\mathrm{5d,1\text{-}loop}} &= \prod_{\alpha=\lfloor -\frac{N}{2}\rfloor+1}^{\lfloor \frac{N}{2}\rfloor} \widehat{\mathcal{W}}^{(\alpha)}_k(\emptyset,\emptyset) \\ &= \prod_{\alpha=\lfloor -\frac{N}{2}\rfloor+1}^{\lfloor \frac{N}{2}\rfloor} \prod_{1\le b\le c\le k} \frac{\mathcal{M}\left(Q^{(\alpha)}_{mb})^{-1}\mathbb{Q}^{(\alpha)}_{bc}Q^{(\alpha)}_{mc}\right)}{\mathcal{M}\left(\mathbb{Q}^{(\alpha)}_{bc}Q^{(\alpha)}_{mc}\sqrt{\frac{\mathfrak{t}}{\mathfrak{q}}}\right)} \\ &\quad \times \prod_{1\le b<c\le k} \frac{\mathcal{M}\left(\mathbb{Q}^{(\alpha)}_{bc}\frac{\mathfrak{t}}{\mathfrak{q}}\right)}{\mathcal{M}\left((Q^{(\alpha)}_{mb})^{-1}\mathbb{Q}^{(\alpha)}_{bc}\sqrt{\frac{\mathfrak{t}}{\mathfrak{q}}}\right)} \,, \end{aligned} \tag{2.115}$$

We can now abuse the exchange relations detailed in App. A the MacMahon and Nekrasov functions, along with the cyclicity of the product over $\alpha$. First we convert the $\mathcal{N}_{\lambda\mu}$ functions into $\mathrm{N}^\beta_{\lambda\mu}$ for the instanton piece, resulting in

$$\begin{aligned} Z^{\mathrm{U}(k)^N}_{\mathrm{5d,inst}} = \sum_\nu \prod_{\alpha=\lfloor -\frac{N}{2}\rfloor+1}^{\lfloor \frac{N}{2}\rfloor} \mathfrak{q}_{(\alpha)}^{\sum_{b=1}^k |\nu_b^{(\alpha)}|} \prod_{1\le b\le c\le k} \frac{\mathrm{N}^\beta_{\nu_c^{(\alpha+1)}\nu_b^{(\alpha)}}\left(\mathbb{F}^{(\alpha)}_{bc}+m^{(\alpha)}_c+\epsilon_+\right)}{\mathrm{N}^\beta_{\nu_c^{(\alpha+1)}\nu_b^{(\alpha+1)}}\left(\mathbb{F}^{(\alpha)}_{bc}+m^{(\alpha)}_c-m^{(\alpha)}_b\right)} \\ \times \prod_{1\le b<c\le k} \frac{\mathrm{N}^\beta_{\nu_c^{(\alpha)}\nu_b^{(\alpha+1)}}\left(\mathbb{F}^{(\alpha)}_{bc}-m^{(\alpha)}_b+\epsilon_+\right)}{\mathrm{N}^\beta_{\nu_c^{(\alpha)}\nu_b^{(\alpha)}}\left(\mathbb{F}^{(\alpha)}_{bc}+2\epsilon_+\right)} \,, \end{aligned} \tag{2.116}$$

with $\epsilon_+ = \frac{\epsilon_1+\epsilon_2}{2}$ and

$$\begin{aligned} \mathrm{N}^\beta_{\lambda\mu}(m;\epsilon_1,\epsilon_2) &= \prod_{(i,j)\in\lambda} 2\sinh\frac{\beta}{2}\left[m+\epsilon_1(\lambda_i-j+1)+\epsilon_2(i-\mu^t_j)\right] \\ &\quad \times \prod_{(i,j)\in\mu} 2\sinh\frac{\beta}{2}\left[m+\epsilon_1(j-\mu_i)+\epsilon_2(\lambda^t_j-i+1)\right] \,. \end{aligned} \tag{2.117}$$

We also used the following definitions for our fugacities

$$\mathbb{Q}^{(\alpha)}_{bc} = e^{-\beta\mathbb{F}^{(\alpha)}_{bc}} \,, \qquad Q^{(\alpha)}_{mb} = e^{-\beta m^{(\alpha)}_b} \,. \tag{2.118}$$

Note that the above can be interpreted with the help of our diagram using the positions of the D5 branes, $a^{(\alpha)}_b$. Specifically

$$\mathbb{F}^{(\alpha)}_{bc} = a^{(\alpha)}_c - a^{(\alpha)}_b \,, \qquad m^{(\alpha)}_b = a^{(\alpha+1)}_b - a^{(\alpha)}_b + m^{(\alpha)}_{\mathrm{bif}} \,, \tag{2.119}$$

where the second variable is the distance between D5 branes over an NS5, with the bif standing for bifundamental, since these contributions will come from bifundamental

hypermultiplets. These will be expanded upon more in Chapter 4. This identification allows us to write

$$
\begin{aligned}
Z^{\mathrm{U}(k)^N}_{\mathrm{5d,inst}} &= \sum_{\nu} \prod_{\alpha=\lfloor -\frac{N}{2}\rfloor+1}^{\lfloor \frac{N}{2}\rfloor} \mathfrak{q}_{(\alpha)}^{\sum_{b=1}^{k}|\nu_b^{(\alpha)}|} \prod_{1\le b\le c\le k} \frac{\mathrm{N}^{\beta}_{\nu_c^{(\alpha+1)}\nu_b^{(\alpha)}}\left(a_c^{(\alpha+1)}-a_b^{(\alpha)}+m_{\mathrm{bif}}^{(\alpha)}-\epsilon_+\right)}{\mathrm{N}^{\beta}_{\nu_c^{(\alpha+1)}\nu_b^{(\alpha+1)}}\left(a_c^{(\alpha+1)}-a_b^{(\alpha+1)}\right)} \\
&\quad \times \prod_{1\le b<c\le k} \frac{\mathrm{N}^{\beta}_{\nu_c^{(\alpha)}\nu_b^{(\alpha+1)}}\left(a_c^{(\alpha)}-a_b^{(\alpha+1)}-m_{\mathrm{bif}}^{(\alpha)}-\epsilon_+\right)}{\mathrm{N}^{\beta}_{\nu_c^{(\alpha)}\nu_b^{(\alpha)}}\left(a_c^{(\alpha)}-a_b^{(\alpha)}-2\epsilon_+\right)} \\
&= \sum_{\nu} \prod_{\alpha=\lfloor -\frac{N}{2}\rfloor+1}^{\lfloor \frac{N}{2}\rfloor} \mathfrak{q}_{(\alpha)}^{\sum_{b=1}^{k}|\nu_b^{(\alpha)}|} \prod_{1\le b\le c\le k} \frac{\mathrm{N}^{\beta}_{\nu_c^{(\alpha+1)}\nu_b^{(\alpha)}}\left(a_c^{(\alpha+1)}-a_b^{(\alpha)}+m_{\mathrm{bif}}^{(\alpha)}-\epsilon_+\right)}{\mathrm{N}^{\beta}_{\nu_c^{(\alpha)}\nu_b^{(\alpha)}}\left(a_c^{(\alpha)}-a_b^{(\alpha)}\right)} \\
&\quad \times \prod_{1\le b<c\le k} \frac{\mathrm{N}^{\beta}_{\nu_c^{(\alpha)}\nu_b^{(\alpha+1)}}\left(a_c^{(\alpha)}-a_b^{(\alpha+1)}-m_{\mathrm{bif}}^{(\alpha)}-\epsilon_+\right)}{\mathrm{N}^{\beta}_{\nu_c^{(\alpha)}\nu_b^{(\alpha)}}\left(a_c^{(\alpha)}-a_b^{(\alpha)}-2\epsilon_+\right)} \,,
\end{aligned}
\tag{2.120}
$$

where we used the cyclicity of $\alpha$ in the denominator of the first line to arrive at the second equality. The exchange relation that we need to use is

$$
\mathrm{N}^{\beta}_{\lambda\mu}(-x;\epsilon_1,\epsilon_2) = (-1)^{|\mu|+|\lambda|}\mathrm{N}^{\beta}_{\mu\lambda}(x-\epsilon_1-\epsilon_2;\epsilon_1,\epsilon_2) \,, \tag{2.121}
$$

which we can apply to the last line giving

$$
\prod_{1\le b<c\le k} \frac{(-1)^{|\nu_c^{(\alpha)}|+|\nu_b^{(\alpha+1)}|}\mathrm{N}^{\beta}_{\nu_b^{(\alpha+1)}\nu_c^{(\alpha)}}\left(a_b^{(\alpha+1)}-a_c^{(\alpha)}+m_{\mathrm{bif}}^{(\alpha)}-\epsilon_+\right)}{(-1)^{|\nu_c^{(\alpha)}|+|\nu_b^{(\alpha)}|}\mathrm{N}^{\beta}_{\nu_b^{(\alpha)}\nu_c^{(\alpha)}}\left(a_b^{(\alpha)}-a_c^{(\alpha)}\right)} \,. \tag{2.122}
$$

The cyclicity of $\alpha$ will take care of the minus sign factors, and then we can relabel $b \leftrightarrow c$ to finally write

$$
Z^{\mathrm{U}(k)^N}_{\mathrm{5d,inst}} = \sum_{\nu}\prod_{\alpha} \mathfrak{q}_{(\alpha)}^{\sum_{b=1}^{k}|\nu_b^{(\alpha)}|} \prod_{b,c=1}^{k} \frac{\mathrm{N}^{\beta}_{\nu_c^{(\alpha+1)}\nu_b^{(\alpha)}}\left(a_c^{(\alpha+1)}-a_b^{(\alpha)}+m_{\mathrm{bif}}^{(\alpha)}-\epsilon_+\right)}{\mathrm{N}^{\beta}_{\nu_c^{(\alpha)}\nu_b^{(\alpha)}}\left(a_c^{(\alpha)}-a_b^{(\alpha)}\right)} \,. \tag{2.123}
$$

We recognise the denominator as coming from a 5d vector multiplet and the numerator coming from a bifundamental chiral multiplet [52].

For the perturbative piece we simply need to use the relation from App. A

$$
\mathcal{M}(Q^{-1}) = \left(-Q^{-1}\sqrt{\frac{\mathfrak{q}}{\mathfrak{t}}}\right)^{\frac{1}{12}} \mathcal{M}\left(Q\frac{\mathfrak{t}}{\mathfrak{q}}\right) \,, \tag{2.124}
$$

and do the relabelling trick to get

$$Z^{\mathrm{U}(k)^N}_{\text{5d,1-loop}} = \prod_{\alpha} \left( \mathfrak{m}^{(\alpha)} \sqrt{\frac{\mathfrak{t}}{\mathfrak{q}}} \right)^{\frac{1}{24}k(k-1)} \prod_{b,c=1}^{k} \frac{\mathcal{M}\left( e^{-\beta\left(a_c^{(\alpha)} - a_b^{(\alpha)}\right)} \right)}{\mathcal{M}\left( e^{-\beta\left(a_c^{(\alpha+1)} - a_b^{(\alpha)}\right)} \mathfrak{m}^{(\alpha)} \sqrt{\frac{\mathfrak{t}}{\mathfrak{q}}} \right)} , \tag{2.125}$$

where we used the cyclicity of $\alpha$ again and $\mathfrak{m}^{(\alpha)} = e^{-\beta m^{(\alpha)}_{\text{bif}}}$.

Before we take the 4d limit, we note that if we specify the number of nodes in the quiver to be $N = 1$, then we have a 5d $\mathcal{N} = 1^*$ theory. This is precisely one way of obtaining the 6d (2,0) index via [19, 20] and is what we use in Section 4 for the 6d partition function.

If we had chosen the preferred direction to be horizontal instead of vertical then the calculation would have yielded a equivalent partition function, rephrased in terms of sum over the Coulomb branch parameters of $\theta$ functions.

The elliptic structure comes from the fact that, with the chosen preferred direction to be horizontal, one can never use the Cauchy identities in (2.100) to permute an empty partition into the correct position in the skew-Schur functions. One needs to perform a recursion relation on the topological string amplitude and use the fact that the Kähler parameters satisfy $\lim_{n\to\infty} Q^n = 0$. This is a beautiful calculation and is detailed in Appendix B of [71], but since we do not use this form of the partition function we leave it as an exercise to the interested reader.

A similar calculation is done for the Little String Theories (LST) by identifying both sets of external edges depicted in Fig. 2, which just amounts to having the same partition on each side for each horizontal strip rather than the empty partition. This will yield a 6d (1,0) LST partition function and was performed in [81–83], and reproduced in [3] with the number of nodes equal to one.

### The 4d limit

The 4d $\mathcal{N} = 2$ $\mathrm{U}(k)^N$ circular-quiver result is obtained by reducing the 5d answer along the circle.

$$Z^{\mathrm{U}(k)^N}_{4D} = \lim_{\beta\to 0} Z^{\mathrm{U}(k)^N}_{5D} . \tag{2.126}$$

This operation can be straightforwardly performed, since having a Lagrangian description implies that the limit and sum over partitions commute [73]. Armed with details from App. A, this is a simple matter. In fact we can simply state the results of this

reduction

$$Z^{\mathrm{U}(k)^N}_{\mathrm{4d,inst}} = \sum_{\nu} \prod_{\alpha} \mathfrak{q}_{(\alpha)}^{\sum_{b=1}^{k} |\nu_b^{(\alpha)}|} \prod_{b,c=1}^{k} \frac{\mathrm{N}_{\nu_c^{(\alpha+1)} \nu_b^{(\alpha)}} \left( a_c^{(\alpha+1)} - a_b^{(\alpha)} + m_{\mathrm{bif}}^{(\alpha)} - \epsilon_+ \right)}{\mathrm{N}_{\nu_c^{(\alpha)} \nu_b^{(\alpha)}} \left( a_c^{(\alpha)} - a_b^{(\alpha)} \right)} , \tag{2.127}$$

and

$$Z^{\mathrm{U}(k)^N}_{\mathrm{4D,1\text{-}loop}} = \prod_{\alpha} \prod_{b,c=1}^{k} \frac{\Gamma_2 \left( a_c^{(\alpha+1)} - a_b^{(\alpha)} + m_{\mathrm{bif}}^{(\alpha)} + \epsilon_+ | \epsilon_1, \epsilon_2 \right)}{\Gamma_2 \left( a_c^{(\alpha)} - a_b^{(\alpha)} | \epsilon_1, \epsilon_2 \right)} , \tag{2.128}$$

where

$$\begin{aligned} \mathrm{N}_{\lambda\nu}(x; \epsilon_1, \epsilon_2) = & \prod_{(i,j) \in \lambda} \left( x + \epsilon_1 (\lambda_i - j + 1) + \epsilon_1 (i - \nu_j^t) \right) \\ & \times \prod_{(i,j) \in \nu} \left( x + \epsilon_1 (j - \nu_i) + \epsilon_2 (\lambda_j^t - i + 1) \right) . \end{aligned} \tag{2.129}$$

Combining (2.128) with (2.127) one gets the full 4d partition function which matches the results of [17, 69, 84]. Recall that, in this regime, $\epsilon_1 > 0$ and $\epsilon_2 < 0$.

We recognise the denominators of both the perturbative and instanton contributions as coming from a 4d vector multiplet; while the numerators come from bifundamental hypermultiplets. This concludes our introduction to the refined topological vertex.

# Chapter 3

# Algebraic Techniques for the Superconformal Index

This chapter is based on the paper [1]. Section 3.4.5 is based on unpublished work. There is an accompanying `python` package for the explicit enumeration of the various superconformal modules. Note that the package works for any representation of any superconformal algebra, and is reviewed in App. B.

## 3.1 Introduction and Summary

The basic building blocks of a superconformal field theory (SCFT) are the multiplets of local operators. By studying the unitary irreducible representations (UIRs) of the corresponding superconformal algebra (SCA) one can make broad statements about these theories, and their associated spectra.

These UIRs are of two general types: short representations and long representations. Short UIRs have primaries that are annihilated by certain non-trivial combinations of the Poincaré supercharges while long representations do not. Moreover, short representations can contribute to the superconformal index [39,40,42], can realise non-trivial structures like chiral algebras [24,85] and chiral rings that enjoy various non-renormalisation properties, can be used to study the structure of anomalies [86], and can describe the SUSY-preserving relevant and marginal deformations of SCFTs [87, 88]. Furthermore, by understanding how short representations recombine to form long representations one can hope, when sufficient symmetry is present, to bootstrap non-trivial correlation functions of local operators and perhaps even whole theories (see [15,24,89] for important recent progress on this front).

In this chapter, we perform the conceptually straightforward, but calculationally non-trivial, task of giving the level-by-level construction of all UIRs for the five-dimensional $\mathcal{N} = 1$ and six-dimensional (2,0) SCA. We also calculate the most general superconfor-

mal index associated with these multiplets. Our approach throughout is based on the presentation and conventions of [36, 42].[7]

We expect the results assembled here to be useful for more detailed studies of the many still-mysterious SCFTs in five and six dimensions (see, e.g., the theories described in the classic works [93–97] and the more recent literature [98, 99]) as well as for more general explorations of the space of SCFTs in these dimensions; *c.f.* [100–105] and their gravity duals [106–108].

The methodology we use to extract our results is rather general and well established [24, 36, 37, 42, 88, 109]. Indeed, we use a simple Verma-module construction to obtain all irreducible representations of the full SCA from irreducible representations of its maximal compact subalgebra. The UIRs are labelled by highest weights corresponding to superconformal primaries, from which all descendants are recovered by the action of momentum operators and supercharges. Hence, each UIR is uniquely identified by a string of quantum numbers, which characterises the superconformal primary state. As we described above, there are both long and short multiplets. The short multiplets have null states, which can be consistently deleted (hence the moniker, "short"). A complete classification of short UIRs can be obtained by imposing the condition of unitarity. For special values of the quantum numbers characterising short UIRs, additional null states can occur. The precise enumeration and analysis of all such possibilities using unitarity is an intricate task.

Once all null states have been identified, the Racah–Speiser (RS) algorithm simplifies the multiplet construction and clarifies the origin of equations of motion and conservation equations, whenever these are present.[8] The RS algorithm provides a prescription for the Clebsch–Gordan decomposition of states in representation space. Since representations of the maximal compact subalgebra are labelled by highest weights, these take values in the dominant Weyl chamber and the corresponding Dynkin labels are positive. After the Clebsch–Gordan decomposition, a representation in the sum with negative Dynkin labels lies outside the dominant Weyl chamber and can no longer label an irreducible representation. The RS prescription involves applying successive Weyl reflections, which bounce the weight vector off the boundaries of the Weyl chamber. Each time a Weyl reflection is performed, the multiplicity of the representation flips sign. Therefore, if a representation is labelled by negative Dynkin labels, it gets reflected back into the dominant Weyl chamber up to a sign. If it is labelled by a weight which lies exactly on the boundary of the dominant Weyl chamber, the state

[7] Note that a comprehensive classification of unitary irreducible representations (UIRs) for all SCAs was carried out in [36,38,42,90–92] and further discussed in [88]. However, in this section we supplement these works by giving the level-by-level construction of the corresponding multiplets as well as the resulting superconformal index contributions. Part of this work was already done in [24] for the 6d $(2,0)$ SCA (but we will provide the full set of multiplets and index contributions for this algebra).

[8] A concise summary of the Racah–Speiser algorithm can be found in App. B of [37] and in App. B.

has zero multiplicity and should be removed from the sum. A natural interpretation for representations with negative multiplicities is in terms of constraints imposed on operators inside the multiplet [37].

Since we study the 5d $\mathcal{N} = 1$ and 6d SCAs, our presentation is split into three corresponding sections, one for each algebra; all of which are largely self-contained. Each multiplet is labelled by the quantum numbers designating its superconformal primary and the shortening conditions the latter obeys. Some multiplets with special values for their quantum numbers admit a distinct physical interpretation; these are dealt with separately. We provide a detailed discussion for the case of the 5d $\mathcal{N} = 1$ SCA in Sec. 3.2, which extends naturally to 6d cases in Sec. 3.3 and Sec. 3.4. Special emphasis is put on identifying operator constraints, whenever present. Each section also contains expressions for recombination rules and indices for the superconformal multiplets under study.

The last section of the chapter is devoted to formally obtaining the superconformal index from the corresponding multiplet supercharacters.

## 3.2 Multiplets and Superconformal Indices for 5d $\mathcal{N} = 1$

We begin by providing a systematic analysis of all short multiplets admitted by the 5d $\mathcal{N} = 1$ SCA, $\mathfrak{f}(4)$. This involves a derivation of the superconformal unitarity bounds. By doing so we reproduce the results of [42]. We then proceed to write the complete multiplet spectra and compute their indices. Our notation and conventions for the 5d SCA are provided in Sec. 2.1.2. Unitarity for all these multiplets were proven in [1] by paying special attention to new developments in [110–112]. We omit the proofs in this thesis.

### 3.2.1 UIR Building with Auxiliary Verma Modules

The superconformal primaries of the 5d SCA $\mathfrak{f}(4)$ are designated $|\Delta; l_1, l_2; k\rangle$, where $\Delta$ is the conformal dimension, $l_1 \geq l_2 > 0$ are Lorentz symmetry quantum numbers in the orthogonal basis and $k$ is an $R$-symmetry label. Each primary is in one-to-one correspondence with a highest weight state of the maximal compact subalgebra $\mathfrak{so}(5) \oplus \mathfrak{so}(2) \oplus \mathfrak{su}(2)_R \subset \mathfrak{f}(4)$.[9] There are eight Poincaré and eight superconformal supercharges, denoted by $\mathcal{Q}_{\mathbf{A}a}$ and $\mathcal{S}_{\mathbf{A}a}$ respectively—where $a = 1, \cdots, 4$ is an $\mathfrak{so}(5)$ Lorentz spinor index and $\mathbf{A} = \mathbf{1}, \mathbf{2}$ an index of $\mathfrak{su}(2)_R$. One also has five momenta $P_\mu$ and special conformal generators $K_\mu$, where $\mu = 1, \cdots, 5$ is a Lorentz vector index. The superconformal primary is annihilated by all $\mathcal{S}_{\mathbf{A}a}$ and $K_\mu$. A basis for the representation

[9] The quantum numbers labelling the primary are eigenvalues for the Cartans of the maximal compact subalgebra in a particular basis.

space of $\mathfrak{f}(4)$ can be constructed by considering the following Verma module

$$\prod_{\mathbf{A},a}(\mathcal{Q}_{\mathbf{A}a})^{n_{\mathbf{A},a}}\prod_{\mu}P_{\mu}{}^{n_{\mu}}\,|\Delta;l_1,l_2;k\rangle^{hw} \tag{3.1}$$

for some ordering of operators,[10] where $n=\sum_{\mathbf{A}a}n_{\mathbf{A},a}$ and $\hat{n}=\sum_{\mu}n_{\mu}$ denote the "level" of a superconformal or conformal descendant respectively. In order to obtain UIRs, the requirement of unitarity needs to be imposed level-by-level on the Verma module. This leads to bounds on the conformal dimension $\Delta$.

There exists a natural basis for constructing the UIRs of the 5d SCA, in which particular combinations of supercharges map highest weights of the maximal compact subalgebra, $\mathfrak{so}(5)\oplus\mathfrak{su}(2)_R$, to other highest weights. This is particularly helpful since it allows for a far more compact way of writing out modules of superconformal symmetry. Furthermore, each state is a conformal primary, which means that we can implicitly take the infinite tower of derivatives along for the ride, and only deal with a module of conformal primaries which are highest weight. We define

$$\Lambda^a_{\mathbf{1}}:=\sum_{b=1}^{a}\mathcal{Q}_{\mathbf{1}b}\lambda^a_b \qquad \text{and} \qquad \Lambda^a_{\mathbf{2}}:=\sum_{b=1}^{a}\mathcal{Q}_{\mathbf{2}b}\lambda^a_b-\sum_{b=1}^{a}\mathcal{Q}_{\mathbf{1}b}\mathcal{R}^-\lambda^a_b\frac{1}{2\hat{\mathcal{R}}}\,. \tag{3.2}$$

The $\lambda^a_b$ are given by

$$\begin{aligned}
&\lambda^a_a=1\,,\quad \text{where } a \text{ is not summed over}\,,\\
&\lambda^2_1=-\mathcal{M}^-_2\frac{1}{2\mathcal{H}_2}\,,\\
&\lambda^3_1=\left(-\mathcal{M}^-_1\mathcal{M}^-_2+\mathcal{M}^-_2\mathcal{M}^-_1\frac{(\mathcal{H}_1-\mathcal{H}_2+1)}{(\mathcal{H}_1-\mathcal{H}_2)}\right)\frac{1}{4(\mathcal{H}_1+1)}\,,\\
&\lambda^3_2=-\mathcal{M}^-_1\frac{1}{2(\mathcal{H}_1-\mathcal{H}_2)}\,,\\
&\lambda^4_1=\Big(-\mathcal{M}^-_2\mathcal{M}^-_1\mathcal{M}^-_2\frac{(2+\mathcal{H}_1+5\mathcal{H}_2+4\mathcal{H}_1\mathcal{H}_2)}{(\mathcal{H}_1+1)\mathcal{H}_2}+\mathcal{M}^-_1(\mathcal{M}^-_2)^2\frac{(2\mathcal{H}_2+1)}{\mathcal{H}_2}\\
&\qquad\qquad+(\mathcal{M}^-_2)^2\mathcal{M}^-_1\frac{(2\mathcal{H}_1+3)}{(\mathcal{H}_1+1)}\Big)\frac{1}{8(\mathcal{H}_1+\mathcal{H}_2+1)}\,,\\
&\lambda^4_2=\left(-\mathcal{M}^-_2\mathcal{M}^-_1+\mathcal{M}^-_1\mathcal{M}^-_2\frac{(\mathcal{H}_2+1)}{\mathcal{H}_2}\right)\frac{1}{4(\mathcal{H}_1+1)}\,,\\
&\lambda^4_3=-\mathcal{M}^-_2\frac{1}{2\mathcal{H}_2}\,.
\end{aligned} \tag{3.3}$$

These coefficients can be uniquely determined by imposing the requirement that all Lorentz raising operators and R-symmetry raising operators annihilate $\Lambda^a_{\mathbf{A}}\,|\Delta;l_1,l_2;k\rangle^{hw}$.

[10] Any other ordering can be obtained using the superconformal algebra.

**Unitarity Bounds for $l_1 \geq l_2 > 0$**

In order to derive unitarity bounds for the superconformal descendent states, we need the norms of level-one states. These can be calculated using the above basis in (3.3) and the algebra relations in Sec 2.19. They are

$$
\begin{aligned}
||\Lambda^4_{\mathbf{1}} |\Delta; l_1, l_2; k\rangle^{hw}||^2 &= (\Delta - 3k - l_1 - l_2 - 4)\,\frac{(2l_1+3)\,(l_1+l_2+2)\,(2l_2+1)}{4\,(l_1+1)\,l_2\,(l_1+l_2+1)}\,, \\
||\Lambda^3_{\mathbf{1}} |\Delta; l_1, l_2; k\rangle^{hw}||^2 &= (\Delta - 3k - l_1 + l_2 - 3)\,\frac{(2l_1+3)\,(l_1-l_2+1)}{2\,(l_1+1)\,(l_1-l_2)}\,, \\
||\Lambda^2_{\mathbf{1}} |\Delta; l_1, l_2; k\rangle^{hw}||^2 &= (\Delta - 3k + l_1 - l_2 - 1)\frac{(2l_2+1)}{2l_2}\,, \\
||\Lambda^1_{\mathbf{1}} |\Delta; l_1, l_2; k\rangle^{hw}||^2 &= (\Delta - 3k + l_1 + l_2) \\
||\Lambda^4_{\mathbf{2}} |\Delta; l_1, l_2; k\rangle^{hw}||^2 &= (\Delta + 3k - l_1 - l_2 - 1)\frac{(2l_1+3)\,(l_1+l_2+2)\,(2l_2+1)}{4\,(l_1+1)\,l_2\,(l_1+l_2+1)}\Big(1+\frac{1}{2k}\Big)\,, \\
||\Lambda^3_{\mathbf{2}} |\Delta; l_1, l_2; k\rangle^{hw}||^2 &= (\Delta + 3k - l_1 + l_2)\frac{(2l_1+3)\,(l_1-l_2+1)}{2\,(l_1+1)\,(l_1-l_2)}\Big(1+\frac{1}{2k}\Big)\,, \\
||\Lambda^2_{\mathbf{2}} |\Delta; l_1, l_2; k\rangle^{hw}||^2 &= (\Delta + 3k + l_1 - l_2 + 2)\frac{(2l_2+1)}{2l_2}\Big(1+\frac{1}{2k}\Big)\,, \\
||\Lambda^1_{\mathbf{2}} |\Delta; l_1, l_2; k\rangle^{hw}||^2 &= (\Delta + 3k + l_1 + l_2 + 3)\Big(1+\frac{1}{2k}\Big)\,,
\end{aligned}
\tag{3.4}
$$

where we have normalised $\Big\||\Delta; l_1, l_2; k\rangle^{hw}\Big\|^2 = 1$. Observe that these norms are all of the form

$$
\begin{aligned}
\Big\|\Lambda^a_{\mathbf{A}} |\Delta; l_1, l_2; k\rangle^{hw}\Big\|^2 &= \Big(\Delta - f^a_{\mathbf{A}}(l_1, l_2, k)\Big) g^a_{\mathbf{A}}(l_1, l_2, k) \\
&:= B^a_{\mathbf{A}}(l_1, l_2, k) g^a_{\mathbf{A}}(l_1, l_2, k)\,,
\end{aligned}
\tag{3.5}
$$

where $g^a(l_1, l_2)$ is a positive-definite rational function in the fundamental Weyl chamber, $l_1 \geq l_2 > 0$. Unitarity demands that the norms are positive semi-definite and this imposes a bound on the conformal dimension via the functions $B^a_{\mathbf{A}}(l_1, l_2, k)$. The strongest bound on the conformal dimension is provided by $B^4_{\mathbf{A}}(l_1, l_2, k) \geq 0$. When $B^4_{\mathbf{A}}(l_1, l_2, k) > 0$ the UIR can be obtained using (3.1). The resulting multiplet is called "long" and labelled $\mathcal{L}$.

When $B^4_{\mathbf{A}}(l_1, l_2, k) = 0$ the state is null. This means that the primary obeys the "shortening condition" $\Lambda^4_{\mathbf{1}} |\Delta; l_1, l_2; k\rangle^{hw} = 0$. All such states can be consistently removed from the superconformal representation. The resulting multiplet is "short" and labelled as type $\mathcal{A}$. Since it can be reached from a long multiplet by continuously dialling $\Delta$ it is called a "regular" short multiplet. At higher levels, $\prod_{a=1}^n \Lambda^a_{\mathbf{1}} |\Delta; l_1, l_2; k\rangle^{hw}$ with $n > 1$, the norms involve products of $B^a_{\mathbf{A}}(l_1, l_2, k)$s and the strongest bound still comes from $B^4_{\mathbf{1}}(l_1, l_2, k) \geq 0$. Therefore, there will be no change to the bounds obtained

at level one.

We will shortly be interested in constructing the spectrum of UIRs using highest weight states, which are only sensitive to quantum numbers. For this purpose, it will be sufficient to use the following simplification: Instead of removing the null state $\Lambda^4_{\mathbf{1}}\left|\Delta;l_1,l_2;k\right\rangle^{hw}$ one can remove the supercharge with the same quantum numbers (that is $\mathcal{Q}_{\mathbf{14}}$) from the Verma module basis (3.1) and use the remaining supercharges to obtain the quantum numbers for the superconformal descendants of the highest weight. For this reason we will be identifying such "absent supercharges" for all short multiplets of the SCA [24, 42, 109, 113]. We emphasise that this is an *auxiliary* Verma-module construction which leads to the same spectrum in terms of highest weights. If one is interested in the precise form of the operators, the much more involved $\Lambda$-basis should be used.

### Unitarity Bounds for $l_1 > l_2 = 0$

We now turn to the special case with $l_1 > 0$, $l_2 = 0$. When $l_2 = 0$ the operator $\Lambda^4_{\mathbf{1}}$ is not well defined and we have to omit the level-one state $\Lambda^4_{\mathbf{1}}\left|\Delta;l_1,0;k\right\rangle^{hw}$ from our spectrum—and as a result $\mathcal{Q}_{\mathbf{14}}$ from the basis of auxiliary Verma-module generators (3.1). Naively, the strongest bound then arises from the norm of the state $\Lambda^3_{\mathbf{1}}\left|\Delta;l_1,0;k\right\rangle^{hw}$. However, the level-two state $\Lambda^3_{\mathbf{1}}\Lambda^4_{\mathbf{1}}\left|\Delta;l_1,0;k\right\rangle^{hw}$ is actually well defined, as can be explicitly checked. Its norm is proportional to

$$\begin{aligned}\left\|\Lambda^3_{\mathbf{1}}\Lambda^4_{\mathbf{1}}\left|\Delta;l_1,0;k\right\rangle^{hw}\right\|^2 &\propto (\Delta-3k-l_1-4)\,(\Delta-3k-l_1-3)\\ &= B^3_{\mathbf{1}}(l_1,0,k)B^4_{\mathbf{1}}(l_1,0,k)\end{aligned} \tag{3.6}$$

and the corresponding set of restrictions come from $B^4_{\mathbf{1}}(l_1,0,k)\geq 0$ or $B^3_{\mathbf{1}}(l_1,0,k)=0$.

When $B^4_{\mathbf{1}}(l_1,0,k)=0$ one recovers a regular short representation of type $\mathcal{A}$ and the null-state condition translates to the removal of $\mathcal{Q}_{\mathbf{13}}\mathcal{Q}_{\mathbf{14}}$ from the basis of Verma-module generators. Instead, one could also have $B^3_{\mathbf{1}}(l_1,0,k)=0$; this gives rise to the null state $\Lambda^3_{\mathbf{1}}\left|\Delta;l_1,0;k\right\rangle^{hw}$. Making that choice (and removing the corresponding vector $\mathcal{Q}_{\mathbf{13}}\left|\Delta;l_1,0;k\right\rangle^{hw}$ in addition to $\mathcal{Q}_{\mathbf{14}}\left|\Delta;l_1,0;k\right\rangle^{hw}$ from the auxiliary Verma module) leads to an "isolated" short multiplet of type $\mathcal{B}$.[11]

### Unitarity Bounds for $l_1 = l_2 = 0$

The same logic extends to $l_1 = l_2 = 0$: At level one the only well-defined state is $\Lambda^1_{\mathbf{1}}|\Delta;0,0;k\rangle^{hw}$. However, there exist well-defined states at levels two and four, obtained by $\Lambda^2_{\mathbf{1}}\Lambda^3_{\mathbf{1}}\left|\Delta;0,0;k\right\rangle^{hw}$, $\Lambda^1_{\mathbf{1}}\Lambda^2_{\mathbf{1}}\Lambda^3_{\mathbf{1}}\Lambda^4_{\mathbf{1}}\left|\Delta;0,0;k\right\rangle^{hw}$. These give rise to the conditions

[11] The name isolated is due to the fact that there are no unitary states in the gap between $B^3(l_1,0,k)=0$ and $B^4(l_1,0,k)\geq 0$.

$B^1_{\mathbf{1}}(0,0,k) = 0$, $B^3_{\mathbf{1}}(0,0,k) = 0$ or $B^4_{\mathbf{1}}(0,0,k) \geq 0$ and lead to the new set of isolated short multiplets $\mathcal{D}$. We summarise their properties and list all short multiplets for the 5d SCA in Table 2.

### Additional Unitarity Bounds

It is important to note that for $k = 0$ additional null states can be generated by acting on the existing ones with Lorentz and $R$-symmetry lowering operators.[12] This results in the removal of more combinations of supercharges from the set of Verma-module generators in (3.1). We will mention explicitly whenever this will be the case in our upcoming analysis.

Finally, there are supplementary unitarity restrictions and associated null states originating from conformal descendants. These have been analysed in detail in [36,109], the results of which we use. Saturating a conformal bound results in a "momentum-null" state, where the corresponding shortening condition is an operator constraint involving momentum analogues of the superconformal $\Lambda$s [109]. In that reference, a prescription is given for removing the associated states, $P_\mu \, |\Delta; l_1, l_2; k\rangle^{hw}$, from the auxiliary Verma-module construction, again in analogy with the superconformal procedure.[13] However, we will choose not to exclude any momenta from the basis of Verma-module generators (3.1). After using the RS algorithm this choice will allow us to explicitly recover highest weight states corresponding to the operator constraints from the general multiplet structure.

One can combine the conformal and superconformal bounds to predict that operator constraints will appear in the following short multiplets:

$$\mathcal{B}[d_1, 0; 0] \, , \quad \mathcal{D}[0, 0; \{1, 2\}] \, . \tag{3.7}$$

The multiplet $\mathcal{D}[0,0;0]$ does not belong to this list as it is the vacuum.

### The Procedure

Based on the above ingredients, let us summarise our strategy for constructing the superconformal UIRs:

1. Begin with a superconformal primary and consider the highest weight component of the corresponding irreducible representation of the Lorentz and $R$-symmetry algebras.

[12] See e.g. the discussion in App. 6.2.1 of [24] in the context of the 6d (2,0) SCA.

[13] Note that this does not mean that all conformal descendants of a particular type should be removed from the set of local operators.

| Multiplet | Shortening Condition | Conformal Dimension |
|---|---|---|
| $\mathcal{A}[l_1, l_2; k]$ | $\Lambda_{\mathbf{1}}^4 \Psi = 0$ | $\Delta = 3k + l_1 + l_2 + 4$ |
| $\mathcal{A}[l_1, 0; k]$ | $\Lambda_{\mathbf{1}}^3 \Lambda_{\mathbf{1}}^4 \Psi = 0$ | $\Delta = 3k + l_1 + 4$ |
| $\mathcal{A}[0, 0; k]$ | $\Lambda_{\mathbf{1}}^1 \Lambda_{\mathbf{1}}^2 \Lambda_{\mathbf{1}}^3 \Lambda_{\mathbf{1}}^4 \Psi = 0$ | $\Delta = 3k + 4$ |
| $\mathcal{B}[l_1, 0; k]$ | $\Lambda_{\mathbf{1}}^3 \Psi = 0$ | $\Delta = 3k + l_1 + 3$ |
| $\mathcal{B}[0, 0; k]$ | $\Lambda_{\mathbf{1}}^2 \Lambda_{\mathbf{1}}^3 \Psi = 0$ | $\Delta = 3k + 3$ |
| $\mathcal{D}[0, 0; k]$ | $\Lambda_{\mathbf{1}}^1 \Psi = 0$ | $\Delta = 3k$ |

**Table 2:** A list of all short multiplets for the 5d $\mathcal{N} = 1$ SCA, along with the conformal dimension of the superconformal primary and the corresponding shortening condition. The $\Lambda_{\mathbf{1}}^a$ in the shortening conditions are defined in (3.2) and (3.3). The first of these multiplets ($\mathcal{A}$) is a regular short representation, whereas the rest ($\mathcal{B}, \mathcal{D}$) are isolated short representations. Here $\Psi$ denotes the superconformal primary state for each multiplet.

2. Determine all combinations of supercharges which need to be removed from the auxiliary Verma-module basis (3.1) due to null or ill-defined states.[14]

3. Use the remaining Verma-module generators to determine the highest weights for all descendant states. This may result in some of the quantum numbers labelling the highest weight state becoming negative.

4. Use the Racah–Speiser algorithm to recover a spectrum with only positive quantum numbers. This could result in some states being projected out, while others acquiring a "negative multiplicity". The latter can cancel out against other states with the same quantum numbers but positive multiplicity. Any remaining states with negative multiplicity can be interpreted as operator constraints. This conjectural identification follows [37] and is based on a large number of examples, but can be additionally supported using supercharacters; c.f. Sec. B.1.3.

The spectrum of a given superconformal multiplet can always be obtained following these steps. However, there also exist—and we will implement— case-specific alternative ways to map out the multiplet content. We will explicitly identify these occurrences when applicable. Particular care should be taken with the identification of the unitarity bounds in step 2, where one needs to explicitly calculate the norms of all well-defined, distinct (i.e. not related through commutation relations) products of $\Lambda$s.[15]

[14] We will occasionally use a simplified version of this step in our construction by listing and removing only a subset of supercharges associated with ill-defined states. This is possible because in all cases the remaining ones lead to zero-multiplicity states after the application of the RS algorithm. This is computationally much cheaper.

[15] For example, in our discussion of unitarity bounds for $l_1 = l_2 = 0$, $\Lambda_{\mathbf{1}}^3 |\Delta; 0, 0; k\rangle^{hw}$ and $\Lambda_{\mathbf{1}}^2 |\Delta; 0, 0; k\rangle^{hw}$ are individually ill defined, while $\Lambda_{\mathbf{1}}^2 \Lambda_{\mathbf{1}}^3 |\Delta; 0, 0; k\rangle^{hw}$ is not. This can in turn lead to the wrong identification of shortening conditions, since $||\Lambda_{\mathbf{1}}^2 \Lambda_{\mathbf{1}}^3 |\Delta; 0, 0; k\rangle^{hw}||^2 = B_{\mathbf{1}}^3(0, 0, k) B_{\mathbf{1}}^1(0, 0, k)$, whereas $||\Lambda_{\mathbf{1}}^1 \Lambda_{\mathbf{1}}^2 |\Delta; 0, 0; k\rangle^{hw}||^2 = B^2(0, 0, k) B^1(0, 0, k)$, with the first one leading to more stringent unitarity bounds.

### 3.2.2 5d $\mathcal{N}=1$ Multiplet Recombination Rules

For the purposes of listing the recombination rules as well as for explicitly constructing the multiplets, we will find it more convenient to switch to the Dynkin basis for the various quantum numbers. That is, we will use

$$d_1 = l_1 - l_2 \ , \quad d_2 = 2l_2 \ , \quad K = 2k \ . \tag{3.8}$$

Short multiplets can recombine to form long multiplets when the conformal dimension for the latter approaches the unitarity bound, that is when $\Delta + \epsilon \to \frac{3}{2}K + d_1 + d_2 + 4$. It can then be checked, using the results that we will present in the following sections, that

$$\begin{aligned}
\mathcal{L}[\Delta+\epsilon; d_1, d_2; K] &\xrightarrow{\epsilon\to 0} \mathcal{A}[d_1, d_2; K] \oplus \mathcal{A}[d_1, d_2 - 1; K+1] \ , \\
\mathcal{L}[\Delta+\epsilon; d_1, 0; K] &\xrightarrow{\epsilon\to 0} \mathcal{A}[d_1, 0; K] \oplus \mathcal{B}[d_1 - 1, 0; K+2] \ , \\
\mathcal{L}[\Delta+\epsilon; 0, 0; K] &\xrightarrow{\epsilon\to 0} \mathcal{A}[0, 0; K] \oplus \mathcal{D}[0, 0; K+4] \ .
\end{aligned} \tag{3.9}$$

The following multiplets do not appear in a recombination rule:

$$\begin{aligned}
&\mathcal{B}\left[d_1, 0; \{0, 1\}\right] \ , \\
&\mathcal{D}\left[0, 0; \{0, 1, 2, 3\}\right] \ .
\end{aligned} \tag{3.10}$$

### 3.2.3 The 5d $\mathcal{N}=1$ Superconformal Index

We define the superconformal index with respect to the supercharge $\mathcal{Q}_{\mathbf{14}}$, in accordance with [42, 114]. This is given by

$$\mathcal{I}(x, y) = \mathrm{Tr}_{\mathcal{H}}(-1)^F e^{-\beta\delta} x^{\frac{2}{3}\Delta + \frac{1}{3}(d_1+d_2)} y^{d_1} \ , \tag{3.11}$$

where making use of the spin-statistics theorem the fermion number is $F = d_2$ and the trace is over the Hilbert space of operators of the theory. The states that are counted by this index satisfy $\delta = 0$, where

$$\delta := \{\mathcal{Q}_{\mathbf{14}}, \mathcal{S}_{\mathbf{21}}\} = \Delta - \frac{3}{2}K - d_1 - d_2 \ . \tag{3.12}$$

It is easy to see that as a result long multiplets can never contribute to the index, since none of their states are annihilated by any supersymmetry generators. The charges $d_1$ and $\frac{2}{3}\Delta + \frac{1}{3}(d_1 + d_2)$ appearing in the exponents of (3.11) are eigenvalues for the generators commuting with $\mathcal{Q}_{\mathbf{14}}, \mathcal{S}_{\mathbf{21}}$ and consequently with $\delta$. In practice, this index can be explicitly evaluated as a supercharacter for each of the multiplets constructed below. A detailed construction of characters for superconformal representations is

reviewed in Section 3.5.

### 3.2.4 5d $\mathcal{N}=1$ Multiplets

#### Long Multiplets

We can now go ahead with the explicit construction of multiplets. Since long multiplets are not associated with any shortening conditions, we can proceed as per (3.1) acting with all supercharges and momenta on the superconformal primary to obtain the unitary superconformal representation.

We will choose to group the supercharges together as $Q=(\mathcal{Q}_{\mathbf{A}1},\mathcal{Q}_{\mathbf{A}2})$ and $\tilde{Q}=(\mathcal{Q}_{\mathbf{A}3},\mathcal{Q}_{\mathbf{A}4})$, purely for book-keeping purposes. The explicit quantum numbers of these supercharges are given by

$$\begin{aligned}
&\mathcal{Q}_{\mathbf{1}1}\sim(1)_{(0,1)}\,, && \mathcal{Q}_{\mathbf{1}2}\sim(1)_{(1,-1)}\,, && \mathcal{Q}_{\mathbf{1}3}\sim(1)_{(-1,1)}\,, && \mathcal{Q}_{\mathbf{1}4}\sim(1)_{(0,-1)}\,,\\
&\mathcal{Q}_{\mathbf{2}1}\sim(-1)_{(0,1)}\,, && \mathcal{Q}_{\mathbf{2}2}\sim(-1)_{(1,-1)}\,, && \mathcal{Q}_{\mathbf{2}3}\sim(-1)_{(-1,1)}\,, && \mathcal{Q}_{\mathbf{2}4}\sim(-1)_{(0,-1)}\,.
\end{aligned} \tag{3.13}$$

With this information in hand, it is straightforward to map out their action starting from a superconformal primary, labelled by $(K)_{(d_1,d_2)}$:

$$\begin{aligned}
(K)_{(d_1,d_2)} &\xrightarrow{Q} (K+1)_{(d_1,d_2+1),(d_1+1,d_2-1)}\,,\ (K-1)_{(d_1,d_2+1),(d_1+1,d_2-1)}\,,\\
&\xrightarrow{Q^2} (K+2)_{(d_1+1,d_2)}\,,\ (K)_{(d_1,d_2+2),(d_1+1,d_2)^2,(d_1+2,d_2-2)}\,,\ (K-2)_{(d_1+1,d_2)}\,,\\
&\xrightarrow{Q^3} (K+1)_{(d_1+1,d_2+1),(d_1+2,d_2-1)}\,,\ (K-1)_{(d_1+1,d_2+1),(d_1+2,d_2-1)}\,,\\
&\xrightarrow{Q^4} (K)_{(d_1+2,d_2)}\,,\\
(K)_{(d_1,d_2)} &\xrightarrow{\tilde{Q}} (K+1)_{(d_1,d_2-1),(d_1-1,d_2+1)}\,,\ (K-1)_{(d_1,d_2-1),(d_1-1,d_2+1)}\,,\\
&\xrightarrow{\tilde{Q}^2} (K+2)_{(d_1-1,d_2)}\,,\ (K)_{(d_1,d_2-2),(d_1-1,d_2)^2,(d_1-2,d_2+2)}\,,\ (K-2)_{(d_1-1,d_2)}\,,\\
&\xrightarrow{\tilde{Q}^3} (K+1)_{(d_1-1,d_2-1),(d_1-2,d_2+1)}\,,\ (K-1)_{(d_1-1,d_2-1),(d_1-2,d_2+1)}\,,\\
&\xrightarrow{\tilde{Q}^4} (K)_{(d_1-2,d_2)}\,,
\end{aligned} \tag{3.14}$$

where we have split the actions of $Q$ and $\tilde{Q}$ into two "chains". Since the Dynkin labels here are generic, there is no need to implement the RS algorithm. By definition, these multiplets do not contribute to the superconformal index. Should these quantum numbers become negative after specifying the superconformal primary then the algorithm would be required, but it is omitted here since the resulting multiplet would be large and unwieldy. The states are of course obtainable by using the package detailed in Appendix B.2.

### $\mathcal{A}$-type multiplets

Recall from Table 2 that $\mathcal{A}$-type multiplets obey three types of shortening conditions depending on the quantum numbers of the superconformal primary. These result in the removal of the following combinations of supercharges from the basis of Verma-module generators (3.1):[16]

$$\begin{aligned} \mathcal{A}[d_1,d_2;K]: &\quad \mathcal{Q}_{\mathbf{14}}\ , \\ \mathcal{A}[d_1,0;K]: &\quad \mathcal{Q}_{\mathbf{13}}\mathcal{Q}_{\mathbf{14}}\ , \\ \mathcal{A}[0,0;K]: &\quad \mathcal{Q}_{\mathbf{11}}\mathcal{Q}_{\mathbf{12}}\mathcal{Q}_{\mathbf{13}}\mathcal{Q}_{\mathbf{14}}\ . \end{aligned} \tag{3.15}$$

Let us consider the first case. On the one hand, acting with the allowed set of supercharges yields the same result as found in (3.14) for the $Q$-supercharge set. On the other, for the $\tilde{Q}$-supercharge set we have

$$\begin{aligned} (K)_{(d_1,d_2)} &\xrightarrow{\tilde{Q}} (K+1)_{(d_1-1,d_2+1)}\ ,\ (K-1)_{(d_1,d_2-1),(d_1-1,d_2+1)}\ , \\ &\xrightarrow{\tilde{Q}^2} (K)_{(d_1-2,d_2+2),(d_1-1,d_2)}\ ,\ (K-2)_{(d_1-1,d_2)}\ , \\ &\xrightarrow{\tilde{Q}^3} (K-1)_{(d_1-2,d_2+1)}\ . \end{aligned} \tag{3.16}$$

The two remaining cases with $d_2 = 0$ and $d_1 = d_2 = 0$ can be obtained by implementing the recipe at the end of Sec. 3.2.1, by e.g. first constructing all the states using the combinations of the $Q$-chain of Eq. (3.14) and $\tilde{Q}$-chain of (3.16) and then setting $d_2 = 0$. Applying the RS algorithm will produce some negative-multiplicity states, all of which cancel with positive-multiplicity states with the same quantum numbers. The remaining states comprise the spectrum of the $\mathcal{A}[d_1,0;K]$ multiplet and one can proceed analogously for $\mathcal{A}[0,0;K]$.

For $K = 0$ and $d_1, d_2$ generic the primary still lies above the unitarity bound for all conformal descendants and there are no momentum-null states. Moreover, there are additional ill-defined states, which translates into also removing $\mathcal{Q}_{\mathbf{24}}$, $\mathcal{Q}_{\mathbf{23}}\mathcal{Q}_{\mathbf{24}}$ and $\mathcal{Q}_{\mathbf{21}}\mathcal{Q}_{\mathbf{22}}\mathcal{Q}_{\mathbf{23}}\mathcal{Q}_{\mathbf{24}}$ from the construction of the respective multiplets for $d_1, d_2 > 0$, $d_2 = 0$ and $d_1 = d_2 = 0$ using the auxiliary Verma module. The resulting spectrum is no different from setting $K = 0$ and running the RS algorithm for $\mathfrak{su}(2)_R$.

As with the long multiplets, we choose not to include the explicit spectra of these multiplets in the main body, as they would be too large. Again, the states are obtainable by using the package detailed in Appendix B.

[16] Once again, we are using a Dynkin basis for the quantum numbers.

The index over the spectrum of all $\mathcal{A}$-type multiplets is given by

$$\mathcal{I}_{\mathcal{A}[d_1,d_2;K]}(x,y) = (-1)^{d_2+1}\frac{x^{d_1+d_2+K+4}}{(1-xy^{-1})(1-xy)}\chi_{d_1}(y)\ , \tag{3.17}$$

by appropriately tuning $d_1, d_2$ and $K$, including $d_2 = 0$ and $d_1 = d_2 = 0$, where we have used the $\mathfrak{su}(2)$ character for the spin-$\frac{l}{2}$ representation

$$\chi_l(y) = \frac{y^{l+1} - y^{-l-1}}{y - y^{-1}}\ . \tag{3.18}$$

One readily sees that (3.17) is compatible with the recombination rule (3.9):

$$\lim_{\epsilon\to 0}\mathcal{I}_{\mathcal{L}[\Delta+\epsilon;d_1,d_2;K]}(x,y) = \mathcal{I}_{\mathcal{A}[d_1,d_2;K]}(x,y) + \mathcal{I}_{\mathcal{A}[d_1,d_2-1;K+1]}(x,y) = 0\ . \tag{3.19}$$

### $\mathcal{B}$-type multiplets

For $\mathcal{B}$-type multiplets, the supercharges that need to be removed from the Verma-module basis (3.1) due to null states are

$$\begin{aligned} \mathcal{B}[d_1,0;K]:&\quad \mathcal{Q}_{\mathbf{13}}\ , \\ \mathcal{B}[0,0;K]:&\quad \mathcal{Q}_{\mathbf{12}}\mathcal{Q}_{\mathbf{13}}\ . \end{aligned} \tag{3.20}$$

Note that one should also remove $\mathcal{Q}_{\mathbf{14}}$ since the state $\Lambda^4_{\mathbf{1}}\Psi$ is ill defined for $d_2 = 0$. Acting on the primary—while keeping the quantum numbers generic—one has the same action as (3.14) for $Q$, while the $\tilde{Q}$-chain is

$$\begin{aligned} (K)_{(d_1,d_2)} &\xrightarrow{\tilde{Q}} (K-1)_{(d_1,d_2-1),(d_1-1,d_2+1)}\ , \\ &\xrightarrow{\tilde{Q}^2} (K-2)_{(d_1-1,d_2)}\ . \end{aligned} \tag{3.21}$$

We may then combine the action of these supercharges to construct the following grid; acting with $Q$ is captured by *southwest* motion on the diagram, while $\tilde{Q}$ by *southeast*

motion. This module is well defined for all $d_1 \geq 1$ values:

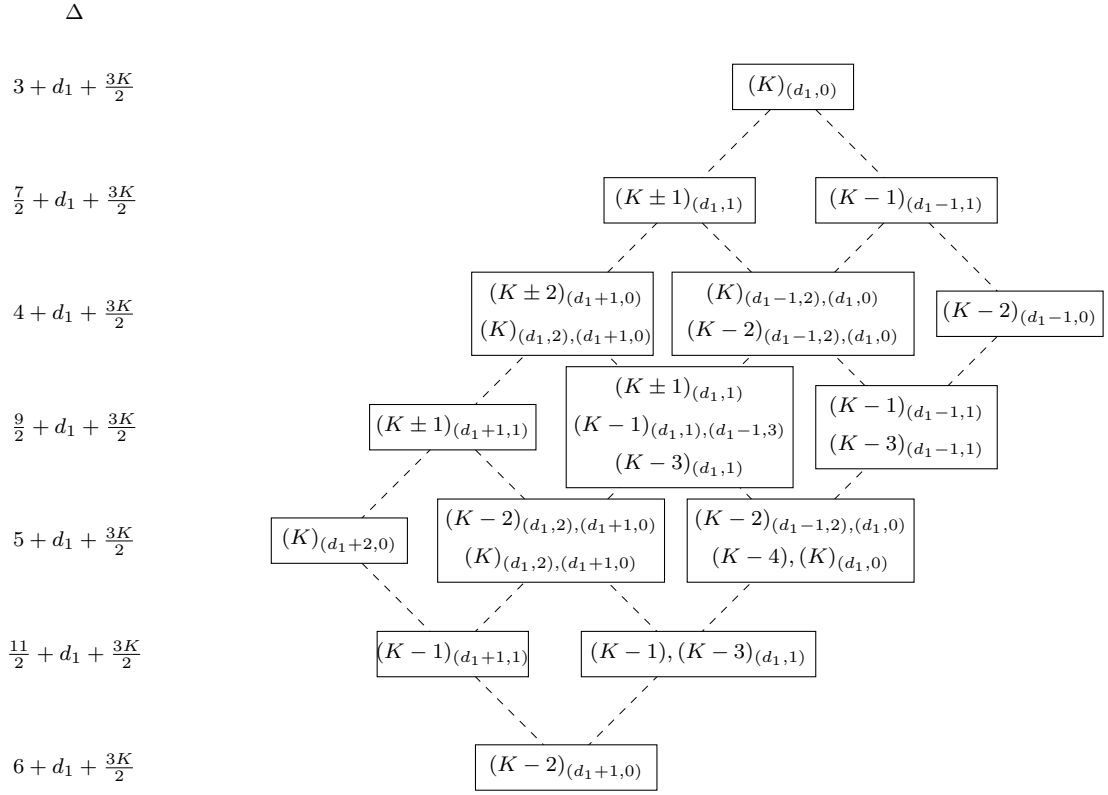


(3.22)

Let us next look at some special values of the $R$-symmetry quantum number. For $K = 1$ the states with values $(K-4)$ and $(K-3)$ are reflected to $-(1)$ and $-(0)$ respectively via the RS algorithm, where they subsequently cancel with other descendants with identical quantum numbers but non-negative multiplicity. The $(K-2)$ states are simply deleted as they lie on the boundary of the Weyl chamber for $K = 1$. Likewise if $K = 2$, the $(K-3)$ states are deleted and the $(K-4)$ state is reflected to $-(0)$ where it cancels against another state with non-negative multiplicity.

Following this reasoning, it quickly becomes obvious that only through setting $K = 0$ does one end up with negative multiplicities being present after cancellations, which we can observe from the last two levels of the module. In that case, the $(K-1)$ highest weights are deleted to leave the states $-[11/2 + d_1; d_1, 1; 1]$ and $-[6 + d_1; d_1 + 1, 0; 0]$. We will study this $\mathcal{B}[d_1, 0; 0]$ multiplet separately below.

The second type of $\mathcal{B}$-multiplet to consider is $\mathcal{B}[0, 0; K]$, for which one is instructed to remove from the Verma-module basis (3.1) the supercharge combinations $\mathcal{Q}_{\mathbf{12}}\mathcal{Q}_{\mathbf{13}}$.

The superconformal representation constructed using the remaining supercharges is

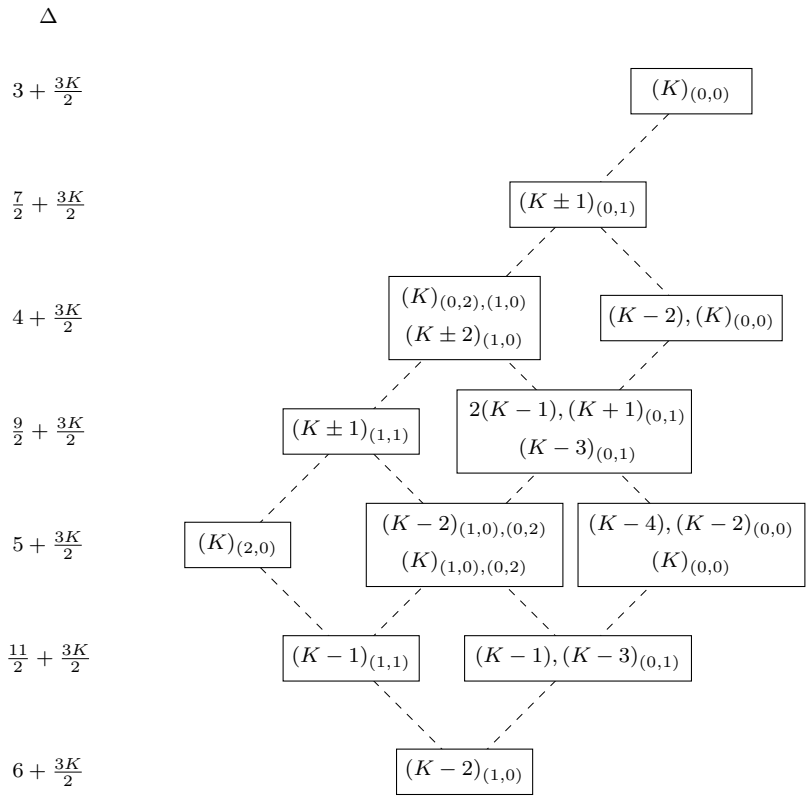


(3.23)

This UIR can also be obtained from $\mathcal{B}[d_1, 0; K]$ by setting $d_1 = 0$. The same arguments as in the $\mathcal{B}[d_1, 0; K]$ case can be applied to study the behaviour of the multiplet for concrete $K$ values. Again, we find that non-cancelling negative-multiplicity states only appear at $K = 0$.

The superconformal index for all values of $d_1$ and $K > 0$ is calculated to be

$$\mathcal{I}_{\mathcal{B}[d_1,0;K]}(x,y) = \frac{x^{d_1+K+3}}{(1-xy^{-1})(1-xy)}\chi_{d_1+1}(y) \ . \tag{3.24}$$

One observes that this satisfies the recombination rules (3.9):

$$\lim_{\epsilon\to 0}\mathcal{I}_{\mathcal{L}[\Delta+\epsilon;d_1,0;K]}(x,y) = \mathcal{I}_{\mathcal{A}[d_1,0;K]}(x,y) + \mathcal{I}_{\mathcal{B}[d_1-1,0;K+2]}(x,y) = 0 \ . \tag{3.25}$$

**Higher-Spin-Current Multiplets: $\mathcal{B}[d_1, 0; 0]$**

Let us now address the special case with $K = 0$. For $d_1 \neq 0$ this family of $\mathcal{B}$-type multiplets contains higher-spin currents and has a primary corresponding to the symmetric traceless representation of $\mathfrak{so}(5)$. One finds that $\mathcal{Q}_{\mathbf{A}3}$ and $\mathcal{Q}_{\mathbf{A}4}$ need to be removed from the Verma-module basis (3.1). Therefore the entire representation is built by just

acting on the superconformal primary with the set of $Q$s from (3.13) and is

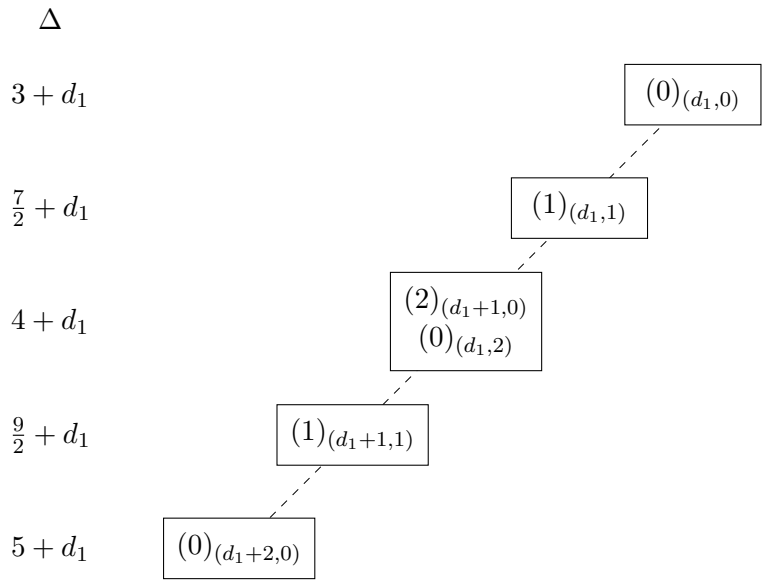


(3.26)

This result seems to contradict (3.7), which predicted the presence of operator constraints. However, note that the absent $\mathcal{Q}$s anticommute into $P_5$, which has therefore been implicitly removed from the Verma-module generators. This has the effect of projecting out states corresponding to operator constraints; we will henceforth refer to the remaining states as "reduced states". Note that, if one studies the conformal dimensions of the operators in this multiplet, $P_5$ is exactly the operator responsible for the conservation equation constraint detailed in [109].

The operator constraints can actually be restored—c.f. Sec. B.1— by utilising the following relationship between characters

$$\hat{\chi}[\Delta; d_1, d_2; K] = \chi[\Delta; d_1, d_2; K] - \chi[\Delta + 1; d_1 - 1, d_2; K] \,, \tag{3.27}$$

where $\Delta = 3 + d_1 + \frac{1}{2}d_2$. Here the $\hat{\chi}$ and $\chi$ correspond to taking a character of the superconformal representation without/with the $P_5$ respectively. It is clear that every operator in this multiplet can satisfy a conservation equation, in fact, if $d_1 > 0$, then every operator does. We can appropriately account for the negative contributions to

the RHS via negative-multiplicity states. The full multiplet can then be expressed as:

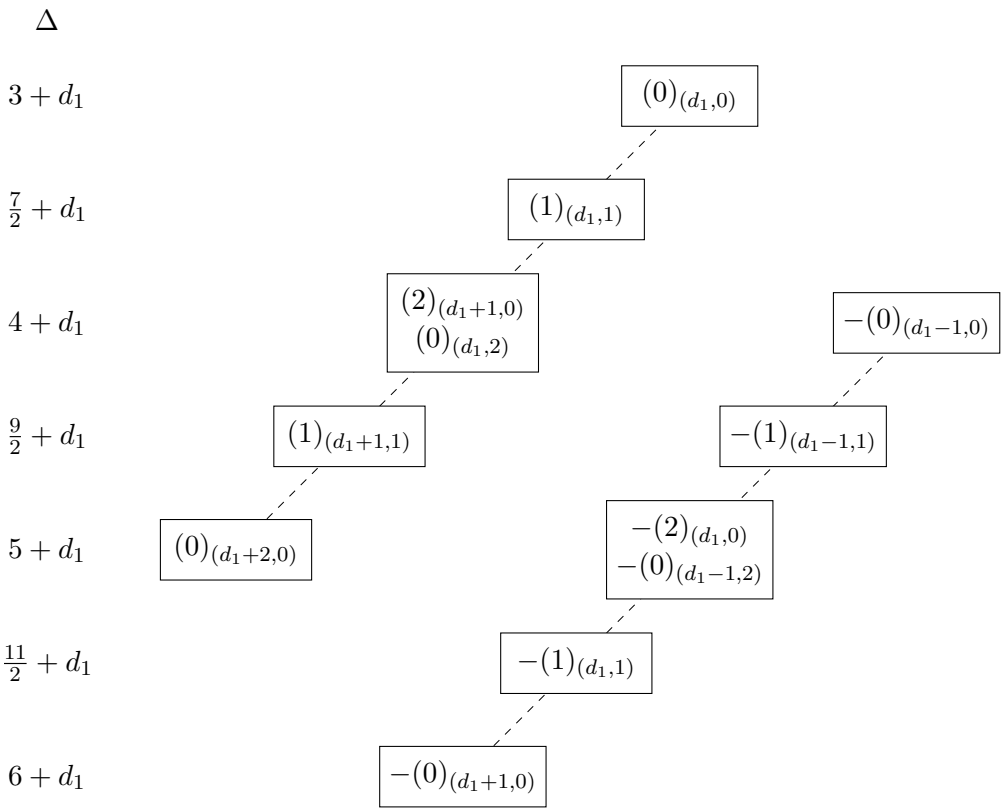


(3.28)

An example of the above $[3+d_1; d_1, 0; 0]$ primary is the operator

$$\mathcal{O}_{\mu_1\cdots\mu_{d_1}} = \epsilon_{\mathbf{AB}}\phi^{\mathbf{A}}\overset{\leftrightarrow}{\partial}_{\mu_1}\cdots\overset{\leftrightarrow}{\partial}_{\mu_{d_1}}\phi^{\mathbf{B}} \,, \tag{3.29}$$

where $\phi^A$ is a free hypermultiplet scalar. This object satisfies the generalised conservation equation

$$\partial^{\mu}\mathcal{O}_{\mu\mu_2\cdots\mu_{d_1-1}} = 0 \,, \tag{3.30}$$

which is identified with the state $-[4+d_1; d_1-1, 0; 0]$, which we need to remove, lest we over-count states in the multiplet.

It is interesting to point out that for $d_1 = 1$ the superconformal primary is an $R$-neutral $\Delta = 4$ conserved current, which is not itself a higher-spin current. The higher-spin currents are instead found as its descendants. This logic also shows that the commutator of the conserved charge, $\mathcal{T}$, associated with the primary has a non-vanishing commutator with the supercharges

$$[\mathcal{Q}_{\mathbf{11}}, \mathcal{T}] = \mathcal{T}'_{\mathbf{11}} \,, \tag{3.31}$$

where $\mathcal{T}'_{\mathbf{11}}$ is the charge associated with the level-one descendant current. This commutator explains why we do not refer to $\mathcal{T}$ as a flavour symmetry.

The index is of course insensitive to the above discussion; it gives the same answer when evaluated either on (3.26) or (3.28) and that is

$$\mathcal{I}_{\mathcal{B}[d_1,0;0]}(x,y) = \frac{x^{d_1+3}}{(1-xy^{-1})(1-xy)}\chi_{d_1+1}(y)\ . \tag{3.32}$$

**The Stress-Tensor Multiplet: $\mathcal{B}[0,0;0]$**

Let us finally turn to the case where one also sets $d_1 = 0$. The supercharges removed from the Verma-module basis (3.1) should be those for $\mathcal{B}[0,0;K]$, but since $K=0$ one can also act on its shortening conditions with the $R$-symmetry lowering operator. This results in needing to remove $Q_{\mathbf{12}}Q_{\mathbf{23}}$. Consequently the module is:

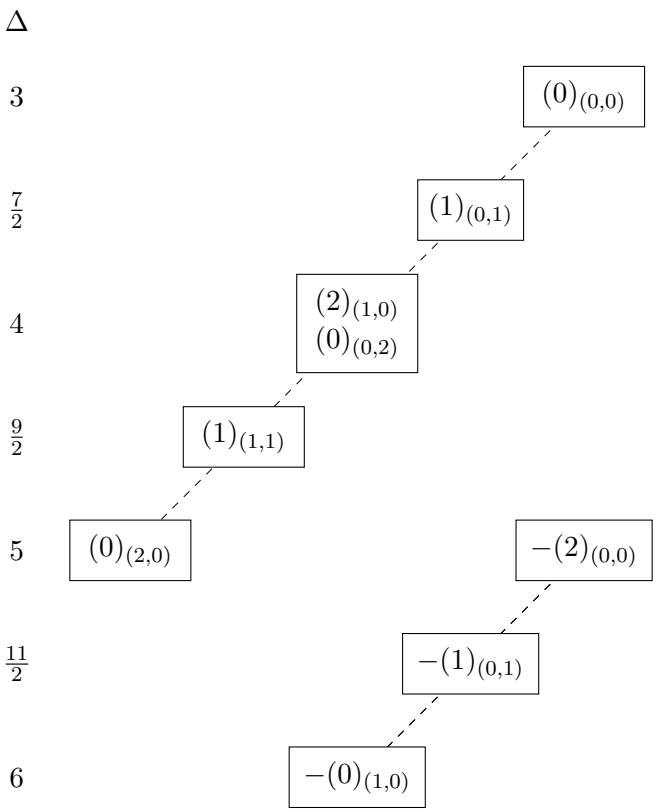


(3.33)

We recognise that this multiplet contains the $R$-symmetry current, the supersymmetry current and the stress tensor, as well as their corresponding equations of motion. In particular, we identify:

$$\begin{aligned} [4;1,0;2]: &\quad J_\mu^{(\mathbf{AB})}\ , & -[5;0,0;2]: &\quad \partial^\mu J_\mu^{(\mathbf{AB})} = 0\ , \\ [9/2;1,1;1]: &\quad S_{\mu a}^{\mathbf{A}}\ , & -[11/2;0,1;1]: &\quad \partial^\mu S_{\mu a}^{\mathbf{A}} = 0\ , \end{aligned} \tag{3.34}$$

$$[5;2,0;0]: \quad \Theta_{\mu\nu}\ , \qquad\qquad -[6;1,0;0]: \quad \partial^{\mu}\Theta_{\mu\nu}=0\ .$$

This multiplet also contains three states that do not obey conservation equations.

The index over this multiplet counts just two components of the $R$-symmetry current, $J_1^{\mathbf{11}}$ and $J_4^{\mathbf{11}}$. It is given by

$$\mathcal{I}_{\mathcal{B}[0,0;0]}(x,y)=\frac{x^3}{(1-xy^{-1})\,(1-xy)}\chi_1(y)\ . \tag{3.35}$$

**$\mathcal{D}$-type multiplets**

For the $\mathcal{D}[0,0;K]$ multiplet unitarity requires that the conformal dimension of the primary is $\Delta=\frac{3K}{2}$. The null state associated with this condition instructs us to remove $\mathcal{Q}_{\mathbf{1}1}$ from the basis of Verma-module generators, but due to having $d_1=d_2=0$ one actually needs to remove the larger set of supercharges $\mathcal{Q}_{\mathbf{1}a}$, $a=1,\ldots,4$. In fact, in this case $\Lambda^1_{\mathbf{1}}\Psi=\mathcal{Q}_{\mathbf{1}1}\Psi=0$ and one has the shortening condition

$$\mathcal{Q}_{\mathbf{1}a}\Psi=0\ , \tag{3.36}$$

which renders the multiplet $\frac{1}{2}$-BPS.

The action of the remaining supercharges on a primary state where the quantum numbers are kept generic is then

$$\begin{aligned}
(K)_{(d_1,d_2)} &\xrightarrow{Q} (K-1)_{(d_1,d_2+1),(d_1+1,d_2-1)}\ ,\\
&\xrightarrow{Q^2} (K-2)_{(d_1+1,d_2)}\ ,\\
(K)_{(d_1,d_2)} &\xrightarrow{\tilde{Q}} (K-1)_{(d_1,d_2-1),(d_1-1,d_2+1)}\ ,\\
&\xrightarrow{\tilde{Q}^2} (K-2)_{(d_1-1,d_2)}\ .
\end{aligned} \tag{3.37}$$

After setting $d_1 = d_2 = 0$ and employing RS the full multiplet is

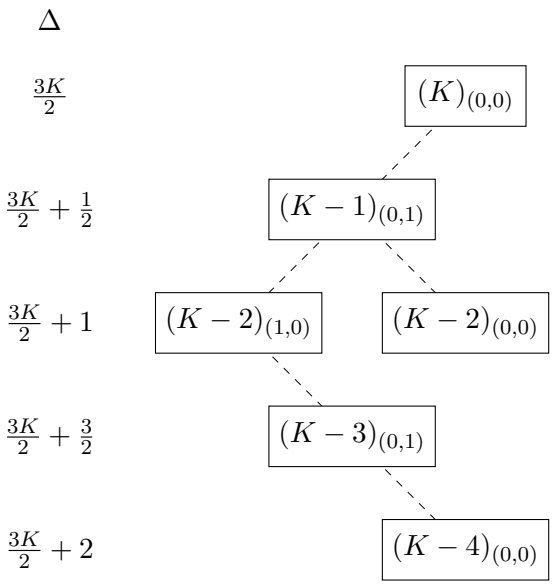


(3.38)

For low enough values of $K$ there can be additional reflections. If $K = 1$ or $K = 2$ these will correspond to operator constraints, to be discussed below. If $K = 3$ then the only problematic state will be the level four $[0, 0; K - 4]$, which becomes $[0, 0; -1]$; this is on the boundary of the Weyl chamber, and hence will also be deleted.

The index for this multiplet is

$$\mathcal{I}_{\mathcal{D}[0,0;K]}(x, y) = \frac{x^K}{(1 - xy^{-1})(1 - xy)} , \tag{3.39}$$

which satisfies a recombination rule from (3.9):

$$\lim_{\epsilon \to 0} \mathcal{I}_{\mathcal{L}[\Delta+\epsilon;0,0;K]}(x, y) = \mathcal{I}_{\mathcal{A}[0,0;K]}(x, y) + \mathcal{I}_{\mathcal{D}[0,0;K+4]}(x, y) = 0 . \tag{3.40}$$

**The Hypermultiplet:** $\mathcal{D}[0,0;1]$

When $K = 1$ no additional shortening conditions arise, therefore we may proceed directly using (3.38). One recovers:

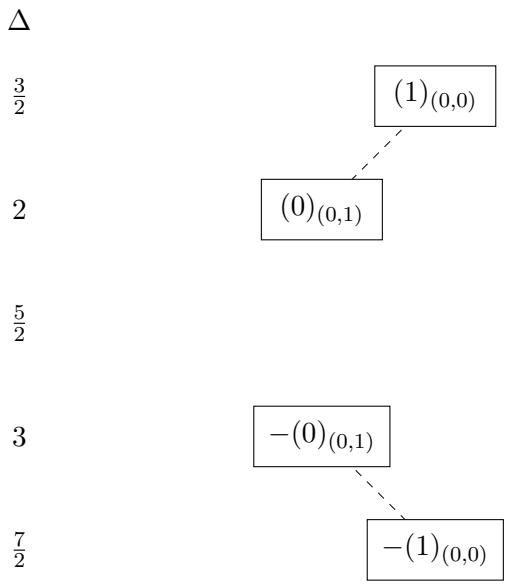


(3.41)

We can recognise these highest weight states as

$$\begin{aligned} [3/2;0,0;1]: &\quad \phi^{\mathbf{A}}\,, \\ [2;0,1;0]: &\quad \lambda_a\,, \\ -[3;0,1;0]: &\quad \partial^{ab}\overline{\lambda}_b = 0\,, \\ -[7/2;0,0;1]: &\quad \partial^2\phi^{\mathbf{A}} = 0\,. \end{aligned} \tag{3.42}$$

The index for this multiplet counts the first operator in the primary, $\phi^{\mathbf{1}}$ along with the $P_1$ and $P_2$ conformal descendants. Therefore we have

$$\mathcal{I}_{\mathcal{D}[0,0;1]}(x,y) = \frac{x}{(1-xy^{-1})\,(1-xy)}\,. \tag{3.43}$$

This is the single-letter index obtained in [114, 115].

**The Flavour-Current Multiplet:** $\mathcal{D}[0,0;2]$

One of the $\mathcal{D}$-type multiplets predicted to contain operator constraints is $\mathcal{D}[0,0;2]$. As above, we may jump straight into the multiplet structure by setting $K = 2$ in the

$\mathcal{D}[0,0;K]$ module. This produces

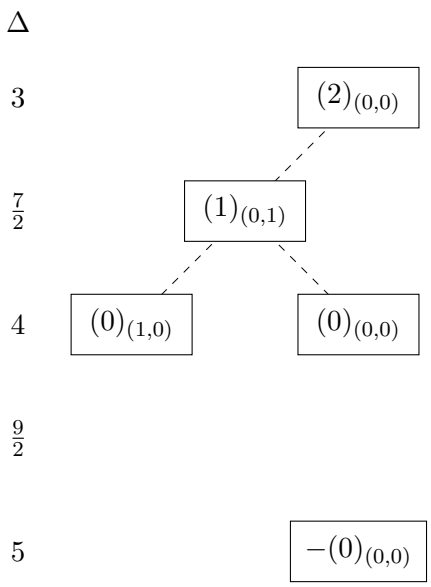


(3.44)

We recognise these fields to be a scalar $\mu^{(\mathbf{AB})}$ in the **3** of $\mathfrak{su}(2)_R$, a fermion $\psi_a^{\mathbf{A}}$ in the **2** of $\mathfrak{su}(2)_R$, a vector $J_\mu$ and an R-neutral scalar $M$. Furthermore the negative-multiplicity state is the equation of motion for the vector current $\partial^\mu J_\mu = 0$. This multiplet is also known as the linear multiplet and appeared in the UV symmetry-enhancement discussion of [116].

The corresponding index is:

$$\mathcal{I}_{\mathcal{D}[0,0;2]}(x,y) = \frac{x^2}{(1-xy^{-1})(1-xy)} \,. \tag{3.45}$$

This concludes our listing of superconformal multiplets for the 5d SCA.

### 3.2.5 Index Spectroscopy

In five dimensions, it was conjectured in [94] that the UV fixed points of Sp($N$) gauge theories should exhibit a flavour symmetry enhancement. Specifically, the enhanced flavour group is one of the exceptional series, $\mathrm{E}_N$. This was confirmed for $N = 1$ by localisation in [114] and then with topological strings; firstly in [80] for the first flavour two ranks, with the remaining ranks being completed in [72]. We can make statements about the spectrum of these theories using our knowledge of indices from the various superconformal multiplets using the sieve algorithm developed in [117].

For $N_f = 0$ where the global symmetry is U(1) which gets enhanced to $\mathrm{E}_1 = \mathrm{SU}(2)$. The index is given by

$$\mathcal{I}_{N_f=0} = 1 + \chi_{\mathbf{3}}^{E_1} x^2 + \chi_1(y)\left[1+\chi_{\mathbf{3}}^{E_1}\right]x^3 + \left(\chi_2(y)\left[1+\chi_{\mathbf{3}}^{E_1}\right] + 1 + \chi_{\mathbf{5}}^{E_1}\right)x^4$$

$$+\left(\chi_3(y)\left[1+\chi_{\mathbf{3}}^{E_1}\right]+\chi_1(y)\left[1+\chi_{\mathbf{3}}^{E_1}+\chi_{\mathbf{5}}^{E_1}\right]\right)x^5+\left(\chi_4(y)\left[1+\chi_{\mathbf{3}}^{E_1}\right]\right.$$
$$\left.+\chi_2(y)\left[1+\chi_{\mathbf{3}}^{E_1}+\chi_{\mathbf{5}}^{E_1}+\chi_{\mathbf{3}}^{E_1}\chi_{\mathbf{3}}^{E_1}\right]+\chi_{\mathbf{3}}^{E_1}+\chi_{\mathbf{7}}^{E_1}-1\right)x^6+\mathcal{O}(x^7)\,. \quad (3.46)$$

This index can be concisely decomposed as

$$\mathcal{I}_{N_f=0}=1+\chi_{\mathbf{3}}^{E_1}\mathcal{D}[0,0;2]+\mathcal{B}[0,0;0]+\chi_{\mathbf{5}}^{E_1}\mathcal{D}[0,0;4]+\chi_{\mathbf{3}}^{E_1}\mathcal{B}[0,0;2]$$
$$+\chi_{\mathbf{3}}^{E_1}\chi_{\mathbf{3}}^{E_1}\mathcal{B}[1,0;2]+\chi_{\mathbf{7}}^{E_1}\mathcal{D}[0,0;6]+\mathcal{A}[0,0;2]+\dots\,. \quad (3.47)$$

We see the familiar flavour current multiplet coming with the adjoint character of $\mathrm{E}_1$ along with the stress tensor with no multiplicative factor as expected. Perhaps the most interesting part is the appearance of the $\mathcal{A}$ multiplets in the decomposition. This is because, with the exception of $\mathcal{A}[d_1,1;K]$, these multiplets do not admit a free field decomposition.[17] It is possible that these more mysterious contributions to the index are a result of the instantons.

When $N_F=1$ the global symmetry is $\mathrm{SO}(2)\times\mathrm{U}(1)$ which gets enhanced to $\mathrm{E}_2=\mathrm{SU}(2)\times\mathrm{U}(1)$. The index is

$$\mathcal{I}_{N_f=1}=$$
$$1+\chi_{\mathbf{4}}^{E_2}x^2+\chi_1(y)\left[1+\chi_{\mathbf{4}}^{E_2}\right]x^3+\left(\chi_2(y)\left[1+\chi_{\mathbf{4}}^{E_2}\right]+1+\chi_{\mathbf{5}}^{SU(2)}-\chi_{\mathbf{4}}(f)\right)x^4$$
$$+\left(\chi_3(y)\left[1+\chi_{\mathbf{4}}^{E_2}\right]+\chi_1(y)\left[1+\chi_{\mathbf{4}}^{E_2}+\chi_{\mathbf{3}}^{SU(2)}+\chi_{\mathbf{5}}^{SU(2)}-\chi_{\mathbf{4}}(f)\right]\right)x^5$$
$$+\left(\chi_4(y)\left[1+\chi_{\mathbf{4}}^{E_2}\right]+\chi_2(y)\left[4\chi_{\mathbf{4}}^{E_2}+2\chi_{\mathbf{5}}^{SU(2)}-\chi_{\mathbf{4}}(f)\right]+\chi_{\mathbf{7}}^{SU(2)}+3\chi_{\mathbf{3}}^{SU(2)}+1\right)x^6$$
$$+\mathcal{O}(x^7)\,. \quad (3.49)$$

This can be rewritten as

$$\mathcal{I}_{N_f=1}=1+\chi_{\mathbf{4}}^{E_2}\mathcal{D}[0,0;2]+\mathcal{B}[0,0;0]+\chi_{\mathbf{4}}(f)\mathcal{A}[0,0;0]+\chi_{\mathbf{5}}^{SU(2)}\mathcal{D}[0,0;4]$$
$$+2\chi_{\mathbf{3}}^{SU(2)}\mathcal{B}[0,0;2]+(1+2\chi_{\mathbf{4}}^{E_2}+\chi_{\mathbf{5}}^{SU(2)})\mathcal{B}[1,0;2]$$
$$+(\chi_{\mathbf{4}}^{E_2}+\chi_{\mathbf{7}}^{SU(2)})\mathcal{D}[0,0;6]+\dots \quad (3.50)$$

with that $\chi_{\mathbf{4}}^{E_2}=1+\chi_{\mathbf{3}}^{SU(2)}$ and $\chi_{\mathbf{4}}(f)=(p+p^{-1})\chi_{\mathbf{2}}^{SU(2)}$ with $p=e^{\frac{i\rho}{2}}$. Again, note the appearance of the $\mathcal{A}$ multiplets. Now is even more curious since the contribution to the index comes with a minus sign, and is charged under the fundamental of the SU(2) but with opposite U(1) charges. This is no coincidence, as fermionic terms such as this appear at higher orders of $x$ [114] with non-trivial flavour charges. It would

[17] The free field decomposition of the aforementioned multiplet is

$$\mathcal{O}_{a,\mu_1\cdots\mu_{d_1}}^{(\mathbf{A}_1\cdots\mathbf{A}_K)}=\epsilon_{\mathbf{BC}}\phi^{\mathbf{B}}\overleftrightarrow{\partial}_{\mu_1}\cdots\overleftrightarrow{\partial}_{\mu_{d_1}}\phi^{\mathbf{B}}\lambda_a\phi^{(\mathbf{A}_1}\cdots\phi^{\mathbf{A}_K)}\,. \quad (3.48)$$

be interesting to see if by studying the multiplet structure of these fermionic operators could shed some light on these instanton contributions.

## 3.3 Multiplets and Superconformal Indices for 6d (1,0)

We now switch to six dimensions. In this section we provide a systematic analysis of all superconformal multiplets admitted by the 6d $\mathcal{N} = (1,0)$ algebra, $\mathfrak{osp}(8^*|2)$.[18] Since the method for building UIRs is completely analogous to Sec. 3.2.1 we will be brief and merely sketch the derivation of the unitarity bounds obtained in detail by [36, 42]. We then proceed to write out the complete set of spectra for superconformal multiplets along with their corresponding superconformal indices.

### 3.3.1 UIR Building with Auxiliary Verma Modules

The superconformal primaries of the algebra $\mathfrak{osp}(8^*|2)$ are designated $|\Delta; c_1, c_2, c_3; K\rangle$ and labelled by the conformal dimension $\Delta$, the Lorentz quantum numbers for $\mathfrak{su}(4)$ in the Dynkin basis $c_i$ and an $R$-symmetry label $K$. Each primary is in one-to-one correspondence with a highest weight labelling irreducible representations of the maximal compact subalgebra $\mathfrak{so}(6) \oplus \mathfrak{so}(2) \oplus \mathfrak{su}(2)_R \subset \mathfrak{osp}(8^*|2)$. There are eight Poincaré and superconformal supercharges, denoted by $\mathcal{Q}_{\mathbf{A}a}$ and $\mathcal{S}_{\mathbf{A}\dot{a}}$—where $a, \dot{a} = 1, \cdots, 4$ are $\mathfrak{su}(4)$ (anti)fundamental indices and $\mathbf{A} = 1, 2$ an index of $\mathfrak{su}(2)_R$. One also has six momenta $P_\mu$ and special conformal generators $K_\mu$, where $\mu = 1, \cdots, 6$ is a Lorentz vector index. The superconformal primary is annihilated by all $\mathcal{S}_{\mathbf{A}\dot{a}}$ and $K_\mu$. A basis for the representation space of $\mathfrak{osp}(8^*|2)$ can be constructed by considering the following Verma module

$$\prod_{\mathbf{A},a} (\mathcal{Q}_{\mathbf{A}a})^{n_{\mathbf{A},a}} \prod_{\mu} {P_\mu}^{n_\mu} |\Delta; c_1, c_2, c_3; K\rangle^{hw} \ , \tag{3.51}$$

where $n = \sum_{\mathbf{A}a} n_{\mathbf{A},a}$ and $\hat{n} = \sum_\mu n_\mu$ denote the level of a superconformal or conformal descendant respectively. UIRs can be obtained from the above after also imposing the requirement of unitarity level-by-level.

We will now review the conditions imposed by unitarity, starting with the superconformal descendants [42]. For descendants of level $n > 0$ it suffices to calculate the norms of states in the highest weight of $\mathfrak{su}(2)_R$, since these provide the most stringent set of unitarity bounds [36, 42, 92]. Hence the unitarity bounds stem from the study of superconformal descendants arising from the action of supercharges of the form $\mathcal{Q}_{\mathbf{1}a}$.

[18] Some of the multiplets up to spin 2 discussed in this section have been previously constructed using the dual gravity description in [118].

| Multiplet | Shortening Condition | Conformal Dimension |
|---|---|---|
| $\mathcal{A}[c_1,c_2,c_3;K]$ | $A^4\Psi=0$ | $\Delta=2K+\frac{c_1}{2}+c_2+\frac{3c_3}{2}+6$ |
| $\mathcal{A}[c_1,c_2,0;K]$ | $A^3A^4\Psi=0$ | $\Delta=2K+\frac{c_1}{2}+c_2+6$ |
| $\mathcal{A}[c_1,0,0;K]$ | $A^2A^3A^4\Psi=0$ | $\Delta=2K+\frac{c_1}{2}+6$ |
| $\mathcal{A}[0,0,0;K]$ | $A^1A^2A^3A^4\Psi=0$ | $\Delta=2K+6$ |
| $\mathcal{B}[c_1,c_2,0;K]$ | $A^3\Psi=0$ | $\Delta=2K+\frac{c_1}{2}+c_2+4$ |
| $\mathcal{B}[c_1,0,0;K]$ | $A^2A^3\Psi=0$ | $\Delta=2K+\frac{c_1}{2}+4$ |
| $\mathcal{B}[0,0,0;K]$ | $A^1A^2A^3\Psi=0$ | $\Delta=2K+4$ |
| $\mathcal{C}[c_1,0,0;K]$ | $A^2\Psi=0$ | $\Delta=2K+\frac{c_1}{2}+2$ |
| $\mathcal{C}[0,0,0;K]$ | $A^1A^2\Psi=0$ | $\Delta=2K+2$ |
| $\mathcal{D}[0,0,0;K]$ | $A^1\Psi=0$ | $\Delta=2K$ |

**Table 3:** A list of all short multiplets for the 6d $(1,0)$ SCA, along with the conformal dimension of the superconformal primary and the corresponding shortening condition. The $A^a$ in the shortening conditions are defined in (3.52) and [42]. The first of these multiplets ($\mathcal{A}$) is a regular short representation, whereas the rest ($\mathcal{B},\mathcal{C},\mathcal{D}$) are isolated short representations. Here $\Psi$ denotes the superconformal primary state for each multiplet.

Before proceeding, it is convenient to define the basis $A^a\,|\Delta;c_1,c_2,c_3;K\rangle^{hw}$, where

$$A^a=\sum_{b=1}^{a}\mathcal{Q}_{\mathbf{1}b}\Upsilon^a_b\,. \tag{3.52}$$

The $\Upsilon^a_b$ are functions of $\mathfrak{su}(4)$ Cartans and Lorentz lowering operators analogous to those the (3.2), the explicit form of which can be found in [42]. They map highest weights to highest weights.

One then conducts a level-by-level analysis of the norms for the superconformal descendants, while also keeping track of whether the states $A^a\,|\Delta;c_1,c_2,c_3;K\rangle^{hw}$ are well defined when setting $c_i=0$. This gives rise to a set of regular and isolated short multiplets, obeying certain shortening conditions [42]. The precise form of the $A^a$ is unimportant; they have the same quantum numbers as the supercharge $\mathcal{Q}_{\mathbf{1}a}$. The shortening conditions can then be translated into absent generators in the auxiliary Verma module (3.51) and we are instructed to remove the corresponding combinations of supercharges in a straightforward way. These results are summarised in Table 3. Additional absent supercharges can be obtained when $K=0$ by acting on the existing null states with Lorentz and $R$-symmetry lowering operators. As a result additional supercharges need to be removed from (3.51). These occurrences will be dealt with on a case-by-case basis.

Finally, there can be supplementary unitarity restrictions and associated null states arising from considering conformal descendants. These have been studied in detail in [36, 109]. In analogy with the 5d approach, we will choose not to exclude any momenta from the basis of auxiliary Verma-module generators (3.51); with the help of

the RS algorithm this will account for states corresponding to equations of motion and conservation equations.

We can combine the information from the conformal and superconformal unitarity bounds to predict when a multiplet will contain operator constraints. These are found to be

$$\mathcal{B}[c_1, c_2, 0; 0] \ , \quad \mathcal{C}[c_1, 0, 0; \{0, 1\}] \ , \quad \mathcal{D}[0, 0, 0; \{1, 2\}] \tag{3.53}$$

and will be treated separately in the following sections. The multiplet $\mathcal{D}[0, 0, 0; 0]$ does not belong to this list as it is the vacuum, which is annihilated by all supercharges and momenta.

### 3.3.2 6d (1,0) Recombination Rules

Short multiplets can recombine into a long multiplet $\mathcal{L}$. This occurs when the conformal dimension of $\mathcal{L}$ approaches the unitarity bound, that is when $\Delta + \epsilon \to 2K + \frac{1}{2}(c_1 + 2c_2 + 3c_3) + 6$. We find that

$$\begin{aligned}
\mathcal{L}[\Delta + \epsilon; c_1, c_2, c_3; K] &\xrightarrow{\epsilon \to 0} \mathcal{A}[c_1, c_2, c_3; K] \oplus \mathcal{A}[c_1, c_2, c_3 - 1; K + 1] \ , \\
\mathcal{L}[\Delta + \epsilon; c_1, c_2, 0; K] &\xrightarrow{\epsilon \to 0} \mathcal{A}[c_1, c_2, 0; K] \oplus \mathcal{B}[c_1, c_2 - 1, 0; K + 2] \ , \\
\mathcal{L}[\Delta + \epsilon; c_1, 0, 0; K] &\xrightarrow{\epsilon \to 0} \mathcal{A}[c_1, 0, 0; K] \oplus \mathcal{C}[c_1 - 1, 0, 0; K + 3] \ , \\
\mathcal{L}[\Delta + \epsilon; 0, 0, 0; K] &\xrightarrow{\epsilon \to 0} \mathcal{A}[0, 0, 0; K] \oplus \mathcal{D}[0, 0, 0; K + 4] \ .
\end{aligned} \tag{3.54}$$

These identities can be explicitly checked, e.g. by using supercharacters for the multiplets that we discuss below.

A small number of short multiplets do not appear in any recombination rule. These are

$$\begin{aligned}
&\mathcal{B}\left[c_1, c_2, 0; \{0, 1\}\right] \ , \\
&\mathcal{C}\left[c_1, 0, 0; \{0, 1, 2\}\right] \ , \\
&\mathcal{D}\left[0, 0, 0; \{0, 1, 2, 3\}\right] \ .
\end{aligned} \tag{3.55}$$

### 3.3.3 The 6d (1,0) Superconformal Index

We define the 6d (1,0) superconformal index with respect to the supercharge $\mathcal{Q}_{\mathbf{14}}$, in accordance with [42]. This is given by

$$\mathcal{I}(p, q, s) = \mathrm{Tr}_{\mathcal{H}}(-1)^F e^{-\beta\delta} q^{\Delta - \frac{1}{2}K} p^{c_2} s^{c_1} \ , \tag{3.56}$$

where the fermion number is $F = c_1 + c_3$. The states that are counted satisfy $\delta = 0$, where

$$\delta := \{\mathcal{Q}_{\mathbf{1}4}, \mathcal{S}_{\mathbf{2}\dot{4}}\} = \Delta - 2K - \frac{1}{2}(c_1 + 2c_2 + 3c_3) \ . \tag{3.57}$$

The Cartan combinations $\Delta - \frac{1}{2}K$, $c_2$ and $c_1$ are generators of the subalgebra that commutes with $\mathcal{Q}_{\mathbf{1}4}, \mathcal{S}_{\mathbf{2}\dot{4}}$ and $\delta$. This index can be evaluated as a 6d supercharacter, as discussed in Sec. 3.5.

### 3.3.4 6d (1,0) Multiplets

#### Long multiplets

Long multiplets are generated by the action of all supercharges. We will choose to group them into $Q = (\mathcal{Q}_{\mathbf{A}1}, \mathcal{Q}_{\mathbf{A}2})$ and $\tilde{Q} = (\mathcal{Q}_{\mathbf{A}3}, \mathcal{Q}_{\mathbf{A}4})$, with their individual quantum numbers given by

$$\begin{aligned}
&\mathcal{Q}_{\mathbf{1}1} \sim (1)_{(1,0,0)} \ , \quad && \mathcal{Q}_{\mathbf{1}2} \sim (1)_{(-1,1,0)} \ , \quad && \mathcal{Q}_{\mathbf{1}3} \sim (1)_{(0,-1,1)} \ , \quad && \mathcal{Q}_{\mathbf{1}4} \sim (1)_{(0,0,-1)} \ , \\
&\mathcal{Q}_{\mathbf{2}1} \sim (-1)_{(1,0,0)} \ , \quad && \mathcal{Q}_{\mathbf{2}2} \sim (-1)_{(-1,1,0)} \ , \quad && \mathcal{Q}_{\mathbf{2}3} \sim (-1)_{(0,-1,1)} \ , \quad && \mathcal{Q}_{\mathbf{2}4} \sim (-1)_{(0,0,-1)} \ .
\end{aligned} \tag{3.58}$$

The action of these supercharges on a superconformal primary $(K)_{(c_1,c_2,c_3)}$ is given by

$$\begin{aligned}
(K)_{(c_1,c_2,c_3)} &\xrightarrow{Q} (K \pm 1)_{(c_1+1,c_2,c_3),(c_1-1,c_2+1,c_3)} \ , \\
&\xrightarrow{Q^2} (K \pm 2)_{(c_1,c_2+1,c_3)} \ , \ (K)_{(c_1+2,c_2,c_3),(c_1,c_2+1,c_3)^2,(c_1-2,c_2+2,c_3)} \ , \\
&\xrightarrow{Q^3} (K \pm 1)_{(c_1+1,c_2+1,c_3),(c_1-1,c_2+2,c_3)} \ , \\
&\xrightarrow{Q^4} (K)_{(c_1,c_2+2,c_3)} \ , \\
(K)_{(c_1,c_2,c_3)} &\xrightarrow{\tilde{Q}} (K \pm 1)_{(c_1,c_2-1,c_3+1),(c_1,c_2,c_3-1)} \ , \\
&\xrightarrow{\tilde{Q}^2} (K \pm 2)_{(c_1,c_2-1,c_3)} \ , \ (K)_{(c_1,c_2-2,c_3+2),(c_1,c_2-1,c_3)^2,(c_1,c_2,c_3-2)} \ , \\
&\xrightarrow{\tilde{Q}^3} (K \pm 1)_{(c_1,c_2-1,c_3-1),(c_1,c_2-2,c_3+1)} \ , \\
&\xrightarrow{\tilde{Q}^4} (K)_{(c_1,c_2-2,c_3)} \ .
\end{aligned} \tag{3.59}$$

As in 5d, the explicit form of the multiplets are obtainable by using the package detailed in Appendix B.2; and indeed this case is considered for the primary $[0,0,0,0]$ in the first example.

### $\mathcal{A}$-type multiplets

Recall from Table 3 that the $\mathcal{A}$–multiplets obey four kinds of shortening conditions. These result in the removal of the following combinations of supercharges from the basis of Verma module generators (3.51):

$$\begin{aligned}
\mathcal{A}[c_1,c_2,c_3;K] &: \mathcal{Q}_{\mathbf{14}}\ , \\
\mathcal{A}[c_1,c_2,0;K] &: \mathcal{Q}_{\mathbf{13}}\mathcal{Q}_{\mathbf{14}}\ , \\
\mathcal{A}[c_1,0,0;K] &: \mathcal{Q}_{\mathbf{12}}\mathcal{Q}_{\mathbf{13}}\mathcal{Q}_{\mathbf{14}}\ , \\
\mathcal{A}[0,0,0;K] &: \mathcal{Q}_{\mathbf{11}}\mathcal{Q}_{\mathbf{12}}\mathcal{Q}_{\mathbf{13}}\mathcal{Q}_{\mathbf{14}}\ .
\end{aligned} \tag{3.60}$$

With regards to the spectrum, let us first consider the $\mathcal{A}[c_1,c_2,c_3;K]$ multiplet. The action of the $Q$-set of supercharges is the same as for the long multiplet (3.59), however since we are also instructed to remove $\mathcal{Q}_{\mathbf{14}}$ the $\tilde{Q}$-chain becomes

$$\begin{aligned}
(K)_{(c_1,c_2,c_3)} &\xrightarrow{\tilde{Q}} (K\pm 1)_{(c_1,c_2-1,c_3+1)}\ ,\ (K-1)_{(c_1,c_2,c_3-1)}\ , \\
&\xrightarrow{\tilde{Q}^2} (K)_{(c_1,c_2-2,c_3+2),(c_1,c_2-1,c_3)}\ ,\ (K-2)_{(c_1,c_2-1,c_3)}\ , \\
&\xrightarrow{\tilde{Q}^3} (K-1)_{(c_1,c_2-2,c_3+1)}\ .
\end{aligned} \tag{3.61}$$

The remaining four cases can be obtained straightforwardly in a similar way. The resulting multiplet spectra turn out to be the same as starting with (3.61), substituting for specific $c_i$ values and running the RS algorithm.

Additional ill-defined states occur for $K=0$, when one should also remove the supercharge combinations

$$\begin{aligned}
\mathcal{A}[c_1,c_2,c_3;0] &: \mathcal{Q}_{\mathbf{24}}\ , \\
\mathcal{A}[c_1,c_2,0;0] &: \mathcal{Q}_{\mathbf{23}}\mathcal{Q}_{\mathbf{24}}\ , \\
\mathcal{A}[c_1,0,0;0] &: \mathcal{Q}_{\mathbf{22}}\mathcal{Q}_{\mathbf{23}}\mathcal{Q}_{\mathbf{24}}\ , \\
\mathcal{A}[0,0,0;0] &: \mathcal{Q}_{\mathbf{21}}\mathcal{Q}_{\mathbf{22}}\mathcal{Q}_{\mathbf{23}}\mathcal{Q}_{\mathbf{24}}\ ,
\end{aligned} \tag{3.62}$$

from the basis of Verma-module generators. Once again, the resulting spectra are equivalent to starting with the $K\neq 0$ multiplets, explicitly setting $K=0$ and running the RS algorithm for $\mathfrak{su}(2)_R$.

The superconformal index for all values of $c_i$ and $K$ is given by

$$\begin{aligned}
\mathcal{I}_{\mathcal{A}[c_1,c_2,c_3;K]}(p,q,s) = &\frac{(-1)^{c_1+c_3}q^{6+\frac{3K}{2}+\frac{1}{2}(c_1+2c_2+3c_3)}}{(pq-1)\,(p^2-s)\,(ps-1)\,(p-s^2)\,(q-s)(p-qs)} \\
&\times\Big\{p^{-c_2+1}s^{c_2+4}\left(p^{-c_1}-ps^{c_1+1}\right)+p^{c_2+4}s^{c_1+4}
\end{aligned}$$

$$p^{-c_1+2}s^{2-c_2}+p^{c_1+4}s^{-c_1+1}\left(s^{-c_2}-sp^{c_2+1}\right)\Big\}\,. \tag{3.63}$$

This index satisfies the following recombination rules

$$\begin{aligned}&\lim_{\epsilon\to 0}\mathcal{I}_{\mathcal{L}[\Delta+\epsilon;c_1,c_2,c_3;K]}(p,q,s)=\\&\quad\mathcal{I}_{\mathcal{A}[c_1,c_2,c_3;K]}(p,q,s)+\mathcal{I}_{\mathcal{A}[c_1,c_2,c_3-1;K+1]}(p,q,s)=0\,.\end{aligned} \tag{3.64}$$

### $\mathcal{B}$-type multiplets

For the $\mathcal{B}$-type multiplets, the supercharges that need to be removed from the basis (3.51) are

$$\begin{aligned}\mathcal{B}[c_1,c_2,0;K]&:\mathcal{Q}_{\mathbf{13}}\,,/cr\mathcal{B}[c_1,0,0;K] &&:\mathcal{Q}_{\mathbf{12}}\mathcal{Q}_{\mathbf{13}}\,,\\ \mathcal{B}[0,0,0;K]&:\mathcal{Q}_{\mathbf{11}}\mathcal{Q}_{\mathbf{12}}\mathcal{Q}_{\mathbf{13}}\,. &&\end{aligned} \tag{3.65}$$

For the first type of multiplet, $\mathcal{B}[c_1,c_2,0;K]$, one should also remove $\mathcal{Q}_{\mathbf{14}}$ as the state $A^4\Psi$ is ill defined for $c_3=0$. Acting on a primary with generic quantum numbers, $(K)_{(c_1,c_2,c_3)}$, one has the same action as (3.59) for $Q$. The $\tilde{Q}$-chain is modified to

$$\begin{aligned}(K)_{(c_1,c_2,c_3)}&\xrightarrow{\tilde{Q}}(K-1)_{(c_1,c_2-1,c_3+1),(c_1,c_2,c_3-1)}\,,\\ &\xrightarrow{\tilde{Q}^2}(K-2)_{(c_1,c_2-1,c_3)}\,.\end{aligned} \tag{3.66}$$

We can represent this multiplet on a grid, where acting with $Q$s corresponds to *south-west* motion on the diagram, while acting with $\tilde{Q}$ to *southeast* motion

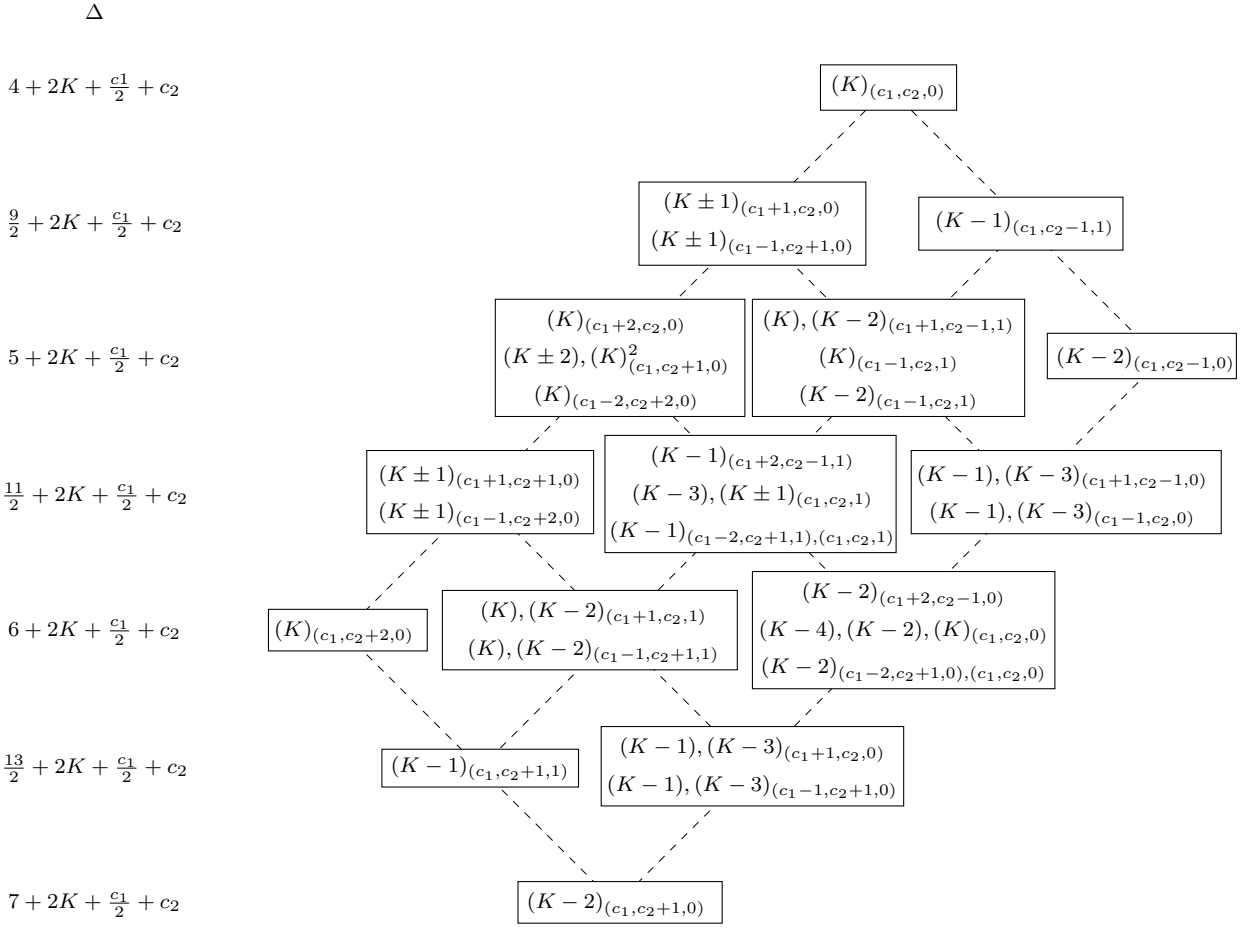


(3.67)

The next multiplet type is $\mathcal{B}[c_1,0,0;K]$, where one is instructed to remove $\mathcal{Q}_{\mathbf{12}}\mathcal{Q}_{\mathbf{13}}$. Similarly, $\mathcal{Q}_{\mathbf{12}}\mathcal{Q}_{\mathbf{14}}$ and $\mathcal{Q}_{\mathbf{13}}\mathcal{Q}_{\mathbf{14}}$ should also be removed as the states $A^2A^4\Psi$ and $A^3A^4\Psi$ are ill defined for $c_2=c_3=0$. The multiplet spectrum is given by

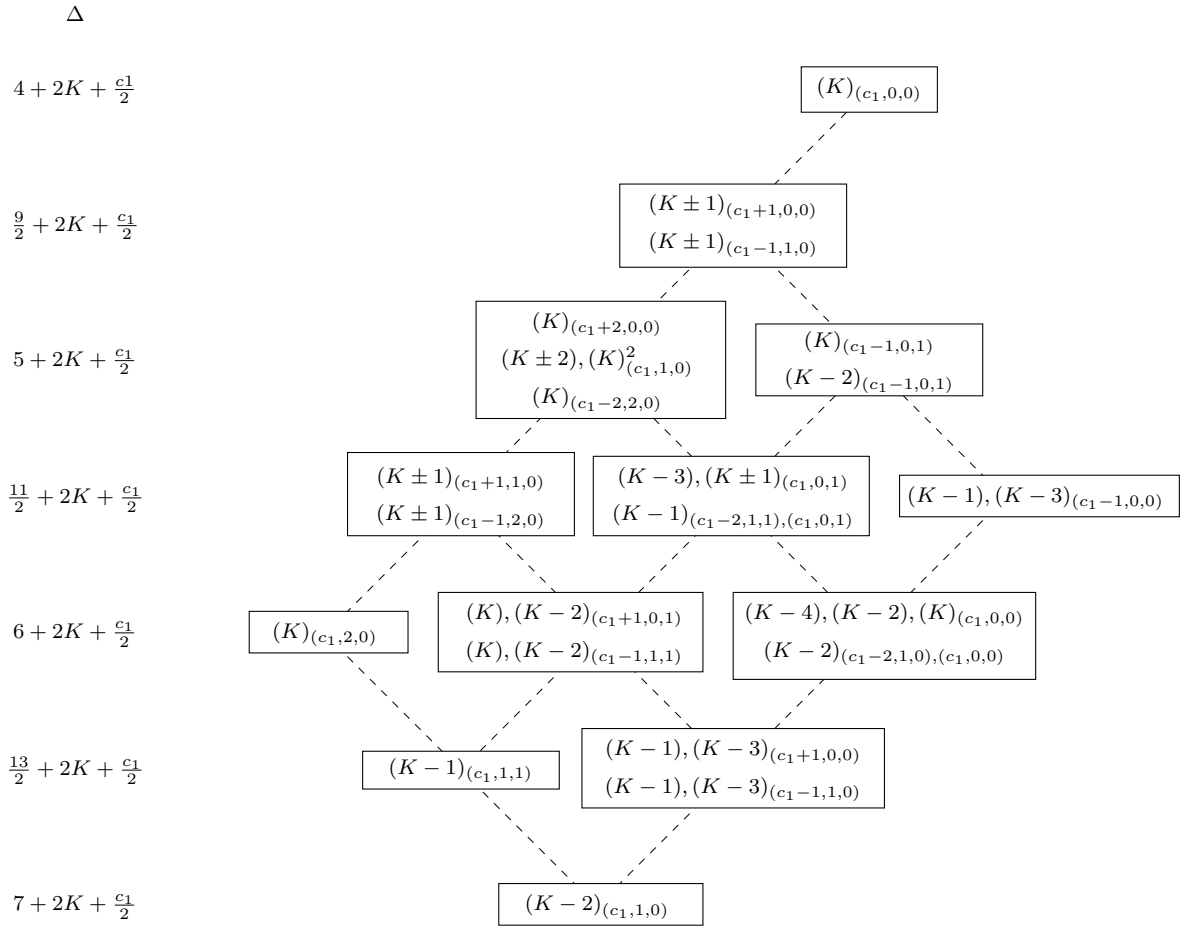


(3.68)

The last $\mathcal{B}$-type multiplet to consider is $\mathcal{B}[0,0,0;K]$. Its shortening condition is $A^1A^2A^3\Psi = 0$. All other combinations of three $A^a$ are ill defined and one is therefore required to remove $\mathcal{Q}_{\mathbf{1}a}\mathcal{Q}_{\mathbf{1}b}\mathcal{Q}_{\mathbf{1}c}$ from (3.51). The multiplet spectrum is determined to be

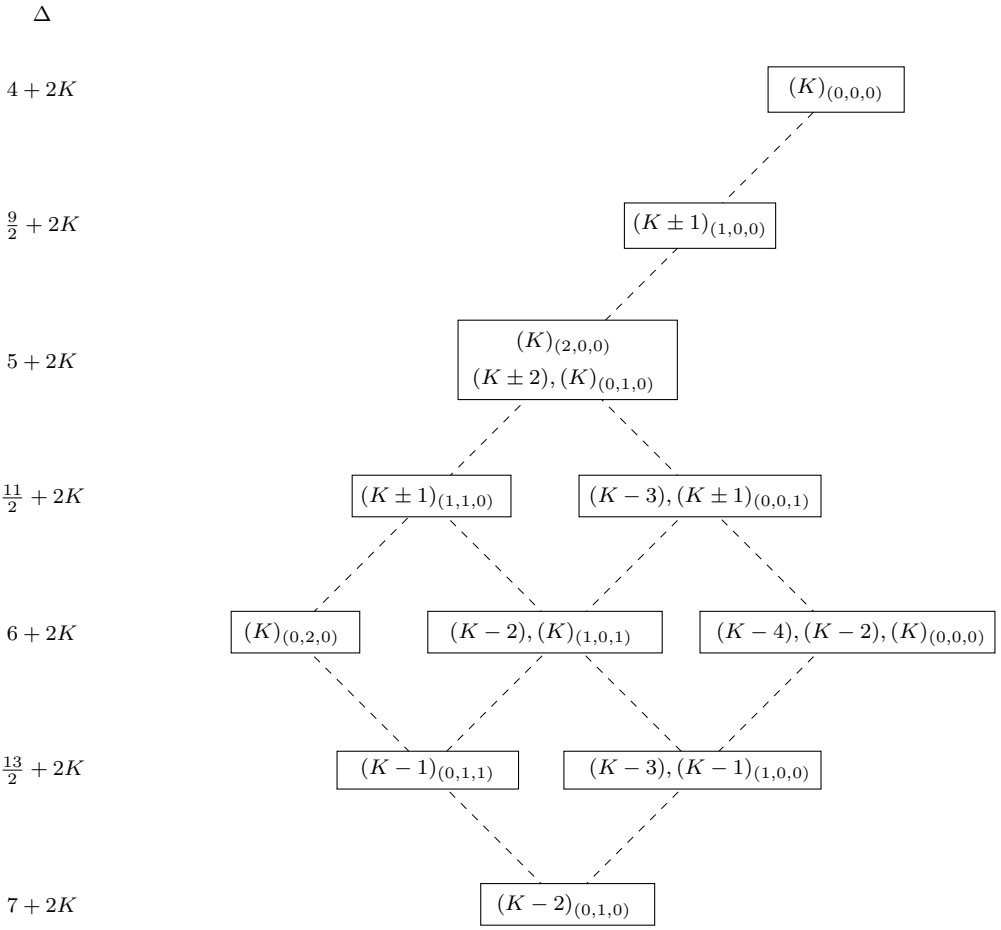


(3.69)

The index over $\mathcal{B}$-type multiplets for all values of $c_i$ and $K \neq 0$ is given by

$$\begin{aligned}
&\mathcal{I}_{\mathcal{B}[c_1,c_2,0;K]}(p,q,s) = \\
&(-1)^{c_1+1} q^{4+\frac{3K}{2}+\frac{c_1}{2}+c_2} \left\{ \frac{p^{-c_2} s^{c_2+5} \left(p^{-c_1} - p s^{c_1+1}\right) - p^{-c_1+2} s^{1-c_2}}{(pq-1)\,(p^2-s)\,(ps-1)\,(p-s^2)\,(q-s)(p-qs)} \right. \\
&\left. + \frac{p^{c_2+5} s^{c_1+4} + p^{c_1+4} s^{-c_1} \left(s^{-c_2} - s^2 p^{c_2+2}\right)}{(pq-1)\,(p^2-s)\,(ps-1)\,(p-s^2)\,(q-s)(p-qs)} \right\} .
\end{aligned} \tag{3.70}$$

**Higher-Spin-Current Multiplets: $\mathcal{B}[c_1, c_2, 0; 0]$**

In Eq. (3.53) we claimed that the special subset of $\mathcal{B}$-type multiplets with $K = 0$ should contain operator constraints. Recall that for $\mathcal{B}[c_1, c_2, 0; K]$ one should remove $\mathcal{Q}_{\mathbf{1}4}$ and $\mathcal{Q}_{\mathbf{1}3}$ from the basis of Verma-module generators. Since $K = 0$ we also remove two more supercharges, $\mathcal{Q}_{\mathbf{2}4}$ and $\mathcal{Q}_{\mathbf{2}3}$. That is, we should completely remove the set of $\tilde{Q}$ supercharges of (3.58) and the spectrum is generated solely by acting with the set of

all $Q$s:

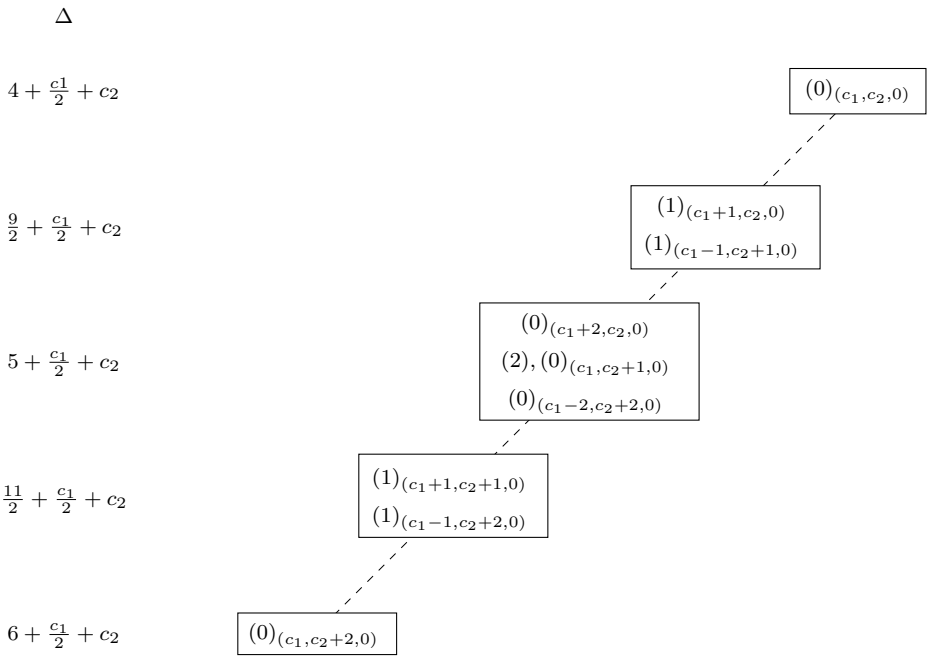


(3.71)

Note that the absent $\mathcal{Q}$s anticommute into $P_6$, which has therefore been implicitly removed from the Verma-module generators. This has the effect of projecting out states corresponding to operator constraints and hence the spectrum only contains reduced states. The operator constraints can be restored using the dictionary developed in App. B.1. This can be done using the character expression

$$\hat{\chi}[\Delta;c_1,c_2,c_2;K]=\chi[\Delta;c_1,c_2,c_3;K]-\chi[\Delta+1;c_1,c_2-1,c_3;K]\,, \tag{3.72}$$

where $\Delta=4+\frac{c_1}{2}+c_2$. The hat indicates a character of the reduced (i.e. $P_6$-removed) Verma module. The result is

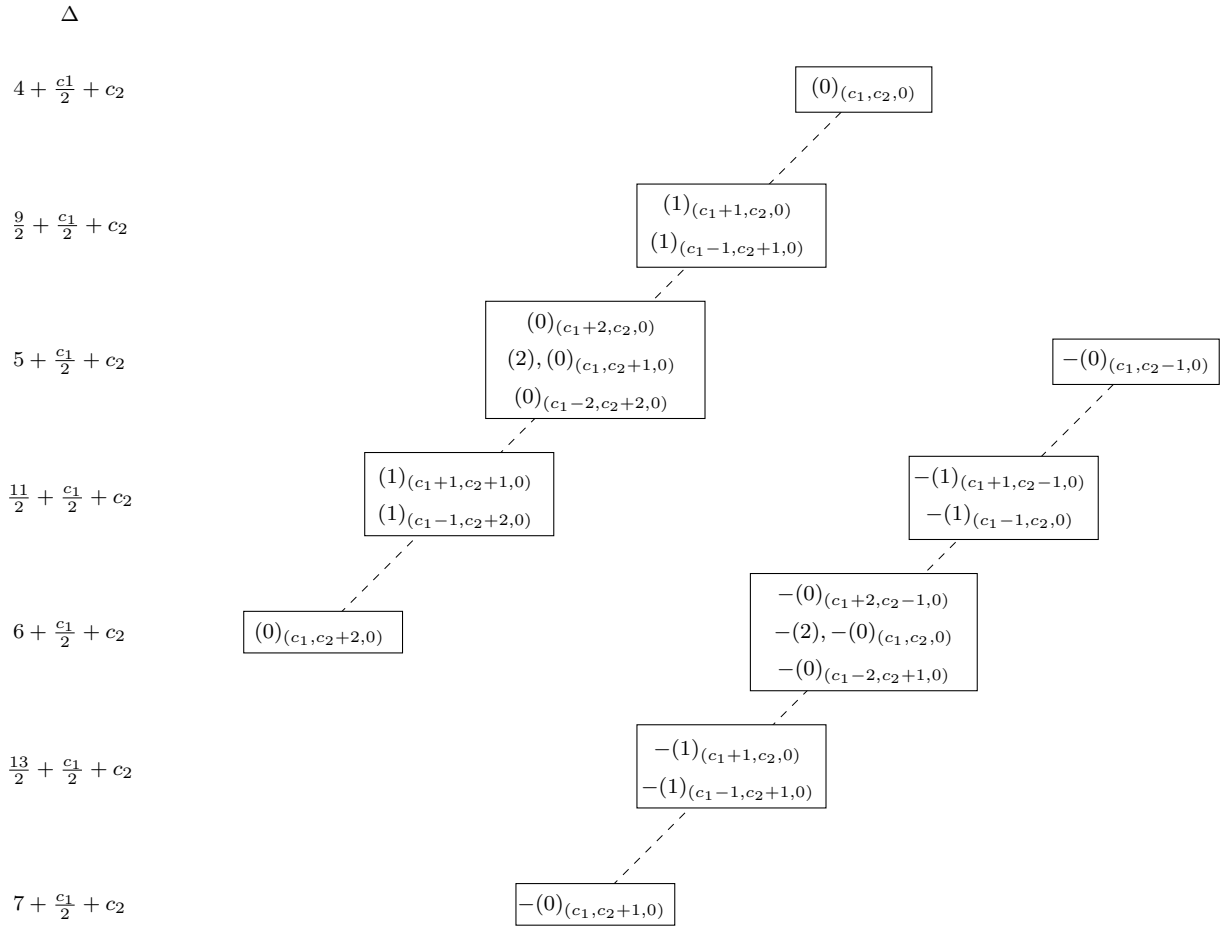


(3.73)

An example of a superconformal primary for a $\mathcal{B}[0, c_2, 0; 0]$ multiplet with $c_2 > 0$ is

$$\mathcal{O}_{\mu_1 \cdots \mu_{c_2}} = \epsilon_{\mathbf{AB}} \phi^{\mathbf{A}} \overset{\leftrightarrow}{\partial}_{\mu_1} \cdots \overset{\leftrightarrow}{\partial}_{\mu_{c_2}} \phi^{\mathbf{B}} \,, \tag{3.74}$$

where $\phi^A$ is a free hypermultiplet scalar. It is interesting to point out that for $c_1 = 1, c_2 = 0$ or $c_1 = 0, c_2 = 1$ the superconformal primary is not higher spin. The higher-spin currents are instead found as their descendants. Moreover, the superconformal primary in the multiplet of $\mathcal{B}[0, 1, 0; 0]$ is a $\Delta = 5$, R-neutral conserved current. However, as explained around (3.31) in the case of 5d, this is not a flavour current.

The corresponding superconformal index for any $c_1, c_2 \geq 0$ reads

$$\mathcal{I}_{\mathcal{B}[c_1,c_2,0;0]}(p,q,s) =$$
$$(-1)^{c_1+1} q^{4+\frac{1}{2}(c_1+2c_2)} \left\{ \frac{p^{-c_2} s^{c_2+5} \left(p^{-c_1} - p s^{c_1+1}\right) - p^{-c_1+2} s^{1-c_2}}{(pq-1)\,(p^2-s)\,(ps-1)\,(p-s^2)\,(q-s)(p-qs)} \right.$$

$$+\left.\frac{p^{c_2+5}s^{c_1+4}+p^{c_1+4}s^{-c_1}\left(s^{-c_2}-s^2p^{c_2+2}\right)}{(pq-1)\,(p^2-s)\,(ps-1)\,(p-s^2)\,(q-s)(p-qs)}\right\}. \tag{3.75}$$

**The Stress-Tensor Multiplet:** $\mathcal{B}[0,0,0;0]$

The last $\mathcal{B}$-type multiplet of note is the stress tensor. Ordinarily, the shortening conditions require that we remove $\mathcal{Q}_{\mathbf{1}a}\mathcal{Q}_{\mathbf{1}b}\mathcal{Q}_{\mathbf{1}c}$ from the basis of generators, but since $K=0$ we also obtain that $\mathcal{Q}_{\mathbf{A}a}\mathcal{Q}_{\mathbf{B}b}\mathcal{Q}_{\mathbf{C}c}$ should be removed from the auxiliary Verma module for $a\neq b\neq c$ and $\mathbf{A},\mathbf{B},\mathbf{C}=\mathbf{1},\mathbf{2}$. The resulting multiplet is therefore

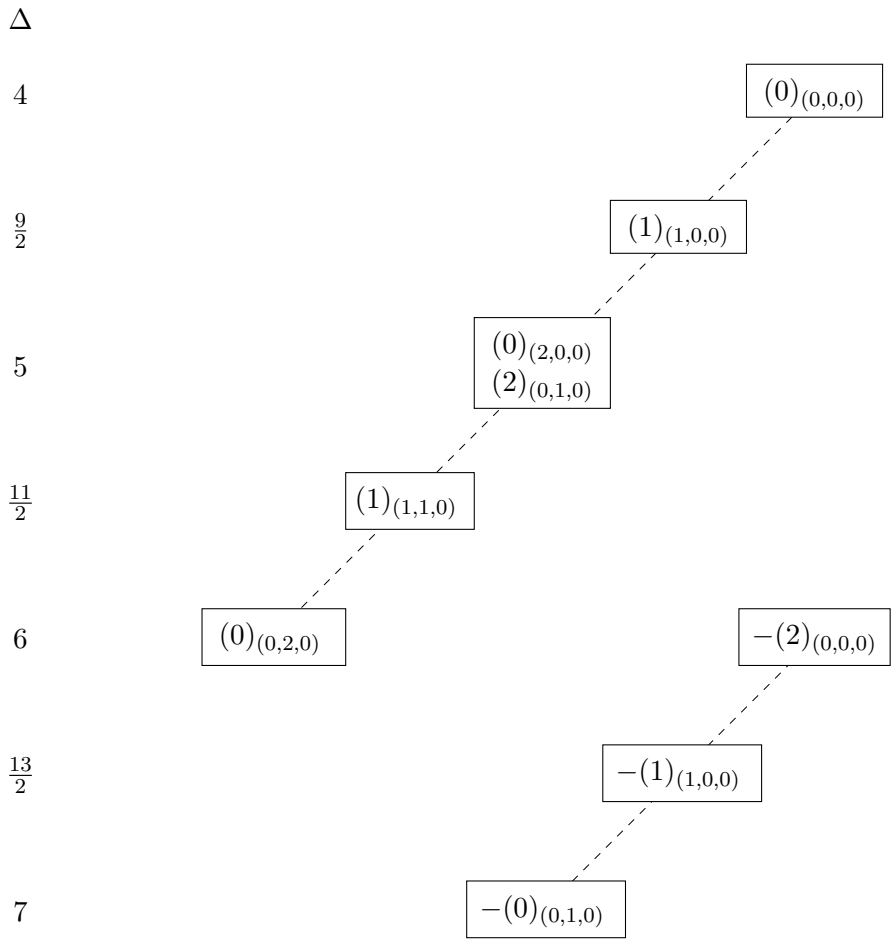


(3.76)

We recognise these states as being associated with the fields

$$\begin{aligned}
[5;0,1,0;2]: &\quad J_\mu^{(\mathbf{AB})}\,, & -[6;0,0,0;2]: &\quad \partial^\mu J_\mu^{(\mathbf{AB})}=0\,,\\
[11/2;1,1,0;1]: &\quad S_{\mu a}^{\mathbf{A}}\,, & -[13/2;1,0,0;1]: &\quad \partial^\mu S_{\mu a}^{\mathbf{A}}=0\,,\\
[6;0,2,0;0]: &\quad \Theta_{\mu\nu}\,, & -[7;0,1,0;0]: &\quad \partial^\mu\Theta_{\mu\nu}=0\,,
\end{aligned} \tag{3.77}$$

namely the 6d $R$-symmetry current, supersymmetry current and stress tensor. We also have three states that do not obey equations of motion. These are

$$\begin{aligned} [4;0,0,0;0]: &\quad \Sigma\ , \\ [9/2;1,0,0;1]: &\quad \zeta_a^{\mathbf{A}}\ , \\ [5;2,0,0;0]: &\quad Z^+_{(ab)}\ , \end{aligned} \tag{3.78}$$

where + denotes the selfdual part of the operator.

The index over this stress-tensor multiplet is

$$\mathcal{I}_{\mathcal{B}[0,0,0;0]}(p,q,s) = q^4 \frac{s^{-1}+p+p^{-1}s}{(1-pq)(1-qs^{-1})(1-p^{-1}qs)}\ , \tag{3.79}$$

counting three components of the $R$-symmetry current plus conformal descendants.

### $\mathcal{C}$-type Multiplets

The two distinct $\mathcal{C}$-type multiplets are $\mathcal{C}[c_1,0,0;K]$ and $\mathcal{C}[0,0,0;K]$, with the requirement that we remove $\mathcal{Q}_{\mathbf{1}a}$ for $a\neq 1$ and $\mathcal{Q}_{\mathbf{1}a}\mathcal{Q}_{\mathbf{1}b}$ respectively from the basis of Verma-module generators. On the one hand, since the generators $\mathcal{Q}_{\mathbf{1}3}$ and $\mathcal{Q}_{\mathbf{1}4}$ are absent, the set of available $\tilde{Q}$s is the same as for the $\mathcal{B}[c_1,c_2,0;K]$ case, that is $\mathcal{Q}_{\mathbf{2}3}$, $\mathcal{Q}_{\mathbf{2}4}$. On the other, only $\mathcal{Q}_{\mathbf{1}2}$ is removed from the set of $Q$s. Therefore the two resulting chains of supercharge actions on a generic state $(K)_{(c_1,c_2,c_3)}$ are

$$\begin{aligned} (K)_{(c_1,c_2,c_3)} &\xrightarrow{Q} (K\pm 1)_{(c_1+1,c_2,c_3)}\ , (K-1)_{(c_1-1,c_2+1,c_3)}\ , \\ &\xrightarrow{Q^2} (K-2)_{(c_1,c_2+1,c_3)}\ ,\ (K)_{(c_1+2,c_2,c_3),(c_1,c_2+1,c_3)}\ , \\ &\xrightarrow{Q^3} (K-1)_{(c_1+1,c_2+1,c_3)}\ , \\ (K)_{(c_1,c_2,c_3)} &\xrightarrow{\tilde{Q}} (K-1)_{(c_1,c_2-1,c_3+1),(c_1,c_2,c_3-1)}\ , \\ &\xrightarrow{\tilde{Q}^2} (K-2)_{(c_1,c_3+1,c_3)}\ . \end{aligned} \tag{3.80}$$

After substituting in the relevant $c_i$ values for the primary and implementing the RS algorithm we obtain for $\mathcal{C}[c_1,0,0;K]$

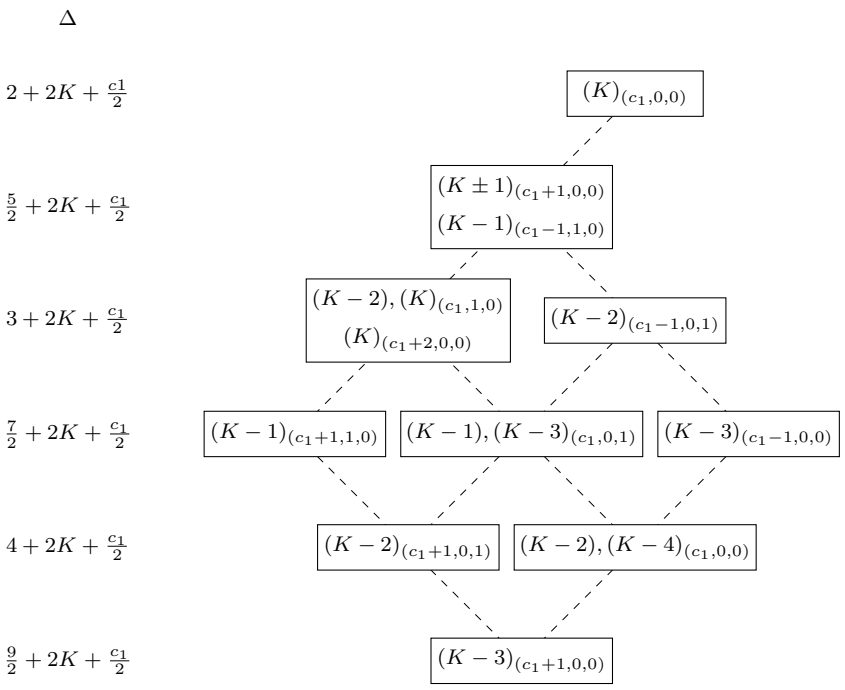


(3.81)

The corresponding superconformal index

$$\mathcal{I}_{\mathcal{C}[c_1,0,0;K]}(p,q,s) = (-1)^{c_1} q^{2+\frac{3K}{2}+\frac{c_1}{2}} \frac{p^{c_1+5}s^{-c_1}(ps-1)+p^2s^{c_1+5}\left(s-p^2\right)+p^{-c_1}s^2\left(p-s^2\right)}{(pq-1)\left(p^2-s\right)(ps-1)\left(p-s^2\right)(q-s)(qs-p)} , \quad (3.82)$$

which can be used in conjunction with $\mathcal{A}[c_1,0,0;K]$ to verify the recombination rules

$$\lim_{\epsilon\to 0}\mathcal{I}_{\mathcal{L}[\Delta+\epsilon;c_1,0,0;K]}(p,q,s) = \mathcal{I}_{\mathcal{A}[c_1,0,0;K]}(p,q,s)+\mathcal{I}_{\mathcal{C}[c_1-1,0,0;K+3]}(p,q,s) = 0 . \quad (3.83)$$

Turning our attention to $\mathcal{C}[0,0,0;K]$, we recall that the shortening conditions require the combinations $\mathcal{Q}_{\mathbf{1}a}\mathcal{Q}_{\mathbf{1}b}$ to be absent from the basis of Verma-module generators. The resulting spectrum is alternatively obtained by setting $c_1=0$ in $\mathcal{C}[c_1,0,0;K]$ and running the RS algorithm. This is a simple task: the lowest value of $c_1$ that appears in $\mathcal{C}[c_1,0,0;K]$ is $c_1-1$ and only these states are deleted when setting $c_1=0$—they will be on the boundary of the Weyl chamber. There is no need to perform any of the more elaborate Weyl reflections on any other state.

Therefore the spectrum for $\mathcal{C}[0,0,0;K]$ is given by

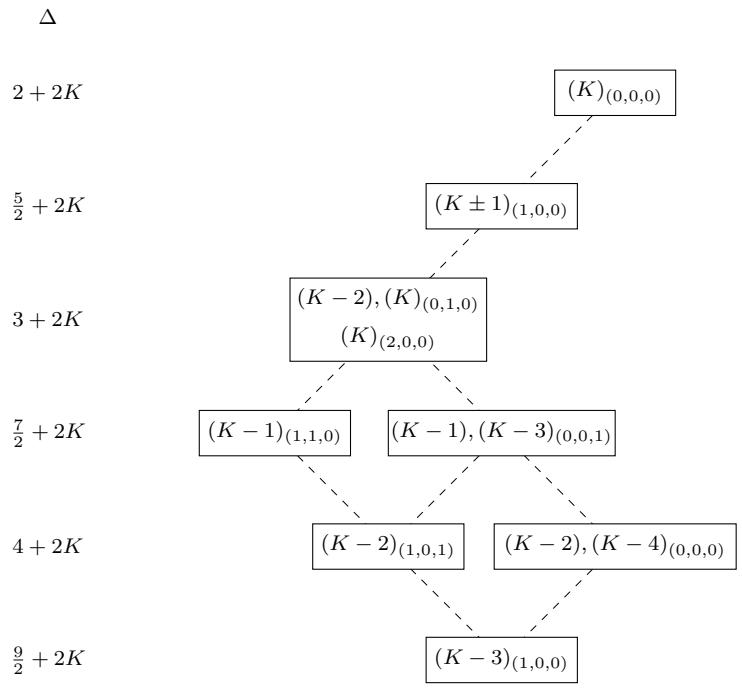


(3.84)

The associated index for $K > 1$ evaluates to

$$\mathcal{I}_{\mathcal{C}[0,0,0;K]}(p,q,s) = -q^{2+\frac{3K}{2}} \frac{s^{-1}p + s + p^{-1}}{(1-pq)(1-qs^{-1})(1-p^{-1}qs)} \,. \tag{3.85}$$

The cases with $K = 0, 1$ are predicted to contain operator constraints from (3.53) and will be dealt with separately below.

$\mathcal{C}[c_1,0,0;0]$

For this class of multiplets, $K = 0$ and we obtain additional shortening conditions. These can be translated into the requirement that $\mathcal{Q}_{\mathbf{A}a}$ for $a \neq 1$ be removed from the basis of Verma-module generators. The latter then in turn imply that $P_{23} \sim \{\mathcal{Q}_{\mathbf{12}}, \mathcal{Q}_{\mathbf{23}}\}$, $P_{24} \sim \{\mathcal{Q}_{\mathbf{12}}, \mathcal{Q}_{\mathbf{24}}\}$ and $P_{34} \sim \{\mathcal{Q}_{\mathbf{13}}, \mathcal{Q}_{\mathbf{24}}\}$ have also been removed from the auxiliary Verma-module basis. In vector notation, these momentum operators correspond respectively to $P_3$, $P_5$ and $P_6$. The implication of this fact is that the multiplet construction will only reproduce the reduced states, with the operator constraints hav-

ing been projected out. Thus the $\mathcal{C}[c_1,0,0;0]$ multiplet is very simply:

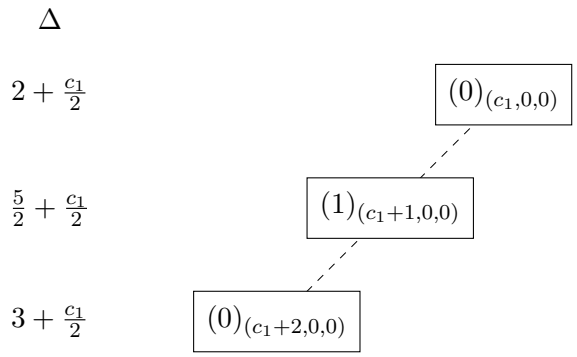


(3.86)

The operator constraints can be restored by means of App. B.1. Implementing this would result in introducing—for each of the three states in (3.86)—the following combinations

$$(K)^{\Delta}_{(c_1,0,0)}: \qquad -(K)^{\Delta+1}_{(c_1-1,0,1)}+(K)^{\Delta+2}_{(c_1-2,1,0)}-(K)^{\Delta+3}_{(c_1-2,0,0)}\,, \tag{3.87}$$

for a total of nine additional states corresponding to equations of motion. As a side comment, note that this spectrum is not the one we would have obtained had we just set $K=0$ in (3.81) and implemented the RS algorithm. As such, the index that one obtains is different to just setting $K=0$ in (3.82), and is given by

$$\begin{aligned}&\mathcal{I}_{\mathcal{C}[c_1,0,0;0]}=\\&(-1)^{c_1}q^{2+\frac{c_1}{2}}\left\{\frac{p^{c_1+5}s^{-c_1}(ps-1)+p^2s^{c_1+5}\left(s-p^2\right)+s^2p^{-c_1}\left(p-s^2\right)}{(pq-1)\left(p^2-s\right)(ps-1)\left(p-s^2\right)(q-s)(qs-p)}\right.\\&\left.-q\frac{p^{c_1+4}s^{1-c_1}(ps-1)+p^2s^{c_1+4}\left(s-p^2\right)+s^2p^{1-c_1}\left(p-s^2\right)}{(pq-1)\left(p^2-s\right)(ps-1)\left(p-s^2\right)(q-s)(qs-p)}\right\},\end{aligned} \tag{3.88}$$

where we see the appearance of more $\delta=0$ states being counted (or, rather, being removed due to equations of motion).

**The Free-Tensor Multiplet: $\mathcal{C}[0,0,0;0]$**

When $c_1=0$ we recover the free-tensor multiplet. In this case the lowering operator of $\mathfrak{su}(2)_R$ acts on the null-state condition $\mathcal{Q}_{\mathbf{11}}\mathcal{Q}_{\mathbf{12}}\Psi=0$ to create additional shortening conditions. This translates into the requirement that $\mathcal{Q}_{\mathbf{A}a}\mathcal{Q}_{\mathbf{B}b}$ for $a\neq b$ should be removed from the basis of Verma-module generators. The multiplet can be constructed

using the remaining supercharges and is given by

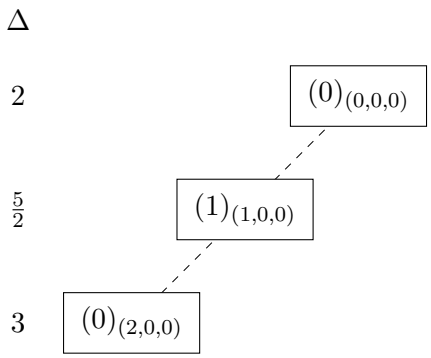


(3.89)

We identify the states with the following fields

$$\begin{aligned} [2;0,0;0;0]: &\quad \varphi\ , \\ [5/2;1,0,0;1]: &\quad \lambda_a^{\mathbf{A}}\ , \\ [3;2,0,0;0]: &\quad H^+_{[\mu\nu\rho]}\ . \end{aligned} \tag{3.90}$$

Similar to the previous subsection, (3.89) only contains reduced states and no equations of motion. When the latter are restored by means of App. B.1 we recover the expected

$$\begin{aligned} \partial^2\varphi = 0\ : &\quad -[4;0,0,0;0]\ , \\ \partial\!\!\!/^{\dot{a}b}\tilde{\lambda}_{\dot{b}}^{\mathbf{A}} = 0\ : &\quad -[7/2;0,0,1;1]\ , \\ \partial_{[\sigma}H^+_{\mu\nu\rho]} = 0\ : &\quad -[4;1,0,1;0]+[5;0,1,0;0]-[6;0,0,0;0]\ . \end{aligned} \tag{3.91}$$

The index for this configuration evaluates to

$$\mathcal{I}_{\mathcal{C}[0,0,0;0]}(p,q,s) = -q^2\frac{s^{-1}p+s+p^{-1}-q}{(1-pq)(1-qs^{-1})(1-p^{-1}qs)}\ , \tag{3.92}$$

counting three components of the fermion $\lambda_a^{\mathbf{A}}$ alongside its equation of motion. This matches the index later found in [119].

**Higher-Spin-Current Multiplets: $\mathcal{C}[c_1,0,0;1]$**

These multiplets are simple to construct since, contrary to the above case, we need not act with the $R$-symmetry lowering operator. As such, we can take the spectrum of (3.81) and set $K=1$ without incurring new shortening conditions. The resulting

$\mathcal{C}[c_1,0,0;1]$ multiplet is

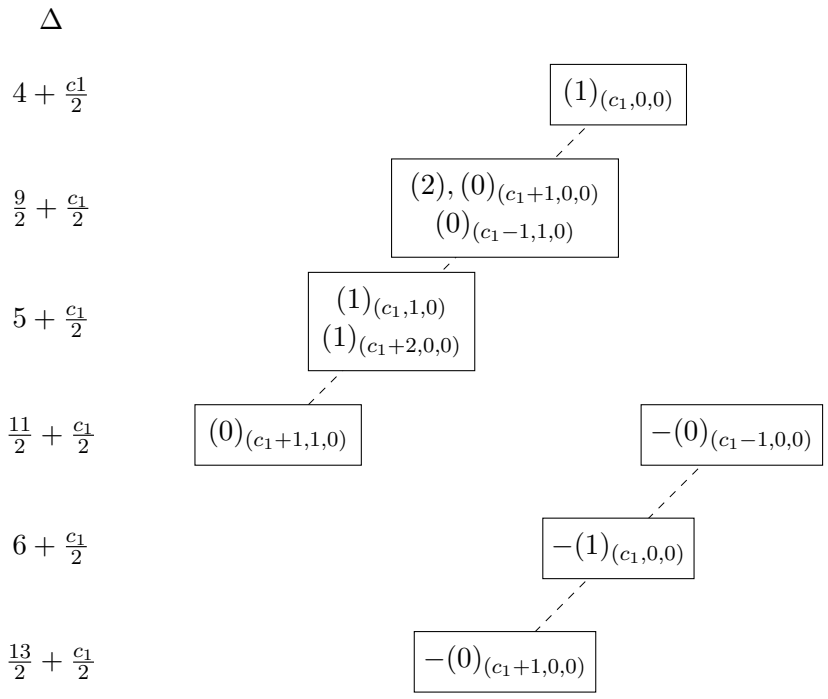


(3.93)

which includes conservation equations. It is worth pointing out that the multiplet with $c_1 = 1$ contains a $\Delta = 5$, R-neutral conserved current as a level one descendant. However, we see that there is also a spin-2 current with $\Delta = 6$ at level three.

The corresponding index evaluates to

$$\mathcal{I}_{\mathcal{C}[c_1,0,0;1]}(p,q,s) = q^{\frac{7}{2}+\frac{c_1}{2}} \frac{p^{c_1+5}s^{-c_1}(ps-1) + p^2 s^{c_1+5}\left(s-p^2\right) + p^{-c_1}s^2\left(p-s^2\right)}{(pq-1)\left(p^2-s\right)(ps-1)\left(p-s^2\right)(q-s)(qs-p)} \,. \tag{3.94}$$

Note that this index is valid for $c_1 = 0$. This is because setting $K = 1$ does not introduce any additional shortening conditions. However, when $c_1 = 0$ this multiplet does not contain currents with spin $j \geq 2$, and will be discussed below.

**"Extra"-Supercurrent Multiplet:** $\mathcal{C}[0,0,0;1]$

These multiplets can be constructed by substituting $K = 1$ into the spectrum of $\mathcal{C}[0,0,0;K]$. The result is

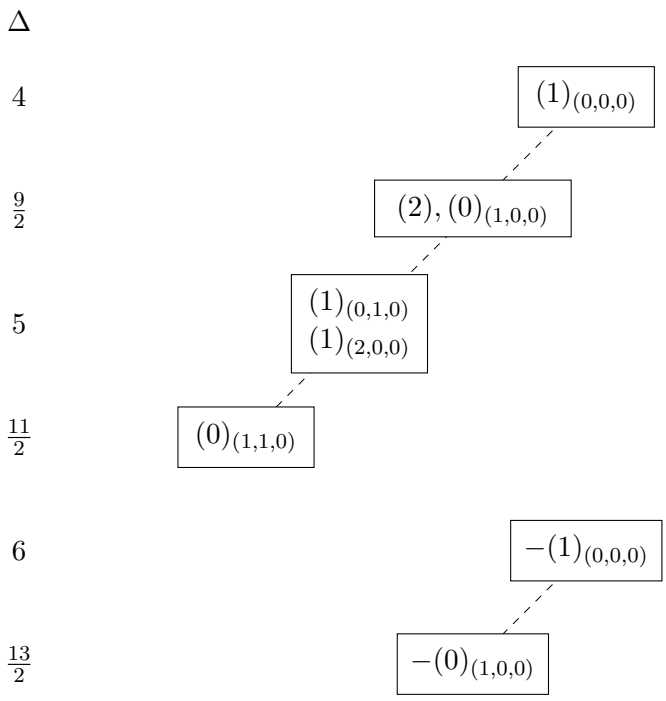


(3.95)

This multiplet contains a conserved $K = 1$ spin-1 current and a conserved R-neutral spin-$\frac{3}{2}$ current. These generate additional global and supersymmetry transformations, which—as we will discuss in Sec. 3.3.5—are necessary for the description of the (2,0) stress-tensor multiplet in the language of the (1,0) SCA.

Its index is then given by

$$\mathcal{I}_{\mathcal{C}[0,0,0;1]}(p,q,s) = -q^{\frac{7}{2}} \frac{s^{-1}p + s + p^{-1}}{(1-pq)(1-qs^{-1})(1-p^{-1}qs)} \,. \tag{3.96}$$

### $\mathcal{D}$-type multiplets

We finally turn to the $\mathcal{D}[0,0,0;K]$ multiplets. These are the simplest of the 6d $(1,0)$ SCA for generic values of $K$. Since the shortening condition is $A^1\Psi = \mathcal{Q}_{\mathbf{11}}\Psi = 0$, acting with all Lorentz lowering operators leads to

$$\mathcal{Q}_{\mathbf{1}a}\Psi = 0 \tag{3.97}$$

and hence the multiplet is $\frac{1}{2}$–BPS.

Starting with a generic superconformal primary state $(K)_{(c_1,c_2,c_3)}$, the two chains obtained from the action of $Q$s and $\tilde{Q}$s are

$$\begin{aligned}(K)_{(c_1,c_2,c_3)} &\xrightarrow{Q} (K-1)_{(c_1+1,c_2,c_3),(c_1-1,c_2+1,c_3)} \,, \\ &\xrightarrow{Q^2} (K-2)_{(c_1,c_2+1,c_3)} \,,\end{aligned}$$

$$(K)_{(c_1,c_2,c_3)} \xrightarrow{\tilde{Q}} (K-1)_{(c_1,c_2-1,c_3+1),(c_1,c_2,c_3-1)} \,, \tag{3.98}$$

$$\xrightarrow{\tilde{Q}^2} (K-2)_{(c_1,c_3+1,c_3)} \,. \tag{3.99}$$

One then needs to set $c_i = 0$ and run the RS algorithm. Upon doing so, the result is

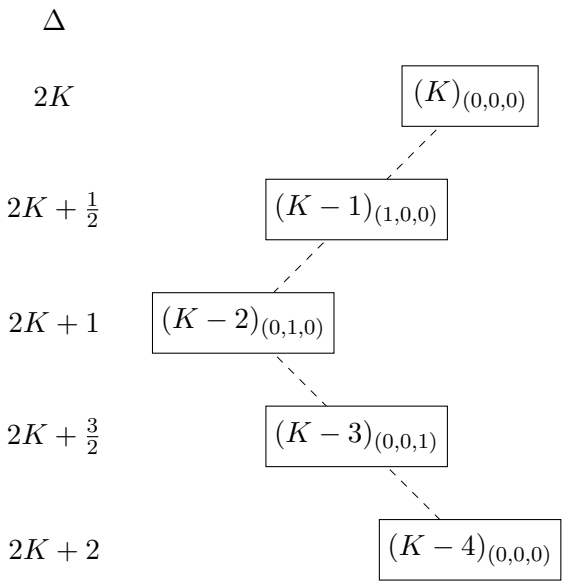


(3.100)

We notice that for $K \leq 2$ the above will lead to negative-multiplicity representations via the RS algorithm and hence operator constraints, to be discussed in the next section.

The superconformal index for $K > 2$ is given by

$$\mathcal{I}_{\mathcal{D}[0,0,0;K]}(p,q,s) = \frac{q^{\frac{3K}{2}}}{(1-pq)(1-qs^{-1})(1-p^{-1}qs)} \,. \tag{3.101}$$

**The Hypermultiplet: $\mathcal{D}[0,0,0;1]$**

Setting $K = 1$ in the $\mathcal{D}[0,0,0;K]$ multiplet will not incur any nontrivial changes to the spectrum, as it does not lead to additional shortening conditions. As a result, we may

simply write the multiplet out as

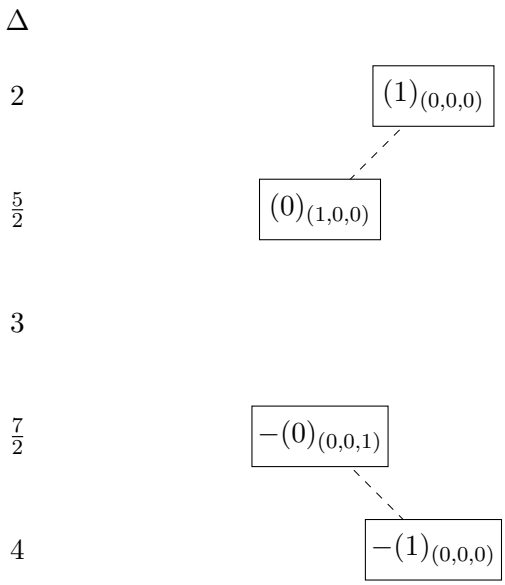


(3.102)

These states can be interpreted as a scalar $\phi^{\mathbf{A}}$ with its associated Klein–Gordon equation $\partial^2\phi^{\mathbf{A}} = 0$ and a fermion $\psi_a$ alongside the Dirac equation $\partial^{\dot{a}b}\tilde{\psi}_{\dot{b}} = 0$.

The corresponding index is given by

$$\mathcal{I}_{\mathcal{D}[0,0,0;1]}(p,q,s) = \frac{q^{\frac{3}{2}}}{(1-pq)(1-qs^{-1})(1-p^{-1}qs)} \,. \tag{3.103}$$

**The Flavour-Current Multiplet:** $\mathcal{D}[0,0,0;2]$

As above, we can simply substitute $K=2$ into $\mathcal{D}[0,0,0;K]$ to generate this spectrum, as there are no additional shortening conditions. The result is

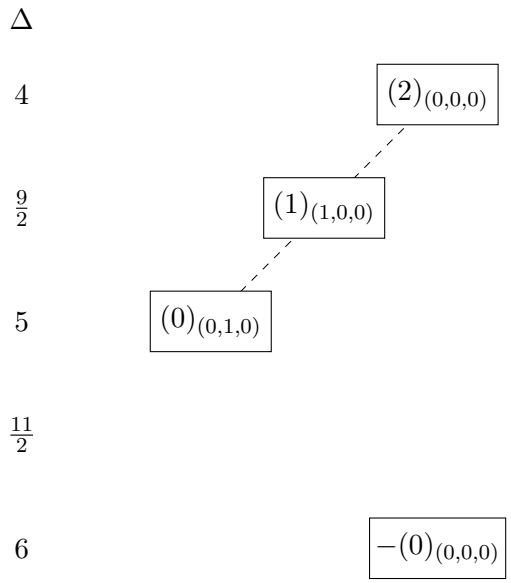


(3.104)

These states can be identified with the operators $\mu^{(\mathbf{AB})}$, $\psi_a^{\mathbf{A}}$ and the $\mathfrak{su}(2)_R$-singlet conserved current $J_\mu$, with $\partial^\mu J_\mu = 0$. This multiplet is also known as a linear multiplet and appears in [116, 120, 121].

The index for this multiplet is given by

$$\mathcal{I}_{\mathcal{D}[0,0,0;2]}(p,q,s) = \frac{q^3}{(1-pq)(1-qs^{-1})(1-p^{-1}qs)} \,. \tag{3.105}$$

We conclude our discussion of the superconformal multiplets for the 6d (1,0) SCA by noting that all these indices admit a nice rewriting in terms of characters of the maximally commuting subalgebra:

$$\begin{aligned}
\mathcal{I}_{\mathcal{A}[c_1,c_2,c_3;K]}(p,q,s) &= (-1)^{c_1+c_3+1}\frac{q^{\frac{c_1+2c_2+3c_3}{2}+\frac{3K}{2}+6}}{(1-pq)\,(1-qs^{-1})\,(1-p^{-1}qs)}\chi^{\mathfrak{su}(3)}_{(c_2,c_1)}(p,s)\,,\\
\mathcal{I}_{\mathcal{B}[c_1,c_2,0;K]}(p,q,s) &= (-1)^{c_1}\frac{q^{\frac{c_1+2c_2}{2}+\frac{3K}{2}+4}}{(1-pq)\,(1-qs^{-1})\,(1-p^{-1}qs)}\chi^{\mathfrak{su}(3)}_{(c_2+1,c_1)}(p,s)\,,\\
\mathcal{I}_{\mathcal{C}[c_1,0,0;K]}(p,q,s) &= (-1)^{c_1+1}\frac{q^{\frac{c_1}{2}+\frac{3K}{2}+2}}{(1-pq)\,(1-qs^{-1})\,(1-p^{-1}qs)}\chi^{\mathfrak{su}(3)}_{(0,c_1+1)}(p,s)\,,\\
\mathcal{I}_{\mathcal{C}[c_1,0,0;0]}(p,q,s) &= (-1)^{c_1+1}\frac{q^{\frac{c_1}{2}+2}}{(1-pq)\,(1-qs^{-1})\,(1-p^{-1}qs)}\chi^{\mathfrak{su}(3)}_{(0,c_1+1)}(p,s)\\
&\quad+(-1)^{c_1}\frac{q^{\frac{c_1}{2}+3}}{(1-pq)\,(1-qs^{-1})\,(1-p^{-1}qs)}\chi^{\mathfrak{su}(3)}_{(0,c_1)}(p,s)\,,
\end{aligned}$$

$$\mathcal{I}_{\mathcal{D}[0,0,0;K]}(p,q,s)=\frac{q^{\frac{3K}{2}}}{(1-pq)\,(1-qs^{-1})\,(1-p^{-1}qs)}\,, \tag{3.106}$$

where

$$\chi^{\mathfrak{su}(3)}_{(m,n)}(p,s)=\frac{\begin{vmatrix} p^{m+n+2} & s^{-2-m-n} & \left(\frac{s}{p}\right)^{m+n+2} \\ p^{n+1} & s^{-n-1} & \left(\frac{s}{p}\right)^{n+1} \\ 1 & 1 & 1 \end{vmatrix}}{\begin{vmatrix} p^{2} & s^{-2} & \left(\frac{s}{p}\right)^{2} \\ p^{1} & s^{-1} & \left(\frac{s}{p}\right) \\ 1 & 1 & 1 \end{vmatrix}}\,. \tag{3.107}$$

### 3.3.5 Supersymmetry Enhancement of 6d $(1,0)$ Multiplets

An important consistency condition for the 6d $\mathcal{N}=1$ multiplets is that they can combine to form $\mathcal{N}=2$ multiplets. For instance, one should be able to construct the additional supersymmetry and $R$-symmetry currents of the $\mathcal{N}=2$ SCA from these multiplets. The $\mathcal{N}=2$ case will be treated in more detail in the next section, so we will only focus on two of the simplest multiplets: the free tensor and the stress tensor. This will use the results and naming conventions of the upcoming section.

For the first, we need only consider the $R$ symmetry, since the Lorentz quantum numbers are the same for both cases. We identify the $\mathfrak{su}(2)_R \subset \mathfrak{so}(5)_R$ by choosing $K=d_1$; note that as a result distinct states for $\mathcal{N}=2$ can give rise to the same state for $\mathcal{N}=1$. The free tensor in $\mathcal{N}=2$ has the $R$-symmetry highest weight $(1,0)$, which corresponds to a representation with Dynkin values $(1,0)$, $(-1,2)$, $(0,0)$, $(1,-2)$ and $(-1,0)$. Reducing this to $\mathfrak{su}(2)_R$ results in the states $2\times(1)$, $(0)$ and $2\times(-1)$. Another way of writing this is in terms of three modules, two with highest weights labelled by $(1)$ and one labelled by $(0)$. Thus the superconformal primary of $\mathcal{D}[0,0,0;1,0]$ can be identified with two primaries from the $\mathcal{N}=1$ hypermultiplet and one from the $\mathcal{N}=1$ tensor multiplet. Indeed one can repeat this for every state in $\mathcal{D}[0,0,0;1,0]$ and the result is that the entire multiplet is written as

$$\mathcal{D}[0,0,0;1,0]\simeq 2\mathcal{D}[0,0,0;1]\oplus\mathcal{C}[0,0,0;0]\,, \tag{3.108}$$

where the equivalence is up to the identification $d_1=K$.

One can similarly rewrite the stress-tensor multiplet of $\mathcal{N}=2$, as a collection of $\mathcal{N}=1$ multiplets. The result is that

$$\mathcal{D}[0,0,0;2,0]\simeq 3\mathcal{D}[0,0,0;2]\oplus 2\mathcal{C}[0,0,0;1]\oplus\mathcal{B}[0,0,0;0]\,, \tag{3.109}$$

where the equivalence is again up to the identification $d_1 = K$, confirming the original expectation.[19]

## 3.4 Multiplets and Superconformal Indices for 6d (2,0)

We lastly turn to the construction of superconformal multiplets for the 6d (2,0) SCA, $\mathfrak{osp}(8^*|4)$. Since we now have sixteen Poincaré supercharges, the UIRs will be much larger compared to the ones obtained in Sec. 3.2 and Sec. 3.3 and representing them diagrammatically would not be particularly instructive. Similarly, the full expressions for the most general ("refined") superconformal indices are unwieldy. In [24] the "Schur" limit was provided, and the accompanying `mathematica` notebook of [1]. Here we do something slightly different, and define a MacDonald-like index, analagous to the one defined in [48].[20]

In contrast to the other sections, we will only explicitly display the half-BPS multiplets and those that contain generalised equations of motion. This is because, with sixteen supercharges, the modules rapidly grow in size. Full details can be found by using the `python` package detailed in Section B.2.

### 3.4.1 UIR Building with Auxiliary Verma Modules

The superconformal primaries of the algebra $\mathfrak{osp}(8^*|4)$ are designated $|\Delta; c_1, c_2, c_3; d_1, d_2\rangle$ and labelled by the conformal dimension $\Delta$, the Lorentz quantum numbers for $\mathfrak{su}(4)$ in the Dynkin basis $c_i$ and the $R$-symmetry quantum numbers in the Dynkin basis $d_i$. Each primary is in one-to-one correspondence with a highest weight labeling irreducible representations of the maximal compact subalgebra $\mathfrak{so}(6) \oplus \mathfrak{so}(2) \oplus \mathfrak{so}(5)_R \subset \mathfrak{osp}(8^*|4)$. There are sixteen Poincaré and superconformal supercharges, denoted by $\mathcal{Q}_{\mathbf{A}a}$ and $\mathcal{S}_{\mathbf{A}\dot{a}}$, where $\dot{a}, a = 1, \ldots, 4$ are (anti)fundamental indices of $\mathfrak{su}(4)$ and $\mathbf{A} = 1, \ldots, 4$ a spinor index of $\mathfrak{so}(5)_R$. One also has six momenta $P_\mu$ and special conformal generators $K_\mu$, where $\mu$ is a vector index of the Lorentz group, $\mu = 1, \cdots, 6$. The superconformal primary is annihilated by all $\mathcal{S}_{\mathbf{A}\dot{a}}$ and $K_\mu$. A basis for the representation space of $\mathfrak{osp}(8^*|4)$ can be constructed by considering the Verma module

$$\prod_{\mathbf{A},a} (\mathcal{Q}_{\mathbf{A}a})^{n_{\mathbf{A},a}} \prod_{\mu} {P_\mu}^{n_\mu} |\Delta; c_1, c_2, c_3; d_1, d_2\rangle^{hw} \ , \tag{3.110}$$

[19] For example, note that we find precisely the expected decomposition of the $\mathfrak{so}(5)_R$ currents (recall that these are level two superconformal descendants of the $\mathcal{D}[0,0,0;2,0]$ multiplet) in terms of representations of $\mathfrak{su}(2)_R$: $\mathbf{10} = 3 \times \mathbf{1} + 2 \times \mathbf{2} + 1 \times \mathbf{3}$.

[20] A discussion of the null states for the 6d (2,0) SCA, along with the calculation of Schur indices for the various short multiplets, can be found in App. C of [24]. Here we additionally construct the full multiplets with an emphasis on the equations of motion and conservation equations.

| Multiplet | Shortening Condition | Conformal Dimension |
|---|---|---|
| $\mathcal{A}[c_1,c_2,c_3;d_1,d_2]$ | $A^4\Psi=0$ | $\Delta=2d_1+2d_2+\frac{c_1}{2}+c_2+\frac{3c_3}{2}+6$ |
| $\mathcal{A}[c_1,c_2,0;d_1,d_2]$ | $A^3A^4\Psi=0$ | $\Delta=2d_1+2d_2+\frac{c_1}{2}+c_2+6$ |
| $\mathcal{A}[c_1,0,0;d_1,d_2]$ | $A^2A^3A^4\Psi=0$ | $\Delta=2d_1+2d_2+\frac{c_1}{2}+6$ |
| $\mathcal{A}[0,0,0;d_1,d_2]$ | $A^1A^2A^3A^4\Psi=0$ | $\Delta=2d_1+2d_2+6$ |
| $\mathcal{B}[c_1,c_2,0;d_1,d_2]$ | $A^3\Psi=0$ | $\Delta=2d_1+2d_2+\frac{c_1}{2}+c_2+4$ |
| $\mathcal{B}[c_1,0,0;d_1,d_2]$ | $A^2A^3\Psi=0$ | $\Delta=2d_1+2d_2+\frac{c_1}{2}+4$ |
| $\mathcal{B}[0,0,0;d_1,d_2]$ | $A^1A^2A^3\Psi=0$ | $\Delta=2d_1+2d_2+4$ |
| $\mathcal{C}[c_1,0,0;d_1,d_2]$ | $A^2\Psi=0$ | $\Delta=2d_1+2d_2+\frac{c_1}{2}+2$ |
| $\mathcal{C}[0,0,0;d_1,d_2]$ | $A^1A^2\Psi=0$ | $\Delta=2d_1+2d_2+2$ |
| $\mathcal{D}[0,0,0;d_1,d_2]$ | $A^1\Psi=0$ | $\Delta=2d_1+2d_2$ |

**Table 4:** A list of all short multiplets for the 6d $(2,0)$ SCA, along with the shortening condition and conformal dimension of the superconformal primary. The $A^a$ in the shortening conditions are defined in (3.52) and [42]. The first of these multiplets ($\mathcal{A}$) is a regular short representation, whereas the rest ($\mathcal{B},\mathcal{C},\mathcal{D}$) are isolated short representations. Here $\Psi$ denotes the superconformal primary state for each multiplet.

where $n=\sum_{\mathbf{A}a}n_{\mathbf{A},a}$ and $\hat{n}=\sum_\mu n_\mu$ denote the level of a superconformal or conformal descendant respectively. In order to obtain UIRs, the requirement of unitarity needs to be imposed level-by-level on the Verma module. This leads to bounds on the conformal dimension $\Delta$.

Starting with the superconformal descendants, the conditions imposed by unitarity can be deduced as follows. In principle, one needs to calculate the norms of superconformal descendants for $n>0$. However, since it is sufficient to perform this analysis in the highest weight of the $R$-symmetry group [36, 42, 92], the results of Sec. 3.52 can be easily imported to the (2,0) case and we may still use the basis $A^{a_i}\cdots A^{a_j}\,|\Delta;c_1,c_2,c_3;d_1,d_2\rangle^{hw}$.[21] We need only convert the Cartan for the highest weight of $\mathfrak{su}(2)_R$ to $\mathfrak{so}(5)_R$, which is done by simply replacing $K\to d_1+d_2$. This gives rise to a group of similar short multiplets, which we collect in Table 4. We will provide more details regarding the generators that are absent from the auxiliary Verma module when discussing individual multiplets. Furthermore, it will be important to clarify which additional absent generators can occur from tuning the $R$-symmetry quantum numbers, $d_1$ and $d_2$. These turn out to be far more intricate than for (1,0). The null states arising from conformal descendants are identical to Sec. 3.3. One can combine the information from the conformal and superconformal unitarity bounds to predict when a multiplet will contain operator constraints [36, 109]. These special cases are

$$\mathcal{B}[c_1,c_2,0;0,0]\ ,\quad \mathcal{C}[c_1,0,0;d_1,d_2]\quad \text{for } d_1+d_2\leq 1\ ,$$

[21] The analysis in [36, 42, 92] was performed for generic $R$-symmetry $\mathfrak{sp}(\mathcal{N})$. The construction is largely focussed around the Lorentz Cartans and raising operators.

$$\mathcal{D}[0,0,0;d_1,d_2] \quad \text{for } d_1+d_2\leq 2\ . \tag{3.111}$$

The multiplet $\mathcal{D}[0,0,0;0,0]$ does not belong to this list as it is the vacuum, which is annihilated by all supercharges and momenta.

### 3.4.2 6d (2,0) Recombination Rules

Short multiplets can recombine into a long multiplet $\mathcal{L}$. This occurs when the conformal dimension of $\mathcal{L}$ approaches the unitarity bound, that is when $\Delta+\epsilon\to 2d_1+2d_2+\frac{1}{2}(c_1+2c_2+3c_3)+6$. As in [24], we find that

$$\begin{aligned}
\mathcal{L}[\Delta+\epsilon;c_1,c_2,c_3;d_1,d_2] &\xrightarrow{\epsilon\to 0} \mathcal{A}[c_1,c_2,c_3;d_1,d_2]\oplus\mathcal{A}[c_1,c_2,c_3-1;d_1,d_2+1]\ ,\\
\mathcal{L}[\Delta+\epsilon;c_1,c_2,0;d_1,d_2] &\xrightarrow{\epsilon\to 0} \mathcal{A}[c_1,c_2,0;d_1,d_2]\oplus\mathcal{B}[c_1,c_2-1,0;d_1,d_2+2]\ ,\\
\mathcal{L}[\Delta+\epsilon;c_1,0,0;d_1,d_2] &\xrightarrow{\epsilon\to 0} \mathcal{A}[c_1,0,0;d_1,d_2]\oplus\mathcal{C}[c_1-1,0,0;d_1,d_2+3]\ ,\\
\mathcal{L}[\Delta+\epsilon;0,0,0;d_1,d_2] &\xrightarrow{\epsilon\to 0} \mathcal{A}[0,0,0;d_1,d_2]\oplus\mathcal{D}[0,0,0;d_1,d_2+4]\ .
\end{aligned} \tag{3.112}$$

A small number of short multiplets do not appear in a recombination rule. These are

$$\begin{aligned}
&\mathcal{B}\left[c_1,c_2,0;d_1,\{0,1\}\right]\ ,\\
&\mathcal{C}\left[c_1,0,0;d_1,\{0,1,2\}\right]\ ,\\
&\mathcal{D}\left[0,0,0;d_1,\{0,1,2,3\}\right]\ .
\end{aligned} \tag{3.113}$$

### 3.4.3 The 6d (2,0) Superconformal Index

We define the 6d (2,0) superconformal index with respect to the supercharge $\mathcal{Q}_{\mathbf{2}4}$. This is given by

$$\mathcal{I}(p,q,s,t)=\mathrm{Tr}_{\mathcal{H}}(-1)^F e^{-\beta\delta}q^{\Delta-d_1-\frac{1}{2}d_2}p^{c_2+c_3-d_2}t^{d_1+d_2}s^{c_1+c_2}\ , \tag{3.114}$$

where the fermion number is $F=c_1+c_3$. The states that are counted satisfy $\delta=0$, with

$$\delta:=\{\mathcal{Q}_{\mathbf{2}4},\mathcal{S}_{\mathbf{3}\dot{4}}\}=\Delta-2d_1-\frac{1}{2}(c_1+2c_2+3c_3)\ . \tag{3.115}$$

The exponents appearing in (3.114) are the eigenvalues for the generators commuting with $\mathcal{Q}_{\mathbf{2}4}$, $\mathcal{S}_{\mathbf{3}\dot{4}}$ and $\delta$. This index can be evaluated as a 6d supercharacter; this is discussed in our Sec. 3.5 and App. C of [24].

### The 6d MacDonald limit

The authors of [24] define the 6d Schur limit by taking $t \to 1$ in (3.114). We define a one-parameter refinement of this index, which single out the same set of multiplets but with an additional fugacity. The limit is obtained by taking $p \to 0$

$$\mathcal{I}^{Mac}(t,q,s) = \mathrm{Tr}_{\mathcal{H}}(-1)^F e^{-\beta\,\delta} q^{\Delta - d_1 - \frac{1}{2}d_2} t^{d_1+d_2} s^{c_1+c_2} \ , \tag{3.116}$$

subject to the constraint that $d_2 = c_2 + c_3$. Note that under this constraint

$$\delta' := \{\mathcal{Q}_{\mathbf{12}}, \mathcal{S}_{\mathbf{4}\dot{2}}\} = \Delta - 2d_1 - 2d_2 - \frac{1}{2}(c_1 - 2c_2 - c_3) = \delta \ . \tag{3.117}$$

We therefore have that both $\delta = 0 = \delta'$, hence the exponents in (3.116) commute with the supercharge $\mathcal{Q}_{\mathbf{12}}$ and the 6d MacDonald index consequently counts operators annihilated by two supercharges. The operators contributing to the index in this limit satisfy

$$\begin{aligned} \Delta &= 2d_1 + d_2 + \frac{1}{2}(c_1 + c_3) \ , \\ d_2 &= c_2 + c_3 \ , \end{aligned} \tag{3.118}$$

which project onto the same subset of states as the Schur limit that was defined in [24]. Of course, one can unrefine this index by sending $t \to 1$ whereupon it becomes the Schur index. An additional limit exists, known as the half-BPS limit, which only receives non-zero contributions from the half-BPS multiplets. This is obtained by holding the combination $x := qt$ fixed and sending $q \to 0$. This is a very simple limit which does not count derivatives. It was calculated for the interacting $A_N$ type $(2,0)$ theories in [122].

## 3.4.4 6d (2,0) Multiplets

### Long multiplets

Long multiplets are constructed by acting with all supercharges on a superconformal primary $(d_1, d_2)_{(c_1,c_2,c_3)}$. This leads to lengthy expressions which, although not presented here, are available from the `python` package. For book-keeping purposes we will group the supercharges into $Q = (\mathcal{Q}_{\mathbf{2}a}, \mathcal{Q}_{\mathbf{3}a})$ and $\tilde{Q} = (\mathcal{Q}_{\mathbf{1}a}, \mathcal{Q}_{\mathbf{4}a})$ for the remaining of the 6d (2,0) discussion.

### $\mathcal{A}$-type multiplets

Recall from Table 4 that the $\mathcal{A}$-type multiplets obey four kinds of shortening conditions. These result in the removal of the following supercharges from the basis of Verma

module generators in (3.110)

$$\begin{aligned}\mathcal{A}[c_1,c_2,c_3;d_1,d_2] &: \mathcal{Q}_{\mathbf{14}}\ ,\\ \mathcal{A}[c_1,c_2,0;d_1,d_2] &: \mathcal{Q}_{\mathbf{13}}\mathcal{Q}_{\mathbf{14}}\ ,\\ \mathcal{A}[c_1,0,0;d_1,d_2] &: \mathcal{Q}_{\mathbf{12}}\mathcal{Q}_{\mathbf{13}}\mathcal{Q}_{\mathbf{14}}\ ,\\ \mathcal{A}[0,0,0;d_1,d_2] &: \mathcal{Q}_{\mathbf{11}}\mathcal{Q}_{\mathbf{12}}\mathcal{Q}_{\mathbf{13}}\mathcal{Q}_{\mathbf{14}}\ .\end{aligned} \tag{3.119}$$

The $\mathcal{A}$-type multiplets cannot contain operator constraints for any $d_1$ or $d_2$.

One can arrive at new shortening conditions—and as a result a reduced number of $\mathcal{Q}$-generators—for $d_1 \neq 0$, $d_2 = 0$ and $d_1 = d_2 = 0$. Consider for instance the case $\mathcal{A}[c_1,c_2,c_3;d_1,0]$. From Table 4 the null state reads $A^4\Psi = 0$. In the auxiliary Verma-module basis, this corresponds to $\mathcal{Q}_{\mathbf{14}}\Psi = 0$. However, since $d_2 = 0$ one also finds that $\mathcal{R}_2^-\mathcal{Q}_{\mathbf{14}}\Psi = 0$. This corresponds to having to additionally remove $\mathcal{Q}_{\mathbf{24}}$ from our Verma-module basis. Following on from this, when $d_1 = 0$ the operator $\mathcal{R}_1^-$ also annihilates the superconformal primary and two new conditions are obtained: $\mathcal{R}_1^-\mathcal{R}_2^-\mathcal{Q}_{\mathbf{14}}\Psi = 0$ and $\mathcal{R}_2^-\mathcal{R}_1^-\mathcal{R}_2^-\mathcal{Q}_{\mathbf{14}}\Psi = 0$. These correspond to also removing $\mathcal{Q}_{\mathbf{34}}$ and $\mathcal{Q}_{\mathbf{44}}$ respectively from the basis of Verma-module generators.

All $\mathcal{A}$-type multiplets have zero contribution to the MacDonald limit of the 6d (2,0) index. In the fully refined case they are non-zero and satisfy

$$\begin{aligned}&\lim_{\epsilon\to 0}\mathcal{I}_{\mathcal{L}[\Delta+\epsilon;c_1,c_2,c_3;d_1,d_2]}(p,q,s,t) =\\ &\quad\mathcal{I}_{\mathcal{A}[c_1,c_2,c_3;d_1,d_2]}(p,q,s,t) + \mathcal{I}_{\mathcal{A}[c_1,c_2,c_3-1;d_1,d_2+1]}(p,q,s,t) = 0\ ,\end{aligned} \tag{3.120}$$

when $\Delta = 6 + 2d_1 + 2d_2 + \frac{1}{2}(c_1 + 2c_2 + 3c_3)$.

As with the long multiplets, these multiplets are too enormous to display neatly, so we can defer to the `python` package for the explicit structure.

### $\mathcal{B}$-type multiplets

For the $\mathcal{B}$-type multiplets, the supercharges that need to be removed from the Verma-module basis (3.110) are

$$\begin{aligned}\mathcal{B}[c_1,c_2,0;d_1,d_2] &: \mathcal{Q}_{\mathbf{13}}\ ,\\ \mathcal{B}[c_1,0,0;d_1,d_2] &: \mathcal{Q}_{\mathbf{12}}\mathcal{Q}_{\mathbf{13}}\ ,\\ \mathcal{B}[0,0,0;d_1,d_2] &: \mathcal{Q}_{\mathbf{11}}\mathcal{Q}_{\mathbf{12}}\mathcal{Q}_{\mathbf{13}}\ .\end{aligned} \tag{3.121}$$

For the first type of multiplet, $\mathcal{B}[c_1,c_2,0;d_1,d_2]$, one should also remove $\mathcal{Q}_{\mathbf{14}}$ as the state $A^4\Psi$ is ill defined. A similar argument can be made regarding $\mathcal{B}[c_1,0,0;d_1,d_2]$ to reach the conclusion that $\mathcal{Q}_{\mathbf{12}}\mathcal{Q}_{\mathbf{13}}$, $\mathcal{Q}_{\mathbf{12}}\mathcal{Q}_{\mathbf{14}}$ and $\mathcal{Q}_{\mathbf{13}}\mathcal{Q}_{\mathbf{14}}$ should be removed from the

Verma-module basis. For $\mathcal{B}[0,0,0;d_1,d_2]$ these additional supercharges are $\mathcal{Q}_{\mathbf{1}a}\mathcal{Q}_{\mathbf{1}b}\mathcal{Q}_{\mathbf{1}c}$ with $a \neq b \neq c$, exactly as in Sec. 3.3.4.

There are three distinct sub-cases that need to be considered when dialling $d_1$, $d_2$. These are:

1. $\mathcal{B}[c_1,c_2,0;d_1,1]$: When $d_2 = 1$ we find that $(\mathcal{R}_2^-)^2\Psi = 0$. This leads to the combination $\mathcal{Q}_{\mathbf{2}3}\mathcal{Q}_{\mathbf{2}4}$ being additionally removed from the basis of Verma-module generators [24].

2. $\mathcal{B}[c_1,c_2,0;d_1,0]$: Having $d_2 = 0$ implies that $\mathcal{R}_2^-\Psi = 0$. This means that $\mathcal{R}_2^-\mathcal{Q}_{\mathbf{1}3}\Psi = 0$. Furthermore, since $A^4\Psi$ is ill defined, the combination $\mathcal{R}_2^- A^4\Psi$ is similarly ill defined. Thus we remove $\mathcal{Q}_{\mathbf{2}3}$ and $\mathcal{Q}_{\mathbf{2}4}$ from the basis of Verma-module generators as they are associated with ill-defined states.

3. $\mathcal{B}[c_1,c_2,0;0,0]$: When $d_1 = d_2 = 0$ all $R$-symmetry lowering operators annihilate the primary. Hence we can apply the above logic while including the lowering operator $\mathcal{R}_1^-$. One finds that the supercharges $\mathcal{Q}_{\mathbf{3}3}$, $\mathcal{Q}_{\mathbf{4}3}$, $\mathcal{Q}_{\mathbf{3}4}$, $\mathcal{Q}_{\mathbf{4}4}$ should also be removed as well as the above from the basis of Verma-module generators as they are associated with ill-defined states.

According to (3.111) the multiplets $\mathcal{B}[c_1,c_2,0;0,0]$ should contain operator constraints. However, the removal of $\mathcal{Q}_{\mathbf{A}3}$ and $\mathcal{Q}_{\mathbf{A}4}$ from the basis of generators implicitly also removes

$$P_{34} = \{\mathcal{Q}_{\mathbf{1}3}, \mathcal{Q}_{\mathbf{4}4}\} = \{\mathcal{Q}_{\mathbf{2}3}, \mathcal{Q}_{\mathbf{3}4}\} \propto P_6 \ . \tag{3.122}$$

This corresponds to projecting out all states associated with a conservation equation from the UIR and the resulting module will not include negative-multiplicity representations. The operator constraints can be restored using the dictionary of Sec. B.1.

The contribution to the Macdonald limit of the 6d (2,0) superconformal index for these multiplets is vanishing, with the exception of $\mathcal{B}[c_1,c_2,0;d_1,0]$, for which

$$\mathcal{I}^{Mac}_{\mathcal{B}[c_1,c_2,0;d_1,0]}(q,s,t) = (-1)^{c_1}\frac{q^{4+d_1+\frac{c_1}{2}+c_2}t^{d_1+2}}{1-q}\chi_{c_1+1}(s) \ . \tag{3.123}$$

The refined indices satisfy

$$\begin{aligned}&\lim_{\epsilon\to 0}\mathcal{I}_{\mathcal{L}[\Delta+\epsilon;c_1,c_2,0;d_1,d_2]}(p,q,s,t) = \\ &\qquad \mathcal{I}_{\mathcal{A}[c_1,c_2,0;d_1,d_2]}(p,q,s,t) + \mathcal{I}_{\mathcal{B}[c_1,c_2-1,0;d_1,d_2+2]}(p,q,s,t) = 0 \ ,\end{aligned} \tag{3.124}$$

when $\Delta = 6 + 2d_1 + 2d_2 + \frac{1}{2}(c_1 + 2c_2)$.

**Higher-Spin-Current Multiplets:** $\mathcal{B}[c_1, c_2, 0; 0, 0]$

Recall that we are only constructing the auxiliary Verma module with the supercharges $\mathcal{Q}_{\mathbf{A}1}$ and $\mathcal{Q}_{\mathbf{A}2}$. Their action on a superconformal primary with generic Dynkin labels $(d_1, d_2)_{(c_1,c_2,c_3)}$ are given by

$$\begin{aligned}
(d_1,d_2)_{(c_1,c_2,c_3)} &\xrightarrow{\mathcal{Q}} (d_1-1,d_2+1),(d_1+1,d_2-1)_{(c_1+1,c_2,c_3),(c_1-1,c_2+1,c_3)}\ ,\\
&\xrightarrow{\mathcal{Q}^2} (d_1,d_2)_{(c_1+2,c_2,c_3),(c_1-2,c_2+2,c_3),(c_1,c_2+1,c_3)^2},(d_1-2,d_2+2)_{(c_1,c_2+1,c_3)},\\
&\qquad (d_1+2,d_2-2)_{(c_1,c_2+1,c_3)}\ ,\\
&\xrightarrow{\mathcal{Q}^3} (d_1+1,d_2-1),(d_1-1,d_2+1)_{(c_1+1,c_2+1,c_3),(c_1-1,c_2+2,c_3)}\ ,\\
&\xrightarrow{\mathcal{Q}^4} (d_1,d_2)_{(c_1,c_2+2,c_3)}\ ,\\
(d_1,d_2)_{(c_1,c_2,c_3)} &\xrightarrow{\tilde{Q}} (d_1,d_2+1),(d_1,d_2-1)_{(c_1+1,c_2,c_3),(c_1-1,c_2+1,c_3)}\ ,\\
&\xrightarrow{\tilde{Q}^2} (d_1,d_2)_{(c_1+2,c_2,c_3),(c_1-2,c_2+2,c_3),(c_1,c_2+1,c_3)^2},(d_1,d_2+2)_{(c_1,c_2+1,c_3)}\ ,\\
&\qquad (d_1,d_2-2)_{(c_1,c_2+1,c_3)}\ ,\\
&\xrightarrow{\tilde{Q}^3} (d_1,d_2-1),(d_1,d_2+1)_{(c_1+1,c_2+1,c_3),(c_1-1,c_2+2,c_3)}\ ,\\
&\xrightarrow{\tilde{Q}^4} (d_1,d_2)_{(c_1,c_2+2,c_3)}\ .
\end{aligned} \tag{3.125}$$

The full representation is then built from these chains of supercharges. Clearly since $d_1 = d_2 = 0$ we would only use the $\mathfrak{so}(5)$ Weyl reflections in the implementation of the RS algorithm. As mentioned in the beginning of this section, we will omit the explicit depiction of this multiplet since it is large and unwieldy. As always, though, one can use the provided `python` package as desired. Note that this would give the reduced spectrum because, as predicted from the discussion around (3.122), there are no negative-multiplicity states. In order to restore them we would the character relation

$$\hat{\chi}[\Delta; c_1, c_2, c_3; d_1, d_2] = \chi[\Delta; c_1, c_2, c_3; d_1, d_2] - \chi[\Delta+1; c_1, c_2-1, c_3; d_1, d_2]\ , \tag{3.126}$$

where the hat denotes a character over the reduced (i.e. $P_6$–removed) Verma module. Reconstructing this module with the conservation equation states simply amounts to

the following pairings

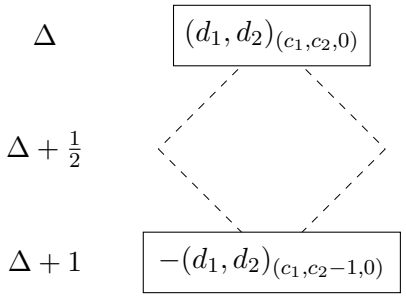


(3.127)

when $c_2 \geq 1$. If $c_2 = 0$ on the primary then there is no vector index with which to contract in a conservation equation, which is mirrored by the fact that the would-be negative multiplicity state sits on the boundary of the Weyl chamber at $c_2 = -1$, and would therefore be deleted.

This leads to the observation that, for arbitrary values of $c_1$ and $c_2$, we have an infinite family of conserved currents which have higher spin. A subset of these conserved higher-spin currents are the ones belonging to the multiplet $\mathcal{B}[0, c_2, 0; 0, 0]$. This multiplet has a superconformal primary in the rank-$c_2$ symmetric traceless representation of $\mathfrak{su}(4)$, which corresponds to the higher-spin currents that one expects to find in the free 6d $(2, 0)$ theory.

For example, we may take

$$\mathcal{O}_{\mu_1 \cdots \mu_{c_2}} = \sum_{\mathbf{I}} \Phi^{\mathbf{I}} \overset{\leftrightarrow}{\partial}_{\mu_1} \cdots \overset{\leftrightarrow}{\partial}_{\mu_{c_2}} \Phi^{\mathbf{I}}, \tag{3.128}$$

where $\mathbf{I} = 1, \cdots, 5$ is an $\mathfrak{so}(5)_R$ vector index, and $\Phi^I$ is a free-tensor primary. Therefore, this object satisfies the conservation equation

$$\partial^{\mu} \mathcal{O}_{\mu\mu_2 \ldots \mu_{c_2-1}} = 0 \, . \tag{3.129}$$

For generic $c_1, c_2$, the MacDonald index for this type of multiplet is given by

$$\mathcal{I}^{Mac}_{\mathcal{B}[c_1,c_2,0;0,0]}(q, s, t) = (-1)^{c_1} \frac{q^{\frac{c_1}{2}+c_2+4} t^2}{1-q} \chi_{c_1+1}(s) \, . \tag{3.130}$$

### $\mathcal{C}$-type multiplets

From Table 4 the two distinct $\mathcal{C}$-type multiplets are $\mathcal{C}[c_1, 0, 0; d_1, d_2]$ and $\mathcal{C}[0, 0, 0; d_1, d_2]$. Upon repeating the null-state analysis, one finds that for generic values of $d_1, d_2$ one is required to remove $\mathcal{Q}_{\mathbf{1}a}$ for $a \neq 1$ and $\mathcal{Q}_{\mathbf{1}a}\mathcal{Q}_{\mathbf{1}b}$ respectively from the basis of Verma-module generators.

One also obtains additional absent Verma-module generators for certain values of

$d_1$ and $d_2$. The procedure for identifying these is the same as the one presented in Sec. 3.4.4, so we simply summarise the additional set of $\mathcal{Q}$s that are to be removed:

$$\begin{aligned}
\mathcal{C}[c_1,0,0;d_1,2]: &\quad \mathcal{Q}_{\mathbf{2}2}\mathcal{Q}_{\mathbf{2}3}\mathcal{Q}_{\mathbf{2}4}\ ,\\
\mathcal{C}[c_1,0,0;d_1,1]: &\quad \mathcal{Q}_{\mathbf{2}a}\mathcal{Q}_{\mathbf{2}b}\quad \text{for } a\neq b\neq 1\ ,\\
\mathcal{C}[c_1,0,0;d_1,0]: &\quad \mathcal{Q}_{\mathbf{2}a}\quad \text{for } a\neq 1\ ,\\
\mathcal{C}[c_1,0,0;0,0]: &\quad \mathcal{Q}_{\mathbf{A}a}\quad \text{for } a\neq 1\ .
\end{aligned} \tag{3.131}$$

There are three combinations of $d_1, d_2$ for which the multiplet contains operator constraints. The first two $\mathcal{C}[c_1,0,0;1,0]$, $\mathcal{C}[c_1,0,0;0,1]$ contain conservation equations, whereas $\mathcal{C}[c_1,0,0;0,0]$ contains generalised equations of motion. The latter will be discussed in detail below.

The only non-vanishing MacDonald indices for the $\mathcal{C}$–multiplets are

$$\begin{aligned}
\mathcal{I}^{Mac}_{\mathcal{C}[c_1,0,0;d_1,1]}(q,s,t) &= (-1)^{c_1+1}\frac{q^{\frac{7}{2}+d_1+\frac{c_1}{2}}t^{d_1+2}}{1-q}\chi_{c_1+1}(s)\ ,\\
\mathcal{I}^{Mac}_{\mathcal{C}[c_1,0,0;d_1,0]}(q,s,t) &= (-1)^{c_1}\frac{q^{2+d_1+\frac{c_1}{2}}t^{d_1+1}}{1-q}\chi_{c_1+2}(s)\ .
\end{aligned} \tag{3.132}$$

The refined indices of course satisfy

$$\begin{aligned}
&\lim_{\epsilon\to 0}\mathcal{I}_{\mathcal{L}[\Delta+\epsilon;c_1,0,0;d_1,d_2]}(p,q,s,t) =\\
&\quad \mathcal{I}_{\mathcal{A}[c_1,0,0;d_1,d_2]}(p,q,s,t)+\mathcal{I}_{\mathcal{C}[c_1-1,0,0;d_1,d_2+3]}(p,q,s,t)=0\ ,
\end{aligned} \tag{3.133}$$

when $\Delta = 6+2d_1+2d_2+\frac{1}{2}c_1$.

$\mathcal{C}[c_1,0,0;0,0]$

Recall from (3.131) that the associated Verma module is constructed by the action of $\mathcal{Q}_{\mathbf{A}1}$. Since we are removing all other supercharges, we also have to remove several momenta from the basis of generators of the Verma module. These are

$$\begin{aligned}
P_{23} &= \{\mathcal{Q}_{\mathbf{1}2},\mathcal{Q}_{\mathbf{4}3}\} = \{\mathcal{Q}_{\mathbf{2}2},\mathcal{Q}_{\mathbf{3}3}\}\propto P_3,\\
P_{24} &= \{\mathcal{Q}_{\mathbf{1}2},\mathcal{Q}_{\mathbf{4}4}\} = \{\mathcal{Q}_{\mathbf{2}2},\mathcal{Q}_{\mathbf{3}4}\}\propto P_5,\\
P_{34} &= \{\mathcal{Q}_{\mathbf{1}3},\mathcal{Q}_{\mathbf{4}4}\} = \{\mathcal{Q}_{\mathbf{2}3},\mathcal{Q}_{\mathbf{3}4}\}\propto P_6\ ,
\end{aligned} \tag{3.134}$$

where in the last column we have converted to Lorentz vector indices. Thus for generic Dynkin labels the actions of the supercharges lead to

$$(d_1,d_2)_{(c_1,c_2,c_3)}\xrightarrow{Q}(d_1-1,d_2+1),(d_1+1,d_2-1)_{(c_1+1,c_2,c_3)},$$

$$
\begin{aligned}
&\xrightarrow{Q^2} (d_1, d_2)_{(c_1+2,c_2,c_3)}, \\
(d_1, d_2)_{(c_1,c_2,c_3)} &\xrightarrow{\tilde{Q}} (d_1, d_2+1), (d_1, d_2-1)_{(c_1+1,c_2,c_3)}, \\
&\xrightarrow{\tilde{Q}^2} (d_1, d_2)_{(c_1+2,c_2,c_3)}.
\end{aligned} \tag{3.135}
$$

Denoting the action of $Q = (\mathcal{Q}_{\mathbf{2}a}, \mathcal{Q}_{\mathbf{3}a})$ as moving *southwest* on the diagram and $\tilde{Q} = (\mathcal{Q}_{\mathbf{1}a}, \mathcal{Q}_{\mathbf{4}a})$ as moving *southeast*, we can represent this multiplet as:

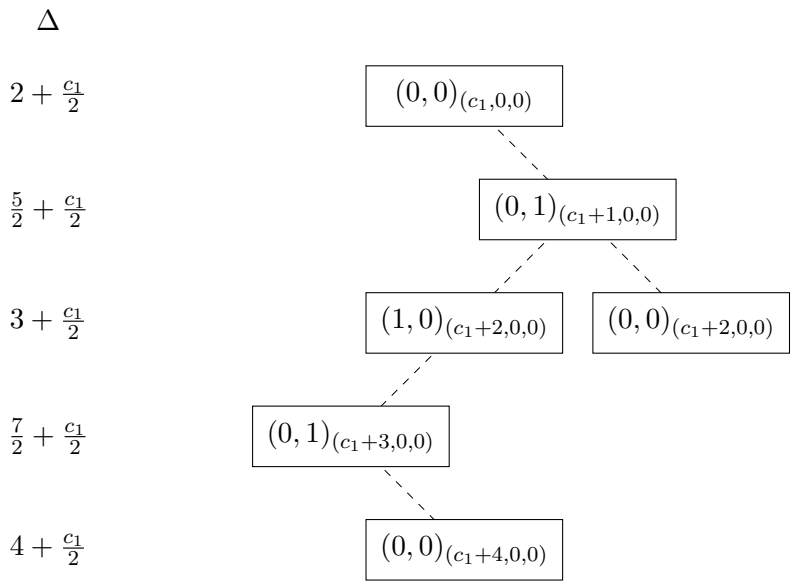


(3.136)

As in the $\mathcal{B}[c_1, c_2, 0; 0, 0]$ case, we can restore the negative-multiplicity states by making use of the character relation

$$
\begin{aligned}
&\hat{\chi}[\Delta; c_1, 0, 0; d_1, d_2] = \\
&\quad \chi[\Delta; c_1, 0, 0; d_1, d_2] - \chi[\Delta+1; c_1-1, 0, 1; d_1, d_2] + \chi[\Delta+2; c_1-2, 1, 0; d_1, d_2] \\
&\quad - \chi[\Delta+3; c_1-2, 0, 0; d_1, d_2] \ ,
\end{aligned} \tag{3.137}
$$

where a hat denotes the $P$-reduced character. This will lead to a set of equations of motion.

The index over this multiplet in the MacDonald limit is

$$
\mathcal{I}^{Mac}_{\mathcal{C}[c_1,0,0;0,0]}(q, s, t) = (-1)^{c_1} \frac{q^{\frac{c_1}{2}+2} t}{1-q} \chi_{c_1+2}(s) \ . \tag{3.138}
$$

### $\mathcal{D}$-type multiplets

These multiplets, summarised in Table 4, are the smallest of the $\mathfrak{osp}(8^*|4)$ algebra. The associated null state is $A^1\Psi = 0$, which implies that $\mathcal{Q}_{\mathbf{1}a}\Psi = 0$ and the multiplet is

thus $\frac{1}{4}$-BPS.

These multiplets contain additional vectors for $d_2 \leq 3$, when one also needs to remove the following combinations of supercharges from the basis of Verma-module generators:

$$\begin{aligned}
\mathcal{D}[0,0,0;d_1,3]: &\quad \mathcal{Q}_{\mathbf{2}1}\mathcal{Q}_{\mathbf{2}2}\mathcal{Q}_{\mathbf{2}3}\mathcal{Q}_{\mathbf{2}4}\ , \\
\mathcal{D}[0,0,0;d_1,2]: &\quad \mathcal{Q}_{\mathbf{2}a}\mathcal{Q}_{\mathbf{2}b}\mathcal{Q}_{\mathbf{2}c} \\
\mathcal{D}[0,0,0;d_1,1]: &\quad \mathcal{Q}_{\mathbf{2}a}\mathcal{Q}_{\mathbf{2}b}\ , \\
\mathcal{D}[0,0,0;d_1,0]: &\quad \mathcal{Q}_{\mathbf{2}a}\ .
\end{aligned} \tag{3.139}$$

When $d_1 = d_2 = 0$ this corresponds to the vacuum, because all supercharges annihilate the superconformal primary.

For generic $d_1, d_2$ we have the $Q$-chain

$$\begin{aligned}
(d_1,d_2)_{(c_1,c_2,c_3)} &\xrightarrow{Q} (d_1,d_2-1)_{(c_1+1,c_2,c_3),(c_1-1,c_2+1,c_3),(c_1,c_2-1,c_3+1),(c_1,c_2,c_3-1)}\ , \\
&\xrightarrow{Q^2} (d_1,d_2-2)_{(c_1,c_2+1,c_3),(c_1+1,c_2-1,c_3+1),(c_1+1,c_2,c_3-1),(c_1-1,c_2,c_3+1)}\ , \\
&\qquad (d_1,d_2-2)_{(c_1-1,c_2+1,c_3-1),(c_1,c_2-1,c_3)}\ , \\
&\xrightarrow{Q^3} (d_1,d_2-3)_{(c_1,c_2,c_3+1),(c_1,c_2+1,c_3-1),(c_1+1,c_2-1,c_3),(c_1-1,c_2,c_3)}\ , \\
&\xrightarrow{Q^4} (d_1,d_2-4)_{(c_1,c_2,c_3)}\ .
\end{aligned} \tag{3.140}$$

The action of the $\tilde{Q}$ supercharges will be dealt with on a case-by-case basis as we dial $d_2$ for the examples that we provide.

The non-zero contributions to the MacDonald limit of the index are given by

$$\begin{aligned}
\mathcal{I}^{Mac}_{\mathcal{D}[0,0,0;d_1,2]}(q,s,t) &= \frac{q^{3+d_1}t^{d_1+2}}{1-q} \qquad d_1 \geq 0\ , \\
\mathcal{I}^{Mac}_{\mathcal{D}[0,0,0;d_1,1]}(q,s,t) &= -\frac{q^{\frac{3}{2}+d_1}t^{d_1+1}}{1-q}\chi_1(s) \qquad \text{for} \quad d_1 \geq 0\ , \\
\mathcal{I}^{Mac}_{\mathcal{D}[0,0,0;d_1,0]}(q,s,t) &= \frac{q^{d_1}t^{d_1}}{1-q} \qquad \text{for} \quad d_1 > 0\ .
\end{aligned} \tag{3.141}$$

The $\mathcal{D}$-type multiplets contain negative-multiplicity states for $d_1 + d_2 \leq 2$. These include the free-tensor and stress-tensor multiplet.

**Half–BPS Multiplets:** $\mathcal{D}[0,0,0;d_1,0]$

Recall that in this case we are prescribed to remove $\mathcal{Q}_{\mathbf{2}a}$ from the basis of Verma-module generators. This is because $A^1\Psi = \mathcal{Q}_{\mathbf{1}1}\Psi = 0$ and using $R$-symmetry lowering operators we find that all $\mathcal{Q}_{\mathbf{1}a}$, $\mathcal{Q}_{\mathbf{2}a}$ annihilate the primary. As a result, the multiplet

is $\frac{1}{2}$–BPS. The set of $\tilde{Q}$s consist entirely of $\mathcal{Q}_{\mathbf{3}a}$ supercharges. Acting on a generic superconformal primary state $(d_1, d_2)_{(c_1,c_2,c_3)}$ with the $\tilde{Q}$s yields

$$\begin{aligned}(d_1,d_2)_{(c_1,c_2,c_3)} &\xrightarrow{\tilde{Q}} (d_1-1,d_2+1)_{(c_1+1,c_2,c_3),(c_1-1,c_2+1,c_3),(c_1,c_2-1,c_3+1),(c_1,c_2,c_3-1)}\ ,\\ &\xrightarrow{\tilde{Q}^2} (d_1-2,d_2+2)_{(c_1,c_2+1,c_3),(c_1+1,c_2-1,c_3+1),(c_1+1,c_2,c_3-1),(c_1,c_2-1,c_3)}\ ,\\ &\qquad (d_1-2,d_2+2)_{(c_1-1,c_2+1,c_3-1),(c_1-1,c_2,c_3+1)}\ ,\\ &\xrightarrow{\tilde{Q}^3} (d_1-3,d_2+3)_{(c_1,c_2,c_3+1),(c_1,c_2+1,c_3-1),(c_1+1,c_2-1,c_3),(c_1-1,c_2,c_3)}\ ,\\ &\xrightarrow{\tilde{Q}^4} (d_1-4,d_2+4)_{(c_1,c_2,c_3)}\ .\end{aligned} \tag{3.142}$$

The Verma module is then built out of $\mathcal{Q}_{\mathbf{3}a}$, $\mathcal{Q}_{\mathbf{4}a}$ and we obtain

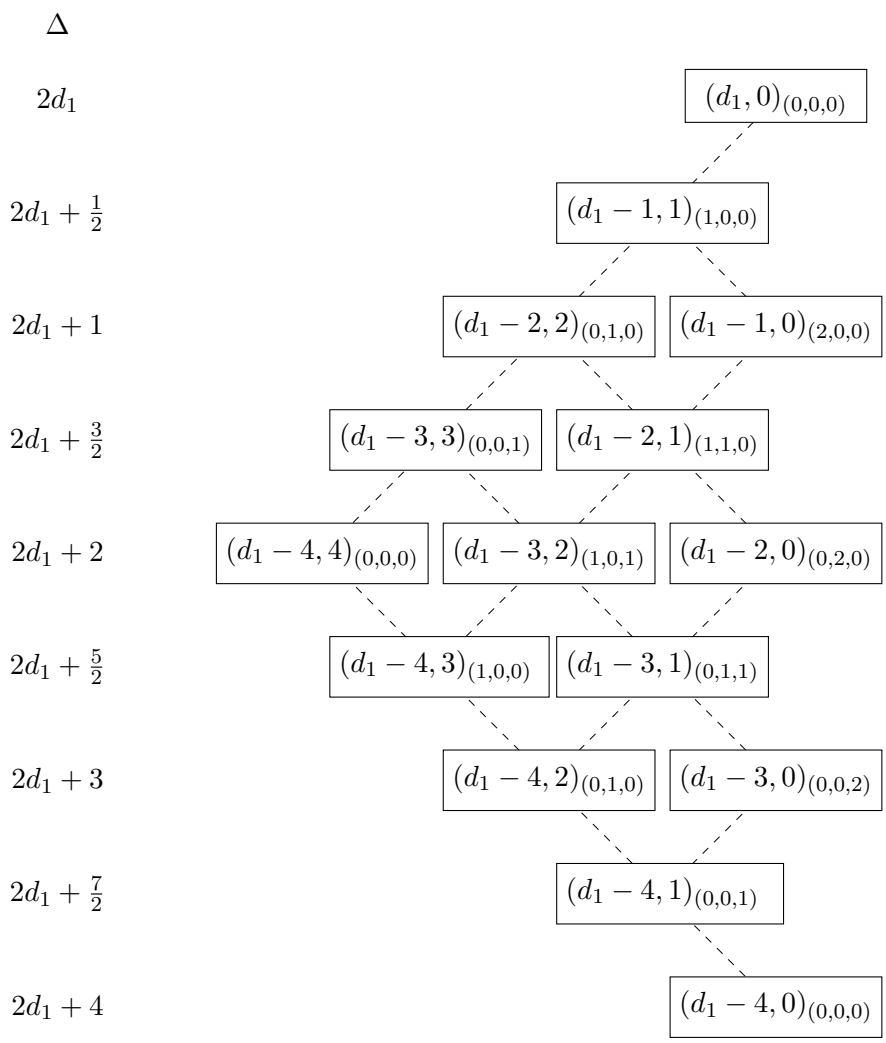


(3.143)

The half-BPS index limit of this index is very simple:

$$\mathcal{I}^{\frac{1}{2}\text{-BPS}}_{\mathcal{D}[0,0,0;d_1,0]}(x) = x^{d_1} \ , \tag{3.144}$$

which is the only non-vanishing class of half-BPS indices, as the name might suggest.

**The Free-Tensor Multiplet:** $\mathcal{D}[0,0,0;1,0]$

This spectrum can be obtained by substituting $d_1 = 1$ into that of $\mathcal{D}[0,0,0;d_1,0]$ and running the RS algorithm. The resulting states match a scalar $\Phi^{\mathbf{I}}$, $\mathbf{I} = 1,\ldots,5$, a fermion $\lambda^{\mathbf{A}}_a$ and a selfdual tensor $H^+_{[\mu\nu\rho]}$. The negative-multiplicity representations are naturally matched with the equations of motion $\partial^2\Phi^{\mathbf{I}} = 0$, $\not{\partial}^{\dot{a}b}\tilde{\lambda}^{\mathbf{A}}_{\dot{b}} = 0$ and the Bianchi identity for the selfdual tensor $\partial_{[\mu}H^+_{\nu\rho\sigma]} = 0$.

The full multiplet is given by

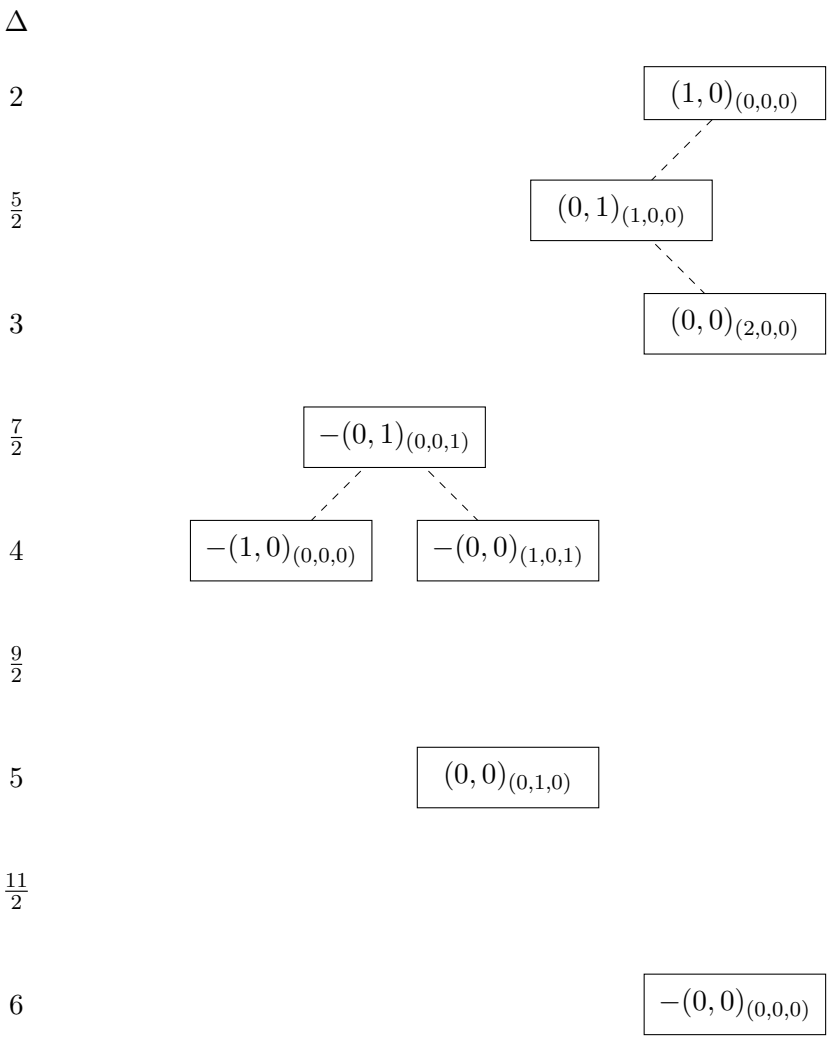


(3.145)

The refined index over this multiplet is compact enough to be presented in full

$$\mathcal{I}_{\mathcal{D}[0,0,0;1,0]}(p,q,s,t) = \frac{qt + q^2p^2t^{-1} - q^2p(s+p+s^{-1}) + q^3p^2}{(1-q)(1-qps)(1-qps^{-1})} \,. \tag{3.146}$$

**The Stress-Tensor Multiplet:** $\mathcal{D}[0,0,0;2,0]$

This spectrum can be obtained by substituting $d_1 = 2$ into that of $\mathcal{D}[0,0,0;d_1,0]$ and running the RS algorithm. The resulting representation is

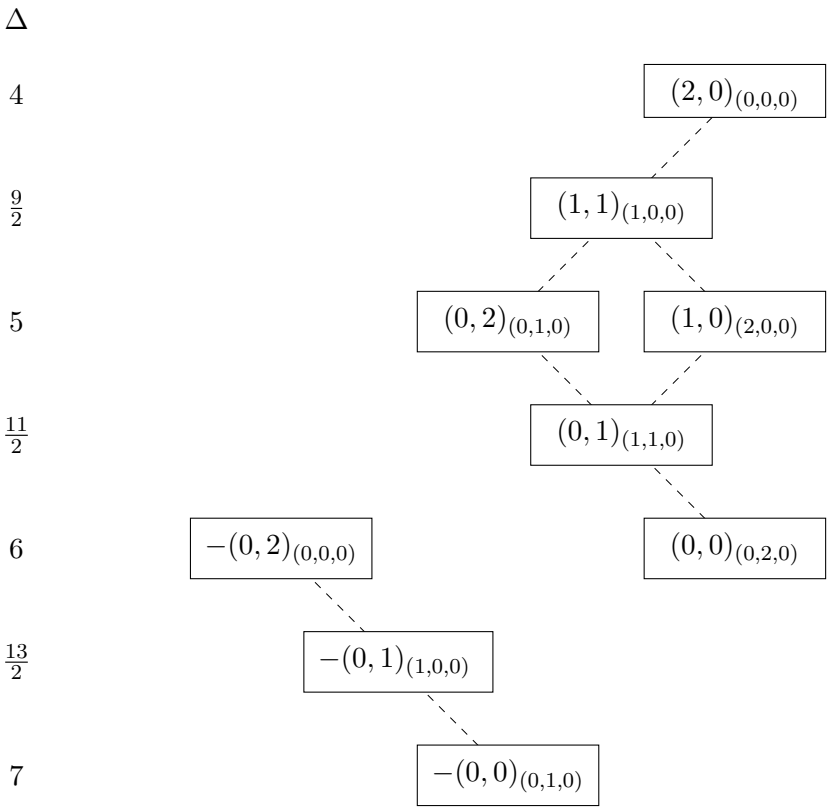


(3.147)

The superconformal primary is now the diboson

$$\mathcal{O}^{\mathbf{IJ}} := :\Phi^{(\mathbf{I}}\Phi^{\mathbf{J})}: \,. \tag{3.148}$$

We can identify the important states with the following currents and their conservation equations; namely the $R$-symmetry current $J_\mu^{(\mathbf{AB})}$, supersymmetry current $S_{\mu a}^{\mathbf{A}}$ and stress tensor $\Theta_{\mu\nu}$. We also have three states with no associated conservation equations. The refined index for this multiplet is calculated to be

$$\mathcal{I}_{\mathcal{D}[0,0,0;2,0]}(p,q,s,t) = -\frac{pq^3(st + s^{-1}t + pt + p^3qt^{-1} + p^2qst^{-1} + p^2qs^{-1}t^{-1})}{(1-q)(1-qps)(1-qps^{-1})}$$

$$+\frac{q^2t^2+p^2q^3(1+p^2qt^{-2})+p^2q^4(1+ps+ps^{-1})}{(1-q)(1-qps)(1-qps^{-1})}\,. \quad (3.149)$$

$\mathcal{D}[0,0,0;0,1]$

The shortening conditions for this follow from (3.139) by setting $d_1 = 0$. The full spectrum of states, including those corresponding to operator constraints, is given by the diagram:

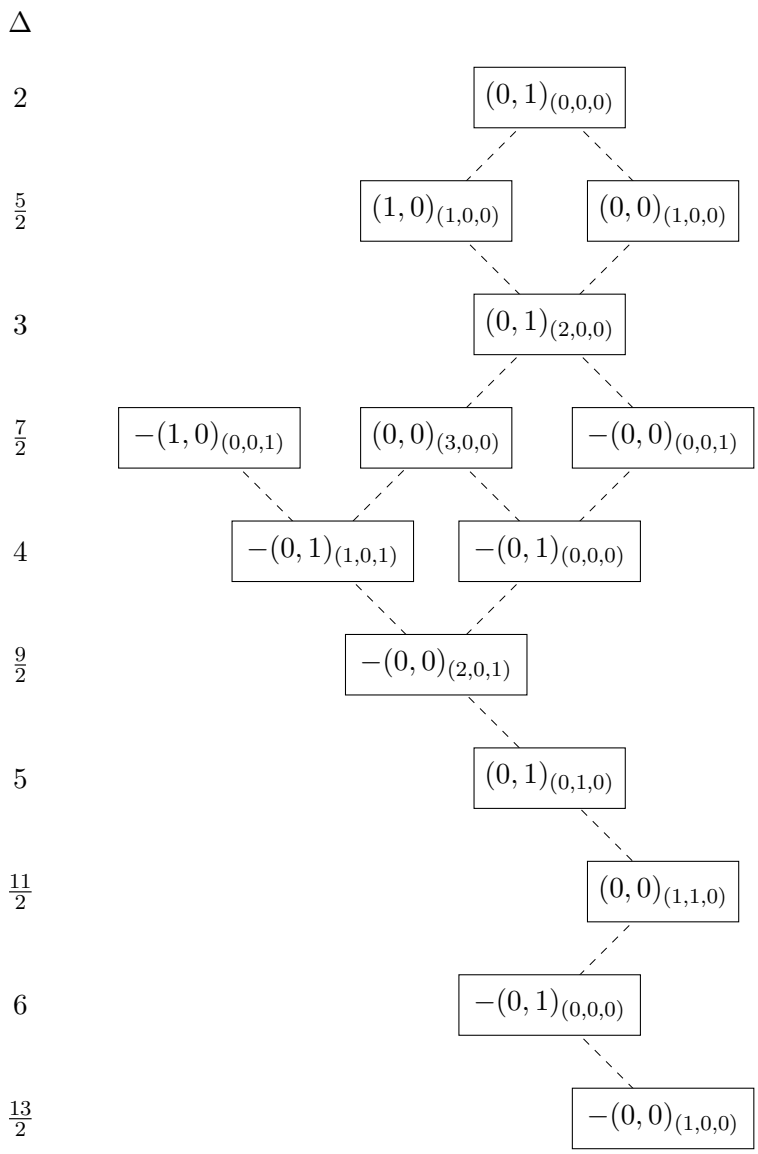


(3.150)

### 3.4.5 Index Spectroscopy

Despite years of progress, the $(2,0)$ theory remains a very mysterious theory. One approach in gaining some insight is to study its superconformal indices. Fully refined

indices obtained in integral form were found by appealing to the (2,0) theory's relationship to 5d super Yang Mills (sYM). They were calculated through localisation as in [122, 123] and by topological strings in [70]. Note that, through topological strings, one need not necessarily appeal to 5d sYM, as was shown in [71] via a change of preferred direction in the topological vertex.

While these integral representations are incredibly complicated and difficult to manipulate (aside from a series expansion of the integrand), there exist limits of the integrand where the integral is able to be computed exactly; largely due to the limit trivialising the sum over instanton contributions. It was shown in [21, 122] that the Schur limits of the interacting theories are given by

$$\begin{aligned}\mathcal{I}^{Schur}_{A_{N-1}}(q) &= \text{P.E}\left[\frac{q^2+\ldots+q^N}{1-q}\right], \\ \mathcal{I}^{Schur}_{D_N}(q) &= \text{P.E}\left[\frac{q^N+(q^2+\ldots+q^{2N-2})}{1-q}\right],\end{aligned} \tag{3.151}$$

which was later reproduced by [24] using the fact that a 2d subsector of the theory can be mapped to a $\mathcal{W}_N$ algebra. The character of this algebra is what reproduces these limits of the index. They then conjectured the following forms of the exceptional indices

$$\begin{aligned}\mathcal{I}^{Schur}_{E_6}(q) &= \text{P.E}\left[\frac{q^2+q^5+q^6+q^8+q^9+q^{12}}{1-q}\right], \\ \mathcal{I}^{Schur}_{E_7}(q) &= \text{P.E}\left[\frac{q^2+q^6+q^8+q^{10}+q^{12}+q^{14}+q^{18}}{1-q}\right], \\ \mathcal{I}^{Schur}_{E_8}(q) &= \text{P.E}\left[\frac{q^2+q^8+q^{12}+q^{14}+q^{18}+q^{20}+q^{24}+q^{30}}{1-q}\right],\end{aligned} \tag{3.152}$$

using the same method. It was then noted by the authors that these indices all have no dependence on the fugacity $s$. Due to the structure of the unrefined indices, no state with the appropriate power of $s$ can be cancelled by another state with with the opposite sign once one fixes the corresponding power of $q$. Since there are no cancellations available in this Schur limit, they immediately ruled out representations whose index counts states with non-zero $c_1$. Therefore the set of allowed Schur multiplets that can contribute to interacting $(2,0)$ theories are

$$\mathcal{B}[0,c_2,0;d_1,0], \qquad \mathcal{D}[0,0,0,;d_1,\{0,2\}]\,. \tag{3.153}$$

whose Schur indices are

$$\begin{aligned}\mathcal{I}^{Schur}_{\mathcal{B}[0,c_2,0;d_1,0]}(q) &= \frac{q^{4+d_1+c_2}}{1-q}\ ,\\ \mathcal{I}^{Schur}_{\mathcal{D}[0,0,0;d_1,2]}(q) &= \frac{q^{3+d_1}}{1-q}\ ,\\ \mathcal{I}^{Schur}_{\mathcal{D}[0,0,0;d_1,0]}(q) &= \frac{q^{d_1}}{1-q}\ .\end{aligned} \tag{3.154}$$

This is already huge progress, but when performing index spectroscopy, the simplicity of the Schur limits of these multiplets is both a gift and a curse. It is not clear *a priori* how one would differentiate contributions coming from, *e.g.* $\mathcal{D}[0,0,0;4,0]$, $\mathcal{D}[0,0,0;1,2]$ or $\mathcal{B}[0,0,0;0,0]$.

This is where the MacDonald index comes in. The additional fugacity $t$ distinguishes all three of these multiplets, such that there could never be any confusion. We simply need the MacDonald versions of these interacting indices. The authors of [21, 123] note that the numerator that appears in the Plethystic exponential comes from contributions of the half-BPS primary operators, while the denominator comes from derivative contributions. Since our MacDonald index counts primary half-BPS operators with $q^{d_1}t^{d_1}$ as opposed to $q^{d_1}$, while both count the derivative with $q$, we conjecture that the MacDonald indices for the interacting $(2,0)$ theories are given by

$$\begin{aligned}\mathcal{I}^{Mac}_{A_{N-1}}(q,t) &= \text{P.E}\left[\frac{(qt)^2+\ldots+(qt)^N}{1-q}\right],\\ \mathcal{I}^{Mac}_{D_N}(q,t) &= \text{P.E}\left[\frac{(qt)^N+((qt)^2+\ldots+(qt)^{2N-2})}{1-q}\right],\\ \mathcal{I}^{Mac}_{E_6}(q,t) &= \text{P.E}\left[\frac{(qt)^2+(qt)^5+(qt)^6+(qt)^8+(qt)^9+(qt)^{12}}{1-q}\right],\\ \mathcal{I}^{Mac}_{E_7}(q,t) &= \text{P.E}\left[\frac{(qt)^2+(qt)^6+(qt)^8+(qt)^{10}+(qt)^{12}+(qt)^{14}+(qt)^{18}}{1-q}\right],\\ \mathcal{I}^{Mac}_{E_8}(q,t) &= \text{P.E}\left[\frac{(qt)^2+(qt)^8+(qt)^{12}+(qt)^{14}+(qt)^{18}+(qt)^{20}+(qt)^{24}+(qt)^{30}}{1-q}\right].\end{aligned} \tag{3.155}$$

Armed with these, one can show that the MacDonal index for the $A_1$ theory has an exact expansion as

$$\begin{aligned}&\text{P.E}\left[\frac{(qt)^2}{1-q}\right] =\\ &\quad 1+\sum_{d_1=1}^{\infty}\mathcal{I}^{Mac}_{\mathcal{D}[0,0,0;2d_1,0]}(q,t)+\sum_{c_2,d_1=0}^{\infty}\text{mult}(c_2,d_1)\mathcal{I}^{Mac}_{\mathcal{B}[0,c_2,0;2d_1+2,0]}(q,t)\ ,\end{aligned} \tag{3.156}$$

where $\text{mult}(c_2, d_1)$ are the multiplicities given by the generating function

$$\text{mult}(c_2, d_1) = \frac{1}{(d_1+2)!}\frac{\partial^{d_1+2}}{\partial x^{d_1+2}}\prod_{k=2}^{c_2}\frac{1}{1-x^k}\bigg|_{x=0} . \tag{3.157}$$

Notice the lack of $\mathcal{D}[0,0,0;d_1,2]$ contributions. This is not a general statement, however, as when one considers the $A_2$ index one finds contributions coming from two towers

$$\sum_{i_1,i_2=1}^{\infty}\mathcal{I}^{Mac}_{\mathcal{D}[0,0,0;2i_1+3i_2-2,2]}(q,t) . \tag{3.158}$$

This can be seen by noting that

$$\begin{aligned}\text{P.E}\left[\frac{(qt)^N}{1-q}\right] = 1 &+ \sum_{d_1=1}^{\infty}\mathcal{I}^{Mac}_{\mathcal{D}[0,0,0;Nd_1,0]}(q,t) \\ &+ \sum_{c_2,d_1=0}^{\infty}\text{mult}(c_2,d_1)\mathcal{I}^{Mac}_{\mathcal{B}[0,c_2,0;Nd_1+2(N-1),0]}(q,t) ,\end{aligned} \tag{3.159}$$

along with the following "fusion" rules:

$$\begin{aligned}\mathcal{I}^{Mac}_{\mathcal{D}[0,0,0;i,0]}(q,t)\times\mathcal{I}^{Mac}_{\mathcal{D}[0,0,0;j,0]}(q,t) =& \mathcal{I}^{Mac}_{\mathcal{D}[0,0,0;i+j,0]}(q,t)+\mathcal{I}^{Mac}_{\mathcal{D}[0,0,0;i+j-2,2]}(q,t) \\ &+\sum_{k=0}^{\infty}\mathcal{I}^{Mac}_{\mathcal{B}[0,k,0;i+j-2,0]}(q,t) , \\ \mathcal{I}^{Mac}_{\mathcal{D}[0,0,0;i,0]}(q,t)\times\mathcal{I}^{Mac}_{\mathcal{B}[0,m,0;j,0]}(q,t) =& \sum_{k=0}^{\infty}\mathcal{I}^{Mac}_{\mathcal{B}[0,k+m,0;i+j,0]}(q,t) , \\ \mathcal{I}^{Mac}_{\mathcal{B}[0,m,0;i,0]}(q,t)\times\mathcal{I}^{Mac}_{\mathcal{B}[0,n,0;j,0]}(q,t) =& \sum_{k=0}^{\infty}\mathcal{I}^{Mac}_{\mathcal{B}[0,k+m+n+2,0;i+j+2,0]}(q,t) .\end{aligned} \tag{3.160}$$

One can simply write

$$\mathcal{I}^{Mac}_{A_2}(q,t) = \text{P.E}\left[\frac{(qt)^2+(qt)^3}{1-q}\right] = \text{P.E}\left[\frac{(qt)^2}{1-q}\right]\times\text{P.E}\left[\frac{(qt)^3}{1-q}\right] , \tag{3.161}$$

expand in the two Plethystic exponentials using Eq. 3.159 and use the "fusion" rules. This then recovers, among other terms, the aforementioned contributions from the $\mathcal{D}[0,0,0;d_1,2]$ multiplets. While we have not been able to rule out any more multiplets, we have been able to find a decomposition in terms of Schur multiplets; and in the $A_1$ case, obtain a closed form expression for the coefficients of all these multiplets. It would be interesting to explore these coefficients more for two reasons. Firstly, it may be that we are able to find a closed form expression for these coefficients. Secondly,

these coefficients are of particular interest in the area of combinatorics and might be interesting in their own right.

Another interesting route in this spirit is to see whether one can probe more refined limits of the interacting superconformal indices; either as a series expansion up to high order or by finding a particular limit that simplifies the Nekrasov partition function in a non-trivial way. We leave both these questions as areas for future investigation.

## 3.5 From Supercharacters to Indices

In the previous two sections we had simply quoted the results for the indices of the mentioned multiplets. While one could simply try letter counting to extract these quantities, for generic quantum numbers, this process becomes rather arduous. A better way is to calculate the supercharacter and perform a redefinition of parameters to match the index. A supercharacter is defined in a general way as

$$\mathrm{Tr}_{\mathcal{R}}(-1)^F \prod_i p_i^{d_i} \ , \tag{3.162}$$

where the $p_i$ are fugacities and $d_i$ are the corresponding Dynkin labels associated with the charges of the representation of a particular algebra. An index is similarly defined as (see Sec 2.2)

$$\mathrm{Tr}_{\mathcal{H}}(-1)^F e^{-\beta\delta} \prod_i x_i^{\mu_i} \ , \tag{3.163}$$

where $\mu_i$ are the charges associated with a maximally commuting subalgebra. Since these $\mu_i$ are a subalgebra of the larger algebra, one simply needs to express the $\mu_i$ in terms of the $d_i$, then find the corresponding map for the character fugacities such that we are left with

$$\mathrm{Tr}_{\mathcal{R}}(-1)^F \prod_i^n x_i(p_1, \ldots, p_n)^{\mu_i} \ . \tag{3.164}$$

This endows us with a map from $p_i$ to $x_i$. Note that once we perform this map, since the exponents are all in terms of the commuting subalgebra, all states that do not satisfy $\delta = 0$ will be pair-wise cancelled which enforces the $e^{-\beta\delta}$ term. This will be made more precise when we discuss specific examples.

For now let us a consider a representation of a Lie algebra $\mathfrak{g}$ with highest weight $\lambda$. The Weyl character formula is given by [66]

$$\chi_\lambda = \frac{\sum_{w\in W} \mathrm{sgn}(w) e^{w(\lambda+\rho)}}{e^\rho \prod_{\alpha\in\Phi_-}(1-e^\alpha)}, \tag{3.165}$$

where $W$ is the Weyl group of the Lie algebra root system and $\rho$ is the half sum of the positive roots $\Phi_+$. Note that $\text{sgn}(w) = (-1)^{l(w)}$ where $l(w)$ is the length of the Weyl group element, i.e. how many simple reflections it is comprised of.

One can alternatively obtain this formula using a Verma-module construction: Decompose the algebra $\mathfrak{g}$ as

$$\mathfrak{g} = \Phi_+ \oplus \mathfrak{h} \oplus \Phi_- \ , \tag{3.166}$$

where $\mathfrak{h}$ corresponds to the Cartan subalgebra and $\Phi_-$ ($\Phi_+$ ) are the negative (positive) roots. We construct the Verma module $\mathcal{V}$ corresponding to some highest (lowest) weight $|\lambda\rangle$ by considering the space comprised of the states $f(\Phi_-)\,|\lambda\rangle$ ($f(\Phi_+)\,|\lambda\rangle$), where $f$ is any polynomial of the negative (positive) roots modulo algebraic relations. The character of this module is defined to be [66]

$$\chi_{\mathcal{V}} = \frac{e^{\lambda}}{\prod_{\alpha\in\Phi_-}(1-e^{\alpha})} \ . \tag{3.167}$$

The character of the representation labelled by $\Lambda$ is recovered by summing over the Weyl group action on the roots

$$\chi_\lambda = \sum_{w\in W} w(\chi_{\mathcal{V}}) = \sum_{w\in W} \frac{e^{w(\lambda)}}{\prod_{\alpha\in\Phi_-}(1-e^{w(\alpha)})}. \tag{3.168}$$

We can utilise the identity $w(e^{-\rho-\lambda}\chi_{\mathcal{V}}) = \text{sgn}(w)e^{-\rho-\lambda}\chi_{\mathcal{V}}$ along with the fact that $w$ acts naturally—i.e. we may take $w(e^{-\rho-\lambda}\chi_{\mathcal{V}}) = w(e^{-\rho-\lambda})w(\chi_{\mathcal{V}})$ [66]—to show that

$$\chi_\lambda = \sum_{w\in W} w(\chi_{\mathcal{V}}) = \frac{\sum_{w\in W}(-1)^{l(w)}e^{w(\lambda+\rho)}}{e^{\rho+\lambda}}\chi_{\mathcal{V}} = \frac{\sum_{w\in W}(-1)^{l(w)}e^{w(\lambda+\rho)}}{e^{\rho}\prod_{\alpha\in\Phi_-}(1-e^{\alpha})}. \tag{3.169}$$

The formulation of the Weyl character formula (3.168) is particularly useful in the context of UIRs of the SCA [24, 113].

### 3.5.1 Characters of 5d $\mathcal{N}=1$ Multiplets

We are now in a position to compute the characters of $\mathfrak{f}(4)$.[22] Let us consider a representation the highest weight of which has conformal dimension $\Delta$ with $\mathfrak{so}(5)$ Lorentz quantum numbers $(d_1, d_2)$ and $\mathfrak{su}(2)_R$ quantum numbers $K$. Note that these are expressed in the Dynkin basis and hence are integer. The highest weight can be decomposed as

$$\lambda = \omega_1^{\beta} d_1 + \omega_2^{\beta} d_2 + \omega^{\alpha} K \ , \tag{3.170}$$

[22] A summary of this discussion for the case of the (2,0) SCA can be found in App. C of [24].

where $\omega_i^\beta$ $(i=1,2)$ are the fundamental weights associated with the $\mathfrak{so}(5)$ simple roots $\beta_i$, while $\omega^\alpha$ is the fundamental weight associated with the $\mathfrak{su}(2)_R$ simple root $\alpha$. We may in turn express the fundamental weights in terms of the simple roots (for reasons which will become apparent) by using the Cartan matrix $A_{ij}$

$$\begin{aligned}\omega_i^\beta &= (A_{B_2}^{-1})_{ij}\beta_j = \begin{pmatrix} 1 & 1 \\ \frac{1}{2} & 1 \end{pmatrix}\begin{pmatrix}\beta_1 \\ \beta_2\end{pmatrix} , \\ \omega^\alpha &= \frac{1}{2}\alpha \, . \end{aligned} \tag{3.171}$$

Let us next consider $e^\lambda$ by defining the fugacities

$$b_1 = e^{\beta_1+\beta_2} \ , \ \ b_2 = e^{\frac{1}{2}(\beta_1+2\beta_2)} \ , \ \ a = e^{\frac{1}{2}\alpha} \ , \tag{3.172}$$

hence

$$e^\lambda = b_1^{d_1} b_2^{d_2} a^K \, . \tag{3.173}$$

The character of a particular representation $\mathcal{R}$ is then defined to be

$$\chi_{\mathcal{R}}(a,\mathbf{b},q) = \mathrm{Tr}_{\mathcal{R}}(q^\Delta b_1^{d_1} b_2^{d_2} a^K) \, , \tag{3.174}$$

where we have included the $\mathfrak{so}(2)$ Cartan, $\Delta$. For example we can read off the character for the supercharges $\mathcal{Q}_{\mathbf{A}1}$ as (recall that we are in the Dynkin basis)

$$\sum_{\mathbf{A}=\mathbf{1}}^{\mathbf{4}} \chi(\mathcal{Q}_{\mathbf{A}1}) = ab_2 q^{\frac{1}{2}} + \frac{ab_1 q^{\frac{1}{2}}}{b_2} + \frac{ab_2 q^{\frac{1}{2}}}{b_1} + \frac{aq^{\frac{1}{2}}}{b_2} \, . \tag{3.175}$$

We can then apply this to specific representations of the SCA.

### Long Representations

For the long representation $\mathcal{L}_{[\Delta;d_1,d_2;K]}$ we construct the superconformal multiplet by acting on the highest weight state $|\Delta;d_1,d_2;K\rangle^{hw}$ with momentum operators and supercharges as in Eq. (3.1). Thus for a generic long representation we can decompose the character of the superconformal Verma module using (3.167) as

$$\chi_{\mathcal{L}}(a,\mathbf{b},q) = q^\Delta \chi_{[d_1,d_2]}(\mathbf{b})\chi_{[K]}(a) f(a,\mathbf{b},q) \, . \tag{3.176}$$

The polynomial appearing above can be decomposed as $f(a,\mathbf{b},q) = Q(a,\mathbf{b},q)P(\mathbf{b},q)$ since the momentum operators and supercharges commute. Explicitly these functions

are

$$Q(a,\mathbf{b},q)=\prod_{\mathbf{A},a}(1+\chi(\mathcal{Q}_{\mathbf{A}a}))\ ,$$
$$P(\mathbf{b},q)=\prod_{\mu=1}^{5}(1-\chi(P_\mu))^{-1}\ . \tag{3.177}$$

The characters $\chi_{[d_1,d_2]}(\mathbf{b})$ and $\chi_{[K]}(a)$ can be obtained through their Weyl orbits. As a result one has

$$\chi_{[d_1,d_2]}(\mathbf{b})=\sum_{w\in W_{\mathrm{SO}(5)}} w(b_1)^{d_1}w(b_2)^{d_2}M(w(\mathbf{b}))\ ,$$
$$\chi_{[K]}(a)=\sum_{w\in W_{\mathrm{SU}(2)}} w(a)^{K}R(w(a))\ , \tag{3.178}$$

where the $M(\mathbf{b})$ and $R(a)$ are the products of the characters of negative roots, explicitly

$$M(\mathbf{b})=\frac{1}{\left(1-\frac{1}{b_1}\right)\left(1-\frac{1}{b_2^2}\right)\left(1-\frac{b_1}{b_2^2}\right)\left(1-\frac{b_2^2}{b_1^2}\right)}\ ,$$
$$R(a)=\frac{a^2}{a^2-1}\ . \tag{3.179}$$

As an aside it will be worthwhile to explicitly demonstrate the Weyl group actions appearing in (3.178). In the orthogonal basis the generators of $W_{\mathrm{SO}(5)}=\mathcal{S}_2\ltimes(\mathbb{Z}_2)^2$ and $W_{\mathrm{SU}(2)}=\mathcal{S}_2$ have the form

$$w_1^B=\begin{pmatrix}0&1\\1&0\end{pmatrix}\ ,\quad w_2^B=\begin{pmatrix}1&0\\0&-1\end{pmatrix}\ ,\quad w^A=\begin{pmatrix}0&1\\1&0\end{pmatrix}\ . \tag{3.180}$$

There are eight elements in $\mathcal{S}_2\ltimes(\mathbb{Z}_2)^2$ and two in $\mathcal{S}_2$. These act on the simple roots as

$$w_i^B\beta_j=f(\beta_1,\beta_2)\ ,\quad w^A\alpha=g(\alpha)\ , \tag{3.181}$$

where the RHS is a combination of simple roots depending on the particular example. In fact, the simple reflections on the simple roots will generate every other root minus the Cartans of the algebra. For example, the simple roots of $\mathfrak{so}(5)$ in the orthogonal basis are $\beta_1=(1,-1)$ and $\beta_2=(0,1)$. Acting on them with $w_2^B$ produces

$$w_2^B\beta_1=(1,1)=\beta_1+2\beta_2\ ,$$
$$w_2^B\beta_2=(0,-1)=-\beta_2\ . \tag{3.182}$$

Similarly, acting with $w_1^B$ will produce $-\beta_1$ and $\beta_1+\beta_2$ respectively. Furthermore, since the Weyl group has a natural action on $e^\lambda$ (i.e. $w(e^\lambda)=e^{w(\lambda)}$), this action can be directly translated to the fugacities. Following the same example

$$\begin{aligned} w_2^B(b_1) &= e^{w_2^B(\beta_1+\beta_2)} = e^{(\beta_1+\beta_2)} = b_1 \ , \\ w_2^B(b_2) &= e^{\frac{1}{2}w_2^B(\beta_1+2\beta_2)} = e^{\frac{1}{2}\beta_1} = \frac{b_1}{b_2} \ . \end{aligned} \tag{3.183}$$

Combining the Weyl groups leads to $W_{\mathrm{SO}(5)\times\mathrm{SU}(2)}$, which has sixteen elements acting on $a$ and $b_i$. The $Q(a,\mathbf{b},q)$ and $P(\mathbf{b},q)$ are both invariant under the action of any element of this combined Weyl group. Using this fact, the character for long representations can be rewritten in terms of

$$\chi_{\mathcal{L}}(a,\mathbf{b},q) = \left[\!\left[q^\Delta b_1^{d_1} b_2^{d_2} a^K M(\mathbf{b}) R(a) P(\mathbf{b},q) Q(a,\mathbf{b},q)\right]\!\right]_W , \tag{3.184}$$

where $[\![\cdots]\!]_W$ is shorthand for the Weyl symmetriser, a notation adopted from [24].

### Short Representations

Consider now the short multiplets of Table 2. In order to calculate their characters, one is instructed [42, 109, 113] to remove certain combinations of $\mathcal{Q}$s and $P$s from the expressions $Q(a,\mathbf{b},q)$ and $P(\mathbf{b},q)$ given in (3.177).[23] We explicitly consider a few examples to elucidate this point:

a. Take the most basic short multiplet, $\mathcal{A}[d_1,d_2;K]$, with $d_1,d_2,K>0$. Its superconformal primary is annihilated by the supercharge $\mathcal{Q}_{\mathbf{14}}$ and the associated character would be

$$\chi_{\mathcal{A}}(a,\mathbf{b},q) = \left[\!\left[ q^\Delta b_1^{d_1} b_2^{d_2} a^K M(\mathbf{b}) R(a) P(\mathbf{b},q) Q(a,\mathbf{b},q) \left(1+\frac{aq^{\frac{1}{2}}}{b_2}\right)^{-1} \right]\!\right]_W ,$$

with $\Delta = 4+3K+d_1+d_2$. Notice that this includes the character for the product over $\mathcal{Q}_{\mathbf{A}a}$ but now with the $\mathcal{Q}_{\mathbf{14}}$ contribution removed; hence the Weyl symmetrisation removes descendant states associated with the action of $\mathcal{Q}_{\mathbf{14}}$.

b. Take the $\mathcal{B}[d_1,0;K]$ multiplet with $K\neq 0$. One is instructed to remove $\mathcal{Q}_{\mathbf{13}}$ and $\mathcal{Q}_{\mathbf{14}}$ and the supercharacter is

$$\chi_{\mathcal{B}}(a,\mathbf{b},q) =$$

[23] There is a subtlety with removing momentum operators, which will be addressed in the following section.

$$\left[\left[q^{\Delta}b_1^{d_1}a^K M(\mathbf{b})R(a)P(\mathbf{b},q)Q(a,\mathbf{b},q)\left(1+\frac{ab_2q^{\frac{1}{2}}}{b_1}\right)^{-1}\left(1+\frac{aq^{\frac{1}{2}}}{b_2}\right)^{-1}\right]\right]_W ,$$

with $\Delta = 3+3K+d_1$.

c. Suppose now we consider the multiplet $\mathcal{B}[d_1,0;0]$. In this case the $R$-symmetry lowering operator in the Dynkin basis $\mathcal{R}^-$ also annihilates the superconformal primary and two additional shortening conditions are generated

$$\begin{aligned}\mathcal{R}^-\mathcal{Q}_{\mathbf{13}}\Psi &= \mathcal{Q}_{\mathbf{23}}\Psi = 0\ ,\\ \mathcal{R}^-\mathcal{M}_2^-\mathcal{Q}_{\mathbf{13}}\Psi &= \mathcal{Q}_{\mathbf{24}}\Psi = 0\ ,\end{aligned} \tag{3.185}$$

where we remind the reader that $\mathcal{M}_2^-$ is a Lorentz lowering operator in the Dynkin basis. Therefore, for the purposes of building the Verma module we can remove both of these from the basis of Verma-module generators. As a result, the modified product over supercharges, now indicated by $\hat{Q}(\mathbf{a},\mathbf{b},q)$, is

$$\begin{aligned}\hat{Q}(a,\mathbf{b},q) &= Q(a,\mathbf{b},q)\\ &\times\left(1+\frac{ab_2q^{\frac{1}{2}}}{b_1}\right)^{-1}\left(1+\frac{aq^{\frac{1}{2}}}{b_2}\right)^{-1}\left(1+\frac{b_2q^{\frac{1}{2}}}{b_1a}\right)^{-1}\left(1+\frac{q^{\frac{1}{2}}}{b_2a}\right)^{-1}.\end{aligned} \tag{3.186}$$

The last thing to take into account is the possible removal of $P$s from $P(\mathbf{b},q)$ when some components of the multiplet correspond to operator constraints. This will be discussed at length in App. B.1.

### The 5d Superconformal Index

The supercharacter for a given multiplet can be readily converted into the superconformal index. The five-dimensional superconformal index, as we have previously defined it in the Dynkin basis in Sec. 3.2.3, is given by[24]

$$\mathcal{I}(x,y) = \mathrm{Tr}_{\mathcal{H}}(-1)^F e^{-\beta\delta}x^{\frac{2}{3}\Delta+\frac{1}{3}(d_1+d_2)}y^{d_1}\ . \tag{3.187}$$

The states that are counted satisfy $\delta = 0$, where

$$\delta := \{\mathcal{S}_{\mathbf{21}},\mathcal{Q}_{\mathbf{14}}\} = \Delta - \frac{3}{2}K - d_1 - d_2\ . \tag{3.188}$$

[24]The fermion number in this case is $F = 2d_1+d_2 \simeq d_2$, since $d_1$ is always integer.

In order to make contact between the character of a 5d superconformal representation and this index, one can simply make the following fugacity reparametrisations

$$q \to x^{2/3} \ , \quad b_1 \to x^{1/3} y \ , \quad b_2 \to x^{1/3} \tag{3.189}$$

and introduce a factor of $(-1)^F$. The resulting object is precisely the index since every state without $\delta = 0$ pairwise cancels.

### 3.5.2 Characters of 6d $(\mathcal{N}, 0)$ Multiplets

Consider a representation, the highest weight of which has conformal dimension $\Delta$ with $\mathfrak{su}(4)$ quantum numbers $(c_1, c_2, c_3)$ and $R$-symmetry quantum numbers $\mathbf{R}$. For $\mathcal{N} = 1$ we have that $\mathbf{R} = K$, the Dynkin label of $\mathfrak{su}(2)_R$, while for $\mathcal{N} = 2$ the Dynkin labels of $\mathfrak{so}(5)_R$ are $\mathbf{R} = (d_1, d_2)$. The highest weight can be decomposed as

$$\lambda = \omega_1^\alpha c_1 + \omega_2^\alpha c_2 + \omega_3^\alpha c_3 + \omega_i^R R^i \ , \tag{3.190}$$

where the index in $\omega_i^R R^i$ is summed over. The $\omega_i^\alpha$ are the fundamental weights associated with the $\mathfrak{su}(4)$ simple roots $\alpha_i$ and $\vec{\omega}^R$ are the fundamental weights associated with the simple roots of the $R$-symmetry algebra, $\vec{\beta}$.[25] For $\mathfrak{su}(2)_R$ $\vec{\beta}$ has only one component, while for $\mathfrak{so}(5)_R$ $\vec{\beta}$ has two components, $(\beta_1, \beta_2)$. Again, we can express the fundamental weights in terms of the simple roots by using the Cartan matrix $A_{ij}$

$$\omega_i^\alpha = (A_{A_3}^{-1})_{ij} \alpha_j = \begin{pmatrix} \frac{3}{4} & \frac{1}{2} & \frac{1}{4} \\ \frac{1}{2} & 1 & \frac{1}{2} \\ \frac{1}{4} & \frac{1}{2} & \frac{3}{4} \end{pmatrix} \begin{pmatrix} \alpha_1 \\ \alpha_2 \\ \alpha_3 \end{pmatrix} \ , \tag{3.191}$$

alongside the expressions for $\mathfrak{su}(2)_R$ and $\mathfrak{so}(5)_R$ given in (3.171).

This allows for a rewriting of $e^\lambda$ by defining the $\mathfrak{su}(4)$ fugacities

$$a_1 = e^{\frac{1}{4}(3\alpha_1 + 2\alpha_2 + \alpha_3)} \ , \ a_2 = e^{\frac{1}{2}(\alpha_1 + 2\alpha_2 + \alpha_3)} \ , \ a_3 = e^{\frac{1}{4}(\alpha_1 + 2\alpha_2 + 3\alpha_3)} \ . \tag{3.192}$$

Similarly, we define the $R$-symmetry fugacities $\mathbf{b}$ using (3.172). For $\mathcal{N} = 1$ we have that

$$\mathbf{b} = b = e^{\frac{1}{2}\beta} \ , \tag{3.193}$$

[25] Recall that in the previous subsection, we had defined the simple root of $\mathfrak{su}(2)_R$ as $\alpha$. In order to avoid confusion with the $\mathfrak{su}(4)$ Lorentz-algebra simple roots, we label all simple roots associated with the 6d $R$-symmetry algebras as $\vec{\beta}$.

while for $\mathcal{N}=2$ we have $\mathbf{b}=(b_1,b_2)$ with

$$b_1 = e^{\beta_1+\beta_2}\ ,\quad b_2 = e^{\frac{1}{2}(\beta_1+2\beta_2)}\ . \tag{3.194}$$

hence

$$e^{\lambda} = a_1^{c_1}a_2^{c_2}a_3^{c_3}\prod_i b_i^{R^i}. \tag{3.195}$$

The character of a particular representation $\mathcal{R}$ is then given by

$$\chi_{\mathcal{R}}(\mathbf{a},\mathbf{b},q) = \mathrm{Tr}_{\mathcal{R}}\left(a_1^{c_1}a_2^{c_2}a_3^{c_3}\prod_i b_i^{R^i}\right) \tag{3.196}$$

and for $\mathcal{N}=1,2$ respectively we have:

$$\begin{aligned}\chi^{(1,0)}_{\mathcal{R}}(\mathbf{a},b,q) &= \mathrm{Tr}_{\mathcal{R}}\left(a_1^{c_1}a_2^{c_2}a_3^{c_3}b^{K}\right)\ ,\\ \chi^{(2,0)}_{\mathcal{R}}(\mathbf{a},\mathbf{b},q) &= \mathrm{Tr}_{\mathcal{R}}\left(a_1^{c_1}a_2^{c_2}a_3^{c_3}b_1^{d_1}b_2^{d_2}\right)\ .\end{aligned} \tag{3.197}$$

We can then apply this to specific irreducible representations of the 6d $(\mathcal{N},0)$ SCA.

### Long Representations

For the long representation $\mathcal{L}_{[\Delta;c_1,c_2,c_3;\mathbf{R}]}$ we construct the superconformal multiplet by acting on the highest weight state $|\Delta;c_1,c_2,c_3;\mathbf{R}\rangle^{hw}$ with momentum operators and supercharges $f(\mathcal{Q},P)\,|\Delta;c_1,c_2,c_3;\mathbf{R}\rangle^{hw}$. This polynomial can be factorised as $f(\mathbf{a},\mathbf{b},q) = Q(\mathbf{a},\mathbf{b},q)P(\mathbf{a},q)$, since the momentum operators and supercharges commute. Explicitly these functions are

$$\begin{aligned}Q(\mathbf{a},\mathbf{b},q) &= \prod_{\mathbf{A},a}(1+\chi(\mathcal{Q}_{\mathbf{A}a}))\ ,\\ P(\mathbf{a},q) &= \prod_{\mu=1}^{6}(1-\chi(P_\mu))^{-1}\ ,\end{aligned} \tag{3.198}$$

where the range of the sum over $\mathbf{A}$ depends on the amount of supersymmetry.

Thus for a generic long representation we can decompose the character of the superconformal Verma module using (3.167) as

$$\chi_{\mathcal{L}}(\mathbf{a},\mathbf{b},q) = q^{\Delta}\chi_{[c_1,c_2,c_3]}(\mathbf{a})\chi_{[d_1,d_2]}(\mathbf{b})P(\mathbf{a},q)Q(\mathbf{a},\mathbf{b},q). \tag{3.199}$$

The characters $\chi_{[c_1,c_2,c_3]}(\mathbf{a})$ and $\chi_{[d_1,d_2]}(\mathbf{R})$ can in turn be obtained through their Weyl orbits. The relevant Weyl groups are $W_{\mathrm{SU}(4)} = \mathcal{S}_4$, $W_{\mathrm{SO}(5)} = \mathcal{S}_2 \ltimes (\mathbb{Z}_2)^2$ and $W_{\mathrm{SU}(2)} =$

$\mathbb{Z}_2$ so one has

$$\chi_{[c_1,c_2,c_3]}(\mathbf{a}) = \sum_{w\in W_{\mathrm{SU}(4)}} w(a_1)^{c_1} w(a_2)^{c_2} w(a_3)^{c_3} M(w(\mathbf{a})), \tag{3.200}$$

$$\chi_{[\mathbf{R}]}(\mathbf{b}) = \sum_{w\in W_R} \left(\prod_i w(b_i)^{R^i}\right) R^{(\mathcal{N},0)}(w(\mathbf{b})). \tag{3.201}$$

We use $W_R$ to indicate the Weyl group appropriate for the $R$ symmetry of the $(\mathcal{N},0)$ SCA. The $M(\mathbf{a})$ and $R^{(\mathcal{N},0)}(\mathbf{b})$ are the products of characters of negative roots as defined in (3.167); explicitly

$$\begin{aligned} M(\mathbf{a}) &= \frac{1}{\left(1-\frac{a_2}{a_1^2}\right)\left(1-\frac{a_2}{a_3^2}\right)\left(1-\frac{1}{a_1a_3}\right)\left(1-\frac{a_1}{a_2a_3}\right)\left(1-\frac{a_1a_3}{a_2^2}\right)\left(1-\frac{a_3}{a_1a_2}\right)}\,, \\ R^{(2,0)}(\mathbf{b}) &= \frac{1}{\left(1-\frac{1}{b_1}\right)\left(1-\frac{1}{b_2^2}\right)\left(1-\frac{b_1}{b_2^2}\right)\left(1-\frac{b_2^2}{b_1^2}\right)}\,, \\ R^{(1,0)}(b) &= \frac{b^2}{b^2-1}\,. \end{aligned} \tag{3.202}$$

Again, we note that both $Q(\mathbf{a},\mathbf{b},q)$ and $P(\mathbf{a},q)$ are invariant under the appropriate Weyl symmetrisations and one can write for $\mathcal{N}=2$

$$\chi^{(2,0)}_{\mathcal{L}}(\mathbf{a},\mathbf{b},q) = \left[\!\left[q^{\Delta} a_1^{c_1} a_2^{c_2} a_3^{c_3} b_1^{d_1} b_2^{d_2} M(\mathbf{a}) R^{(2,0)}(\mathbf{b}) P(\mathbf{a},q) Q(\mathbf{a},\mathbf{b},q)\right]\!\right]_W\,, \tag{3.203}$$

matching [24], while for $\mathcal{N}=1$

$$\chi^{(1,0)}_{\mathcal{L}}(\mathbf{a},b,q) = \left[\!\left[q^{\Delta} a_1^{c_1} a_2^{c_2} a_3^{c_3} b^{K} M(\mathbf{a}) R^{(1,0)}(b) P(\mathbf{a},q) Q(\mathbf{a},b,q)\right]\!\right]_W\,, \tag{3.204}$$

where $[\![\cdots]\!]_W$ denotes the Weyl symmetriser.

### Short Representations

Consider now the short multiplets of Table 3 for $\mathcal{N}=1$ or Table 4 for $\mathcal{N}=2$. To calculate their characters we remove certain combinations of $\mathcal{Q}$s from the expressions $Q(\mathbf{a},\mathbf{b},q)$ given in (3.198). This discussion is completely analogous to Sec. 3.5.1. There are a few cases when one is also prescribed to remove certain $P_\mu$ from $P(\mathbf{a},q)$. This is discussed at length in App. B.1.

### The 6d $(1,0)$ Superconformal Index

Once we have obtained the full supercharacter we can readily covert it into the superconformal index. For $\mathcal{N}=1$ the index as defined in (3.3.3) is given by[26]

$$\mathcal{I}(p,q,s) = \mathrm{Tr}_{\mathcal{H}}(-1)^F e^{-\beta\delta} q^{\Delta-\frac{1}{2}K} p^{c_2} s^{c_1} \ . \tag{3.205}$$

The states that are counted satisfy $\delta = 0$, where

$$\delta = \Delta - 2K - \frac{1}{2}(c_1 + 2c_2 + 3c_3) \ . \tag{3.206}$$

We can therefore write the character of a representation as an index via the following fugacity reparametrisations

$$a_1 \to s \ , \quad a_2 \to p \ , \quad a_3 \to 1 \ , \quad b \to \frac{1}{q^{\frac{1}{2}}} \tag{3.207}$$

and inserting $(-1)^F$. The resulting object is precisely the index since every state without $\delta = 0$ pairwise cancels.

### The 6d $(2,0)$ Superconformal Index

The 6d $(2,0)$ superconformal index, as previously defined in (3.4.3), is given by

$$\mathcal{I}(p,q,s,t) = \mathrm{Tr}_{\mathcal{H}}(-1)^F e^{-\beta\delta} q^{\Delta-d_1-\frac{1}{2}d_2} p^{c_2+c_3-d_2} t^{-d_1-d_2} s^{c_1+c_2} \ . \tag{3.208}$$

The states that are counted satisfy $\delta = 0$, where

$$\delta = \Delta - 2d_1 - \frac{1}{2}c_1 - c_2 - \frac{3}{2}c_3 \ . \tag{3.209}$$

In order to make contact between the character and this index, we make the following fugacity reparametrisations

$$a_1 \to s \ , \quad a_2 \to ps \ , \quad a_3 \to p \ , \quad b_1 \to \frac{t}{q} \ , \quad b_2 \to \frac{q^{\frac{1}{2}}t}{p} \tag{3.210}$$

and insert $(-1)^F$. The resulting object is precisely the index since every state previously counted by the character without $\delta = 0$ pairwise cancels. This concludes our discussion about obtaining general multiplet superconformal indices from supercharacters.

[26] The fermion number in this case is $F = c_1 + c_3$.

# Chapter 4

# Deconstructing Six Dimensional Theories

This chapter is based on the papers [2] and [3]. It has two main sections, each corresponding to the two aforementioned articles. Useful identities and definitions pertinent to this Chapter have been included in Appendix A.

Over the last few years, there has been significant progress in the study of six-dimensional supersymmetric field theories. This progress relied on advances in the exact calculation of protected quantities, such as the superconformal index [39, 40, 42], using *e.g.* the method of supersymmetric localisation [53] or the refined topological vertex [68]. The two six-dimensional theories that we will focus on are the 6d (2,0) theory and the 6d little string theory (LST).

These are the only two UV-complete interacting 6d theories that are thought to exist with sixteen supercharges. The (2,0) theory is conformal and can be understood as a low energy description of $k$ coincident M5-branes in M-theory, commonly denoted as $(2,0)_k$. LST with (1,1) SUSY can be found as a $g_s \to 0$ limit of $k$ coincident NS5-branes in type IIB string theory. Note that this is a non-local quantum field theory since one keeps $\alpha'$ fixed. It is believed that this theory is a UV completion of 6d MSYM. There is a T-dual description for NS5 branes in type IIA string theory with (2,0) supersymmetry. Both of these 6d theories lack a Lagrangian description, and so one needs to get quite creative with how we probe them.

The 6d ADE (2,0) theories have no known Lagrangian descriptions, however, various supersymmetric partition functions have been calculated by appealing to the relationship between 5d maximally-supersymmetric Yang–Mills theory (MSYM) and the 6d (2,0) theory on a circle $\mathbb{S}^1_{R_6}$ of radius $R_6 = g_5^2/2\pi$. The prototypical example of such a protected quantity is the supersymmetric partition function of 5d MSYM on $\mathbb{S}^5$ [124–129] (or $\mathbb{CP}^2 \times \mathbb{S}^1$ [122]), which computes the superconformal index of the (2,0)

theory;[27] for a more complete list of references see [123]. The (2,0) superconformal index was also recovered in [70, 71] using the "refined topological vertex" formalism for constructing topological string amplitudes [68, 132]. Some of these exact tools were subsequently used to help establish a striking connection between BPS subsectors of the $(2,0)_{\mathrm{ADE}}$ theory and 2d $\mathcal{W}_{\mathrm{ADE}}$-algebras. By doing so, the authors of [24] solved for said subsector of the (2,0) theory, since *e.g.* 3-point functions of associated operators can immediately be obtained from the $\mathcal{W}$-algebra literature. Finally, a significant complementary approach was initiated in [15], aiming to constrain the (2,0) theory as an abstract SCFT through the conformal-bootstrap programme, which is solely based on the system's symmetries and a minimal set of initial assumptions.

Conversely for LST, due to its lack of conformal symmetry, there are fewer options available for probing these theories. However, a great deal of progress has been made by using the refined topological vertex to calculate the $\mathbb{R}^4_{\epsilon_1,\epsilon_2} \times \mathbb{T}^2$ partition function, *cf.* [81–83].

These new developments join an older proposal for attacking the (2,0) theory and LST: dimensional deconstruction [23]. In this section we would like to revisit this armed with some modern non-perturbative techniques. Towards that end, we remind the reader of the work of [23]. Two cases were postulated. First, one can start from a superconformal $\mathcal{N} = 2$ four-dimensional circular quiver-gauge theory with SU($k$) gauge-group nodes, and upon taking a specific limit of parameters that takes the theory to the Higgs phase, one recovers the corresponding $\mathrm{A}_{k-1}$ (2,0) theory on a torus of fixed (but arbitrary) size. Evidence for this claim included estimating the Kaluza–Klein (KK) spectrum of the 6d theory on $\mathbb{T}^2$, as well as a string-duality argument where the field theories involved were geometrically engineered using branes. In follow-up work [133], it was confirmed that the circular-quiver theory explicitly deconstructs 5d MSYM on a finite circle $\mathbb{S}^1_{R_5}$, for values of the parameters corresponding to weak coupling (for fixed energies), $g_5^2 = 2\pi R_6$, where the theory is well defined.[28]

The second case was to consider a four-dimensional toroidal quiver-gauge theory with $N_5 \times N_6$ SU($k$) gauge nodes. For a certain set of limits on the field theory parameters it was argued that this theory deconstructs the (1,1) LST with $2\pi R_5 = \frac{N_5}{G\mathrm{v}_5}$ and $2\pi R_6 = \frac{N_6}{G\mathrm{v}_6}$; where $\mathrm{v}_i$ are vacuum expectation values (VEVs) for the chiral multiplets and $G$ is the gauge coupling for each node. This will be expanded on in the subsequent sections.

Although the existing qualitative evidence is highly suggestive, it would be useful to have quantitative tests for the proposals of [23]. The aim of this chapter is to address precisely this point. We perform a detailed comparison between the part of

[27] This is despite the fact that the 5d MSYM theory is perturbatively non-renormalisable [130], although it is also not sufficient evidence to rule in favour of the conjecture of [19, 20, 131].

[28] It naturally follows that for large values of $R_6$ the UV-finite 4d $\mathcal{N} = 2$ theory provides a quantum definition of 5d MSYM through deconstruction [133].

the circular-quiver spectrum that survives deconstruction, and that of the $(2,0)_k$ theory that captures the low-energy dynamics of $k$ M5-branes on a torus. This is carried out via two independent calculations, both of which are only indirectly sensitive to the choice of Higgs VEV. We then test the proposal for (1,1) LST, and along the way propose a refinement for the $\mathbb{S}^4$ partition function for $\mathcal{N}=1$ theories.

## 4.1 The (2,0) Theory

We commence this section with a short summary of the first results of [23] in order to establish conventions and notation. The starting point is an $N$-noded 4d circular-quiver theory, with SU($k$) gauge groups. The nodes are connected by bifundamental chiral superfields, the scalar components of which are denoted by $(X_{\alpha+1,\alpha})^{i_{(\alpha+1)}}{}_{j_{(\alpha)}}$, $(X_{\alpha,\alpha+1})^{j_{(\alpha)}}{}_{i_{(\alpha+1)}}$; here $\alpha = \lfloor -N/2 \rfloor + 1, \ldots, \lfloor N/2 \rfloor$ labels the quiver nodes and the (down) up $i_{(\alpha)}$s are (anti)fundamental gauge indices associated with the $\alpha$-th gauge group. The minimal coupling to the gauge fields occurs via

$$\begin{aligned} D_\mu (X_{\alpha+1,\alpha})^{i_{(\alpha+1)}}{}_{j_{(\alpha)}} &= \partial_\mu (X_{\alpha+1,\alpha})^{i_{(\alpha+1)}}{}_{j_{(\alpha)}} - i (A_\mu^{(\alpha+1)})^{i_{(\alpha+1)}}{}_{k_{(\alpha+1)}} (X_{\alpha+1,\alpha})^{k_{(\alpha+1)}}{}_{j_{(\alpha)}} \\ &\quad + i (X_{\alpha+1,\alpha})^{i_{(\alpha+1)}}{}_{l_{(\alpha)}} (A_\mu^{(\alpha)})^{l_{(\alpha)}}{}_{j_{(\alpha)}} \, . \end{aligned} \tag{4.1}$$

This theory is conformal and enjoys $\mathcal{N}=2$ supersymmetry.

The first step towards implementing the deconstruction prescription of [23] is to give a VEV to the scalar fields

$$\langle (X_{\alpha,\alpha+1})^{j_{(\alpha)}}{}_{i_{(\alpha+1)}} \rangle = \mathrm{v} \, \delta^{j_{(\alpha)}}{}_{i_{(\alpha+1)}} \qquad \forall \, \alpha \, . \tag{4.2}$$

This takes the theory onto the Higgs branch and has the effect of breaking the gauge group down to the diagonal subgroup $\mathrm{SU}(k)^N \to \mathrm{SU}(k)$. Consequently, the previously-independent $N-1$ gauge couplings $g^{(\alpha)}$ are replaced by a single coupling parameter denoted by $G$.

The second step is to consider the limit

$$N \to \infty \, , \qquad G \to \infty \, , \qquad \mathrm{v} \to \infty \, , \tag{4.3}$$

in a fashion that keeps

$$g_5^2 := \frac{G}{\mathrm{v}} \to \text{fixed} \, , \qquad 2\pi R_5 := \frac{N}{G\mathrm{v}} \to \text{fixed} \, . \tag{4.4}$$

For energies small compared to the scale $1/g_5^2$, the resultant theory can be explicitly seen to reproduce 5d MSYM on a continuous circle of radius $R_5$, with bare gauge coupling $g_5$ [133]. Note that supersymmetry is enhanced in the limit, with 16 preserved

| | $x^0$ | $x^1$ | $x^2$ | $x^3$ | $x^4$ | $x^5$ | $x^6$ | $x^7$ | $x^8$ | $x^9$ |
|---|---|---|---|---|---|---|---|---|---|---|
| $k$ D3 branes | – | – | – | – | · | · | · | · | · | · |
| $A_{N-1}$ ALE | · | · | · | · | · | · | – | – | – | – |

**Table 5:** Brane configuration in type IIB string theory. The ALE space extends in the directions $x^6, x^7, x^8, x^9$. The direction $x^6$ is compact with periodicity $x^6 \to x^6 + 2\pi r$.

supercharges. One straightforwardly recovers two towers of massive states:

$$M_{n_1}^2 = \left(\frac{2\pi n_1}{R_5}\right)^2 , \qquad \widetilde{M}_{n_2}^2 = \left(\frac{4\pi^2 n_2}{g_5^2}\right)^2 . \tag{4.5}$$

The first is a tower of KK modes associated with $\mathbb{S}^1_{R_5}$, while the second with the BPS spectrum of $n_2$-instanton-soliton states. The latter can also be identified with another KK tower when the bare 5d coupling is related to the radius of an additional circle,

$$g_5^2 = 2\pi R_6 . \tag{4.6}$$

This identification is implied by Type IIA/M-theory duality, whence 5d mSYM is interpreted as the low-energy effective description for the 6d (2,0) theory on $\mathbb{S}^1_{R_6}$. Even though this 5d picture is expected to break down at high energies, the 4d description is UV complete and valid for all values of parameters (4.4), therefore bypassing the issue of non-completeness of 5d MSYM. The 4d $\mathcal{N} = 2$ circular-quiver theory is thus claimed to be deconstructing the (2,0) theory on a torus $\mathbb{T}^2 = \mathbb{S}^1_{R_5} \times \mathbb{S}^1_{R_6}$ of any size. It is interesting to observe that the S-duality action on the 4d theory, which sends $G \leftrightarrow \frac{N}{G}$, also exchanges the two circles of the $\mathbb{T}^2$.

### Brane Engineering I

The above picture is reinforced using brane engineering and a chain of dualities. The circular-quiver theory can be obtained at low energies on a stack of $k$ D3 branes probing a $\mathbb{C} \times \mathbb{C}^2/\mathbb{Z}_N$ orbifold singularity. This system is parametrised by the orbifold rank, $N$, the string length, $l_s$, and string coupling, $g_s$. Turning on the chiral-multiplet VEVs corresponds to taking the $k$ D3 branes off the orbifold singularity and into the orbifolded transverse space by a distance $d$. The limit (4.4) translates into taking $l_s \to 0$ and $N \to \infty$, while keeping

$$g_s \to \text{fixed} , \qquad \frac{d}{N l_s^2} = \frac{1}{R_5} \to \text{fixed} , \qquad \frac{d}{N l_s^2 g_s} = \frac{1}{R_6} \to \text{fixed} . \tag{4.7}$$

One can use the above to straightforwardly deduce the following relation between the string and gauge-theory parameters

$$\frac{d}{2\pi l_s^2} = G\mathrm{v}\ , \qquad \sqrt{g_s N} = G\ . \tag{4.8}$$

In the limit (4.7) the geometry probed by the $k$ D3s can be locally approximated by $\mathbb{R}^5 \times \mathbb{S}^1_r$, where $r = d/N = l_s^2/R_5$. The D3s can be T-dualised along this circle to obtain $k$ D4s wrapping $\mathbb{S}^1_{R_5}$, with string coupling $g_s' = g_s R_5/l_s$. This becomes strong as $l_s \to 0$ upon which one has $k$ M5 branes on $\mathbb{S}^1_{R_5}$, with the M-theory circle being $R_6 = g_s' l_s = g_s R_5$. Moreover, in the deconstruction limit the 11d Planck length $l_p = l_s {g_s'}^{1/3} \to 0$ and one recovers $(2,0)_k$, the $A_{k-1}$ theory plus a free-tensor multiplet on $\mathbb{T}^2 = \mathbb{S}^1_{R_5} \times \mathbb{S}^1_{R_6}$ [23] .

Note that the low-energy description for this D-brane system is in terms of $\mathrm{U}(k)$ as opposed to $\mathrm{SU}(k)$ gauge groups. On the one hand, this distinction is unimportant for the procurement of the mass spectrum (4.5) as well as for the deconstruction argument reviewed above (since, rather than providing any strong-coupling scale, confinement or any sort of exotic IR phenomena, the U(1) part is IR free and thus decouples). This observation will be important later on and we will therefore explicitly use the $\mathrm{U}(k)^N$ circular-quiver theory in the calculations that follow [23].

### Brane Engineering II

One can also use an alternative description of this brane system, where the T-duality transformation is implemented before taking the branes off the orbifold singularity. This will be more appropriate for our purposes. For the D3-brane probes, the space $\mathbb{C}^2/\mathbb{Z}_N$ resolves to the $A_{N-1}$ ALE metric, as summarised in Table 5. This can be T-dualised along the compact direction to give rise to a configuration of $N$ NS5s on the dual circle, with $k$ D4 branes stretched between them, as summarised in Table 6 [134–137]. There is a $\mathrm{U}(k)^N$ gauge theory associated with open strings that end on the D4 segment between two adjacent NS5s (each of which have their own coupling), massive modes coming from open strings stretching between adjacent D4 segments (across an NS5), as well as an overall centre of mass. At low energies the massive modes freeze out (they become parameters) and the remaining degrees of freedom comprise an $\mathrm{SU}(k)^N \times \mathrm{U}(1)$ theory. Rotations along $x^{7,8,9}$ correspond to the $\mathrm{SU}(2)_R$ of the $\mathcal{N} = 2$ theory while rotations along the $x^{4,5}$ plane to the $\mathrm{U}(1)_r$ symmetry [138, 139].

The gauge theory possesses several deformations, which can be appropriately encoded in terms of distances in the geometric interpretation. In order to parametrise the D4/NS5 brane setup it is useful to define the complex coordinates $v$ and $s$ as follows:

$$v = x^4 + ix^5 \quad \text{and} \quad s = x^6 + ix^{10}\ . \tag{4.9}$$

| | $x^0$ | $x^1$ | $x^2$ | $x^3$ | $x^4$ | $x^5$ | $x^6$ | $x^7$ | $x^8$ | $x^9$ | $(x^{10})$ |
|---|---|---|---|---|---|---|---|---|---|---|---|
| $k$ D4 branes | – | – | – | – | · | · | – | · | · | · | – |
| $N$ NS5 branes | – | – | – | – | – | – | · | · | · | · | · |

**Table 6:** Brane configuration in type IIA string theory. The direction $x^6$ is compact with periodicity $x^6 \to x^6 + 2\pi R_5$. The coordinate $x^{10}$ parametrises the M-theory circle at strong coupling with periodicity $x^{10} \to x^{10} + 2\pi R_6$.

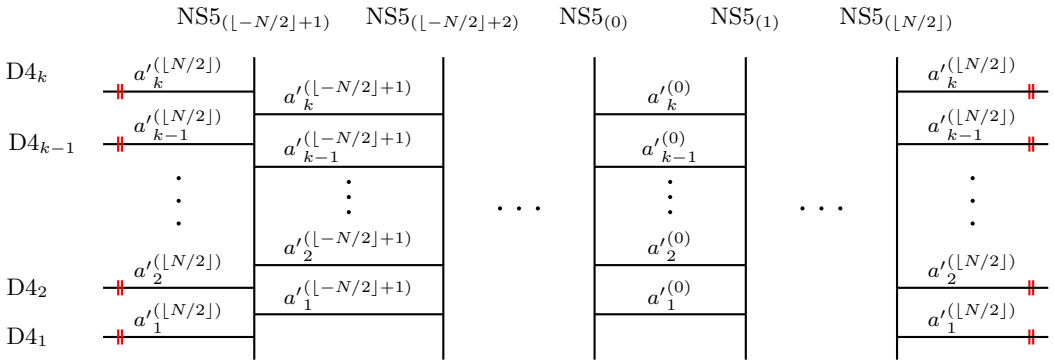


**Figure 3:** The brane set up for the U$(k)^N$ circular-quiver theory. The vertical lines represent NS5 branes while the horizontal lines represent D4 branes. The cyclic identification of the end points is indicated by the double red line on the D4 branes.

Using these variables, the separation of D4 branes can be measured along $v$. Distances in this coordinate, associated with the U$(1)_r$ symmetry, translate into Coulomb parameters $a_b^{(\alpha)}$, as well as bifundamental masses $m_{\text{bif}}^{(\alpha)}$. The Coulomb-branch moduli are straightforwardly encoded as the distances between a colour-D4-brane position and the centre-of-mass position of the colour branes within a single gauge-group factor; see Fig. 3:

$$a_b^{(\alpha)} = \frac{1}{2\pi l_s^2}\left(a'^{(\alpha)}_b - \frac{1}{k}\sum_{c=1}^{k} a'^{(\alpha)}_c\right) . \tag{4.10}$$

The only mass parameters are those of the bifundamental hypermultiplets that capture the relative centre-of-mass positions of two consecutive D4 stacks.[29] For bifundamental fields—fundamental under the gauge group on the left ($(\alpha-1)$-th gauge group) and anti-fundamental under the gauge group on the right ($\alpha$-th gauge group)—the bifundamental mass is given by

$$m_{\text{bif}}^{(\alpha)} = \frac{1}{2\pi l_s^2}\left(\frac{1}{k}\sum_{b=1}^{k} a'^{(\alpha+1)}_b - \frac{1}{k}\sum_{b=1}^{k} a'^{(\alpha)}_b\right) . \tag{4.11}$$

[29] In U$(k)^N$ gauge-theory language this translates into the relative U(1) of the two consecutive colour groups [138].

These definitions were used in the identification of parameters in the calculation of the 4d partition function in Chapter 2.4.1.

In a similar manner, the coordinate $s$ measures the distance between NS5 branes. This encodes the couplings for the $\alpha$-th D4 segment

$$\tau^{(\alpha)} = \frac{4\pi i}{g_{(\alpha)^2}} + \frac{\theta^{(\alpha)}}{8\pi^2} \,. \tag{4.12}$$

Due to the periodic nature of the M-theory circle, $x^{10}$, it is also natural to introduce the exponentiated coordinate $t = e^{-\frac{s}{R_6}}$, where $R_6$ is the radius of M-theory circle [138]. In the $t$ coordinate the distance between two NS5 branes is given by

$$\mathbf{q}_{(\alpha)} = e^{2i\pi\tau^{(\alpha)}} \,. \tag{4.13}$$

For the purposes of deconstruction we are interested in the "maximally-Higgsed" phase, where all chiral multiplets acquire a VEV and the gauge group gets broken to $\mathrm{U}(k)^N \to \mathrm{U}(k)$. In the absence of bifundamental masses, the corresponding classical-brane picture is in terms of coincident endpoints for all adjacent D4 segments. At this point of moduli space, where the Coulomb and Higgs branches meet, the brane segments can reconnect to form a single collection of $k$ D4s wrapping the circle $S^1_{R_5}$, with a single coupling $G$. These can then be moved off the NS5s in the $x^{7,8,9}$ directions. In the limit (4.7) the resultant configuration leads once again to the $(2,0)_k$ theory on the same $\mathbb{T}^2 = \mathbb{S}^1_{R_5} \times \mathbb{S}^1_{R_6}$ as in the previous brane engineering case. We will use this picture of deconstruction as our starting point for the calculation of the partition functions in Sec. 4.1.2.

### 4.1.1 4d/6d Matching: Higgs-Branch Hilbert Series and the (2,0) Index

Having established the proposal of [23], we now set out to test it using some exact methods. We have already discussed in Sec. 4.1 how the 4d $\mathcal{N} = 2$ circular-quiver theory deconstructs the (2,0) theory on a torus of fixed (but arbitrary) size. Nevertheless, a special limit of parameters in Eq. (4.4) can be considered, such that the radii $R_5, R_6 \to \infty$ and the torus decompactifies. The deconstruction limit then relates two fixed-point theories in the UV (4d) and the IR (6d) (at v $\to \infty$) and hence their local operator spectra, up to sectors of the 4d theory decoupling at low energies and large $N$. A quantitative diagnostic of this claim can be performed by setting up a counting problem for local operators on both sides. For instance, one could try and quantify this relationship by comparing appropriate limits of superconformal indices following the procedure of [140], but generalising that approach to the maximally-Higgsed phase of the circular-quiver theory proves difficult.

For this reason, we will focus on very special classes of BPS operators using the

superconformal algebra (SCA) as a guide and analysing the embedding of the $\mathcal{N}=2$ 4d SCA into the 6d (2,0) SCA. This will lead in an identification between a set of simple half-BPS primary operators parametrising the 4d mesonic Higgs branch in the deconstruction limit, and operators in a 6d half-BPS ring. As we will explain in detail below, we will perform the 4d counting using the Higgs-branch Hilbert Series for the $\mathrm{U}(k)^N$ theory, while the 6d counting via the "half-BPS" limit of the superconformal index [141, 142].

### SCA Analysis

The the (2,0) 6d superconformal algebra has been discussed in great detail in Chapter 3, but we will remind the reader of the salient points. The algebra is denoted by $\mathfrak{osp}(8^*|4)$. Primaries in the corresponding modules are in one-to-one correspondence with highest weights in irreducible representations of the maximal compact subalgebra $\mathfrak{so}(6)\oplus\mathfrak{so}(2)\oplus\mathfrak{so}(5)_R\subset\mathfrak{osp}(8^*|4)$. They are thus labelled by the eigenvalues of the respective Cartan generators: the conformal dimension $\Delta$, $\mathfrak{so}(6)$ Lorentz quantum numbers in the orthogonal basis $h_i$, and $R$-symmetry quantum numbers in the orthogonal basis $J_i$. There are also fermionic generators: sixteen Poincaré and superconformal supercharges, denoted by $\mathcal{Q}_{\mathbf{A}a}$ and $\mathcal{S}_{\mathbf{A}\dot{a}}$, where $\dot{a},a=1,\ldots,4$ are (anti)fundamental indices of $\mathfrak{su}(4)$ and $\mathbf{A}=\mathbf{1},\ldots,\mathbf{4}$ a spinor index of $\mathfrak{so}(5)_R$; see *e.g.* [1, 24, 36] for conventions and notation.

Similarly, the $\mathcal{N}=2$ 4d superconformal algebra is denoted by $\mathfrak{su}(2,2|2)$. Primaries in the corresponding modules are in one-to-one correspondence with highest weights in irreducible representations of the maximal compact subalgebra $\mathfrak{so}(4)\oplus\mathfrak{so}(2)\oplus\mathfrak{su}(2)_R\oplus\mathfrak{u}(1)_r\subset\mathfrak{su}(2,2|2)$. They are labelled by the eigenvalues of the respective Cartans: their conformal dimension $\Delta$, $\mathfrak{su}(2)_1\oplus\mathfrak{su}(2)_2\simeq\mathfrak{so}(4)$ Lorentz quantum numbers $m_i$, and $R$-symmetry quantum numbers $R,r$. There are also fermionic generators: eight Poincaré and superconformal supercharges, $Q^I_\alpha$, $\widetilde{Q}_{I\dot{\alpha}}$ and $S^{\dot{\alpha}}_I$, $\widetilde{S}^{I\dot{\alpha}}$, where $\dot{\alpha},\alpha=\pm$ and $I=1,2$ are fundamental indices of $\mathfrak{su}(2)\oplus\mathfrak{su}(2)$ and $\mathfrak{su}(2)_R$ respectively; see *e.g.* [37] for more details. The 4d $\mathcal{N}=2$ SCA is a subalgebra of the (2,0) 6d SCA with the Cartans being related to the 6d ones through

$$\begin{aligned} R=J_1, \qquad & r=J_2\,, \\ m_1=\frac{1}{2}(h_2+h_3), \qquad & m_2=\frac{1}{2}(h_2-h_3)\,. \end{aligned} \tag{4.14}$$

We choose an embedding of the 4d SCA into the 6d SCA, which relates the supercharges as in Table 7 [24].

The (2,0) SCA contains a special class of half-BPS short multiplets, denoted by $\mathcal{D}[0,0,0;J_1,0]$, for which $\Delta=2J_1$ and where the superconformal primary is annihilated by the set of Poincaré supercharges $\mathcal{Q}_{\mathbf{1}a},\mathcal{Q}_{\mathbf{2}a}$ in addition to all the superconformal

| 6d Supercharge | $(h_1, h_2, h_3)$ | $(m_1, m_2)$ | $R$ | $r$ | 4d Supercharge |
|---|---|---|---|---|---|
| $\mathcal{Q}_{\mathbf{11}}$ | $(+,+,+)$ | $(+,0)$ | $+$ | $+$ | $Q^1_+$ |
| $\mathcal{Q}_{\mathbf{21}}$ | $(+,+,+)$ | $(+,0)$ | $+$ | $-$ | |
| $\mathcal{Q}_{\mathbf{31}}$ | $(+,+,+)$ | $(+,0)$ | $-$ | $+$ | $Q^2_+$ |
| $\mathcal{Q}_{\mathbf{41}}$ | $(+,+,+)$ | $(+,0)$ | $-$ | $-$ | |
| $\mathcal{Q}_{\mathbf{12}}$ | $(+,-,-)$ | $(-,0)$ | $+$ | $+$ | $Q^1_-$ |
| $\mathcal{Q}_{\mathbf{22}}$ | $(+,-,-)$ | $(-,0)$ | $+$ | $-$ | |
| $\mathcal{Q}_{\mathbf{32}}$ | $(+,-,-)$ | $(-,0)$ | $-$ | $+$ | $Q^2_-$ |
| $\mathcal{Q}_{\mathbf{42}}$ | $(+,-,-)$ | $(-,0)$ | $-$ | $-$ | |
| $\mathcal{Q}_{\mathbf{13}}$ | $(-,+,-)$ | $(0,+)$ | $+$ | $+$ | |
| $\mathcal{Q}_{\mathbf{23}}$ | $(-,+,-)$ | $(0,+)$ | $+$ | $-$ | $\widetilde{Q}_{2\dot{+}}$ |
| $\mathcal{Q}_{\mathbf{33}}$ | $(-,+,-)$ | $(0,+)$ | $-$ | $+$ | |
| $\mathcal{Q}_{\mathbf{43}}$ | $(-,+,-)$ | $(0,+)$ | $-$ | $-$ | $\widetilde{Q}_{1\dot{+}}$ |
| $\mathcal{Q}_{\mathbf{14}}$ | $(-,-,+)$ | $(0,-)$ | $+$ | $+$ | |
| $\mathcal{Q}_{\mathbf{24}}$ | $(-,-,+)$ | $(0,-)$ | $+$ | $-$ | $\widetilde{Q}_{2\dot{-}}$ |
| $\mathcal{Q}_{\mathbf{34}}$ | $(-,-,+)$ | $(0,-)$ | $-$ | $+$ | |
| $\mathcal{Q}_{\mathbf{44}}$ | $(-,-,+)$ | $(0,-)$ | $-$ | $-$ | $\widetilde{Q}_{1\dot{-}}$ |

**Table 7:** Summary of supercharge quantum numbers in 6d and the 4d embedding. All orthogonal-basis quantum numbers have magnitude one half. The four-dimensional subalgebra acts on the $h_2$ and $h_3$ planes.

$\mathcal{S}_{\mathbf{A}\dot{a}}$ [1, 24, 36]. By inspecting Table 7, one sees that $\mathcal{Q}_{\mathbf{11}}, \mathcal{Q}_{\mathbf{12}}$ and $\mathcal{Q}_{\mathbf{23}}, \mathcal{Q}_{\mathbf{24}}$ can be identified with certain supercharges $Q^1_\alpha, \widetilde{Q}_{2\dot{\alpha}}$ for a 4d $\mathcal{N} = 2$ subalgebra, which can in turn be interpreted as the SCA for the 4d quiver.

Recall now that in four dimensions, operators $\mathcal{H}_\mathcal{I}$ satisfying

$$[Q^1_\alpha, \mathcal{H}_\mathcal{I}] = 0 \,, \qquad [\widetilde{Q}_{2\dot{\alpha}}, \mathcal{H}_\mathcal{I}] = 0 \tag{4.15}$$

form a (non-freely-generated) ring that parametrises the Higgs branch of the theory; see *e.g.* [143]. In the notation of [37] these are in the $\hat{\mathcal{B}}_R$ multiplet with shortening condition $\Delta = 2R$. Therefore, the 4d Higgs-branch operators $\mathcal{H}_\mathcal{I}$ are good candidates for reproducing the 6d half-BPS superconformal primaries in the deconstruction limit. It is these two classes of operators that we will be counting.

### The Half-BPS Index of the 6d (2,0) Theory

Here we briefly review the half-BPS index of the (2,0) theory. For a choice of defining supercharge, $\mathcal{Q}_{\mathbf{44}}$,[30] the 6d (2,0) superconformal index is given by the quantity [42, 142]

$$I = \mathrm{Tr}(-1)^F e^{-\beta\delta} x^{\Delta+J_1} y_1^{h_1-h_2} y_2^{h_2+h_3} q^{h_1+h_2-h_3-3J_2}$$

[30] Note that this is a different choice than we have previously used in Chapter 3. This is in order to faithfully review the result of [141].

$$\delta = \{\mathcal{Q}_{\mathbf{44}}, \mathcal{S}_{\mathbf{1\dot{4}}}\} = \Delta - h_1 - h_2 + h_3 + 2J_1 + 2J_2 \,, \tag{4.16}$$

where the trace is taken over the Hilbert space of the theory in radial quantisation, the $x, y_1, y_2, q$ are a maximal set of fugacities taking values inside the unit circle, such that e.g. $|x| < 1$, and their exponents are the already-defined Cartan generators of the (2,0) SCA [42,142]. The superconformal index receives contributions from operators in short representations of the superconformal algebra with $\delta = 0$, modulo combinations of short representations that can pair up to form long representations.

Let us first consider the abelian case. The index of the free-tensor multiplet in 6d—denoted in [1, 24] as $\mathcal{D}[0,0,0;1,0]$—can be straightforwardly calculated using letter counting and gives[31]

$$\mathcal{I}^{(2,0)_1} = \mathrm{PE}[f], \qquad f = \frac{x + x^2q^3 - x^2q^2(y_1^{-1} + y_1y_2^{-1} + y_2) + x^3q^3}{(1 - xqy_1)(1 - xqy_1y_2^{-1})(1 - xqy_2^{-1})} \,. \tag{4.17}$$

The index for the interacting (2,0) theory is known in closed form only in certain limits of fugacities; see *e.g.* [122] and also [24] for an alternative calculation using the associated $\mathcal{W}$ algebra. A particularly-simple such limit is obtained when $q \to 0$, whence the only operators counted are the half-BPS primaries of the $\mathcal{D}[0,0,0;J_1-J_2,0]$ multiplets. The latter admit a free-field realisation in terms of $\mathcal{D}[0,0,0;1,0]$ for which $\lim_{q\to 0} f = x$. One subsequently has for the "half-BPS" index in the (2,0) theory of $k$ M5 branes (including the c.o.m. free-tensor multiplet) [141, 142]

$$\mathcal{I}^{(2,0)_k}_{\frac{1}{2}\mathrm{BPS}} = \mathrm{PE}\left[\sum_{m=1}^{k} x^m\right] = \prod_{m=1}^{k} \frac{1}{1-x^m} \,. \tag{4.18}$$

Note that this is not the same as the Schur limit of the index, which also counts derivatives acting on the primaries. This can also be obtained from the MacDonald index defined in Chapter 3

$$\mathcal{I}^{Mac}_{A_{k-1}}(q,t) = \mathrm{P.E.}\left[\frac{qt + (qt)^2 + \ldots + (qt)^k}{1-q}\right] \,, \tag{4.19}$$

by taking $x = qt =$ fixed and sending $q \to 0$.

Alternatively, the answer can be rephrased as the coefficient of $\nu^k$ in the expansion of the generating function $\mathrm{PE}[\nu x]$, where $\nu$ an arbitrary parameter. A simple manipulation

[31] Recall that the plethystic exponential is defined as $\mathrm{PE}[f(\mathbf{x})] = \exp\left[\sum_{n=1}^{\infty} \frac{f(\mathbf{x}^n)}{n}\right]$, where $\mathbf{x}$ corresponds to a certain list of fugacities. The inverse operation is called the plethystic logarithm and given by $\mathrm{PL}[f(\mathbf{x})] = \sum_{n=1}^{\infty} \frac{\mu(n)}{n} \log\left[f(\mathbf{x}^n)\right]$, where $\mu(n)$ is the Möbius function.

shows that

$$\mathrm{PE}[\mathcal{I}^{(2,0)_1}_{\frac{1}{2}\mathrm{BPS}}\nu] = \prod_{n=0}^{\infty}\frac{1}{1-x^n\nu} = \frac{1}{(\nu,x)} = \sum_{k=0}^{\infty}\frac{\nu^k}{(x,x)_k} \tag{4.20}$$

and the coefficient of $\nu^k$ is

$$\frac{1}{(x,x)_k} = \prod_{n=1}^{k}\frac{1}{1-x^n} = \mathcal{I}^{(2,0)_k}_{\frac{1}{2}\mathrm{BPS}}\,. \tag{4.21}$$

This method reproduces the $k$-fold-symmetrised product of the quantity multiplying $\nu$ on the left-hand-side of (4.20). We have thus recovered the half-BPS index of the interacting theory from the symmetrised product of the half-BPS index for the free-tensor theory.

### Higgs-Branch Hilbert Series for Circular Quivers

We next proceed to the counting of the primary operators $\mathcal{H}_{\mathcal{I}}$ on the Higgs branch of the 4d circular quiver. These operators can be thought of as holomorphic functions on the Higgs-branch moduli space, and their counting is naturally accomplished by the Higgs-branch Hilbert Series (HS), which we next briefly review [144, 145]. To our knowledge, there is no limit of the 4d index for circular quivers that only receives contributions from such operators, although the Higgs-branch HS is closely related to the Hall-Littlewood limit of the 4d index. The Hall-Littlewood index counts the $\hat{\mathcal{B}}_R$, $\overline{\mathcal{D}}_{R(m_1,0)}$ (or $\mathcal{D}_{R(0,m_2)}$)-type multiplets, while the Higgs-branch HS only counts $\hat{\mathcal{B}}_R$ [48, 146].

Typically, the classical moduli space of a (Lagrangian) $\mathcal{N}=2$ Quantum Field Theory contains a Coulomb branch (where vector multiplet scalars acquire VEVs), a Higgs branch (where hypermultiplet scalars acquire VEVs) and, possibly, a number of mixed Coulomb–Higgs branches. While on the Coulomb branch there is some residual gauge symmetry, on the Higgs branch the gauge group is usually completely broken. The Higgs branch $\mathscr{H}$ does not receive quantum corrections [147] and can be described as a hyper-Kähler quotient by $D$ and $F$ terms.

We proceed to evaluate the Higgs-branch HS for the circular quiver theory with U($k$) gauge symmetry at each of the $N$ nodes; c.f. Fig. 4. In 4d $\mathcal{N}=1$ notation, each node $\alpha = \lfloor -N/2\rfloor+1,\ldots,\lfloor N/2\rfloor$ is associated with an adjoint scalar $X_{\alpha,\alpha}$. The hypermultiplets linking the $\alpha^{\text{th}}$ and $(\alpha+1)^{\text{th}}$ nodes contain bifundamental scalars $X_{\alpha,\alpha+1}$, $X_{\alpha+1,\alpha}$. The superpotential for this theory is given by

$$W = \sum_{\alpha=\lfloor -\frac{N}{2}\rfloor+1}^{\lfloor\frac{N}{2}\rfloor}\mathrm{tr}\Big(\mathrm{X}_{\alpha+1,\alpha}\mathrm{X}_{\alpha,\alpha}\mathrm{X}_{\alpha,\alpha+1} - \mathrm{X}_{\alpha,\alpha-1}\mathrm{X}_{\alpha,\alpha}\mathrm{X}_{\alpha-1,\alpha}\Big)\,, \tag{4.22}$$

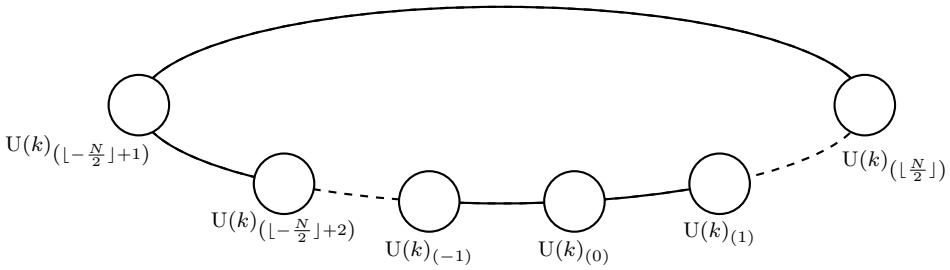


**Figure 4:** The quiver diagram corresponding to the system of D4 and NS5 branes.

where tr denotes the trace over the gauge group. Note that each chiral multiplet scalar is charged under a baryonic $\mathrm{U}(1)_\mathrm{B}$ symmetry, such that $X_{\alpha,\alpha+1}$ has charge +1 and $X_{\alpha+1,\alpha}$ charge -1.

When the gauge group is completely broken, the Higgs-branch HS is typically computed through "letter counting" [145]: On the Higgs branch all vector-multiplet scalars are set to zero and one is left with $F$ terms arising from the derivative of the superpotential $W$ with respect to Coulomb-branch scalars. The $\mathcal{H}_\mathcal{I}$ operators consist of all symmetrised, gauge-invariant combinations (words) made out of the hypermultiplet fields (letters) modulo these $F$ terms. To count them it is sufficient to consider a partition function over the plethystic exponential of the "single-letter" contribution. The $F$ terms are also taken into account but since they act as constraints they appear with opposite-sign coefficients. Taking the result, $g$, and projecting to gauge singlets through integration over the appropriate Haar measure $d\mu$ for a gauge group $G$ leads to the HS:

$$\mathrm{HS} = \int_G d\mu\, g\,. \tag{4.23}$$

Let us now illustrate this procedure with the simple example of the abelian $k = 1$ $\mathrm{U}(1)^N$ theory. Generically, the $k = 1$ HS will depend on the following complex parameters: a fugacity $t$ keeping track of operator scaling dimensions, fugacities for global symmetries (which we will set to one since the index (4.18) only keeps track of scaling dimensions) and $k$ gauge fugacities $u_i$. The $t$ fugacities are complex parameters that take values inside the unit circle, that is $|t| < 1$, while the gauge and possible flavour fugacities lie on the unit circle.

Let us take *e.g.* $N = 2$ where the superpotential is explicitly given by

$$W = X^j_{2,1} X_{1,1} X^i_{1,2} \epsilon_{ij} + X^j_{1,2} X_{2,2} X^i_{2,1} \epsilon_{ij}\,. \tag{4.24}$$

The relevant $F$ terms are $X^i_{1,2}X^j_{2,1}\epsilon_{ij}=0$ and $X^i_{2,1}X^j_{1,2}\epsilon_{ij}=0$, explicitly

$$X^1_{1,2}X^2_{2,1}=X^2_{1,2}X^1_{2,1}\,,\qquad X^1_{2,1}X^2_{1,2}=X^2_{2,1}X^2_{1,2}\,, \tag{4.25}$$

and are obviously identical. This argument generalises to the $N$-noded case, where instead of $N$ $F$ terms, one only has $N-1$ conditions due to the circular nature of the quiver. Since the adjoint character for $k=1$ is equal to one, the $F$-term constraints can easily be accounted for. Thus, in this case, we have that the letter counting of (4.23) should be modified into

$$\mathrm{HS}^N_{k=1}=\mathrm{PE}\left[-(N-1)t^2\right]\int\prod_{\alpha=\lfloor-\frac{N}{2}\rfloor+1}^{\lfloor\frac{N}{2}\rfloor}\frac{du_\alpha}{u_\alpha}\mathrm{PE}\left[t\Big(\frac{u_\alpha}{u_{\alpha+1}}+\frac{u_{\alpha+1}}{u_\alpha}\Big)\right]\,, \tag{4.26}$$

where $u_{\lfloor N/2\rfloor+1}\equiv u_{\lfloor -N/2\rfloor+1}$ from the cyclic identification, the factor outside the integral captures the $F$-term contributions, while the one under the integral the scalar-field contributions. After performing the gauge integrations one has

$$\mathrm{HS}^N_{k=1}=\mathrm{PE}[t^2+2t^N-t^{2N}]\,. \tag{4.27}$$

The above is just the HS of the space $\mathbb{C}^2/\mathbb{Z}_N$ defined as the surface $\mathbb{XY}=\mathbb{W}^N$ embedded in $\mathbb{C}^3$. This is consistent with the fact that the Higgs branch of these quiver theories engineers the moduli space of instantons on ALE space [148]. In order to show this explicitly, note that the generators $\mathbb{X}$, $\mathbb{Y}$ and $\mathbb{W}$ have respective weights $N$, $N$ and 2, such that the defining equation is homogeneous of degree $2N$. From this it can also be deduced that the HS is $\mathrm{PE}[t^2+2t^N-t^{2N}]$ [145]. In terms of operators, the $t^2$ term corresponds to the meson $\mathbb{W}=X_{\alpha,\alpha+1}X_{\alpha+1,\alpha}$—they are all equal due to the $F$ terms—while the $2t^N$ correspond to the two long mesons $\mathbb{X}=X_{1,2}X_{2,3}\dots X_{N,1}$ and $\mathbb{Y}=X_{1,N}X_{N,N-1}\dots X_{2,1}$.[32] These clearly satisfy $\mathbb{XY}=\mathbb{W}^N$.

This result is also to be expected on physical grounds. Upon considering adding $N_\alpha$ flavours to the $\alpha$-th node, the Higgs branch of the circular quiver with generic ranks $k_\alpha$ engineers the moduli space of $\mathrm{U}(\sum N_\alpha)$ instantons on $\mathbb{C}^2/\mathbb{Z}_N$ (see *e.g.* [149] for the details of this identification). For $N_\alpha=0$, $k_\alpha=k=1$, the so-called "rank-zero" instanton only has position moduli and we thus recover the HS of the target-space algebraic variety $\mathbb{C}^2/\mathbb{Z}_N$.

Since $|t|<1$, it is now straightforward to take the large-$N$ limit of (4.27). By

[32] The operators that parametrise the Higgs branch can be constructed out of these generators, such as a meson that "connects" the nodes 1 and 3, $\mathcal{H}_{13}=X_{1,2}X_{2,3}X_{3,2}X_{2,1}$ within contribution $t^4$, a meson that "connects" the nodes 1 and 4, $\mathcal{H}_{14}=X_{1,2}X_{2,3}X_{3,4}X_{4,3}X_{3,2}X_{2,1}$ with contribution $t^6$, and so on.

relating $t^2 = x$ we obtain

$$\mathrm{HS}^{\infty}_{k=1} = \frac{1}{1-x} = \mathrm{PE}\left[\lim_{q\to 0} f\right] = \mathcal{I}^{(2,0)_1}_{\frac{1}{2}\mathrm{BPS}}\,, \tag{4.28}$$

which is the half-BPS index for the 6d free-tensor theory. Note that a 6d scalar has scaling dimension two, while a 4d scalar has dimension one; this accounts for the redefinition $t^2 = x$.

Coming back to the general non-abelian case, it is clear that an obstruction to the direct use of letter counting will arise because of $F$ terms. However, extracting modifications to the single-letter evaluation of higher-rank theories becomes increasingly complicated. Nevertheless, regarding the $\mathrm{U}(k)^N$ quiver as describing $k$ rank-zero instantons on $\mathbb{C}^2/\mathbb{Z}_N$ strongly suggests that one can obtain the general formula for all $k$ and $N$ by simply considering the $k$-fold-symmetrised product of the $k = 1$ case [144,149]. This is because rank-zero instantons do not have internal degrees of freedom and thus are akin to a gas of $k$ non-interacting particles on $\mathbb{C}^2/\mathbb{Z}_N$.[33] This can be implemented by considering the coefficient of $\nu^k$ in the expansion of

$$\mathrm{PE}\left[\mathrm{HS}^{N}_{k=1}(t)\nu\right] = \mathrm{PE}\left[\frac{(1-t^{2N})}{(1-t^2)(1-t^N)^2}\nu\right]\,. \tag{4.29}$$

Taking the large-$N$ limit gives back the coefficient of $\nu^k$ in the expansion of

$$\mathrm{PE}\left[\frac{\nu}{(1-t^2)}\right]\,. \tag{4.30}$$

By setting $t^2 = x$, this expression is precisely (4.20) and one reproduces the superconformal-index result

$$\lim_{N\to\infty} \mathrm{HS}^{N}_{k} = \prod_{m=1}^{k} \frac{1}{1-x^m}\,. \tag{4.31}$$

We have thus confirmed the expectation that, through the deconstruction procedure, the mesonic part of the 4d BPS-operator spectrum properly accounts for the appropriate piece of the 6d (2,0) spectrum.

### 4.1.2 4d/6d Matching: Partition Functions

While the matching that we have just performed is satisfying, it provides but a very simple test of the deconstruction proposal for a collection of protected states. Moreover, since it only involves 6d BPS local operators it is not sensitive to selfdual strings, which

[33] This expectation can be checked explicitly by brute-force calculation for the first few values of $k$, $N$, as shown in Appendix 1 of [2].

should be part of the spectrum and can *e.g.* wrap a torus of finite size. We will next rectify both of these drawbacks by performing a more sophisticated counting on both sides.

We thus switch gears and turn our attention to the deconstruction of the full partition function for the $(2,0)_k$ theory on $\mathbb{S}^4 \times \mathbb{T}^2$. Putting the superconformal circular quiver on $\mathbb{S}^4$ initially lifts the moduli space through the conformal coupling of the scalars to the curvature, thus naively posing a problem for deconstruction. However, this can be easily rectified by appropriately mass-deforming the theory [150]. With this in mind, our starting point will be the BPS partition function in the Coulomb-branch of the mass-deformed 4d $\mathcal{N}=2$ circular-quiver theory on $\mathbb{R}^4_{\epsilon_1,\epsilon_2}$. The latter can be used as a building block for the full 4d partition function on the ellipsoid $\mathbb{S}^4_{\epsilon_1,\epsilon_2}$, upon taking two copies and integrating over the Coulomb-branch parameters with the appropriate Haar measure.[34] Such a construction is typical of (Coulomb-branch) supersymmetric localisation [53, 56]; see also [17, 84].[35]

We propose that the deconstruction limit of [23] be taken directly on these building blocks. Appropriate implementation of this procedure leads to an analogous BPS building block for the 6d partition function on $\mathbb{R}^4_{\epsilon_1,\epsilon_2} \times \mathbb{T}^2_{R_5,R_6}$ [71]. Taking two copies of this result and integrating them over the Coulomb-branch parameters with the appropriate Haar measure leads to the desired answer.

### The 4d Coulomb-Branch Partition Function

We denote the IR partition function of the mass-deformed 4d $\mathcal{N}=2$ theory on $\mathbb{R}_{\epsilon_1,\epsilon_2}$ by $Z_{\rm 4d}(\tau, a, m_{\rm bif}; \epsilon_1, \epsilon_2)$. We use the symbol $a = \{a_b^{(\alpha)}\}$ for the set of Coulomb-branch parameters associated with the brane separations of Fig. 3, with the index $\alpha = \lfloor -N/2 \rfloor + 1, \ldots, \lfloor N/2 \rfloor$ counting the number of colour groups and $b = 1, \ldots, k$ the Coulomb-branch parameters within a given colour group. Moreover, we denote the set of $N$ bifundamental-hypermultiplet masses as $m_{\rm bif} = \{m_{\rm bif}^{(\alpha)}\}$; we will keep these generic for the moment. The partition function $Z_{\rm 4d}(\tau, a, m_{\rm bif}; \epsilon_1, \epsilon_2)$ is the holomorphic half of the integrand of the partition function on the ellipsoid $\mathbb{S}^4_{\epsilon_1,\epsilon_2}$:

$$Z_{\mathbb{S}^4_{\epsilon_1,\epsilon_2}}(\tau, \bar{\tau}, m_{\rm bif}; \epsilon_1, \epsilon_2) = \int [da]\, |Z_{\rm 4d}(\tau, a, m_{\rm bif}; \epsilon_1, \epsilon_2)|^2 \ , \tag{4.32}$$

[34] This IR building block counts BPS particles (monopoles, dyons, etc.) at low energies on the Coulomb branch and is the well-known 4d limit of the "Nekrasov partition function", in the definition of which we include the classical, one-loop and instanton contributions [52, 69].

[35] It is straightforward to convince oneself that the IR partition functions for the mass-deformed $\mathrm{SU}(k)^N \times \mathrm{U}(1)$ circular quiver and the undeformed $\mathrm{U}(k)^N$ circular quiver on $\mathbb{R}^4_{\epsilon_1,\epsilon_2}$ are identical up to U(1) vector-multiplet factors.

where complex conjugation is implemented by:

$$\overline{Z_{\rm 4d}}(\tau, a, m_{\rm bif}; \epsilon_1, \epsilon_2) = Z_{\rm 4d}(-\bar{\tau}, -a, -m_{\rm bif}; -\epsilon_1, -\epsilon_2) \ . \tag{4.33}$$

The Coulomb-branch partition function $Z_{\rm 4d}(a, m_{\rm bif}; \epsilon_1, \epsilon_2)$ comprises of a classical, a one-loop and a non-perturbative piece, all of which can be constructed using existing results from the localisation literature. However, they are also known to arise from the circle reduction of the 5d Nekrasov partition function. In turn, the 5d one-loop and instanton pieces can be calculated using the refined topological vertex formalism [68, 132, 151, 152], the technology of which we employ in the independent rederivation of our expressions in Sec. 2.4.1.[36] Our conventions are given in Sec. 2.4.

Following [17, 84], the classical piece of the Coulomb-branch partition function comprises of the factor

$$Z_{\rm 4d,cl}(\tau, a; \epsilon_1, \epsilon_2) = \exp\left[-\frac{2\pi i}{\epsilon_1\epsilon_2} \sum_{\alpha=-\lfloor\frac{N}{2}\rfloor+1}^{\lfloor\frac{N}{2}\rfloor} \tau^{(\alpha)} \sum_{b=1}^{k} \left(a_b^{(\alpha)}\right)^2\right] \ . \tag{4.34}$$

The one-loop part is obtained by appropriately assigning vector and hypermultiplet contributions for the quiver of Fig. 4,

$$Z_{\rm 4d,1\text{-}loop}(a, m_{\rm bif}; \epsilon_1, \epsilon_2) = \prod_{\alpha=\lfloor-\frac{N}{2}\rfloor+1}^{\lfloor\frac{N}{2}\rfloor} Z^{\rm vec}_{\rm 1\text{-}loop}(a; \epsilon_1, \epsilon_2) Z^{\rm bif}_{\rm 1\text{-}loop}(a, m_{\rm bif}\ ; \epsilon_1, \epsilon_2) \ , \tag{4.35}$$

with the vector and hypermultiplet one-loop determinant contributions given by[37]

$$\begin{aligned} Z^{\rm bif}_{\rm 1\text{-}loop}(a, m_{\rm bif}; \epsilon_1, \epsilon_2) &= \prod_{b,c=1}^{k} \Gamma_2\left(a_c^{(\alpha+1)} - a_b^{(\alpha)} + m_{\rm bif}^{(\alpha)} + \epsilon_+ \middle| \epsilon_1, \epsilon_2\right) \ , \\ Z^{\rm vec}_{\rm 1\text{-}loop}(a; \epsilon_1, \epsilon_2) &= \prod_{b,c=1}^{k} \Gamma_2\left(a_c^{(\alpha)} - a_b^{(\alpha)} \middle| \epsilon_1, \epsilon_2\right)^{-1} \ , \end{aligned} \tag{4.36}$$

where $\epsilon_+ = \frac{\epsilon_1+\epsilon_2}{2}$ and $\Gamma_2(x|\epsilon_1, \epsilon_2)$ is the Barnes double-Gamma function, defined in detail in Appendix A.

[36] The classical contribution in the calculation of the IR partition function cannot be recovered by dimensionally reducing the $\mathbb{R}^4_{\epsilon_1,\epsilon_2} \times \mathbb{S}^1$ result obtained through the topological vertex formalism [74, 80, 153]. However, it is explicitly known from the localisation calculation of [53]. In 5d it can be restored using symmetries, e.g. by imposing fibre-base duality [74].

[37] Note that, compared to [17, 84], the vector multiplet piece includes additional factors arising from the Cartan contributions which we explicitly keep. Furthermore, by virtue of making contact with the topological vertex formalism we have shifted the one-loop contributions by various factors of $\epsilon_{1,2}$. See Appendix B.2 of [17] for details.

Similarly, the instanton part is given by [17]

$$Z_{\text{4d,inst}}(a, m_{\text{bif}}; \epsilon_1, \epsilon_2) = \sum_{\nu} \prod_{\alpha=\lfloor -\frac{N}{2} \rfloor + 1}^{\lfloor \frac{N}{2} \rfloor} \mathbf{q}_{(\alpha)}^{\sum_{b=1}^{k} |\nu_b^{(\alpha)}|} Z_{\text{inst}}^{\text{vec}}(a; \nu) Z_{\text{inst}}^{\text{bif}}(a; \nu) \tag{4.37}$$

where $\mathbf{q}_{(\alpha)}$ is the fugacity keeping track of the instanton number, associated with the complexified coupling $\tau^{(\alpha)}$ for the $\alpha^{th}$ colour group as in (4.13). A Young diagram $\nu_b^{(\alpha)}$ appears for each of the Coulomb moduli $a_b^{(\alpha)}$, collectively denoted by $\nu = \{\nu_b^{(\alpha)}\}$, while the instanton number is given in terms of the total number of boxes of the Young diagram $|\nu_b^{(\alpha)}|$. The vector and hypermultiplet instanton contributions respectively read

$$\begin{aligned} Z_{\text{inst}}^{\text{bif}}(\tau, a, m_{\text{bif}}; \nu) &= \prod_{b,c=1}^{k} \mathrm{N}_{\nu_c^{(\alpha+1)} \nu_b^{(\alpha)}} \left( a_c^{(\alpha+1)} - a_c^{(\alpha+1)} + m_{\text{bif}}^{(\alpha)} - \frac{\epsilon_+}{2} \right) , \\ Z_{\text{inst}}^{\text{vec}}(a, m_{\text{bif}}; \nu) &= \prod_{b,c=1}^{k} \mathrm{N}_{\nu_c^{(\alpha)} \nu_b^{(\alpha)}} \left( a_c^{(\alpha)} - a_b^{(\alpha)} \right)^{-1} , \end{aligned} \tag{4.38}$$

where the functions $\mathrm{N}_{\lambda\mu}(x)$ involved above are defined as[38]

$$\begin{aligned} \mathrm{N}_{\lambda\nu}(x; \epsilon_1, \epsilon_2) = &\prod_{(i,j)\in\lambda} \left( x + \epsilon_1(\lambda_i - j + 1) + \epsilon_1(i - \nu_j^t) \right) \\ &\times \prod_{(i,j)\in\nu} \left( x + \epsilon_1(j - \nu_i) + \epsilon_2(\lambda_j^t - i + 1) \right) , \end{aligned} \tag{4.39}$$

The full Coulomb-branch partition function can be rewritten as

$$Z_{\text{4d}} = Z_{\text{4d,cl}} Z_{\text{4d,1-loop}} Z_{\text{4d,inst}} \, . \tag{4.40}$$

### The 6d Tensor-Branch Partition Function

The IR partition function for the $(2,0)_k$ theory on $\mathbb{R}^4_{\epsilon_1,\epsilon_2} \times \mathbb{T}^2$ was given in [71, 80, 122]. The key point for our purposes is that the BPS sector of the $(2,0)_k$ theory on the (twisted) torus $\mathbb{T}^2_{R_5,R_6} = \mathbb{S}^1_{R_5} \times \mathbb{S}^1_{R_6}$, can be captured by the (mass-deformed) 5d MSYM theory on $\mathbb{R}^4_{\epsilon_1,\epsilon_2} \times \mathbb{S}^1_{R_5}$ [19, 20, 70, 126, 127]. The partition function associated with these BPS states is precisely given by the original calculation of [52, 69] and, as already mentioned, can be straightforwardly reproduced by the refined topological vertex formalism.[39] As in 4d, taking two copies of this building block and integrating over the

[38] See Sec. 2.4 for our conventions on labelling partitions.

[39] The 6d (2,0) theory has no Coulomb branch, since the role of the vector multiplet is played by a tensor multiplet. However, since the 6d result is recovered by a purely 5d calculation, both the Coulomb- and tensor-branch nomenclatures are appropriate.

Coulomb/tensor-branch parameters $\tilde{a} = \{\tilde{a}_b\}$ leads to the full partition function of the 6d theory on $\mathbb{S}^4_{\epsilon_1,\epsilon_2} \times \mathbb{T}^2_{R_5,R_6}$, that is

$$Z_{\mathbb{S}^4_{\epsilon_1,\epsilon_2}\times\mathbb{T}^2_{R_5,R_6}}(\tilde{\tau},\bar{\tilde{\tau}},\tilde{t}_m;\epsilon_1,\epsilon_2) = \int [d\tilde{a}] \left| Z_{\rm 6d}(\widetilde{Q}_\tau, \widetilde{\mathbb{Q}}_{bc}, \widetilde{Q}_m; \mathfrak{q}, \mathfrak{t}) \right|^2 , \tag{4.41}$$

where

$$\overline{Z_{\rm 6d}}(\widetilde{Q}_\tau, \widetilde{\mathbb{Q}}_{bc}, \widetilde{Q}_m; \mathfrak{q}, \mathfrak{t}) = Z_{\rm 6d}\left(\widetilde{Q}_{\bar{\tau}}^{-1}, \widetilde{\mathbb{Q}}_{bc}^{-1}, \widetilde{Q}_m^{-1}; \mathfrak{q}^{-1}, \mathfrak{t}^{-1}\right) , \tag{4.42}$$

where we have put a tilde over parameters that are only associated with the 6d partition function. The fugacities appearing in the above expressions are related to chemical potentials through

$$\mathfrak{q} = e^{-R_5\epsilon_1} , \quad \mathfrak{t} = e^{R_5\epsilon_2} , \quad \widetilde{\mathbb{Q}}_{bc} = e^{-R_5\tilde{t}_{bc}} , \quad \widetilde{Q}_m = e^{-R_5\tilde{t}_m} , \quad \widetilde{Q}_\tau = e^{2\pi i\tilde{\tau}} , \tag{4.43}$$

which can in turn be readily identified with 6d geometric parameters as follows [71]:

$$\tilde{t}_m = \frac{\tilde{\tau}\tilde{m}}{R_5} , \quad \tilde{t}_{bc} = \tilde{a}_c - \tilde{a}_b = \frac{1}{2\pi l_p^3} i R_6 \delta_{bc} . \tag{4.44}$$

Here $R_5, R_6$ are the radii of the circles, $\tilde{\tau}$ the modulus of $\mathbb{T}^2$, the $\delta_{bc}$ denote the distance between the $b^{th}$ and $c^{th}$ separated M5 branes in the broken phase ($b, c = 1, ..., k$), $\tilde{m}$ and $\epsilon_1, \epsilon_2$ are twists of the torus along $R_5$ and $R_6$ respectively, and $l_p$ is the 11d Planck length.

The 6d holomorphic block comprises of a classical, a one-loop and a non-perturbative piece

$$Z_{\rm 6d} = Z_{\rm 6d,cl} Z_{\rm 6d,\ 1\text{-loop}} Z_{\rm 6d,inst} , \tag{4.45}$$

with [71, 127]

$$\begin{aligned}
Z_{\rm 6d,cl} &= \exp\left[ -\frac{2\pi i\tilde{\tau}}{\epsilon_1\epsilon_2} \left( \sum_{b=1}^k \tilde{a}_b^2 \right) \right] , \\
Z_{\rm 6d,inst} &= \sum_\nu Q_\tau^{\sum_{b=1}^k |\nu_b|} \prod_{b,c=1}^k \frac{\mathrm{N}^{R_5}_{\nu_c\nu_b}\left(\tilde{a}_c - \tilde{a}_b + \tilde{t}_m - \epsilon_+\right)}{\mathrm{N}^{R_5}_{\nu_c\nu_b}\left(a_c - a_b\right)} , \\
Z_{\rm 6d,1\text{-}loop} &= \left( \tilde{Q}_m \sqrt{\frac{\mathfrak{t}}{\mathfrak{q}}} \right)^{\frac{1}{24}k(k-1)} \prod_{b,c=1}^k \frac{\mathcal{M}\left(e^{-R_5(a_c-a_b)}\right)}{\mathcal{M}\left(e^{-R_5(a_c-a_b)}\tilde{Q}_m\sqrt{\frac{\mathfrak{t}}{\mathfrak{q}}}\right)} ,
\end{aligned} \tag{4.46}$$

where

$$\mathcal{M}(Q;\mathfrak{t},\mathfrak{q}) = \prod_{i,j=1}^{\infty}(1-Q\mathfrak{t}^{i-1}\mathfrak{q}^{j})^{-1}\,,$$
$$\mathrm{N}^{\beta}_{\lambda\mu}(x;\epsilon_1,\epsilon_2) = \prod_{(i,j)\in\lambda} 2\sinh\frac{\beta}{2}\left[x+\epsilon_1(\lambda_i-j+1)+\epsilon_1(i-\mu^t_j)\right]$$
$$\times\prod_{(i,j)\in\mu} 2\sinh\frac{\beta}{2}\left[x+\epsilon_1(j-\mu_i)+\epsilon_2(\lambda^t_j-i+1)\right]\,. \qquad (4.47)$$

We provide a complete derivation of the one-loop and instanton contributions in Eq. (4.45) using the refined topological vertex formalism in Section 2.4.1 in a more general case from which we recover this as the $N=1$ version of the 5d result.

### Deconstructing the 6d Partition Function

Equipped with both the 4d and 6d expressions, we can finally proceed with our prescription for implementing the dimensional-deconstruction limit at the level of IR partition functions. This was first done in [2] but the prescription was made more precise in [4]. We summarise it here.

The principle of dimensional deconstruction can be extended to exact partition functions with no specific reference to the number of spacetime dimensions. Assuming Lagrangian circular-quiver theories with the appropriate amount of supersymmetry,[40] The $\mathbb{S}^d$ partition functions can be put together in a modular fashion by accounting for the individual contributions coming from the various supersymmetric multiplets appearing in the quiver diagram. Each node will be labelled by an index $\alpha$ and the (integrand of the) corresponding partition function can generically depend on a coupling, Coulomb-branch parameter, mass-deformation parameter etc. Then, exact deconstruction can be implemented directly at the level of partition functions by:

(1) Identifying all parameters between the nodes (couplings, Coulomb-branch parameters, mass deformations etc.)—this reflects the breaking of the gauge symmetry, e.g. $U(k)^N \to U(k)$.

(2) Including a mass parameter $m_\alpha = i\frac{2\pi\alpha}{R}$ for the $\alpha$-th node contribution—this captures the reorganisation of the quiver degrees of freedom into the KK modes of the deconstructed theory—and taking $N\to\infty$.

Deconstruction can be performed separately on the classical, instanton and perturbative piece.

[40] A certain amount of supersymmetry is required to be able to use the localisation method on certain backgrounds such as $\mathbb{S}^d$. This will be discussed in the next section.

Let us begin with the one-loop piece of the 4d partition function

$$Z^{\mathrm{U}(k)^N}_{\text{4d,1-loop}} = \prod_{\alpha}\prod_{b,c=1}^{k} \frac{\Gamma_2\left(a_c^{(\alpha+1)} - a_b^{(\alpha)} + m_{\text{bif}}^{(\alpha)} + \epsilon_+ \middle| \epsilon_1, \epsilon_2\right)}{\Gamma_2\left(a_c^{(\alpha)} - a_b^{(\alpha)} \middle| \epsilon_1, \epsilon_2\right)} \,. \tag{4.48}$$

Applying the prescription we identify all $a_b^{(\alpha)} = a_b$ for all $b$ and $\alpha$. The masses are also identified $m_{\text{bif}}^{(\alpha)} = m$ for all $\alpha$. The arguments of the special functions are shifted by the KK mass and we get

$$Z^{\text{Higgs}}_{\text{4d,1-loop}} = \prod_{\alpha}\prod_{b,c=1}^{k} \frac{\Gamma_2\left(a_c - a_b + m + i\frac{2\pi\alpha}{R_5} + \epsilon_+ \middle| \epsilon_1, \epsilon_2\right)}{\Gamma_2\left(a_c - a_b + i\frac{2\pi\alpha}{R_5} \middle| \epsilon_1, \epsilon_2\right)} \,. \tag{4.49}$$

Using Appendix A, we know that $\Gamma_2$ with $\epsilon_1 > 0$ and $\epsilon_2 < 0$ has the product representation

$$\Gamma_2(x|\epsilon_1, \epsilon_2) \propto \prod_{i,j=0}^{\infty} \left(x + i\epsilon_1 - \epsilon_2(j+1)\right) \,, \tag{4.50}$$

from which we can write

$$\prod_{\alpha=-\infty}^{\infty} \Gamma_2\left(x + i\frac{2\pi\alpha}{R_5} \middle| \epsilon_1, \epsilon_2\right) = \left(\prod_{i,j=0}^{\infty} e^{\frac{R_5}{2}x}\mathfrak{q}^{-\frac{i}{2}}\mathfrak{t}^{-\frac{j+1}{2}}\right) \mathcal{M}\left(e^{-R_5 x}\frac{\mathfrak{t}}{\mathfrak{q}}\right)^{-1} \,, \tag{4.51}$$

where the prefactor will need to be regularised. Putting everything together we get

$$\lim_{N\to\infty} Z^{\text{Higgs}}_{\text{4d,1-loop}} = \prod_{b,c=1}^{k} \left(\prod_{i,j=0}^{\infty} e^{\frac{R_5}{2}(m+\epsilon_+)}\right) \frac{\mathcal{M}\left(e^{-R_5(a_c-a_b)}\frac{\mathfrak{t}}{\mathfrak{q}}\right)}{\mathcal{M}\left(e^{-R_5(a_c-a_b+m+\epsilon_+)}\frac{\mathfrak{t}}{\mathfrak{q}}\right)} \,. \tag{4.52}$$

After regularising the prefactor we get

$$\lim_{N\to\infty} Z^{\text{Higgs}}_{\text{4d,1-loop}} = \prod_{b,c=1}^{k} \left(Q_m\sqrt{\frac{\mathfrak{q}}{\mathfrak{t}}}\right)^{\frac{1}{24}} \frac{\mathcal{M}\left(e^{-R_5(a_c-a_b)}\frac{\mathfrak{t}}{\mathfrak{q}}\right)}{\mathcal{M}\left(e^{-R_5(a_c-a_b)}Q_m\sqrt{\frac{\mathfrak{t}}{\mathfrak{q}}}\right)} \,, \tag{4.53}$$

where we defined $Q_m = e^{-R_5 m}$ alongside the normal definitions for $\mathfrak{q}$ and $\mathfrak{t}$. This almost matches the 6d result. We need to use the reflection formula (2.124)

$$\mathcal{M}(Q^{-1}) = \left(-Q^{-1}\sqrt{\frac{\mathfrak{q}}{\mathfrak{t}}}\right)^{\frac{1}{12}} \mathcal{M}\left(Q\frac{\mathfrak{t}}{\mathfrak{q}}\right) \,, \tag{4.54}$$

to write

$$\lim_{N\to\infty} Z^{\text{Higgs}}_{\text{4d,1-loop}} = \left(Q_m\sqrt{\frac{\mathfrak{t}}{\mathfrak{q}}}\right)^{\frac{1}{24}k^2} \prod_{b,c=1}^{k} \frac{\mathcal{M}\left(e^{-R_5(a_c-a_b)}\right)}{\mathcal{M}\left(e^{-R_5(a_c-a_b)}Q_m\sqrt{\frac{\mathfrak{t}}{\mathfrak{q}}}\right)} \,, \tag{4.55}$$

We now see that, upon identifying $\tilde{a}_b = a_b$, which from the brane point of view makes sense, and $\tilde{t}_m = m$, we have

$$\lim_{N\to\infty} Z^{\text{Higgs}}_{\text{4d,1-loop}} = Z_{\text{6d,1-loop}} \times \left(Q_m\sqrt{\frac{\mathfrak{t}}{\mathfrak{q}}}\right)^{\frac{1}{24}k} \,. \tag{4.56}$$

Note that this prefactor is the regularised version of $\prod_{i,j=0}^{\infty}\left(Q_m^{-2}\frac{\mathfrak{q}}{\mathfrak{t}}\right)^{\frac{k}{4}}$ which is added by hand in [71]. It is interpreted as the gravitational contribution to the topological string partition function. It is explicitly present in the localisation calculation of [122].

The calculation for the non-perturbative piece proceeds in a similar manner. Once again, we begin with the instanton part of the 4d Coulomb-branch partition function from Eq. (4.37)

$$Z^{\text{U}(k)^N}_{\text{4d,inst}} = \sum_{\nu}\prod_{\alpha}\mathfrak{q}_{(\alpha)}^{\sum_{b=1}^{k}|\nu_b^{(\alpha)}|}\prod_{b,c=1}^{k}\frac{\text{N}_{\nu_c^{(\alpha+1)}\nu_b^{(\alpha)}}\left(a_c^{(\alpha+1)}-a_b^{(\alpha)}+m_{\text{bif}}^{(\alpha)}-\epsilon_+\right)}{\text{N}_{\nu_c^{(\alpha)}\nu_b^{(\alpha)}}\left(a_c^{(\alpha)}-a_b^{(\alpha)}\right)} \,, \tag{4.57}$$

and impose the "deconstruction" identifications that we did for the perturbative part, the shifts of the special functions and

$$g_{(\alpha)} \to G \,, \qquad \theta^{(\alpha)} \to \Theta \,, \qquad \nu_b^{(\alpha)} \to \nu_b \,. \tag{4.58}$$

This implies that

$$\prod_{\alpha=-\infty}^{\infty}\mathfrak{q}_{(\alpha)} = \lim_{N\to\infty}\exp\left(-\frac{8\pi^2 N}{G^2}+i\frac{N\Theta}{4\pi}\right) = Q_\tau \,. \tag{4.59}$$

Recall that the combination $N/G^2$ is precisely $R_5/R_6$, so it makes sense for this to be the imaginary part of a complex structure for the emerging torus. This ensures that $\Im\tau > 0$ as required. Furthermore, the theta angles provide a real part for the complex structure, which facilitates a twist along the torus. We have anticipated setting all the couplings to be equal in (4.13) using the brane picture, from which the identification of theta angles and partitions follows naturally. The latter can be see as the D4 branes reconnecting over the NS5 brane.

We then have

$$\lim_{N\to\infty} Z^{\text{Higgs}}_{\text{4d,inst}} = \sum_{\nu} Q_{\tau}^{\sum_{b=1}^{k}|\nu_b|} \prod_{b,c=1}^{k} \prod_{\alpha} \frac{\mathrm{N}_{\nu_c\nu_b}\left(a_c - a_b + m - \epsilon_+ + i\frac{2\pi\alpha}{R_5}\right)}{\mathrm{N}_{\nu_c\nu_b}\left(a_c - a_b + i\frac{2\pi\alpha}{R_5}\right)} \ . \tag{4.60}$$

Perhaps somewhat unsurprising given the definition, the product over $\alpha$ is computed as

$$\prod_{\alpha=-\infty}^{\infty} \mathrm{N}_{\lambda\mu}\left(x + i\frac{2\pi\alpha}{R_5}; \epsilon_1, \epsilon_2\right) = \mathrm{N}^{R_5}_{\lambda\mu}\left(x; \epsilon_1, \epsilon_2\right) \ , \tag{4.61}$$

and is even simpler than the perturbative case. This is mostly due to the fact that no regularisation needs to be taken place, since we are dealing with finite products over partitions. We therefore end up with

$$\lim_{N\to\infty} Z^{\text{Higgs}}_{\text{4d,inst}} = Z_{\text{6d,inst}} \ , \tag{4.62}$$

upon identifying $Q_\tau = \widetilde{Q}_\tau$.

Lastly, we have the classical piece. Recall it is given by

$$Z_{\text{4d,cl}} = \exp\left[-\frac{2\pi i}{\epsilon_1\epsilon_2}\sum_{\alpha}\tau^{(\alpha)}\sum_{b=1}^{k}\left(a_b^{(\alpha)}\right)^2\right] \ . \tag{4.63}$$

Note that a shift in the classical piece by the KK mass will simply result in a factor which is zero due to it being expressible as $\zeta(-2)$, which is itself zero, where $\zeta$ is the Riemann zeta function. Thus upon the deconstruction identifications we obtain

$$\begin{aligned}\lim_{N\to\infty} Z^{\text{Higgs}}_{\text{4d,cl}} &= \exp\left[-\frac{2\pi i}{\epsilon_1\epsilon_2} N\tau\left(\sum_{b=1}^{k} a_b^2\right)\right] \\ &= Z_{\text{6d,cl}} \ ,\end{aligned} \tag{4.64}$$

after imposing the deconstruction identifications.

To summarise, using the map

$$a_b^{(\alpha)} = \tilde{a}_b \ , \qquad m_{\text{bif}}^{(\alpha)} = \tilde{t}_m \ , \qquad \tau^{(\alpha)} = \tau \ , \qquad N\tau = \tilde{\tau} \ , \qquad \nu_b^{(\alpha)} = \nu_b \ , \tag{4.65}$$

along with the prescription of converting the product over $\alpha$ indices to a product over KK masses $M_{KK}^{(\alpha)} = \frac{2\pi i\alpha}{R_5}$ to indicate a reorganisation of the 4d spectrum, we showed that

$$\lim_{N\to\infty} Z^{\text{Higgs}}_{4d} = \left(Q_m\sqrt{\frac{\mathfrak{t}}{\mathfrak{q}}}\right)^{\frac{k}{24}} Z_{6d} \ . \tag{4.66}$$

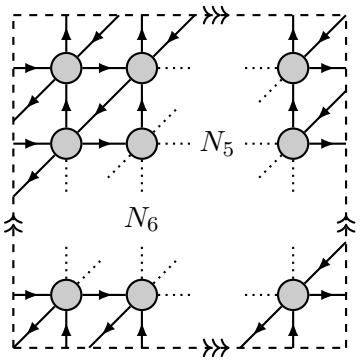


**Figure 5:** The quiver diagram for the $\mathbb{Z}_{N_5} \times \mathbb{Z}_{N_6}$ orbifold theory. Opposite edges are identified. Each directional arrow is a 4d $\mathcal{N} = 1$ bifundamental chiral multiplet and each node is a 4d $\mathcal{N} = 1$ vector multiplet.

This multiplicative piece encodes the genus-one contribution to the topological string partition function [71]. This factor is absent when one uses the glueing prescription to move to the $\mathbb{S}^4 \times \mathbb{T}^2$ partition function.

Upon integrating over the Coulomb/tensor-branch parameters one immediately gets the full partition function for the $(2,0)_k$ theory on $\mathbb{S}^4_{\epsilon_1,\epsilon_2} \times \mathbb{T}^2_{R_5,R_6}$ as per Eq. (4.41)

$$\int [da] \left| \lim_{N\to\infty} Z^{\text{Higgs}}_{\text{4d}} \right|^2 = \int [da] \, |Z_{\text{6d}}|^2 = Z_{\mathbb{S}^4_{\epsilon_1,\epsilon_2} \times \mathbb{T}^2_{R_5,R_6}} \, . \tag{4.67}$$

The quantitative agreement found here provides strong motivation for using the circular quiver—combined with deconstruction—as a tool towards computing observables for the (2,0) theory on $\mathbb{T}^2$. In particular, by reproducing the full 6d partition function from 4d we establish a precise dictionary that could be extended to a number of closely-related exact calculations, including e.g. chiral correlators [58–62, 143], Wilson loop expectation values [53, 154, 155], the radiation emitted by a heavy quark [156, 157], or other protected subsectors of operators [158]. It would be very interesting to import these results to 6d, and compare where possible with other approaches to the (2,0) theory. Ultimately, one would hope to be able to extend this procedure to non-protected sectors [159]. We leave these possibilities open as directions for future research.

## 4.2 Little String Theory

To deconstruct Little String Theory, we effectively need to repeat the procedure we described above, with one additional orbifold in the brane picture described by Table 5. As such, the starting theory that we need to consider is a double $\mathbb{Z}_{N_5} \times \mathbb{Z}_{N_6}$ orbifold of 4d $\mathcal{N} = 4$ sYM. The result is a 4d $\mathcal{N} = 1$ "toroidal-quiver" theory, as depicted in Fig. 5.

Following [23], we would like to explore how the four-dimensional $\mathcal{N} = 1$ toroidal-quiver gauge theory deconstructs the six-dimensional (1,1) LST and test their proposal by comparing the respective partition functions.[41]

Dimensional deconstruction dictates that the horizontal and vertical chiral multiplets in Fig. 5 acquire fixed vacuum expectation values $\mathrm{v}_5$ and $\mathrm{v}_6$, and all couplings are identified as $G$. One then takes the limit

$$N_5, N_6 \to \infty \,, \qquad G \to \infty \,, \tag{4.68}$$

while also fixing the ratios

$$2\pi R_5 \equiv \frac{N_5}{G\mathrm{v}_5} \,, \qquad 2\pi R_6 \equiv \frac{N_6}{G\mathrm{v}_6} \,. \tag{4.69}$$

The latter are identified with the radii of the deconstructed compact dimensions. The theory that emerges at low energies is six-dimensional sYM with (1,1) supersymmetry—the amount of supersymmetry has quadrupled—and gauge coupling $g_6^2 = (\mathrm{v}_5\mathrm{v}_6)^{-1}$. However, on top of the conventional spectrum of massive gauge bosons that deconstructs the Kaluza–Klein (KK) towers associated with the square torus $\mathbb{S}^1_{R_5} \times \mathbb{S}^1_{R_6}$, the four-dimensional quiver contains additional towers of states. This can be seen by acting on the KK towers with the S-duality transformation of the four-dimensional toroidal-quiver theory— sending $G \to N_5 N_6 / G$. From the point of view of the six-dimensional theory, this is a T-duality transformation and the new towers are interpreted as string winding modes on the torus. The combined spectrum of this non-gravitational theory matches that of (1,1) LST with string tension $1/\alpha' = 1/g_6^2$. This remarkable conclusion can also be reached using a complementary brane-engineering argument [23]. To our knowledge there exist no quantitative checks of this claim to date.

In this section, the proposal is tested by using exactly results along the lines of the previous section, but with one additional obstruction.

### 4.2.1 4d $\mathcal{N} = 1$ Ellipsoid Partition Functions

It has been surprisingly difficult to apply the approach of supersymmetric localisation to minimally-supersymmetric theories on the four-sphere, which would be desirable if one were to extend its utility to more realistic settings; see *e.g.* [162–164] for a discussion of associated issues.[42] Note that although $\mathcal{N} = 1$ partition functions on $\mathbb{S}^4$ are known to be scheme dependent and therefore a priori ambiguous [54], one can still use them to extract meaningful physical information, cf. [162, 166].

[41] For an alternative approach to (1,1) LST using *spherical* deconstruction see [160, 161].

[42] It should be mentioned that such localisation calculations have been performed for four-dimensional theories with $\mathcal{N} = 1$ supersymmetry on other manifolds [45, 165].

Given this impasse, it is then intriguing that the issues with the direct computation of the $\mathcal{N}=1$ partition function on $\mathbb{S}^4$ using localisation were recently sidestepped. In [25] known results for the exact, round-sphere partition functions of two- and three-dimensional theories with four supercharges were analytically continued to four dimensions. This culminated into specific expressions for the perturbative contribution of vector and chiral multiplets to the exact $\mathbb{S}^4$-partition function for a particular class of $\mathcal{N}=1$ theories. The proposal passes several checks, including a comparison with the holographic-dual results of [166] for the free energy of $\mathcal{N}=1^*$ super Yang–Mills (sYM), reproducing the generic NSVZ $\beta$ function, and matching a free field calculation of the same result. Overall, this is an important first step in obtaining the full partition function of $\mathcal{N}=1$ theories on $\mathbb{S}^4$.

The approach of [25] closely follows [53]. Starting with $\mathcal{N}=1$ sYM in ten-dimensional Minkowski space, one performs a dimensional reduction to Euclidean 2d/3d and reduces supersymmetry by explicitly performing two successive projections $\Gamma^{6789}\epsilon=\epsilon$, $\Gamma^{4589}\epsilon=\epsilon$, on the 32-component Killing spinors. The result is conformally mapped to the two/three-sphere by adding appropriate curvature couplings, leading to theories with one vector and three adjoint chiral multiplets; one can also turn on mass deformations in the latter.[43] Supersymmetric localisation yields the vector- and chiral-multiplet contributions on $\mathbb{S}^2/\mathbb{S}^3$; these can be combined to give the full partition function. The final two- and three-dimensional answer can be elegantly written in a d-dependent form, which can then be continued to d = 4. Through this operation one arrives at the proposed perturbative partition functions for four-dimensional theories with four supercharges [25].

As appearing in [25] we have

$$\begin{aligned}\mathcal{Z}^{\text{vec}}_{\text{pert}}\prod_{\beta} i\langle\beta,\lambda\rangle &= \prod_{\beta}\prod_{\ell=0}^{\infty}\left[\frac{\ell+i\langle\beta,\lambda\rangle}{\ell+d-1-i\langle\beta,\lambda\rangle}\right]^{n_{\ell,d}}\,,\\ \mathcal{Z}^{\text{chi}}_{\text{pert}}(m) &= \prod_{\beta}\prod_{\ell=0}^{\infty}\left[\frac{\ell+\frac{d}{2}-im-i\langle\beta,\lambda\rangle}{\ell+\frac{d-2}{2}+im+i\langle\beta,\lambda\rangle}\right]^{n_{\ell,d}}\,,\end{aligned} \tag{4.70}$$

where $\beta$ is now a rootspace representative and $\langle\beta,\lambda\rangle$ is valued in whichever representation is required. Note that the vector multiplet piece includes the Haar measure of the gauge group. Without it we can write

$$\mathcal{Z}^{\text{vec}}_{\text{pert}} = \prod_{\beta}\prod_{\ell=0}(\ell+1+i\langle\beta,\lambda\rangle)^{n_{\ell+1,d}}(\ell+d-1-i\langle\beta,\lambda\rangle)^{-n_{\ell,d}}\,. \tag{4.71}$$

This is important, for example, in the U(1) case where there no Haar measure. The

[43] As viewed from ten dimensions, the directions $x^4,\ldots,x^9$ are transverse to the two/three-sphere.

degeneracies are

$$n_{\ell,d} = \frac{\Gamma(\ell+d-1)}{\Gamma(\ell+1)\Gamma(d-1)} \,. \tag{4.72}$$

These expressions can be elegantly recast as

$$\begin{aligned} \mathcal{Z}^{\text{chi}}_{\text{pert}} &= \prod_{\beta\in\mathcal{R}} \frac{\Gamma_3(R^{-1}+iM+i\langle\beta,\lambda\rangle|R^{-1},R^{-1},R^{-1})}{\Gamma_3(2R^{-1}-iM-i\langle\beta,\lambda\rangle|R^{-1},R^{-1},R^{-1})} \,, \\ \mathcal{Z}^{\text{vec}}_{\text{pert}} &= \prod_{\beta\in\text{Adj}} \frac{\Gamma_3(3R^{-1}-i\langle\beta,\lambda\rangle|R^{-1},R^{-1},R^{-1})}{\widehat{\Gamma}_3(i\langle\beta,\lambda\rangle|R^{-1},R^{-1},R^{-1})} \,, \end{aligned} \tag{4.73}$$

where $\widehat{\Gamma}_N$ is a modification of $\Gamma_N$ that only involves a product over $\boldsymbol{\ell} \in \mathbb{N}^N \setminus \{\mathbf{0}\}$ as discussed in Appendix A. In the above, $R$ denotes the radius of the $\mathbb{S}^4$, $M$ is a mass parameter, while $\lambda$ a variable with mass-dimension one that is an element of the Lie algebra to be integrated over in the final expression for the full partition function.[44] Finally, $\beta$ takes values in the weights of the representation $\mathcal{R}$ for the chiral multiplets, or the adjoint for the vector multiplet, and $\langle\beta,\lambda\rangle$ denotes an inner product in weight space.

When phrased in terms of gamma functions, we can compare these expressions to the existing ellipsoid partition functions for 4d $\mathcal{N}=2$ in [84] or 3d $\mathcal{N}=2$ in [57, 67]. These provide a hint as to how to refine the partition functions. We have two conditions that we immediately need to fulfil for the 4d $\mathcal{N}=1$ story. Namely we should reproduce the refined partition functions of [84] when fused together with the appropriate field content and also reduce to those in [25] upon unrefining. Moreover, we know that it should be an unrefinement of a $\Gamma_3$ function. However a squashed four-sphere only has two parameters, $\epsilon_1$ and $\epsilon_2$, hence the third parameter in $\Gamma_3$ cannot be independent. That is, $\omega_3 = \omega_3(\epsilon_1,\epsilon_2)$.

Another fact that we need to bear in mind is that, when $\Re\epsilon_i > 0$, squashed spheres are symmetric under the exchanges of $\epsilon_1 \leftrightarrow \epsilon_2$ and therefore the partition function should reflect this. Indeed this is an observed property of squashed-sphere partition functions across dimensions.

With all this in mind, we propose that the refinements of the functions in Eq. (4.73) to the case of the ellipsoid, $\mathbb{S}^4_{\epsilon_1,\epsilon_2}$ are given by

$$\begin{aligned} \mathcal{Z}^{\text{chi}}_{\text{pert}} &= \prod_{\beta\in\mathcal{R}} \frac{\Gamma_3\left(\epsilon_+ + iM + i\langle\beta,\lambda\rangle|\,\epsilon_1,\epsilon_2,\epsilon_+\right)}{\Gamma_3\left(2\epsilon_+ - iM - i\langle\beta,\lambda\rangle|\,\epsilon_1,\epsilon_2,\epsilon_+\right)} \,, \\ \mathcal{Z}^{\text{vec}}_{\text{pert}} &= \prod_{\beta\in\text{Adj}} \frac{\Gamma_3(3\epsilon_+ - i\langle\beta,\lambda\rangle|\epsilon_1,\epsilon_2,\epsilon_+)}{\widehat{\Gamma}_3(i\langle\beta,\lambda\rangle|\epsilon_1,\epsilon_2,\epsilon_+)} \,, \end{aligned} \tag{4.74}$$

[44] Our definition for the vector-multiplet partition function does not include the Haar measure.

where $\epsilon_\pm = \frac{1}{2}(\epsilon_1 \pm \epsilon_2)$ and the ellipsoid $\mathbb{S}^4_{\epsilon_1,\epsilon_2}$ is defined by

$$\frac{x_1^2}{R^2} + \frac{x_2^2 + x_3^2}{\epsilon_1^{-2}} + \frac{x_4^2 + x_5^2}{\epsilon_2^{-2}} = 1 \tag{4.75}$$

for $\epsilon_1, \epsilon_2 \in \mathbb{R}_{>0}$. Eqs. (4.74) readily reduce to the results for the round $\mathbb{S}^4$, when $\epsilon_1 = R^{-1} = \epsilon_2$.

Moreover, these refined expressions lead to the expected supersymmetry enhancement upon choosing a theory with a vector and a single massless adjoint chiral multiplet. Making use of the identity

$$\Gamma_2(x|\epsilon_1, \epsilon_2) = \frac{\Gamma_3(x|\epsilon_1, \epsilon_2, \epsilon_+)}{\Gamma_3(x + \epsilon_+|\epsilon_1, \epsilon_2, \epsilon_+)} \,, \tag{4.76}$$

one finds that

$$\mathcal{Z}^{\text{chi}}_{\text{pert}}|_{M=0}\mathcal{Z}^{\text{vec}}_{\text{pert}} \quad = \quad \prod_{\beta\in\text{Adj}} \Gamma_2(2\epsilon_+ \; - \; i\langle\beta,\lambda\rangle|\epsilon_1,\epsilon_2)^{-1}\, \widehat{\Gamma}_2(i\langle\beta,\lambda\rangle|\epsilon_1,\epsilon_2)^{-1} \quad . \tag{4.77}$$

Once the Haar measure is also included this matches the answer for the $\mathcal{N} = 2$ vector-multiplet partition function on the ellipsoid, as calculated in [84].

Likewise, pairing up two chiral multiplets with the same mass in conjugate representations $\mathcal{R}$ results in

$$\begin{aligned}\mathcal{Z}^{\text{chi}}_{\text{pert}}|_{M,\lambda}\, \mathcal{Z}^{\text{chi}}_{\text{pert}}|_{-M,-\lambda} = \prod_{\beta\in\mathcal{R}} &\Gamma_2(\epsilon_+ - iM - i\langle\beta,\lambda\rangle|\epsilon_1,\epsilon_2) \\ &\times \Gamma_2(\epsilon_+ + iM + i\langle\beta,\lambda\rangle|\epsilon_1,\epsilon_2) \,,\end{aligned} \tag{4.78}$$

which matches the $\mathcal{N} = 2$ hypermultiplet result in [84].

Eqs. (4.74) form the seed for the perturbative partition function needed in dimensional deconstruction. The gauge theory of interest is obtained by twice-orbifolding the four-dimensional $\mathcal{N} = 4$ sYM with $\mathrm{U}(KN_5N_6)$ gauge group by $\mathbb{Z}_{N_5} \times \mathbb{Z}_{N_6}$. The result is a toroidal quiver-gauge theory with $N_5 \times N_6$ $\mathrm{U}(K)$ nodes and interconnecting bifundamental chiral multiplets as depicted in Fig. 5.

It is at the "orbifold point", that is the coupling at each node takes the same value, which we will denote by $G$. It enjoys superconformal symmetry and is a Lagrangian example of the theories of class $\mathcal{S}_k$ [16, 167].

The dimensional-continuation argument can be directly applied to the $\mathcal{N} = 1$ toroidal-quiver theory: the two orbifold actions lead to the same Killing-spinor projections $\Gamma^{4589}\epsilon = \epsilon$, $\Gamma^{6789}\epsilon = \epsilon$,[45] and although they also break the gauge group to $\mathrm{U}(K)^{N_5\times N_6}$ with bifundamental chirals, these can be individually coupled to the cur-

[45] See [23] for the detailed action of the $\mathbb{Z}_{N_5} \times \mathbb{Z}_{N_6}$ orbifold.

vature of $\mathbb{S}^2/\mathbb{S}^3$.

In accordance with the above, the perturbative part of the integrand of the full partition function for the toroidal-quiver theory on $\mathbb{S}^4_{\epsilon_1,\epsilon_2}$ takes the form

$$\mathcal{Z}^{\text{quiv}}_{\text{pert}} = \prod_{b,\hat{b}} \Delta(\lambda^{(b,\hat{b})})\, \mathcal{Z}^{(b,\hat{b})}_{\text{vec}}\, \mathcal{Z}^{(b,\hat{b})}_{\text{H}}\, \mathcal{Z}^{(b,\hat{b})}_{\text{D}}\, \mathcal{Z}^{(b,\hat{b})}_{\text{V}} \,, \tag{4.79}$$

where

$$\Delta(\lambda^{(b,\hat{b})}) = \prod_{m\neq n=1}^{K} i(\lambda^{(b,\hat{b})}_m - \lambda^{(b,\hat{b})}_n) \tag{4.80}$$

is the Haar measure for each $\mathrm{U}(K)_{(b,\hat{b})}$ gauge node, while the product in $b,\hat{b}$ runs over all $N_5 \times N_6$ nodes. The bifundamental chiral-multiplet contributions for the vertical (V), horizontal (H) and diagonal (D) terms can be organised according to their gauge-group representations, summarised in Tab. 8. The explicit expressions are given by[46]

$$\begin{aligned}
\mathcal{Z}^{(b,\hat{b})}_{\text{H}} &= \prod_{m,n=1}^{K} \frac{\Gamma_3\big(\epsilon_+ + iM^{(b,\hat{b})}_{\text{H}} + i\big(\lambda^{(b,\hat{b})}_m - \lambda^{(b+1,\hat{b})}_n\big)\big)}{\Gamma_3\big(2\epsilon_+ - iM^{(b,\hat{b})}_{\text{H}} - i\big(\lambda^{(b,\hat{b})}_m - \lambda^{(b+1,\hat{b})}_n\big)\big)} \,, \\
\mathcal{Z}^{(b,\hat{b})}_{\text{D}} &= \prod_{m,n=1}^{K} \frac{\Gamma_3\big(\epsilon_+ + iM^{(b,\hat{b})}_{\text{D}} - i\big(\lambda^{(b,\hat{b})}_m - \lambda^{(b+1,\hat{b}+1)}_n\big)\big)}{\Gamma_3\big(2\epsilon_+ - iM^{(b,\hat{b})}_{\text{D}} + i\big(\lambda^{(b,\hat{b})}_m - \lambda^{(b+1,\hat{b}+1)}_n\big)\big)} \,, \\
\mathcal{Z}^{(b,\hat{b})}_{\text{V}} &= \prod_{m,n=1}^{K} \frac{\Gamma_3\big(\epsilon_+ + iM^{(b,\hat{b})}_{\text{V}} + i\big(\lambda^{(b,\hat{b})}_m - \lambda^{(b,\hat{b}+1)}_n\big)\big)}{\Gamma_3\big(2\epsilon_+ - iM^{(b,\hat{b})}_{\text{V}} - i\big(\lambda^{(b,\hat{b})}_m - \lambda^{(b,\hat{b}+1)}_n\big)\big)} \,,
\end{aligned} \tag{4.81}$$

where compared to (4.74) the weight-space inner products have been evaluated on the respective representations.[47] Similarly, the vector-multiplet expressions are given by

$$\mathcal{Z}^{(b,\hat{b})}_{\text{vec}} = \prod_{m,n=1}^{K} \frac{\Gamma_3\big(3\epsilon_+ - i\big(\lambda^{(b,\hat{b})}_m - \lambda^{(b,\hat{b})}_n\big)\big)}{\widehat{\Gamma}_3\big(i\big(\lambda^{(b,\hat{b})}_m - \lambda^{(b,\hat{b})}_n\big)\big)} \,. \tag{4.82}$$

In the unrefined limit $\epsilon_1 = \epsilon_2 = R^{-1}$, and for $N_5 = N_6 = 1$, Eq. (4.79) collapses to the partition function of a single-node theory with a vector and three adjoint chiral

[46] From now on we will suppress the triple-gamma function parameters $\epsilon_1, \epsilon_2, \epsilon_+$ for brevity; the reader should assume that all expressions are given for the ellipsoid.

[47] We note that the lower-dimensional origin of the perturbative partition functions implies that the 4d mass parameters have to satisfy the constraints [25]

$$\begin{aligned}
M^{(b,\hat{b})}_{\text{H}} + M^{(b,\hat{b})}_{\text{D}} + M^{(b+1,\hat{b})}_{\text{V}} &= 0 \,, \\
M^{(b,\hat{b}+1)}_{\text{H}} + M^{(b,\hat{b})}_{\text{D}} + M^{(b,\hat{b})}_{\text{V}} &= 0 \,.
\end{aligned}$$

Our deconstruction prescription will respect these conditions.

| | $\mathrm{U}(K)_{(b,\hat{b})}$ | $\mathrm{U}(K)_{(b,\hat{b}+1)}$ | $\mathrm{U}(K)_{(b+1,\hat{b}+1)}$ |
|---|---|---|---|
| $\mathrm{V}^{(b,\hat{b})}$ | $\square$ | $\overline{\square}$ | $\mathbf{1}$ |
| $\mathrm{H}^{(b,\hat{b}+1)}$ | $\mathbf{1}$ | $\square$ | $\overline{\square}$ |
| $\mathrm{D}^{(b,\hat{b})}$ | $\overline{\square}$ | $\mathbf{1}$ | $\square$ |

**Table 8:** The chiral multiplets for the toroidal quiver and their gauge-group representations. Each chiral multiplet has an associated mass which is also indexed.

multiplets with distinct masses, i.e. $\mathcal{N}=1^*$ sYM as in [25]. In a different limiting case where $N_5=1$ or $N_6=1$, and after appropriately tuning the masses, the theory reduces to an $\mathcal{N}=2$ circular quiver involving the expected partition function Eqs. (4.77), (4.78).

### 4.2.2 Deconstructing Little String Theory

Following the prescription that was clarified in [4] we identify the parameters under the products along with fixing the masses to reflect the fact that we were sitting at the orbifold point. Namely

$$\lambda_m^{(b,\hat{b})}-\lambda_n^{(c,\hat{c})}=\lambda_m-\lambda_n\ ,\quad M_{\mathrm{V}}^{(b,\hat{b})}=0\ ,\quad M_{\mathrm{H}}^{(b,\hat{b})}=-M_{\mathrm{D}}^{(b,\hat{b})}=M\ , \tag{4.83}$$

along with the following shift in the argument for each triple-gamma function

$$\Gamma_3(x^{(b,\hat{b})})\mapsto\Gamma_3(x^{(b,\hat{b})}+2\pi ibR_5^{-1}+2\pi\hat{b}R_6^{-1})\ . \tag{4.84}$$

Furthermore, one needs to extend the range of the products over $b,\hat{b}\in\mathbb{Z}$ when taking the limit $N_5,N_6\to\infty$.

We will explicitly perform the resultant product over $b,\hat{b}$ by zeta-function regularisation. In particular, we will use [168]

$$\prod_{b,\hat{b}\in\mathbb{Z}}\Gamma_N(x+b+\hat{b}\tau|\omega_1,\ldots,\omega_N)=\prod_{\boldsymbol{\ell}\in\mathbb{N}^N}\frac{1}{\theta(q|y)}\ , \tag{4.85}$$

with

$$y=e^{-2\pi i(x+\boldsymbol{\ell}\cdot\boldsymbol{\omega})}\ ,\qquad q=e^{2\pi i\tau} \tag{4.86}$$

and $\theta(q|y)$ a $q$-theta function. Applying (A.36) to the triple-gamma functions that appear in (4.79), and after some algebra, the result for the integrand of the perturbative

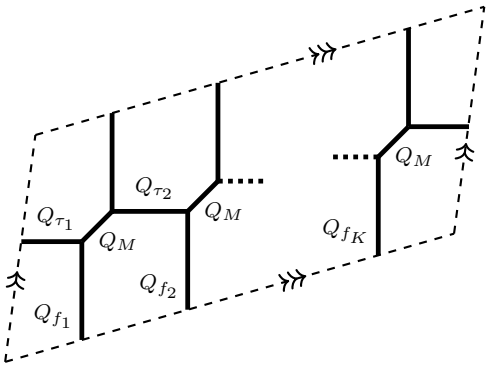


**Figure 6:** The dual toric diagram for the rank-$K$ LST. The vertical direction has been chosen as the preferred one. There are no non-trivial framing factors. Each internal line is associated with a Kähler parameter and a partition. The periodic identification of both horizontal and vertical lines is indicated by the cyclic identification of Kähler parameters and their associated partitions.

partition function of the toroidal theory in the deconstruction limit becomes

$$\mathcal{Z}^{\text{dec}}_{\text{pert}} = \left( \frac{\prod\limits_{\boldsymbol{\ell}\in\mathbb{N}^2} \theta\big(q\big|\mathfrak{q}^{\ell_1+1}\mathfrak{t}^{\ell_2+1}\big) \prod\limits_{\boldsymbol{\ell}\in\mathbb{N}^2\setminus\{\mathbf{0}\}} \theta\big(q\big|\mathfrak{q}^{\ell_1}\mathfrak{t}^{\ell_2}\big)}{\prod\limits_{\boldsymbol{\ell}\in\mathbb{N}^2} \theta\big(q\big|\mathfrak{q}^{\ell_1+\frac{1}{2}}\mathfrak{t}^{\ell_2+\frac{1}{2}}Q_M\big)\, \theta\big(q\big|\mathfrak{q}^{\ell_1+\frac{1}{2}}\mathfrak{t}^{\ell_2+\frac{1}{2}}Q_M^{-1}\big)} \right)^K \times \prod_{m\neq n=1}^{K} \frac{\prod\limits_{\boldsymbol{\ell}\in\mathbb{N}^2} \theta\big(q\big|\mathfrak{q}^{\ell_1+1}\mathfrak{t}^{\ell_2+1}\xi_{mn}\big)\, \theta\big(q\big|\mathfrak{q}^{\ell_1}\mathfrak{t}^{\ell_2}\xi_{mn}\big)}{\prod\limits_{\boldsymbol{\ell}\in\mathbb{N}^2} \theta\big(q\big|\mathfrak{q}^{\ell_1+\frac{1}{2}}\mathfrak{t}^{\ell_2+\frac{1}{2}}Q_M\xi_{mn}\big)\, \theta\big(q\big|\mathfrak{q}^{\ell_1+\frac{1}{2}}\mathfrak{t}^{\ell_2+\frac{1}{2}}Q_M^{-1}\xi_{mn}\big)} \tag{4.87}$$

where $\tau = iR_5/R_6$ and with the following definitions for the fugacities:

$$\mathfrak{q} = e^{-R_5\epsilon_1}\,, \qquad \mathfrak{t} = e^{-R_5\epsilon_2}\,, \qquad Q_M = e^{iR_5M}\,, \qquad \xi_{mn} = e^{iR_5(\lambda_m-\lambda_n)}\,. \tag{4.88}$$

This concludes the application of the deconstruction prescription to the $\mathcal{N}=1$ quiver partition function on $\mathbb{S}^4_{\epsilon_1,\epsilon_2}$.

### The BPS Partition function for (1,1) Little String Theory

Finally, we will show how Eq. (4.87) compares against (1,1) LST, the BPS partition function for which can be calculated by appealing to topological string theory. Via a chain of dualities, the topological string partition function for the toric Calabi–Yau threefold depicted by the dual toric diagram in Fig. 6 evaluates the BPS partition function of (1,1) LST on $\mathbb{R}^4_{\epsilon_1,\epsilon_2}\times\mathbb{T}^2$; cf. [81–83].[48]

[48]The web diagram for $K$ NS5 branes in the Coulomb branch coincides with the dual toric diagram of Fig. 6, where the vertical directions correspond to NS5 branes.

A lengthy calculation using the refined topological vertex formalism [68] leads to a result that factorises into winding sectors, accounting for little strings that wrap one of the toroidal directions. We find

$$\mathcal{Z}^{\text{LST}}_{\mathbb{R}^4_{\epsilon_1,\epsilon_2}\times T^2} = \widehat{\mathcal{Z}}\mathcal{Z}^{\text{wind}} \,, \tag{4.89}$$

where

$$\widehat{\mathcal{Z}} = \left(Q_M\sqrt{\frac{\mathfrak{t}}{\mathfrak{q}}}\right)^{-\frac{K}{24}} \text{P.E.}\left[\frac{q}{1-q} + I_+\left(\frac{q}{1-q}+\frac{1}{2}\right)\sum_{m,n=1}^{K}\xi_{mn}\right] , \tag{4.90}$$

with

$$I_+ = \frac{\mathfrak{q}+\mathfrak{t}-\sqrt{\mathfrak{q}\mathfrak{t}}(Q_M+Q_M^{-1})}{(1-\mathfrak{t})(1-\mathfrak{q})} \tag{4.91}$$

and

$$\mathcal{Z}^{\text{wind}} = \sum_{k=0}^{\infty} w^k \mathcal{Z}^{(k)} \,, \tag{4.92}$$

such that

$$\begin{aligned}\mathcal{Z}^{(k)} = \sum_{Y:\,\sum_m |Y_m|=k}\prod_{m,n=1}^{K}\prod_{s\in Y_m}&\frac{\theta_1\left(\tau|E_{mn}(s)+M-\epsilon_-\right)}{\theta_1\left(\tau|E_{mn}(s)+\epsilon_2\right)}\\ &\times\frac{\theta_1\left(\tau|E_{mn}(s)-M-\epsilon_-\right)}{\theta_1\left(\tau|E_{mn}(s)-\epsilon_1\right)} \,.\end{aligned} \tag{4.93}$$

In the last expression one has that $\mathcal{Z}^{(0)}=1$ and

$$E_{mn} = \lambda_m - \lambda_n - \epsilon_1 h_m(s) + \epsilon_2 v_n(s) \,, \tag{4.94}$$

with $s$ denoting a box in the coloured Young diagram $Y_m$ that labels a given partition, $h_m(s)$ the horizontal distance from the box $s$ to the right edge of $Y_m$ and $v_n(s)$ the vertical distance to the bottom edge.

To reach this answer using the topological vertex formalism one also needs to make the following identifications between the parameters appearing in the toric diagram and the physical ones:

$$\begin{aligned} Q_M\,Q_{\tau_{\alpha>1}} &= e^{iR_5(\lambda_{\alpha-1}-\lambda_\alpha)} \,, & \prod_{i=1}^{K} Q_{\tau_i}Q_M &= q \,,\\ Q_M\,Q_{\tau_1} &= qe^{iR_5(\lambda_K-\lambda_1)} \,, & \prod_{\alpha=1}^{K}(Q_{f_\alpha}Q_M)^{|Y_\alpha|} &= w^k \,, \end{aligned} \tag{4.95}$$

while keeping in mind that

$$\mathfrak{q} = e^{-R_5\epsilon_1} \,, \qquad \mathfrak{t} = e^{R_5\epsilon_2} \,, \tag{4.96}$$

for $\epsilon_1 \in \mathbb{R}_{>0}$ and $\epsilon_2 \in \mathbb{R}_{<0}$. The explicit usage of these identifications should be used alongside the schematic description in Section 2.4.1.

Two copies of the BPS partition functions of LST on $\mathbb{R}^4_{\epsilon_1,\epsilon_2} \times \mathbb{T}^2$ can be "glued together" to construct the corresponding expressions on the ellipsoid [53, 70, 71]:

$$Z_{S^4_{\epsilon_1,\epsilon_2}} = \int [\mathrm{d}\lambda]\; \mathcal{Z}_{\mathbb{R}^4_{\epsilon_1,\epsilon_2}}\, \overline{\mathcal{Z}_{\mathbb{R}^4_{\epsilon_1,\epsilon_2}}} \,, \tag{4.97}$$

with

$$\overline{\mathcal{Z}_{\mathbb{R}^4_{\epsilon_1,\epsilon_2}}}(q,\mathfrak{t},\mathfrak{q},Q_M,\lambda_m) = \mathcal{Z}_{\mathbb{R}^4_{\epsilon_1,\epsilon_2}}(q,\mathfrak{t}^{-1},\mathfrak{q}^{-1},Q_M^{-1},-\lambda_m) \,, \tag{4.98}$$

for $\mathrm{Re}\,\tau = 0$.

Now recall that at low energies (1,1) LST reduces to (1,1) sYM in six dimensions. In turn, the BPS partition function for LST coincides with that of (1,1) sYM, with the zero-winding contributions in the former being reproduced by the perturbative piece in the latter, while the non-trivial winding sectors coming from the tower of instanton-string states, see e.g. [82]. Therefore, for the purpose of comparing with the deconstruction result we will single out the zero-winding sector of the LST partition function.

Since the glueing prescription Eq. (4.97) can be implemented independently for each winding sector, it is straightforward to extract the zero-winding piece of $\mathcal{Z}^{\mathrm{LST}}_{\mathbb{S}^4_{\epsilon_1,\epsilon_2}\times\mathbb{T}^2}$ from (4.89). All in all it can be shown that the 0-winding contributions to the integrand of Eq. (4.97) is given by

$$\mathcal{Z}^{\text{LST, 0-wind}}_{S^4_{\epsilon_1,\epsilon_2}\times\mathbb{T}^2} = \frac{e^{-\frac{\pi i\tau}{6}}}{\eta(\tau)^2} \prod_{m,n=1}^{K} \prod_{\boldsymbol{\ell}\in\mathbb{N}^2} \frac{\theta\big(q\big|\mathfrak{q}^{\ell_1+\frac{1}{2}}\mathfrak{t}^{\ell_2+\frac{1}{2}}Q_M\xi_{mn}\big)}{\theta\left(q\big|\mathfrak{q}^{\ell_1}\mathfrak{t}^{\ell_2+1}\xi_{mn}\right)} \frac{\theta\big(q\big|\mathfrak{q}^{\ell_1+\frac{1}{2}}\mathfrak{t}^{\ell_2+\frac{1}{2}}Q_M^{-1}\xi_{mn}\big)}{\theta\big(q\big|\mathfrak{q}^{\ell_1+1}\mathfrak{t}^{\ell_2}\xi_{mn}\big)} \,. \tag{4.99}$$

As a last step, one needs to analytically continue the above to $\epsilon_2 \in \mathbb{R}_{>0}$ before comparing with Eq. (4.87). Proceeding as e.g. in App. A.2 of [17], the LST result Eq. (4.99) coincides with the one from deconstruction up to an overall geometric factor of $\exp\left(-\pi i\tau/6\right)\eta(\tau)^{-2}$.[49]

Having shown that there is agreement between the perturbative part of the partition functions, one might ask if it is possible to do the same with the instanton parts. Indeed

[49] This a purely geometric factor that does not contain dynamical information and is often dropped outright in the topological strings literature *cf.* [83].

it is quite trivial to show that performing a double deformation of the functions involved in the 4d $\mathcal{N} = 2^*$ partition function reproduces something very similar to (4.93), however, this is simply a mathematical relationship between a rational function and an elliptic one. For it to be genuine, one should start from a purely 4d $\mathcal{N} = 1$ instanton partition function. Unfortunately, no such partition function exists yet; see [169, 170] for recent attempts on this front.

# Chapter 5

# Deconstructing Defects

This chapter is based on the paper [4]. It uses many definitions and identities that are presented in Appendix A.

As previously mentioned in this thesis, there has been remarkable progress in the area of exact results. Somewhat more recently, this success has been extended to include contributions of supersymmetric defects of different codimensionalities [140, 171–176]. The results of the above calculations can often be expressed elegantly in terms of special functions. This reformulation sheds light into various properties of the theory itself, like its duality structure. Furthermore, mathematical relationships between different special functions can lead to connections between supersymmetric partition functions in different dimensions via dimensional reduction [177–180].[50]

In this chapter we explore the above themes in a process which can be thought of as the reverse of dimensional reduction, namely dimensional deconstruction [22, 182]. In its simplest formulation, dimensional deconstruction involves starting with a circular-quiver gauge theory and employing a finely-tuned infinite-node limit to obtain dynamics for a theory in one-compact dimension higher. Although in its original form deconstruction relates four-dimensional quivers to five-dimensional theories on a circle, it is possible under certain conditions to deconstruct theories in any dimension starting from a lower-dimensional compact quiver lattice [183]. Here we will be interested in the version that relates three-dimensional quivers to four-dimensional theories on a circle. Moreover, we will mainly focus on examples that contain supersymmetric defects. Defects have not been considered previously in the context of deconstruction.

It should be noted that the main argument behind the dimensional-deconstruction proposal uses the Lagrangian description of the quiver to identify the classical Kaluza–Klein (KK) spectrum for the higher-dimensional theory. However, one can actually go beyond this perturbative approach and apply the principle of deconstruction at the level of full supersymmetric partition functions on compact manifolds [2, 3]. We will

[50] See also [181] for a related review.

refer to this operation as "exact deconstruction" to distinguish it from the dimensional-deconstruction limit of [22, 182].

Specifically, we will apply exact deconstruction to the squashed-$\mathbb{S}^3$ partition functions[51] of three-dimensional circular-quiver theories in the presence of various defects, to recover the $\mathbb{S}^3 \times \mathbb{S}^1$-partition function—also known as the index—of four-dimensional theories that include $\frac{1}{2}$-BPS defects *wrapping* the emerging circle.

The rest of this chapter is organised as follows: In Sec. 5.1 we provide a summary of the original dimensional-deconstruction proposal and a detailed description of both the technical as well as some conceptual points regarding exact deconstruction. We also review how one can brane engineer our three-dimensional starting points and how to view deconstruction in that language. We also perform a warm-up calculation in a purely 3d setting, where we recover the index of 4d $\mathcal{N} = 2$ super-Yang–Mills (SYM) and super-QCD (SQCD) theories from the squashed-$\mathbb{S}^3$ partition function of a 3d $\mathcal{N} = 2$ circular quiver. This is then extended in Sec. 5.2 to include vortex loops that lead (after deconstruction) to codimension-two defects with 2d $(2, 2)$ supersymmetry. In this discussion, 1d and 2d defects are respectively coupled to 3d and 4d bulk theories before and after deconstruction. The extension of the procedure to 3d Wilson loops, and their potential interpretation in terms of codimension-two defects in 4d post deconstruction, appears in Sec. 5.3. We finally conclude in Sec. 5.4 with a summary of the main results and a list of possible future directions.

## 5.1 Pure Three Dimensional Deconstruction

We begin with a general overview of dimensional deconstruction and its application at the level of supersymmetric sphere partition functions. We refer to the latter application as "exact deconstruction", since the partition functions include contributions from all orders in the coupling, and also to distinguish it from the original proposal that relates theories on flat backgrounds at different energy scales. Some of the details will be omitted at this stage, but will appear when we specialise to the cases of interest in the coming sections. We first focus on the case with no defects.

The dimensional-deconstruction prescription, in the absence of defects, is well known and can be summarised as follows:[52] starting from a supersymmetric $N$-noded circular-quiver theory, where the nodes denote $\mathrm{U}(k)$ vector multiplets with the same bare gauge coupling $G$[53] and the links supersymmetric matter, one takes the theory onto the Higgs

[51] We will focus on squashings of the $\mathbb{S}^3$ that preserve a $\mathrm{U}(1) \times \mathrm{U}(1)$ isometry.

[52] Here we focus on supersymmetric QFTs, which are the main cases of interest in this chapter. Also, in view of the applications that follow we consider unitary gauge groups. Clearly, these assumptions are not necessary features of deconstruction; e.g. one could use special unitary groups instead with no need to modify our prescription.

[53] This is known as the "orbifold point" in the space of couplings.

branch by allowing the scalars in the matter multiplets to simultaneously develop a vacuum expectation value (vev), $v\,\mathbb{1}_{k\times k}$. This has the effect of breaking the gauge group to a diagonal subgroup, $\mathrm{U}(k)^N \to \mathrm{U}(k)$. By flowing to low energies the degrees of freedom get reorganised into the KK modes of a theory in one dimension higher, compactified on a discretised circle with

$$g^2_{\rm dec} \equiv \frac{G}{v} \to \text{fixed}\,, \qquad 2\pi\widehat{R} \equiv \frac{N}{Gv} \to \text{fixed}\,, \qquad a \equiv \frac{1}{Gv}\,. \tag{5.1}$$

In these formulas, $\widehat{R}$ is the radius of the emerging circle, $a$ the lattice spacing and $g_{\rm dec}$ the emerging bare coupling [22, 182]. Although the original deconstruction proposal relates four-dimensional quivers to five-dimensional theories on a circle, it can also be applied to lower-dimensional quivers [183]. It can be further generalised to theories of higher codimensionality by producing products of circles when starting from higher-dimensional periodic lattices in theory space [23, 183].

When the Higgs branch of the theory is not lifted by quantum corrections, e.g. when the quiver is superconformal or by adding an appropriate superpotential term, one can consider taking the combined limit

$$v \to \infty \qquad N \to \infty\,, \qquad G \to \infty\,, \tag{5.2}$$

which sends $a \to 0$ and recovers the continuum theory, while keeping $g_{\rm dec}$ and $\widehat{R}$ fixed; such examples may also exhibit supersymmetry enhancement for the deconstructed theory [23, 184].

Formally this was translated into the replacement rule where the product over gauge nodes was replaced by a product over the KK masses, schematically represented through

$$\prod_\alpha f(x^{(\alpha)}) \mapsto \prod_\alpha f\left(x + 2\pi i\alpha\widehat{R}^{-1}\right)\,. \tag{5.3}$$

This was discussed in Chapter 4 and in [4]. We will now demonstrate how this prescription can be applied to recover four-dimensional partition functions on $\mathbb{S}^3_{\omega_1,\omega_2}\times\mathbb{S}^1_{\widehat{R}}$ from three-dimensional circular-quivers on the squashed three-sphere, $\mathbb{S}^3_{\omega_1,\omega_2}$.

Let us close this discussion with a comment that has to do with the legitimacy of the continuum deconstruction limit (5.2). Unlike the circular-quiver theories of [2, 3, 23], the 3d quivers of this chapter are not superconformal, so one needs to make sure that quantum effects do not lift the Higgs branch—the existence of which is necessary for deconstruction—at low energies. Single-noded $\mathcal{N}=2$ SQCD theories in three dimensions with $N_f \geq N_c$ fundamental/anti-fundamental pairs are believed to have distinct Higgs and Coulomb branches, even after incorporating quantum corrections.

| | $x^0$ | $x^1$ | $x^2$ | $x^3$ | $x^4$ | $x^5$ | $x^6$ | $x^7$ | $x^8$ | $x^9$ |
|---|---|---|---|---|---|---|---|---|---|---|
| D3 | – | – | – | – | · | · | · | · | · | · |
| NS5 | – | – | – | · | · | · | · | – | – | – |
| D5 | – | – | – | · | – | – | – | · | · | · |
| D1 | – | · | · | · | · | · | – | · | · | · |
| NS5′ | – | · | · | · | – | – | · | – | – | – |
| $A_{N-1}$ | · | · | · | · | – | – | · | · | – | – |

**Table 9:** Brane configuration in type IIB string theory engineering 3d vortex-loop operators. The $\mathbb{Z}_N$ orbifold acts in the directions $x^4, x^5, x^8, x^9$. The D3s are stretched between NS5s along an interval $L_3$ in the $x^3$ direction. The D1s are stretched between the D3s and NS5s and/or NS5′s along the $x^6$ direction.

Moreover, at the intersection of these branches such theories flow to interacting critical points in the IR [185,186]. In all the examples that we will consider in this chapter, we have circular quivers where $N_f \geq N_c$ is obeyed at each node. We expect that the above statements about the non-lifting of the Higgs and Coulomb branches extend to the full theory. Although we will not present rigorous arguments to this effect, we will see in the upcoming sections that this picture leads to sensible results. Related statements about the low energy dynamics of 3d $\mathcal{N} = 4$ quivers can be found in [187]. Further evidence that supports the validity of dimensional deconstruction in the cases that we consider is provided in the next subsection with a suitable embedding in string theory.

### 5.1.1 Brane Engineering

Before implementing the technical steps of exact deconstruction it is useful to have complementary evidence that dimensional deconstruction works unobstructed in the full physical theory. In many cases such evidence is encoded naturally in string-theory embeddings. All 3d theories that we will be interested in in this section arise in the low-energy limit of type IIB string theory configurations that involve branes of the type listed in Tables 9 and 10. The precise combinations of these ingredients depend on the specific example under study and we will spell out the pertinent details in the upcoming sections as needed. In the rest of this subsection we summarise the key features of these constructions.

The low-energy dynamics of multiple D3s suspended between NS5s along an interval $L_3$ in the $x^3$ direction are captured by a three-dimensional gauge theory. The inclusion of D5 branes that intersect the D3s corresponds to the introduction of flavour. In order to engineer vortex loops, which are related to codimension-two defects with *non-chiral* 2d supersymmetry through dimensional reduction, one needs to introduce D1s that stretch between the D3s and an NS5 and/or NS5′s along the $x^6$ direction, oriented as in Tab. 9. In order to engineer Wilson loops, which are related to codimension-two defects with *chiral* 2d supersymmetry through dimensional reduction, one needs to

| | $x^0$ | $x^1$ | $x^2$ | $x^3$ | $x^4$ | $x^5$ | $x^6$ | $x^7$ | $x^8$ | $x^9$ |
|---|---|---|---|---|---|---|---|---|---|---|
| D3 | – | – | – | – | · | · | · | · | · | · |
| NS5 | – | – | – | · | · | · | · | – | – | – |
| D5 | – | – | – | · | – | – | – | · | · | · |
| F1 | – | · | · | · | · | · | · | – | · | · |
| D5′ | – | · | · | · | – | – | – | · | – | – |
| $A_{N-1}$ | · | · | · | · | – | – | · | · | – | – |

**Table 10:** Brane configuration in type IIB string theory engineering 3d Wilson-loop operators. The $\mathbb{Z}_N$ orbifold acts in the directions $x^4, x^5, x^8, x^9$. The D3s are stretched between NS5s along an interval $L_3$ in the $x^3$ direction. The F1s are stretched between the D3s and D5s and/or D5′s along the $x^7$ direction.

introduce F1s that stretch between the D3s and a D5 and/or D5′ along the $x^7$ direction, oriented as in Tab. 10. In this fashion, one can engineer a wide variety of examples with $\mathcal{N} = 4$ supersymmetry; see e.g. [174]. Placing various combinations of the above ingredients on a $\mathbb{C}^2/\mathbb{Z}_N$ orbifold singularity, $A_{N-1}$, leads to a circular-quiver gauge theory in three dimensions with $\mathcal{N} = 2$ supersymmetry and vortex/Wilson loops at low energies [148, 188].

In this set-up deconstruction is simply realised by taking the combined brane system off the $A_{N-1}$ singularity and into the orbifolded space, which is locally $\mathbb{R}^3 \times \mathbb{S}^1_{\widetilde{R}}$, by a distance $d$. In the presence of flavour/defect branes this is carried out in one of the directions $x^8$ or $x^9$, with $x^9$ or $x^8$ respectively compactified on a circle of radius $\widetilde{R}$. The continuum limit (5.2) involves taking the string length scale $l_s \to 0$ and $N \to \infty$ while keeping the string coupling $g_s \to$ fixed and $\widetilde{R}/l_s^2 \equiv d/Nl_s^2 \to$ fixed. An equivalent description is in terms of a T-dual system with the various D-branes wrapping a fixed-sized circle $\widehat{R} \equiv l_s^2/\widetilde{R}$ and string coupling $g_s' = g_s\widehat{R}/l_s$ [2, 23]. In order to keep the 3d gauge coupling $1/g_{\rm 3d}^2 \equiv L_3 l_s/g_s$ tunable, as required by deconstruction, one needs to take $L_3 \to \infty$ as $l_s \to 0$. Then, the 4d gauge coupling $1/g_{\rm 4d}^2 \equiv L_3/g_s' l_s = L_3/g_s\widehat{R} \to \infty$ in the limit, resulting in a weakly-coupled 4d gauge theory (with matter and/or defects).

### 5.1.2 4d Indices from $\mathbb{S}^3$ Partition Functions

The exact-deconstruction procedure can be straightforwardly applied in the context of 3d quiver-gauge theories and their partition functions on the U(1) × U(1) isometric hyper-ellipsoid, $\mathbb{S}^3_{\omega_1,\omega_2}$. The latter is given by the equation

$$\omega_1^{-2}(X_1^2 + X_2^2) + \omega_2^{-2}(X_3^2 + X_4^2) = 1 \,. \tag{5.4}$$

Sometimes the squashing parameter can be defined as the dimensionless ratio $b = \sqrt{\frac{\omega_2}{\omega_1}}$; the round three sphere is then recovered in the limit $b \to 1$. However, to remain consistent with the previous chapters, the partition functions will not be in terms of this

parameter. Supersymmetric partition functions on the ellipsoid are readily calculated using supersymmetric localisation [55,57,67]. The unsquashed $\mathbb{S}^3$ partition function for the vector multiplet was also shown explicitly in the review Chapter 2. The answer can be neatly organised by observing that it factorises into individual contributions from vector and chiral multiplets—in the appropriate representations of the Lie algebra—over which one needs to perform a final matrix integral for any symmetries that are gauged. We summarise our notation and the key ingredients in the following.

**Building blocks of sphere partition functions**

The partition function of 3d $\mathcal{N}=2$ theories on $\mathbb{S}^3_{\omega_1,\omega_2}$ can be constructed using the vector- and chiral-multiplet partition functions

$$\begin{aligned} Z^{\mathcal{N}=2}_{\text{vec}}(\lambda) &= \prod_{\beta\in\text{Adj}} \widehat{\Gamma}_h\left(\langle\beta,\lambda\rangle\middle|\omega_1,\omega_2\right)^{-1} \\ &= \widehat{\Gamma}_h\left(0|\omega_1,\omega_2\right)^{-\text{rank}(\mathfrak{g})} \prod_{\beta\in\Delta} \widehat{\Gamma}_h\left(\langle\beta,\lambda\rangle\middle|\omega_1,\omega_2\right)^{-1} \ , \\ Z^{\mathcal{N}=2}_{\text{chi}}(\lambda,r) &= \prod_{\beta\in\mathcal{R}} \Gamma_h\left(r\omega_+ - \langle\beta,\lambda\rangle\middle|\omega_1,\omega_2\right) \ , \end{aligned} \tag{5.5}$$

where $\Gamma_h$ and $\widehat{\Gamma}_h$ are hyperbolic Gamma functions—defined in App. A. Here $\mathcal{R}$ is a generic representation in any product of gauge or global symmetries and $\lambda$ is associated with a set of chemical potentials corresponding to these symmetries, $\beta$ takes values in the weights of the representation $\mathcal{R}$[54] and $r$ denotes the chiral-multiplet $U(1)_R$ charge. The product $\langle\beta,\lambda\rangle$ is an inner product in weight space. We are also using the combination $\omega_+ = \frac{\omega_1+\omega_2}{2}$.

Note that we can combine the vector-multiplet contributions with the matrix-integral Haar measure, $\Delta^{\text{Haar}}(\lambda) = \prod_{\beta\in\Delta} i\langle\beta,\lambda\rangle$, to write

$$\Delta^{\text{Haar}}(\lambda) Z^{\mathcal{N}=2}_{\text{vec}}(\lambda) = \widehat{\Gamma}_h(0|\omega_1,\omega_2)^{-\text{rank}(\mathfrak{g})} \prod_{\beta\in\Delta} \Gamma_h\left(\langle\beta,\lambda\rangle\middle|\omega_1,\omega_2\right)^{-1} \ . \tag{5.6}$$

The above ingredients can be used to construct 3d $\mathcal{N}=4$ multiplet contributions. For the vector multiplet we combine an $\mathcal{N}=2$ vector multiplet with an adjoint $\mathcal{N}=2$ chiral multiplet with $r=1$. For an adjoint chiral $Z^{\mathcal{N}=2}_{\text{Adj chi}}(\lambda, r=1) = 1$,[55] hence

$$\Delta^{\text{Haar}}(\lambda) Z^{\mathcal{N}=4}_{\text{vec}}(\lambda) = \widehat{\Gamma}_h(0|\omega_1,\omega_2)^{-\text{rank}(\mathfrak{g})} \prod_{\beta\in\Delta} \Gamma_h\left(\langle\beta,\lambda\rangle\middle|\omega_1,\omega_2\right)^{-1} \ , \tag{5.7}$$

which is the same function as in $\mathcal{N}=2$. For the 3d $\mathcal{N}=4$ hypermultiplet, one simply

[54] For the adjoint representation the product over $\beta$ can be reduced to a product over the roots $\Delta$ and Cartans $\mathfrak{h}$.

[55] This is due to the result enjoying a symmetry under root reflections.

takes two $\mathcal{N}=2$ chiral multiplets in conjugate representations, both with $r=\frac{1}{2}$. Thus

$$Z_{\rm hyp}^{\mathcal{N}=4}(\lambda)=\prod_{\beta\in\mathcal{R}}\Gamma_h\left(\frac{\omega_+}{2}-\langle\beta,\lambda\rangle|\omega_1,\omega_2\right)\Gamma_h\left(\frac{\omega_+}{2}+\langle\beta,\lambda\rangle|\omega_1,\omega_2\right)\ . \tag{5.8}$$

Post deconstruction, and for the appropriate choice of matter content, the $\mathbb{S}^3$ partition functions of 3d $\mathcal{N}=2$ theories will lift to the superconformal index of 4d $\mathcal{N}=2$ theories [39]. For superconformal $\mathcal{N}=2$ theories in Euclidean $\mathbb{R}^4$, and in radial quantisation, this index is defined as the trace (we use the conventions of [172])

$$\mathcal{I}_{\rm 4d}={\rm Tr}(-1)^F e^{-\beta(E-h_{01}-h_{23}-2R+r)}\mathfrak{p}^{h_{23}-r}\mathfrak{q}^{h_{01}-r}\mathfrak{t}^{R+r}\ , \tag{5.9}$$

where $F$ is the fermion number, $E$ the conformal dimension, $h_{01}=j_1+j_2$ and $h_{23}=-j_1+j_2$ are rotation generators along the two planes 01 and 23 of $\mathbb{R}^4$, $R$ is the $\mathrm{SU}(2)_R$ Cartan, while $r$ is the $\mathrm{U}(1)_r$ Cartan. One can also make the change of variables $\mathfrak{t}\to\mathfrak{v}\sqrt{\mathfrak{p}\mathfrak{q}}$ to arrive at

$$\mathcal{I}_{\rm 4d}={\rm Tr}(-1)^F e^{-\beta(E-h_{01}-h_{23}-2R+r)}\mathfrak{p}^{h_{23}+\frac{1}{2}(R-r)}\mathfrak{q}^{h_{01}+\frac{1}{2}(R-r)}\mathfrak{v}^{R+r}\ , \tag{5.10}$$

which in the limit $\mathfrak{v}\to 1$ reduces to an $\mathcal{N}=1$ superconformal index [41].[56]

The superconformal index of Lagrangian theories can itself be neatly organised in terms of separate contributions from vector multiplets and chiral multiplets, all of which are again expressible via special functions. The special function that dominates the 4d superconformal index is the elliptic Gamma function $\Gamma_e(z|\mathfrak{p},\mathfrak{q})$ (also defined in App. A). In what follows we explain how deconstruction recovers all the details of the 4d superconformal index from three-dimensional data.

### Deconstruction of 4d $\mathcal{N}=2$ pure sYM theory

Let us begin with the simplest possible example, which will allow us to highlight the main points of the exact-deconstruction procedure. In the brane-system description of Tab. 9 this involves $kN$ D3s on the $A_{N-1}$ singularity, suspended between two NS5s that are separated by an interval of size $L_3$. In the string-decoupling limit this set-up gives rise to the three-dimensional quiver-gauge theory with $\mathcal{N}=2$ supersymmetry illustrated in Fig. 7. Up to factors of $\omega_1,\omega_2$, the partition function of this theory on

[56] Via the operator-state map the superconformal index also admits a presentation in terms of a twisted partition function on $\mathbb{S}^3\times\mathbb{S}^1$ with supersymmetric boundary conditions and Hamiltonian $H=E-h_{01}-h_{23}-2R-r$ [40]. This definition is more general as it is also applicable to non-conformal theories, for which the name superconformal index is not quite appropriate. However, since this quantity is independent of the coupling and the theory eventually flows to some SCFT at an IR fixed point, we will still use this nomenclature through a mild abuse of language.

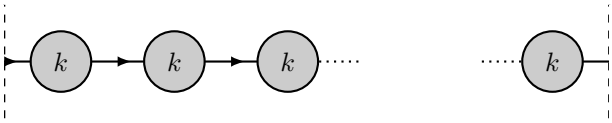


**Figure 7:** 3d $\mathcal{N}=2$ circular quiver with $N$ nodes. The nodes denote U($k$) vector multiplets, while the links bifundamental-chiral multiplets with assigned R charge $r=1$. The endpoints are to be understood as periodically identified.

the ellipsoid, $\mathbb{S}^3_{\omega_1,\omega_2}$, can be immediately written down with the help of (5.5) as

$$\mathcal{Z}^{\text{quiver}}_{\text{3d}} = \prod_{\alpha}\frac{1}{k!}\int\prod_{b=1}^{k}\mathrm{d}\sigma_b^{(\alpha)}\Delta^{\text{Haar}}\left(\sigma^{(\alpha)}\right)\prod_{b,c=1}^{k}\frac{\Gamma_h\left(\omega_+ + \sigma_b^{(\alpha)} - \sigma_c^{(\alpha+1)}\middle|\omega_1,\omega_2\right)}{\widehat{\Gamma}_h\left(\sigma_b^{(\alpha)} - \sigma_c^{(\alpha)}\middle|\omega_1,\omega_2\right)}\,, \tag{5.11}$$

where the $\sigma^{(\alpha)}$ are the Coulomb-branch parameters for the gauge group at each node.

As we have already described in this thesis, the exact-deconstruction prescription has two key elements:

(1) We should identify all $\sigma^{(\alpha)} \to \sigma$. This encodes the breaking of the gauge symmetry $U(k)^N \to U(k)$.

(2) We should shift all the arguments of the hyperbolic Gamma functions by $\Gamma_h(x) \to \Gamma_h(x + i\frac{2\pi\alpha}{R})$ and take $N \to \infty$. This encodes the reorganisation of the spectrum into the KK modes of the higher-dimensional theory with mass parameters $m_\alpha = i\frac{2\pi\alpha}{R}$. In these formulae, $R$ is the radius the deconstructed $\mathbb{S}^1$.

Implementing these steps leads to the partition function

$$\begin{aligned}\mathcal{Z}^{\text{Dec}}_{\text{3d}} = \frac{1}{k!}\int\prod_{b=1}^{k}\mathrm{d}\sigma_b\prod_{\alpha}\frac{\Gamma_h\left(\omega_+ + i\frac{2\pi\alpha}{R}\middle|\omega_1,\omega_2\right)^k}{\widehat{\Gamma}_h(i\frac{2\pi\alpha}{R}|\omega_1,\omega_2)^k} \\ \times\prod_{b\neq c}\frac{\Gamma_h\left(\omega_+ + \sigma_b - \sigma_c + i\frac{2\pi\alpha}{R}\middle|\omega_1,\omega_2\right)}{\Gamma_h\left(\sigma_b - \sigma_c + i\frac{2\pi\alpha}{R}\middle|\omega_1,\omega_2\right)}\,.\end{aligned} \tag{5.12}$$

At this stage one uses the following identity between hyperbolic and elliptic Gamma functions

$$\prod_{\alpha=-\infty}^{\infty}\Gamma_h\left(x + i\frac{2\pi\alpha}{R}\middle|\omega_1,\omega_2\right) = \mathfrak{x}^2\left(\mathfrak{p}\mathfrak{q}\right)^{-\frac{1}{2}}\Gamma_e(\mathfrak{x}|\mathfrak{p},\mathfrak{q}) \tag{5.13}$$

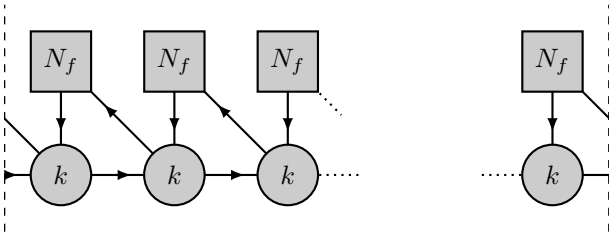


**Figure 8:** 3d $\mathcal{N}=2$ circular quiver with $N$ gauge and flavour nodes. The circular nodes denote U($k$) vector multiplets, while the squares U($N_f$) flavour groups. The links between circles encode bifundamental-chiral multiplets with assigned R charge $r=1$, while the ones between circles and squares (anti)fundamental chirals with assigned R charge $r=\frac{1}{2}$. The endpoints are to be understood as periodically identified.

for $\mathfrak{x}=e^{-Rx}$, $\mathfrak{p}=e^{-R\omega_1}$, $\mathfrak{q}=e^{-R\omega_2}$, as shown in Appendix A. One can therefore write

$$\mathcal{Z}^{\text{Dec}}_{\text{3d}}=\frac{1}{k!}\oint\prod_{b=1}^{k}\frac{\mathrm{d}v_b}{2\pi i v_b}\frac{\Gamma_e(\sqrt{\mathfrak{pq}}|\mathfrak{p},\mathfrak{q})^k}{\widehat{\Gamma}_e(1|\mathfrak{p},\mathfrak{q})^k}\prod_{b\neq c}\frac{\Gamma_e\left(\sqrt{\mathfrak{pq}}v_b v_c^{-1}\middle|\mathfrak{p},\mathfrak{q}\right)}{\Gamma_e\left(v_b v_c^{-1}\middle|\mathfrak{p},\mathfrak{q}\right)}\,, \tag{5.14}$$

where $v_b=e^{-R\sigma_b}$. Finally, using $\widehat{\Gamma}_e(1|\mathfrak{p},\mathfrak{q})=(\mathfrak{p};\mathfrak{p})^{-1}(\mathfrak{q};\mathfrak{q})^{-1}$ and recognising that $\Gamma_e(\sqrt{\mathfrak{pq}}|\mathfrak{p},\mathfrak{q})=1$, as well as $\prod_{b\neq c}\Gamma_e(\sqrt{\mathfrak{pq}}v_b v_c^{-1}|\mathfrak{p},\mathfrak{q})=1$, we arrive at

$$\mathcal{Z}^{\text{Dec}}_{\text{3d}}=\frac{1}{k!}(\mathfrak{p};\mathfrak{p})^k(\mathfrak{q};\mathfrak{q})^k\oint\prod_{b=1}^{k}\frac{\mathrm{d}v_b}{2\pi i v_b}\prod_{b\neq c}\Gamma_e\left(v_b v_c^{-1}\middle|\mathfrak{p},\mathfrak{q}\right)^{-1}\,, \tag{5.15}$$

which reproduces precisely the expression for the $\mathcal{N}=1$ superconformal index of a 4d $\mathcal{N}=2$ vector multiplet.[57] Note that, although the supersymmetry of the deconstructed theory is double that of the original one, the 3d partition function has a single R-charge chemical potential and can therefore only provide the $\mathfrak{v}\to 1$ limit of the full $\mathcal{N}=2$ superconformal index (5.10).[58]

### Deconstruction of 4d $\mathcal{N}=2$ SQCD

One can further enrich the previous example by adding flavour. In the brane picture this corresponds to adding $N_f N$ D5 branes to the $kN$ D3s suspended between two

[57] This corresponds to taking the $\mathfrak{t}\to\sqrt{\mathfrak{pq}}$ limit in the expressions of [172].

[58] It is possible to deconstruct the additional R-symmetry fugacity present in the $\mathcal{N}=2$ index by turning on appropriate real-mass terms in the $\mathbb{S}^3$ partition function. Real masses in the $\mathbb{S}^3$ partition function are related to background-U(1) gauge fields in the $\mathbb{S}^3\times\mathbb{S}^1$ partition function through dimensional reduction [44]. The $\mathbb{S}^3\times\mathbb{S}^1$ partition function in turn provides an alternative presentation of the index via the state-operator map, with generic background-U(1) gauge fields mapping to global fugacities. Therefore, real masses in 3d will generically deconstruct global fugacities in 4d. In particular, turning on real masses, where the accompanying charges specifically correspond to the $R+r$ combination that appears in the $\mathcal{N}=2$ index (-1 for bifundamental chiral multiplets and $\frac{1}{2}$ for the (anti)fundamental chiral multiplets of the next example), reproduces the contributions of the fugacity $\mathfrak{v}$.

NS5s in the presence of the $A_{N-1}$ orbifold singularity, along the directions listed in Tab. 9. In the string-decoupling limit this gives rise to the quiver of Fig. 8, which preserves $\mathcal{N}=2$ supersymmetry in three dimensions. The $\mathbb{S}^3_{\omega_1,\omega_2}$ partition function of this circular-quiver theory is given by the expression

$$\begin{aligned}\mathcal{Z}^{\text{quiver}}_{\text{3d}} = \prod_{\alpha}\frac{1}{k!}\oint\prod_{b=1}^{k}\mathrm{d}\sigma_b^{(\alpha)}\Delta^{\text{Haar}}\left(\sigma^{(\alpha)}\right)\prod_{b,c=1}^{k}\frac{\Gamma_h\left(\omega_+ + \sigma_b^{(\alpha)} - \sigma_c^{(\alpha+1)}\right)}{\widehat{\Gamma}_h\left(\sigma_b^{(\alpha)} - \sigma_c^{(\alpha)}\right)} \\ \times\prod_{b=1}^{k}\prod_{j=1}^{N_f}\Gamma_h\left(\frac{1}{2}\omega_+ - \mu_j^{(\alpha)} + \sigma_b^{(\alpha)}\right)\Gamma_h\left(\frac{1}{2}\omega_+ - \sigma_b^{(\alpha+1)} + \mu_j^{(\alpha)}\right)\,,\end{aligned} \tag{5.16}$$

where we dropped the explicit dependence on $\omega_1$ and $\omega_2$ for brevity.

In order to perform the dimensional-deconstruction procedure, even in the flat-space case, one first needs to explicitly break the flavour group to its diagonal subgroup $\mathrm{U}(N_f)^N \to \mathrm{U}(N_f)$ [184]; this has the effect of identifying all the square nodes in Fig. 8 and sending $\mu_j^{(\alpha)} \to \mu_j$. Apart from this additional detail, the exact-deconstruction procedure can be implemented as in the previous example, by identifying all the Coulomb-branch parameters and shifting all the arguments of the hyperbolic-gamma functions. This leads to the formula

$$\begin{aligned}\mathcal{Z}^{\text{Dec}}_{\text{3d}} = \frac{1}{k!}\int\prod_{b=1}^{k}\mathrm{d}\sigma_b\prod_{\alpha}\frac{\Gamma_h(\omega_+ + i\frac{2\pi\alpha}{R})^k}{\widehat{\Gamma}_h(i\frac{2\pi\alpha}{R})^k}\prod_{b\neq c}\frac{\Gamma_h\left(\omega_+ + \sigma_b - \sigma_c + i\frac{2\pi\alpha}{R}\right)}{\Gamma_h\left(\sigma_b - \sigma_c + i\frac{2\pi\alpha}{R}\right)} \\ \times\prod_{b=1}^{k}\prod_{j=1}^{N_f}\Gamma_h\left(\frac{1}{2}\omega_+ \mp \sigma_b \pm \mu_j + i\frac{2\pi\alpha}{R}\right)\,,\end{aligned} \tag{5.17}$$

where we adopted the notation $f(\pm x) = f(x)f(-x)$. A similar notation will be used for exponents. Finally, using (A.22) we arrive at

$$\begin{aligned}\mathcal{Z}^{\text{Dec}}_{\text{3d}} = \frac{1}{k!}(\mathfrak{p};\mathfrak{p})^k(\mathfrak{q};\mathfrak{q})^k\oint\prod_{b=1}^{k}\frac{\mathrm{d}v_b}{2\pi i v_b}\prod_{b\neq c}\Gamma_e\left(v_b v_c^{-1}\middle|\mathfrak{p},\mathfrak{q}\right)^{-1} \\ \times\prod_{b=1}^{k}\prod_{j=1}^{N_f}\Gamma_e\left((\mathfrak{p}\mathfrak{q})^{\frac{1}{4}}(v_b s_j^{-1})^{\pm}\middle|\mathfrak{p},\mathfrak{q}\right)\,,\end{aligned} \tag{5.18}$$

where $s_j = e^{-R\mu_j}$. When $N_f = 2k$, our $\mathrm{U}(k)$ theory is not conformally invariant. However, it flows to 4d $\mathcal{N}=2$ SQCD with a weak U(1) gauging times a free abelian vector multiplet in the IR. The IR theory admits an honest $\mathcal{N}=1$ superconformal index and, upon a reparametrisation $\tilde{u}_b = u_b a^{-\frac{1}{k}}$,[59] the result (5.18) is in explicit agreement

[59] The $\tilde{u}_b$ are $k$ SU($k$) fugacities obeying $\prod_{b=1}^{k}\tilde{u}_b = 1$, while $a$ denotes the fugacity for the free U(1) sector.

with this quantity.

## 5.2 4d Surface Defects from 3d Vortex Loops

We next examine how exact deconstruction works in the presence of codimension-two defects. Codimension-two defects in three-dimensional QFTs are line operators. In four-dimensional QFTs they are surface operators. We will explain how exact deconstruction lifts $\mathbb{S}^3_{\omega_1,\omega_2}$ partition functions with supersymmetric line-operator insertions in 3d $\mathcal{N}=2$ (or 3d $\mathcal{N}=4$) quiver-gauge theories to $\mathbb{S}^1\times\mathbb{S}^3_{\omega_1,\omega_2}$ partition functions with surface-operator insertions in 4d $\mathcal{N}=2$ (or 4d $\mathcal{N}=4$) gauge theories. Our line defects will always wrap the fibre of the (squashed) Hopf fibration $\mathbb{S}^1\hookrightarrow\mathbb{S}^3\to\mathbb{S}^2$, and will be situated at the North or South pole of the $\mathbb{S}^2$, as in [174]. Note that the squashing deformation breaks the same supersymmetry as the line defect. So even though in flat space the line defects are $\frac{1}{2}$-BPS, on the $\mathbb{S}^3_{\omega_1,\omega_2}$ they do not break any additional supersymmetry.

In 3d $\mathcal{N}=4$ theories one can consider two types of $\frac{1}{2}$-BPS line defects supported on a straight line in flat space. The first type preserves the 1d $\mathcal{N}=4$A supersymmetry algebra, which arises from the dimensional reduction of 2d $\mathcal{N}=(2,2)$ supersymmetry.[60] $\frac{1}{2}$-BPS vortex lines in 3d $\mathcal{N}=4$ QFTs realise this symmetry. The second type preserves the 1d $\mathcal{N}=4$B supersymmetry algebra, which arises from the dimensional reduction of 2d $\mathcal{N}=(4,0)$ supersymmetry. $\frac{1}{2}$-BPS Wilson lines in 3d $\mathcal{N}=4$ QFTs are examples of this type. A review of pertinent details can be found in [174].

Defects of each of these types can generically be studied by coupling a 1d supersymmetric quantum mechanics theory (SQM), supported on the defect worldvolume, to the 3d bulk gauge theory of interest (here a quiver-gauge theory). The supersymmetry of the SQM defines the type of the defect. The typical coupling between the defect and the bulk proceeds via gauging 1d global symmetries with the vector multiplets of the bulk gauge theory. The coupling may also include superpotential terms involving defect and bulk matter fields.

Similarly, in 3d $\mathcal{N}=2$ theories one can consider $\frac{1}{2}$-BPS line defects preserving either 1d $\mathcal{N}=2$A supersymmetry (that arises from the dimensional reduction of 2d $\mathcal{N}=(1,1)$ supersymmetry) or $\frac{1}{2}$-BPS defects preserving 1d $\mathcal{N}=2$B supersymmetry (that arises from the dimensional reduction of 2d $\mathcal{N}=(0,2)$ supersymmetry).

In this chapter we will consider line defects in 3d supersymmetric quiver-gauge theories that preserve the $\mathcal{N}=4$A, $\mathcal{N}=4$B or $\mathcal{N}=2$B supersymmetries. The $\mathcal{N}=2$A supersymmetry will not play any rôle in the cases that we study. In the rest of this section we will discuss how to use exact deconstruction to lift the partition functions

[60] We note in passing that the dimensional reduction of 2d $\mathcal{N}=(2,2)$ surface defects in 4d $\mathcal{N}=2$ gauge theories to three dimensions has been discussed in [189].

of vortex loops with 1d $\mathcal{N}=4$A or $\mathcal{N}=2$B supersymmetry in a 3d bulk, to indices for surface defects with 2d $\mathcal{N}=(4,4)$ or 2d $\mathcal{N}=(2,2)$ supersymmetry in a 4d bulk. Note that in this fashion we will bypass the discussion of dimensionally deconstructing the 4d-2d system from 3d-1d at the level of Lagrangians for the flat-space theories, comparing instead the theories directly at the level of sphere partition functions. The case of Wilson loops is in Sec. 5.3.

### Building blocks of partition functions with vortex-loop insertions

In the presence of codimension-two defects the $\mathbb{S}^3_{\omega_1,\omega_2}$ partition functions will have, in addition to the 3d-multiplet contributions that we discussed in Sec. 5.1.2, contributions coming from the 1d defect theory, which is supported on a circle of radius $\omega^{-1}$;[61] these can also be evaluated using supersymmetric localisation.

Let us first consider building defect theories with 1d $\mathcal{N}=2$B supersymmetry. The basic multiplets in such SQM theories are $\mathcal{N}=2$B vector multiplets, chiral multiplets and Fermi multiplets (we refer the reader to [193] for a review). The one-loop contributions of each of these multiplets to the Witten index of 1d $\mathcal{N}=2$B SQM theories are

$$\begin{aligned}
g_{\text{vec}}^{\mathcal{N}=2}(\lambda) &= \prod_{\beta\in\text{Adj}} \widehat{\Gamma}_1\left(\langle\beta,\lambda\rangle\middle|\omega\right)^{-1}\Gamma_1\left(\omega-\langle\beta,\lambda\rangle\middle|\omega\right)^{-1} \\
&= \Gamma_1\left(\omega\middle|\omega\right)^{-2\times\text{rank}(\mathfrak{g})}\prod_{\beta\in\Delta}\widehat{\Gamma}_1\left(\langle\beta,\lambda\rangle\middle|\omega\right)^{-1}\Gamma_1\left(\omega\langle\beta,\lambda\rangle\middle|\omega\right)^{-1} \ , \\
g_{\text{chi}}^{\mathcal{N}=2}(\lambda,r) &= \prod_{\beta\in\mathcal{R}}\Gamma_1\left(\langle\beta,\lambda\rangle+\frac{r}{2}z\middle|\omega\right)\Gamma_1\left(\omega-\langle\beta,\lambda\rangle-\frac{r}{2}z\middle|\omega\right) \ , \\
g_{\text{fer}}^{\mathcal{N}=2}(\lambda,r) &= \prod_{\beta\in\mathcal{R}}\Gamma_1\left(-\langle\beta,\lambda\rangle-\frac{r}{2}z\middle|\omega\right)^{-1}\Gamma_1\left(\omega+\langle\beta,\lambda\rangle+\frac{r}{2}z\middle|\omega\right)^{-1} \ ,
\end{aligned} \tag{5.19}$$

where $\mathcal{R}$ is a generic representation in any product of gauge or global symmetries and $\lambda$ is associated with a set of chemical potentials corresponding to these symmetries. As part of the global symmetries, we will always include an overall $\text{U}(1)_c$ that rotates the fundamental and anti-fundamental fields in the opposite way, as well as a $\text{U}(1)_d$

[61] In toric coordinates the metric on the ellipsoid is

$$ds^2 = \left(\omega_2^2\cos^2\theta+\omega_1^2\sin^2\theta\right)d\theta^2+\omega_2^2\sin^2\theta\,d\varphi_1^2+\omega_1^2\cos^2\theta\,d\varphi_2^2 \ ,$$

where $\theta\in[0,\frac{\pi}{2}]$ and $\phi_i\in[0,2\pi)$. The Killing vectors of the two U(1) isometries are $K_\pm = \pm\omega_2^{-1}\partial_{\varphi_1}+\omega_1^{-1}\partial_{\varphi_2}$. Details on the structure of supersymmetric field theories on three-dimensional curved manifolds can be found in [190] (see also [191, 192], where the special case of the ellipsoid is worked out in detail). The supersymmetric defects in this chapter are wrapping the orbits of $K_+$. These orbits are periodic when $\frac{\omega_2}{\omega_1}$ is a rational number. Otherwise, they do not close and instead fill out the $(\varphi_1,\varphi_2)$-torus densely. In what follows, we focus on the case of $\frac{\omega_2}{\omega_1}$ being rational (the round $\mathbb{S}^3$ has $\omega_1=\tilde{R}^{-1}=\omega_2$ and is such a case), and $\omega$ is related to the dimensional radius $\mathfrak{R}$ of the closed orbit of $K_+$ by the relation $\mathfrak{R}=(2\pi\omega)^{-1}\sqrt{\omega_1\omega_2}$.

that acts on the adjoint fields. In addition, we have a generic $\mathrm{U}(1)_R$ charge $r$ for chiral and Fermi multiplets, along with its chemical potential $z$. The $\Gamma_1(x|\omega)$ are Barnes 1-Gamma functions, defined in App. A.

Note that we can combine the Haar measure $\Delta^{\mathrm{Haar}}(\sigma)$ with the vector multiplet to obtain

$$\Delta^{\mathrm{Haar}}(\lambda) g_{\mathrm{vec}}^{\mathcal{N}=2}(\lambda) = \Gamma_1\left(\omega|\omega\right)^{-2\times\mathrm{rank}(\mathfrak{g})} \prod_{\beta\in\Delta} \Gamma_1\left(\langle\beta,\lambda\rangle|\omega\right)^{-1} \Gamma_1\left(\omega-\langle\beta,\lambda\rangle|\omega\right)^{-1} \ . \tag{5.20}$$

With these ingredients we can also easily build models with $\mathcal{N}=4$A supersymmetry. For this we simply need to use that a 1d $\mathcal{N}=4$ vector multiplet is a combination of an $\mathcal{N}=2$ vector multiplet and an adjoint $\mathcal{N}=2$ chiral multiplet with $r=2$. Similarly, an $\mathcal{N}=4$ chiral multiplet of charge $r$ comprises of an $\mathcal{N}=2$ chiral multiplet with charge $r$ and an $\mathcal{N}=2$ Fermi multiplet with charge $(r-2)$, in the same representations of the gauge or global symmetry algebras.

Combining this information with an identity given in the appendix, Eq. (A.13), we deduce that the contributions of $\mathcal{N}=4$A vector and chiral multiplets to the SQM index can be succinctly written as

$$\begin{aligned} \Delta^{\mathrm{Haar}}(\lambda) g_{\mathrm{vec}}^{\mathcal{N}=4}(\lambda) &= \left(\frac{\Gamma_1(z|\omega)\Gamma_1(\omega-z|\omega)}{\Gamma_1(\omega|\omega)^2}\right)^{\mathrm{rank}(\mathfrak{g})} \prod_{\beta\in\Delta} \Delta_h\left(\langle\beta,\lambda\rangle|\omega,z\right)^{-1} \ , \\ g_{\mathrm{chi}}^{\mathcal{N}=4}(\lambda,r) &= \prod_{\beta\in\mathcal{R}} \Delta_h\left(\langle\beta,\lambda\rangle+\frac{r}{2}z\Big|\omega,z\right) \ , \end{aligned} \tag{5.21}$$

with

$$\Delta_h(a|\omega,t) \equiv \frac{\Gamma_1(a|\omega)\Gamma_1(\omega-a|\omega)}{\Gamma_1(a+t|\omega)\Gamma_1(\omega-a-t|\omega)} = \frac{\sin(\frac{\pi(a+t)}{\omega})}{\sin(\frac{\pi a}{\omega})} \ . \tag{5.22}$$

Post deconstruction the above will lift to the elliptic-genus contributions of 2d surface defects with $(2,2)$ and $(4,4)$ supersymmetry respectively. As we will see shortly, these results will be dominated by a closely-related function, $\Delta_e$, which will be related to $\Delta_h$ by an identity analogous to the one relating $\Gamma_h$ and $\Gamma_e$ in Appendix A.

### 5.2.1 Indices of Defect Systems

We consider two examples in our analysis. Firstly is a $(4,4)$ defect theory in $\mathcal{N}=4$ sYM and second is a $(2,2)$ defect theory in $\mathcal{N}=2$ SQCD.

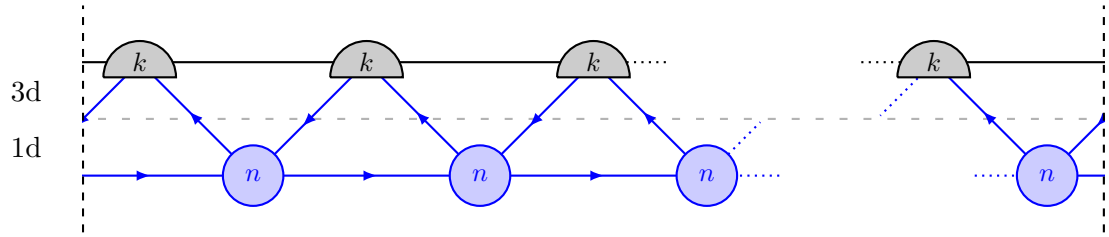


**Figure 9:** The 3d $\mathcal{N}=4$ circular quiver theory in the presence of 1d $\mathcal{N}=4$ defects. Black links and nodes are 3d $\mathcal{N}=4$ hypermultiplets and 3d $\mathcal{N}=4$ vector multiplets respectively of the bulk theory. The blue oriented links and nodes are 1d $\mathcal{N}=4$ chiral multiplets with assigned R charge $r=0$ and 1d $\mathcal{N}=4$ vector multiplets respectively for the defect theory. The diagonal 1d chiral multiplets have been assigned $U(1)_c$ charge $q_c=1$, while the horizontal ones $\mathrm{U}(1)_d$ charge $q_d=1$.

### 2d $\mathcal{N}=(4,4)$ defects in 4d $\mathcal{N}=4$ sYM

For this example, the starting point is an orbifold of a 3d $\mathcal{N}=8$ theory in the presence of a 1d $\mathcal{N}=8$ defect. In the language of the brane system of Tab. 9, the defects are described by $nN$ D1 branes suspended between the $kN$ D3s and an NS5 in the $x^6$ direction. The $x^3$ direction is compactified and the branes are in the presence of the $A_{N-1}$ orbifold singularity. The quiver-gauge theory emerging at low energies is given by Fig. 9 and involves a 3d $\mathcal{N}=4$ bulk quiver with $\mathrm{U}(k)$ gauge group nodes coupled to $\mathcal{N}=4$ 1d defects with $\mathrm{U}(n)$ groups.[62]

The partition function of the combined 3d-1d system can be split into two parts as per

$$\mathcal{Z}_{\mathrm{3d-1d}}=\prod_{\alpha}\frac{1}{k!}\int\prod_{b=1}^{k}\mathrm{d}\sigma_b^{(\alpha)}\mathcal{Z}_{\mathrm{3d}}(\sigma_b^{(\alpha)})\mathcal{Z}_{\mathrm{1d}}(\sigma_b^{(\alpha)})\,. \tag{5.23}$$

The bulk partition function contains the ingredients discussed in Sec. 5.1.2 and for the quiver of Fig. 9 is given by

$$\begin{aligned}\mathcal{Z}_{\mathrm{3d}}(\sigma_b^{(\alpha)})=&\prod_{\alpha}\widehat{\Gamma}_h\left(0|\omega_1,\omega_2\right)^{-k}\prod_{b\neq c}^{k}\Gamma_h\left(\sigma_b^{(\alpha)}-\sigma_c^{(\alpha)}|\omega_1,\omega_2\right)^{-1}\\ &\times\prod_{b,c}^{k}\Gamma_h\left(\frac{\omega_+}{2}-\sigma_b^{(\alpha+1)}+\sigma_c^{(\alpha)}|\omega_1,\omega_2\right)\Gamma_h\left(\frac{\omega_+}{2}+\sigma_b^{(\alpha+1)}-\sigma_c^{(\alpha)}|\omega_1,\omega_2\right)\,.\end{aligned} \tag{5.24}$$

The defect contribution can be evaluated from the ingredients of Sec. 5.2 and is in

[62] A class of closely-related systems with the same amount of supersymmetry appear in [194]. Our brane configurations before deconstruction are related to those appearing in that reference by T duality and the low-energy quiver-gauge theories by dimensional reduction.

turn given by

$$\mathcal{Z}_{\rm 1d}(\sigma_b^{(\alpha)}) = \prod_\alpha \frac{1}{n!}\left(\frac{\Gamma_1(z|\omega)\Gamma_1(\omega-z|\omega)}{\Gamma_1(\omega|\omega)^2}\right)^k \oint \prod_{j=1}^n \mathrm{d}u_j^{(\alpha)} \frac{\prod_{i,j}^n \Delta_h\left(u_i^{(\alpha+1)} - u_j^{(\alpha)} + \kappa|\omega,z\right)}{\prod_{i\neq j}^n \Delta_h\left(u_i^{(\alpha)} - u_j^{(\alpha)}|\omega,z\right)} \times \prod_{i=1}^n\prod_{b=1}^k \Delta_h\left(u_j^{(\alpha)} - \sigma_b^{(\alpha)} + l|\omega,z\right)\Delta_h\left(\sigma_b^{(\alpha)} - u_j^{(\alpha+1)} + l|\omega,z\right) \ . \tag{5.25}$$

Note that this involves integrating the 1d gauge-group parameters $u_j^{(\alpha)}$ over some contour. These integrals can be eventually performed using the Jeffrey–Kirwan residue prescription—as e.g. in [174, 195]—although we will not do so in this chapter.[63] Furthermore, for each defect node there is a $\mathrm{U}(1)_c$ symmetry that rotates the bifundamental chiral multiplets connecting to the bulk theory, with associated chemical potential $l$, as well as a different $\mathrm{U}(1)_d$ symmetry that acts on the bifundamental chiral multiplets between defect gauge nodes—associated with a chemical potential $\kappa$. We have chosen these charges appropriately, $q_c = 1$ and $q_d = 1$, so as to deconstruct a superconformal 4d-2d system.

The exact-deconstruction procedure can now be applied to the 3d piece as in Sec. 5.1.2. It is implemented in a similar fashion for the 1d piece, namely, we identify the parameters $u_i^{(\alpha)} \to u_i$ and shift all the arguments of the functions appearing in (5.25) by $m_\alpha = i\frac{2\pi\alpha}{R}$. Upon performing this operation $\mathcal{Z}_{\rm 3d-1d}$ becomes

$$\mathcal{Z}^{\rm Dec}_{\rm 3d-1d} = \frac{1}{k!}\oint \prod_b^k \frac{\mathrm{d}v_b}{2\pi i v_b} \mathcal{Z}^{\rm Dec}_{\rm 3d}(v)\mathcal{Z}^{\rm Dec}_{\rm 1d}(v) \ , \tag{5.26}$$

with

$$\mathcal{Z}^{\rm Dec}_{\rm 3d}(v) = (\mathfrak{p};\mathfrak{p})^k(\mathfrak{q};\mathfrak{q})^k \frac{\prod_{b,c}^k \Gamma_e(v_b v_c^{-1}(\mathfrak{p}\mathfrak{q})^{\frac{1}{4}}|\mathfrak{p},\mathfrak{q})^2}{\prod_{b\neq c}^k \Gamma_e\left(v_b v_c^{-1}\,|\,\mathfrak{p},\mathfrak{q}\right)} \ , \tag{5.27}$$

which agrees with the index for $\mathcal{N}=4$ SYM as found in [39].[64] In turn, the defect part becomes

$$\mathcal{Z}^{\rm Dec}_{\rm 1d}(v) = \left(\frac{(q;q)^2}{\theta(y^{-1}|q)}\right)^k \oint \prod_j^n \frac{\mathrm{d}\mathfrak{u}_j}{2\pi i \mathfrak{u}_j} \frac{\prod_{i,j}^n \Delta_e\left(d\,\mathfrak{u}_i\mathfrak{u}_j^{-1}|q,y^{-1}\right)}{\prod_{i\neq j}^n \Delta_e\left(\mathfrak{u}_i\mathfrak{u}_j^{-1}|q,y^{-1}\right)}$$

[63] The Jeffrey–Kirwan residue prescription is sensitive to the sign of a Fayet–Iliopoulos (FI) parameter in the SQM. We will implicitly assume that all the 1d gauge theories that appear in this chapter are deformed by an FI term of definite sign.

[64] This can be seen if in the notation of [39] one considers the limit $w \to t^{\frac{1}{2}}$ and by mapping $v \to t^{-\frac{1}{2}}$, with $t = (\mathfrak{p}\mathfrak{q})^{\frac{1}{6}}$ and $y = \left(\mathfrak{p}\mathfrak{q}^{-1}\right)^{\frac{1}{2}}$, after the inclusion of the Haar measure.

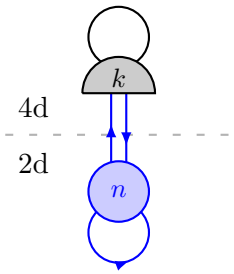


**Figure 10:** The 4d $\mathcal{N}=4$ sYM theory in the presence of a 2d $\mathcal{N}=(4,4)$ surface defect. Black unoriented links and nodes are 4d $\mathcal{N}=2$ hypermultiplets and 4d $\mathcal{N}=2$ vector multiplets respectively of the bulk theory. The blue oriented links and nodes are 2d $\mathcal{N}=(2,2)$ chiral multiplets and 2d $\mathcal{N}=(2,2)$ vector multiplets respectively for the defect theory.

$$\times \prod_{j}^{n} \prod_{b}^{k} \Delta_e\left(\mathfrak{u}_j v_b^{-1} c|q,y^{-1}\right) \Delta_e\left(\mathfrak{u}_j^{-1} v_b\, c|q,y^{-1}\right) \ , \tag{5.28}$$

with $q=e^{-R\omega}$, $y=e^{-Rz}$, $c=e^{-Rl}$ and $d=e^{-R\kappa}$. Here we made use of the identity

$$\Delta_e(A|\Omega,T) = \prod_{\alpha=-\infty}^{\infty} \Delta_h\left(a+i\frac{2\pi\alpha}{R}\Big|\omega,t\right) \ , \tag{5.29}$$

where $A=e^{-Ra}$, $\Omega=e^{-R\omega}$, $T=e^{-Rt}$. The function $\Delta_e(A|\Omega,T)$ is defined as the ratio of theta functions

$$\Delta_e(A|\Omega,T) \equiv \frac{\theta(AT;\Omega)}{\theta(A;\Omega)} \ . \tag{5.30}$$

We would like to identify the above result as the index of a 2d $(4,4)$ theory coupled to the bulk 4d $\mathcal{N}=4$ sYM theory (see Fig. 10). For that purpose it is useful to recall some facts regarding elliptic genera in two-dimensional theories.[65] On the one hand, when considered as a partition function on $\mathbb{T}^2$, e.g. such as in the supersymmetric-localisation calculations of [195,196], the elliptic genus involves tracing over states in the R-R sector of the 2d (2,2) theory; these theories need not necessarily be superconformal. On the other hand, for superconformal theories, the state-operator map exchanges R and NS boundary conditions and therefore when viewed as a generating function for operator counting it is more appropriately defined by tracing over the NS-NS sector, e.g. such as in the superconformal index calculations of [172, 176].

The exact-deconstruction procedure in general takes an $\mathcal{N}=$ 2B SQM partition function on $\mathbb{S}^1$ and lifts it to a (2,2) partition function on $\mathbb{T}^2$. As such, one would expect it to reproduce the R-R elliptic genus. Indeed, in (5.28) one recognises the elliptic-genus contributions attributed to a 2d (2,2) vector, an adjoint chiral (first line)

[65] For a summary of the relevant details we refer the reader to [176].

and two (anti)fundamental chirals (second line) as given in [195]. When combined with the bulk piece they make up the contributions attributed to the 4d-2d system summarised by the quiver of Fig. 10.

The R-R and NS-NS elliptic genera can be related by spectral flow through the relation

$$\mathcal{G}_{\mathrm{R-R}}(q,y) = y^{c/6}\mathcal{G}_{\mathrm{NS-NS}}(q,q^{\frac{1}{2}}y)\ . \tag{5.31}$$

Implementing this dictionary in (5.28) gives rise, up to an overall $c$-dependent coefficient, to

$$\begin{aligned}\widehat{\mathcal{Z}}^{\mathrm{Dec}}_{\mathrm{1d}}(v) = &\left(\frac{(q;q)^2}{\theta(q^{\frac{1}{2}}y^{-1}|q)}\right)^k \oint\prod_j^n \frac{\mathrm{d}u_j}{2\pi i u_j}\frac{\prod_{i,j}^n \Delta_e\left(d\,u_i u_j^{-1}|q,q^{\frac{1}{2}}y^{-1}\right)}{\prod_{i\neq j}^n \Delta_e\left(u_i u_j^{-1}|q,q^{\frac{1}{2}}y^{-1}\right)}\\ &\times\prod_j^n\prod_b^k \Delta_e\left(u_j v_b^{-1}c|q,q^{\frac{1}{2}}y^{-1}\right)\Delta_e\left(u_j^{-1}v_b\,c|q,q^{\frac{1}{2}}y^{-1}\right)\ .\end{aligned} \tag{5.32}$$

The identifications between defect and bulk fugacities

$$q=\mathfrak{q}\ ,\qquad y=\mathfrak{p}^{-\frac{1}{2}}\ ,\qquad c=\mathfrak{p}^{-\frac{3}{8}}\mathfrak{q}^{\frac{1}{8}}\ ,\qquad d=\mathfrak{p}^{-1}\ , \tag{5.33}$$

which was discussed in [4], lead to the final result

$$\begin{aligned}\widehat{\mathcal{Z}}^{\mathrm{Dec}}_{\mathrm{1d}}(v) = &\left(\frac{(\mathfrak{q};\mathfrak{q})^2}{\theta(\sqrt{\mathfrak{p}\mathfrak{q}}|\mathfrak{q})}\right)^k \oint\prod_j^n \frac{\mathrm{d}u_j}{2\pi i u_j}\frac{\prod_{i,j}^n \Delta_e\left(\mathfrak{p}^{-1}\,u_i u_j^{-1}|\mathfrak{q},\sqrt{\mathfrak{p}\mathfrak{q}}\right)}{\prod_{i\neq j}^n \Delta_e\left(u_i u_j^{-1}|\mathfrak{q},\sqrt{\mathfrak{p}\mathfrak{q}}\right)}\\ &\times\prod_j^n\prod_b^k \Delta_e\left(u_j v_b^{-1}\mathfrak{p}^{-\frac{3}{8}}\mathfrak{q}^{\frac{1}{8}}|\mathfrak{q},\sqrt{\mathfrak{p}\mathfrak{q}}\right)\Delta_e\left(u_j^{-1}v_b\,\mathfrak{p}^{-\frac{3}{8}}\mathfrak{q}^{\frac{1}{8}}|\mathfrak{q},\sqrt{\mathfrak{p}\mathfrak{q}}\right)\ .\end{aligned} \tag{5.34}$$

This is precisely the answer for the $\mathcal{N}=1$ limit ($\mathfrak{t}\to\sqrt{\mathfrak{p}\mathfrak{q}}$) of the $\mathcal{N}=2$ superconformal index of the 4d-2d system of Fig. 10, as calculated in [172]. Once again, one needs to perform the 2d gauge integrals using the Jeffrey–Kirwan residue prescription, which can be carried out explicitly as in [172, 195].

### 2d $\mathcal{N}=(2,2)$ defects in 4d $\mathcal{N}=2$ SQCD

Our next example is more general in that it involves half of the supersymmetry of the previous subsection and non-trivial flavour symmetries. The starting point is a brane system consisting of $kN$ D3s stretched between two NS5 branes along the interval $L_3$, with $N_1N$ semi-infinite D3s extending to the left and $N_2N$ to the right. Once again, there are also $nN$ D1s suspended between the rightmost NS5 and an additional NS5 in the $x^6$ direction and the whole system is probing the $A_{N-1}$ orbifold singularity. The

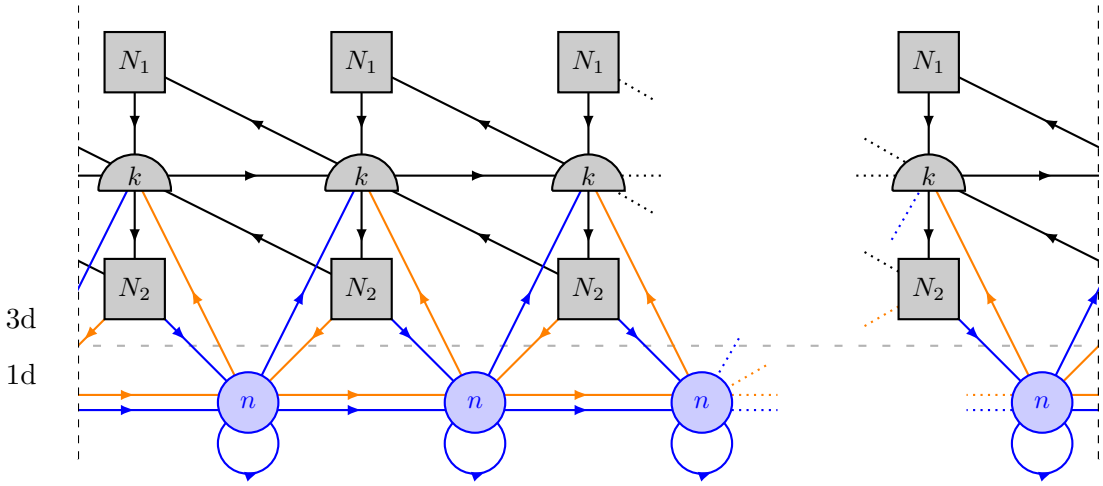


**Figure 11:** The 3d $\mathcal{N}=2$ circular-quiver theory in the presence of 1d $\mathcal{N}=2$ defects. Black oriented links and nodes are 3d $\mathcal{N}=2$ chiral multiplets and 3d $\mathcal{N}=2$ vector multiplets respectively of the bulk theory. The blue oriented links and nodes are 1d $\mathcal{N}=2$ chiral multiplets with R charge $r=0$ and 1d $\mathcal{N}=2$ vector multiplets respectively for the defect theory. The orange oriented links are $\mathcal{N}=2$ Fermi multiplets for the defect theory. The diagonal 1d chiral multiplets have been assigned $\mathrm{U}(1)_c$ charge $q_c=1$, while the horizontal ones $\mathrm{U}(1)_d$ charge $q_d=1$.

corresponding 3d-1d quiver emerging at low energies is depicted in Fig. 11.[66]

From the 1d point of view, the fundamental/antifundamental chiral and Fermi multiplets have unit charge under the $\mathrm{U}(1)_c$ symmetry. The adjoint chiral multiplets and bifundamental Fermi multiplets have unit charge under the $\mathrm{U}(1)_d$ symmetry.

As before, the $\mathbb{S}^3_{\omega_1,\omega_2}$ partition function can be split into 3d and 1d contributions:

$$\mathcal{Z}_{\text{3d}-\text{1d}} = \prod_{\alpha} \frac{1}{k!} \int \prod_{b=1}^{k} \mathrm{d}\sigma_b^{(\alpha)} \mathcal{Z}_{\text{3d}}(\sigma_b^{(\alpha)}) \mathcal{Z}_{\text{1d}}(\sigma_b^{(\alpha)}) \,. \tag{5.35}$$

The 3d part is

$$\begin{aligned}
\mathcal{Z}_{\text{3d}}(\sigma^{(\alpha)}) = &\prod_{\alpha} \Delta^{\text{Haar}}\left(\sigma^{(\alpha)}\right) \prod_{b,c=1}^{k} \frac{\Gamma_h\left(\omega_+ + \sigma_b^{(\alpha)} - \sigma_c^{(\alpha+1)}\right)}{\widehat{\Gamma}_h\left(\sigma_b^{(\alpha)} - \sigma_c^{(\alpha)}\right)} \\
&\times \prod_{b=1}^{k} \prod_{j=1}^{N_1} \Gamma_h\left(\frac{1}{2}\omega_+ - \mu_j^{(\alpha)} + \sigma_b^{(\alpha)}\right) \Gamma_h\left(\frac{1}{2}\omega_+ - \sigma_b^{(\alpha+1)} + \mu_j^{(\alpha)}\right) \\
&\times \prod_{b=1}^{k} \prod_{m=1}^{N_2} \Gamma_h\left(\frac{1}{2}\omega_+ - \sigma_b^{(\alpha+1)} + \nu_m^{(\alpha+1)}\right) \Gamma_h\left(\frac{1}{2}\omega_+ - \nu_m^{(\alpha+1)} + \sigma_b^{(\alpha)}\right) \,,
\end{aligned} \tag{5.36}$$

[66] There also exists a dual UV description of the same vortex loop, obtained by having the D1s end on the leftmost NS5 along $x^3$. This leads to a quiver with $N_1$ and $N_2$ exchanged and the opposite sign for the 1d FI term compared to the system we are using. This sign difference is crucial for recovering the same partition function from both configurations. For a detailed account see [174].

where we suppressed the dependence on $\omega_1$ and $\omega_2$. The $\mu_j^{(\alpha)}, \nu_m^{(\alpha)}$ are new chemical potentials associated with the global symmetries, while the other chemical potentials were defined in Sec. 5.2.1. The 1d part is in turn

$$\begin{aligned}
&\mathcal{Z}_{\rm 1d}(\sigma^{(\alpha)}) = \\
&\oint \prod_\alpha \frac{1}{n!}\Delta^{\rm Haar}\left(u^{(\alpha)}\right)\prod_j \mathrm{d}u_j^{(\alpha)} \prod_{i,j=1}^n \frac{\Gamma_1\left(u_i^{(\alpha)}-u_j^{(\alpha+1)}\right)\Gamma_1\left(\omega-u_i^{(\alpha)}+u_j^{(\alpha+1)}\right)}{\widehat{\Gamma}_1\left(u_i^{(\alpha)}-u_j^{(\alpha)}\right)\Gamma_1\left(\omega+u_i^{(\alpha)}-u_j^{(\alpha)}\right)} \\
&\times \prod_{i,j=1}^n \frac{\Gamma_1\left(u_i^{(\alpha)}-u_j^{(\alpha)}+\kappa\right)\Gamma_1\left(\omega-u_i^{(\alpha)}+u_j^{(\alpha)}-\kappa\right)}{\Gamma_1\left(-u_i^{(\alpha)}+u_j^{(\alpha+1)}+z-\kappa\right)\Gamma_1\left(\omega+u_i^{(\alpha)}-u_j^{(\alpha+1)}-z+\kappa\right)} \\
&\times \prod_{i=1}^n\prod_{b=1}^k \frac{\Gamma_1\left(u_i^{(\alpha)}-\sigma_b^{(\alpha+1)}+l\right)\Gamma_1\left(\omega-u_i^{(\alpha)}+\sigma_b^{(\alpha+1)}-l\right)}{\Gamma_1\left(-u_i^{(\alpha)}+\sigma_b^{(\alpha)}+z-l\right)\Gamma_1\left(\omega+u_i^{(\alpha)}-\sigma_b^{(\alpha)}-z+l\right)} \\
&\times \prod_{i=1}^n\prod_{m=1}^{N_2} \frac{\Gamma_1\left(-u_i^{(\alpha)}+\nu_m^{(\alpha)}+l\right)\Gamma_1\left(\omega+u_i^{(\alpha)}-\nu_m^{(\alpha)}-l\right)}{\Gamma_1\left(u_i^{(\alpha)}-\nu_m^{(\alpha+1)}+z-l\right)\Gamma_1\left(\omega-u_i^{(\alpha)}+\nu_m^{(\alpha+1)}-z+l\right)} \ ,
\end{aligned} \tag{5.37}$$

where again we suppressed the dependence on $\omega$ for brevity. Once again, in order to implement dimensional deconstruction at the level of partition functions, we break the relevant groups involved to a diagonal subgroup and shift the arguments of the Gamma functions, which results in a product over the KK mass parameters, $m_\alpha = i\frac{2\pi\alpha}{R}$.

The resultant expression is much simpler and when expressed in terms of fugacities reads

$$\mathcal{Z}^{\rm Dec}_{\rm 3d-1d} = \frac{1}{k!}\oint \prod_b \frac{\mathrm{d}v_b}{2\pi i v_b}\mathcal{Z}^{\rm Dec}_{\rm 3d}(v)\mathcal{Z}^{\rm Dec}_{\rm 1d}(v) \ , \tag{5.38}$$

with

$$\begin{aligned}
\mathcal{Z}^{\rm Dec}_{\rm 3d}(v) = (\mathfrak{p};\mathfrak{p})^k(\mathfrak{q};\mathfrak{q})^k \prod_{b\neq c}\Gamma_e\left(v_b v_c^{-1}\Big|\mathfrak{p},\mathfrak{q}\right)^{-1}\prod_{b=1}^k\prod_{j=1}^{N_1}\Gamma_e\left((\mathfrak{pq})^{\frac{1}{4}}(v_b s_j^{-1})^{\pm}\Big|\mathfrak{p},\mathfrak{q}\right) \\
\times\prod_{b=1}^k\prod_{m=1}^{N_2}\Gamma_e\left((\mathfrak{pq})^{\frac{1}{4}}(v_b t_m^{-1})^{\pm}\Big|\mathfrak{p},\mathfrak{q}\right) \ ,
\end{aligned} \tag{5.39}$$

where $s_j = e^{R\mu_j}$ and $t_m = e^{R\nu_m}$. The defect piece becomes just

$$\mathcal{Z}^{\rm Dec}_{\rm 1d}(v) = \left(\frac{(q;q)^2}{\theta(y^{-1}|q)}\right)^k \oint \prod_j^n \frac{\mathrm{d}\mathfrak{u}_j}{2\pi i\mathfrak{u}_j}\frac{\prod_{i,j}\Delta_e\left(d\,\mathfrak{u}_i\mathfrak{u}_j^{-1}|q,y^{-1}\right)}{\prod_{i\neq j}\Delta_e\left(\mathfrak{u}_i\mathfrak{u}_j^{-1}|q,y^{-1}\right)}$$

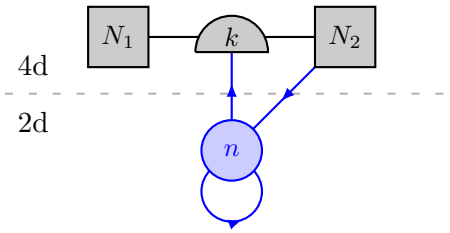


**Figure 12:** The 4d $\mathcal{N}=2$ SYM theory in the presence of a 2d $\mathcal{N}=(2,2)$ surface defect. Black unoriented links and semi-circular nodes are 4d $\mathcal{N}=2$ hypermultiplets and 4d $\mathcal{N}=2$ vector multiplets respectively of the bulk theory. The black squares denote 4d flavour groups. The blue oriented links and nodes are 2d $\mathcal{N}=(2,2)$ chiral multiplets and 2d $\mathcal{N}=(2,2)$ vector multiplets, respectively, for the defect theory.

$$\times \prod_{j=1}^{n}\prod_{b=1}^{k}\Delta_e\left(\mathfrak{u}_j v_b^{-1} c\,|q,y^{-1}\right)\prod_{m=1}^{N_2}\Delta_e\left(\mathfrak{u}_j^{-1} t_m\, c\,|q,y^{-1}\right)\,, \tag{5.40}$$

which upon making use of the identifications that realise the embedding of the defect into the bulk (5.33) leads to

$$\begin{aligned}\mathcal{Z}_{\rm 1d}^{\rm Dec}(z) = &\left(\frac{(\mathfrak{q};\mathfrak{q})^2}{\theta(\mathfrak{p}^{\frac{1}{2}}|\mathfrak{q})}\right)^k \oint\prod_{j}^{n}\frac{\mathrm{d}\mathfrak{u}_j}{2\pi i\mathfrak{u}_j}\frac{\prod_{i,j}\Delta_e\left(\mathfrak{p}^{-1}\,\mathfrak{u}_i\mathfrak{u}_j^{-1}|\mathfrak{q},\mathfrak{p}^{\frac{1}{2}}\right)}{\prod_{i\neq j}\Delta_e\left(\mathfrak{u}_i\mathfrak{u}_j^{-1}|\mathfrak{q},\mathfrak{p}^{\frac{1}{2}}\right)}\\ &\times\prod_{j=1}^{n}\prod_{b=1}^{k}\Delta_e\left(\mathfrak{u}_j v_b^{-1}\mathfrak{p}^{-\frac{3}{8}}\mathfrak{q}^{\frac{1}{8}}\,|\mathfrak{q},\mathfrak{p}^{\frac{1}{2}}\right)\prod_{m=1}^{N_2}\Delta_e\left(\mathfrak{u}_j^{-1}t_m\,\mathfrak{p}^{-\frac{3}{8}}\mathfrak{q}^{\frac{1}{8}}\,|\mathfrak{q},\mathfrak{p}^{\frac{1}{2}}\right)\,.\end{aligned} \tag{5.41}$$

This is the combined $\mathbb{S}^3_{\omega_1,\omega_2}\times S^1_{\widehat{R}}$ partition function for the quiver depicted in Fig. 12 in the R-R sector for the 1d defect partition function. In the case of $N_1=N_2=k$, one can once again implement the spectral flow argument (5.31) to recover the corresponding index result in [172].

We close this discussion by noting that, although we have examined two very specific examples involving vortex loops, one can clearly apply the method of exact deconstruction to more general setups. These can be engineered using branes through various combinations of the ingredients from Tab. 9, including combinations of NS5 and NS5′ branes at different points along the $x^6$ direction connected with different numbers of D1s. As a result, one can obtain e.g. all examples of [174] placed on an orbifold singularity, which will result in product defect gauge groups, additional matter at each quiver node and so on. The implementation of exact deconstruction to these theories is straightforward.

## 5.3 4d Surface Defects from 3d Wilson Loops

In Sec. 5.2 we demonstrated how to deconstruct codimension-two surface defects in 4d $\mathcal{N}=4/\mathcal{N}=2$ theories that preserve non-chiral 2d $\mathcal{N}=(4,4)/\mathcal{N}=(2,2)$ supersymmetry from vortex loops in 3d $\mathcal{N}=4/\ \mathcal{N}=2$ theories. The vortex loops in three dimensions were defined by coupling 1d $\mathcal{N}=4/\mathcal{N}=2$ SQM to the 3d bulk. Similarly, the deconstructed surface defects were defined by coupling 2d $\mathcal{N}=(4,4)/\mathcal{N}=(2,2)$ theories to the 4d bulk.

Another prominent, and perhaps more common, class of line defects in 3d theories arises from Wilson loops. In 3d $\mathcal{N}=4$ theories $\frac{1}{2}$-BPS Wilson-loop operators, which will be the focus of our discussion in the rest of this section, are given by path-ordered traces of the form

$$W_{\mathcal{R}} = \mathrm{Tr}_{\mathcal{R}} P \exp \oint i \left( A_\mu \dot{x}^\mu + \sqrt{-\dot{x}^2}\sigma \right) d\tau \ , \tag{5.42}$$

In this formula $\sigma$ is the real scalar field in the $\mathcal{N}=2$ vector multiplet, which is part of the 3d $\mathcal{N}=4$ vector multiplet. As usual, Wilson loops are labelled by a gauge-group representation $\mathcal{R}$. For concreteness, in what follows we will focus on the fundamental and antisymmetric representations of the unitary gauge group (namely, representations labelled by Young tableaux with a single column). Analogous statements will apply to more general representations. As a one-dimensional defect, the operator (5.42) preserves the 1d $\mathcal{N}=4\mathrm{B}$ supersymmetry that arises from the dimensional reduction of the *chiral* 2d $\mathcal{N}=(4,0)$ supersymmetry. This should be compared against the 2d $\mathcal{N}=(2,2)$ supersymmetry associated by dimensional reduction with the vortex loops.

In supersymmetric localisation the insertion of a Wilson-loop operator (5.42) in the round $\mathbb{S}^3$ partition function[67] is captured by the introduction of a factor

$$\mathrm{Tr}_{\mathcal{R}} \left( e^{2\pi\sigma} \right) = \sum_{\beta \in \mathcal{R}} e^{2\pi\langle \beta, \sigma \rangle} \tag{5.43}$$

in the resultant matrix integral [53, 55]. On the RHS of this expression the sum is performed over all the weights $\beta$ of the representation $\mathcal{R}$.

The question of whether one can implement exact deconstruction with 3d Wilson-loop insertions is an obvious one. However, if there exists a well-defined procedure for lifting 3d Wilson loops in some representation $\mathcal{R}$, what kind of defect does one expect to obtain in four dimensions? The natural answer seems to be a codimension-two defect with chiral supersymmetry labelled by the same representation.

The literature on surface defects with 2d $\mathcal{N}=(4,0)$ supersymmetry is relatively-

[67] For the moment we consider the case of a round $\mathbb{S}^3$. We will soon generalise to squashed three-spheres with arbitrary squashing.

limited.[68] An early discussion of surface defects with 2d $\mathcal{N} = (8,0)$ supersymmetry appears in [199] and is based on the D3-D7 intersection in string theory; see [200] for related work. The surface defects in [199] are formulated by integrating out 2d chiral fermions. Notice that a similar approach to Wilson loops in 4d $\mathcal{N} = 4$ SYM was employed in [201, 202]. In that case the result of integrating out the chiral fermions is not a single Wilson loop, but rather a sum over Wilson loops in different representations; this is a point which we will come back to more explicitly in a moment. Here we stress that the codimension-two operators obtained in this manner are formulated in terms of a Wess–Zumino–Witten action supported on a surface, with no explicit reference to individual representations [199].

Applying deconstruction to 3d Wilson loops is therefore an interesting direction that has the potential to produce novel results about chiral surface operators in 4d theories. In this section, we take the first steps towards this direction by studying deconstruction at the level of $\mathbb{S}^3_{\omega_1,\omega_2}$ partition functions with Wilson loop insertions.[69]

The strategy is straightforward and begins with a 3d circular quiver-gauge theory with a Wilson-loop insertion for each node. That in turn introduces a product of insertions of the type (5.43) into the $\mathbb{S}^3_{\omega_1,\omega_2}$ partition function. Then, one has to implement the deconstruction procedure and evaluate the result in the appropriate limit. We have previously argued that in the context of $\mathbb{S}^3_{\omega_1,\omega_2}$ partition functions the main effect of the exact-deconstruction procedure is to produce a shift in the argument of various Gamma functions. This encoded the reorganisation of the 3d spectrum into the KK modes of a 4d theory on a circle. However, from that point of view it is not immediately clear how we should extend the prescription to treat insertions of the type (5.43). To handle this issue we instead propose the following approach.

First, it is convenient to take a step back and reformulate 3d Wilson loops in terms of a gauged 1d $\mathcal{N} = 2$ Fermi multiplet in analogy with [201]—see [174] for a related discussion in three dimensions.[70] For starters, consider a gauge theory with a single U($k$) node. We insert a one-dimensional defect described by a gauged $\mathcal{N} = 2$ Fermi multiplet in the fundamental representation of the bulk U($k$) gauge group. This can be engineered using the ingredients of Tab. 10 in terms of $k$ D3s suspended between

[68] We note that the generating function for a class of BPS co-dimension two defects on $\mathbb{S}^3 \times \mathbb{S}^1$ with $(2,0)$ supersymmetry was recently obtained from the affinisation of the $\mathbb{S}^3$ partition function including Wilson-loop insertions, followed by a projection with affine characters [197, 198]. This procedure produces results that are very similar to the ones given in this section through deconstruction. It would be very interesting to further explore the relationship between the two prescriptions.

[69] Chiral surface defects in 4d $\mathcal{N} = 2$ or $\mathcal{N} = 4$ SYM theories can also be obtained from the 6d $\mathcal{N} = (2,0)$ theory by dimensionally reducing codimension-two or codimension-four defects. Related brane constructions of such defects appear, for example, in [203, 204]. These constructions produce surface defects that are naturally labelled by representations of the gauge group.

[70] The 3d $\mathcal{N} = 2$ Fermi multiplet is also a representation of the 3d $\mathcal{N} = 4$ supersymmetry algebra, and in that context it is sometimes called a half-Fermi multiplet; see e.g. the appendix of [205] for a 2d version.

two NS5s along $x^3$ and a single D5′ separated by some distance in the $x^7$ direction. The fermion $\chi$ in the Fermi multiplet emerges from the quantisation of open strings connecting the D3s and D5′ and has the action

$$\int dt\, \chi^\dagger \Big[ i\partial_t + (A_0 + \frac{1}{\sqrt{\omega_1\omega_2}}\sigma - \frac{1}{\sqrt{\omega_1\omega_2}} im) \Big] \chi \,, \tag{5.44}$$

where $A_0$ is the temporal component of the bulk gauge field, $\sigma$ is the bulk Coulomb-branch parameter and $m$ is a mass parameter that can be viewed as the vev of a background U(1) gauge field, corresponding to the frozen dynamics of the single D5′. Integrating out this fermion leads to the insertion of a $\frac{1}{2}$-BPS Wilson loop [174, 201]. Let us verify this statement at the level of the $\mathbb{S}^3_{\omega_1,\omega_2}$ partition function. As in the vortex-loop case, we will take the Wilson-loop defect to wrap the Hopf fibre of the ellipsoid.

Up to an overall regularisation-dependent factor, the contribution of such a Fermi multiplet (5.19) can be re-expressed as

$$\begin{aligned} g^{\mathcal{N}=2}_{\text{fer}}(\sigma, m) &= \prod_{b=1}^{k} \sin \pi(i\omega^{-1}\sigma_b + \omega^{-1} m) \propto \prod_{b=1}^{k} \left( e^{-\pi\omega^{-1}\sigma_b + i\pi\omega^{-1} m} - e^{\pi\omega^{-1}\sigma_b - i\pi\omega^{-1} m} \right) \\ &= e^{i\pi\omega^{-1} k m} e^{-\pi\omega^{-1}\sum_b \sigma_b} \prod_{b=1}^{k} \left( 1 - e^{-2\pi i\omega^{-1} m} e^{2\pi\omega^{-1}\sigma_b} \right) \,, \end{aligned} \tag{5.45}$$

The factor $e^{-\pi\omega^{-1}\sum_b \sigma_b}$ is related to a global anomaly for $\mathrm{U}(1) \subset \mathrm{U}(k)$ and is also noted in [174], where it is argued that it is cancelled by a bare supersymmetric Chern-Simons term in the bulk at level $\kappa = \frac{1}{2}$. Since

$$\prod_{b=1}^{k} \left( 1 - e^{-2\pi i\omega^{-1} m} e^{2\pi\omega^{-1}\sigma_b} \right) = \sum_{\rho=0}^{k} (-1)^\rho e^{-2\pi i\omega^{-1} m \rho} \sum_{\beta \in \mathcal{A}_\rho} e^{2\pi\omega^{-1}\langle \beta, \sigma \rangle} \tag{5.46}$$

we recover from (5.45) the expansion of the Fermi-multiplet contribution as a sum over all Wilson loops in the anti-symmetric representations $\mathcal{A}_\rho$. From this result, the contribution of the $\rho$-antisymmetric representation can be recovered by noticing that it is weighted by the $\rho$-th power of the factor $\mu = e^{-2\pi i\omega^{-1} m}$ and hence isolated by evaluating the residue

$$\frac{1}{2\pi i} \oint d\mu \mu^{-\rho-1} g^{\mathcal{N}=2}_{\text{fer}}(\sigma, \mu) \,. \tag{5.47}$$

This observation motivates the following three-step approach for extending exact deconstruction to 3d Wilson loops:

(i) Add a 1d defect described by a Fermi multiplet for each node of the 3d quiver.

(ii) Use this to deconstruct a 4d theory with a chiral 2d surface defect described by a 2d Fermi multiplet.

(iii) Isolate the contributions associated with different powers of $\mu$.

The last point that needs to be addressed is whether the final step in the above prescription truly defines quantities that correspond to $k$ independent objects in 2d. The latter could in turn be interpreted as chiral surface operators labelled by antisymmetric representations of the four-dimensional bulk gauge group U($k$). To address this matter let us examine in detail the results obtained by this prescription.

For the first step, and as in any of the constructions of the previous sections our starting point is a 3d $N$-noded quiver, with each node labelled by $\alpha = \lfloor -\frac{N}{2} \rfloor + 1, \ldots, \lfloor \frac{N}{2} \rfloor$. The specific details of the quiver are not important—we will only assume that it is a 3d $\mathcal{N}=2$ or $\mathcal{N}=4$ quiver that deconstructs to a 4d $\mathcal{N}=2$ or $\mathcal{N}=4$ gauge theory on a circle. For concreteness, one can consider engineering such an example by taking the brane system leading to (5.44) and placing it on the orbifold singularity of Tab. 10. At low energies, each node of the resultant quiver includes a 1d defect with chiral supersymmetry, described by an $\mathcal{N}=2$ Fermi multiplet of mass $m^{(\alpha)}$. This system is placed on $\mathbb{S}^3_{\omega_1,\omega_2}$ and as already mentioned the 1d defect at each node wraps the Hopf fibre.

Before exact deconstruction, the total 1d contribution to the $\mathbb{S}^3_{\omega_1,\omega_2}$ partition function is

$$\mathcal{Z}_{1\mathrm{d}}(\sigma_b^{(\alpha)}, m_b^{(\alpha)}) = \prod_{\alpha} g_{\mathrm{fer}}^{\mathcal{N}=2}(\sigma^{(\alpha)}, m^{(\alpha)}) \tag{5.48}$$

with each Fermi-multiplet contribution given by[71]

$$g_{\mathrm{fer}}^{\mathcal{N}=2}(\sigma^{(\alpha)}, m^{(\alpha)}) = \prod_{b=1}^{k} \Gamma_1\left(-\sigma_b^{(\alpha)} - m^{(\alpha)} \middle| \omega\right)^{-1} \Gamma_1\left(\omega + \sigma_b^{(\alpha)} + m^{(\alpha)} \middle| \omega\right)^{-1} . \tag{5.49}$$

To deconstruct, we set $\sigma^{(\alpha)} \to \sigma$ and $m^{(\alpha)} \to m$, shift the arguments of the $\Gamma_1$ functions and take $N \to \infty$ to obtain

$$\begin{aligned} \mathcal{Z}_{1\mathrm{d}}^{\mathrm{Dec}}(\sigma, m) &= \prod_{\alpha=-\infty}^{\infty} \prod_{b=1}^{k} \Gamma_1\left(-\sigma_b - m + i\frac{2\pi\alpha}{R} \middle| \omega\right)^{-1} \Gamma_1\left(\omega + \sigma_b + m + i\frac{2\pi\alpha}{R} \middle| \omega\right)^{-1} \\ &\propto \prod_{\alpha=-\infty}^{\infty} \prod_{b=1}^{k} \prod_{n=-\infty}^{\infty} \left(-\sigma_b - m + i\frac{2\pi\alpha}{R} + n\omega\right) . \end{aligned} \tag{5.50}$$

[71] We have switched off all other chemical potentials that could appear here for the purposes of this discussion.

Up to an unimportant zeta-function regularisable factor

$$\begin{aligned}\mathcal{Z}^{\text{Dec}}_{\text{1d}}(\sigma,m) &\propto \prod_{\alpha=-\infty}^{\infty}\prod_{b=1}^{k}\prod_{n=-\infty}^{\infty}\left(\omega^{-1}(-\sigma_b-m)+n+\alpha\tau\right)\\ &= \prod_{b=1}^{k}\theta\left(e^{-2\pi i\omega^{-1}\sigma_b}\mu|q\right)\ ,\end{aligned} \tag{5.51}$$

where we defined $\tau=-\frac{i}{\omega R}$, $\mu=e^{-2\pi i\omega^{-1}m}$, $q=e^{2\pi i\tau}$. This completes the second step of our prescription.

For the third and final step we compute the quantity

$$\mathcal{Z}^{\text{Dec }(\rho)}_{\text{1d}}(\sigma)\equiv\frac{1}{2\pi i}\oint d\mu\,\mu^{-\rho-1}\prod_{b=1}^{k}\theta\left(e^{-2\pi i\omega^{-1}\sigma_b}\mu|q\right)\ , \tag{5.52}$$

Since $\theta(z|q)$ is closely related to the Jacobi-theta function,

$$\vartheta(z|q)=\prod_{n=1}^{\infty}(1-q^n)(1+zq^{n-\frac{1}{2}})\left(1+z^{-1}q^{n-\frac{1}{2}}\right)=\sum_{n=-\infty}^{\infty}z^n q^{\frac{n^2}{2}}\ , \tag{5.53}$$

and the eta function, $\eta(q)=q^{\frac{1}{24}}\prod_{n=1}^{\infty}(1-q^n)$, via the relation

$$\theta(z|q)=q^{\frac{1}{24}}\eta^{-1}(q)\vartheta(-zq^{-\frac{1}{2}}|q)\ , \tag{5.54}$$

we can re-write (5.52) as

$$\mathcal{Z}^{\text{Dec }(\rho)}_{\text{1d}}(\sigma)=(-1)^{\rho}q^{\frac{\rho}{2}+\frac{k}{24}}\,\eta^{-k}(q)\sum_{n_1,\ldots,n_k=-\infty}^{\infty}\delta_{\rho,\sum_b n_b}\,e^{-2\pi i\omega^{-1}\sum_b n_b\sigma_b}q^{\frac{1}{2}\sum_{j=b}^{k}n_b^2}\ . \tag{5.55}$$

Therefore, our proposal for the index of a chiral surface defect, labelled by integer $\rho$, in 4d $\mathcal{N}=2$ or $\mathcal{N}=4$ theories is given by

$$\mathcal{I}^{(\rho)}_{\text{4d}-\text{2d}}=\oint\prod_{b=1}^{k}\frac{\mathrm{d}v_b}{2\pi i v_b}\mathcal{Z}^{\text{Dec}}_{\text{3d}}(v)\mathcal{Z}^{\text{Dec }(\rho)}_{\text{1d}}(v^{\tau})\ , \tag{5.56}$$

with $v_b=e^{-2\pi iR\sigma_b}$. Now one can ask whether $\rho$ could be related to the $\rho$-antisymmetric representation in a suitable classification.

At first sight, the association with the fundamental or antisymmetric representations of U($k$) fails because the integer $\rho$ that appears in (5.55) is not restricted to $k$ different values. Nevertheless, we notice that $\mathcal{Z}^{\text{Dec }(\rho)}_{\text{1d}}(\sigma)$ as defined in (5.55) obeys the following

quasi-periodicity relation

$$\mathcal{Z}_{\rm 1d}^{\rm Dec\ (\rho+k)}(\sigma) = (-1)^k q^{k+\rho} e^{-2\pi i\omega^{-1}\sum_b \sigma_b}\, \mathcal{Z}_{\rm 1d}^{\rm Dec\ (\rho)}(\sigma)\ , \tag{5.57}$$

which is easily derived by shifting all sums over $n_b$ by one unit.

The $\sigma$-dependent factor $e^{-2\pi i\omega^{-1}\sum_b \sigma_b}$ would cancel if the definition (5.55) included an extra $e^{2\pi i\omega^{-1}\frac{\rho}{k}\sum_b \sigma_b}$,[72] or if the bulk gauge group was SU($k$). With this cautionary note in mind, the deconstructed 3d-1d squashed $\mathbb{S}^3$ partition function is restricted to $k$ different values that could eventually fit into a classification of chiral surface defects in terms of the fundamental or antisymmetric representations of the gauge group.

As a brief illustration we consider the case of a U(2) gauge group, i.e. $k=2$. Then, it is straightforward to show that $\mathcal{Z}_{\rm 1d}^{\rm Dec\,(\rho)}$ in (5.55) only assumes two different values[73]

$$\begin{aligned} e^{\pi i\omega^{-1}\rho\sum_b \sigma_b} q^{-\frac{\rho^2}{4}}\, \mathcal{Z}_{\rm 1d}^{\rm Dec\ (\rho=even)}(\sigma) &= \vartheta_{00}\left(e^{-2\pi i\omega^{-1}(\sigma_1-\sigma_2)}\middle|q^2\right)\ , \\ e^{\pi i\omega^{-1}\rho\sum_b \sigma_b} q^{-\frac{\rho^2}{4}}\, \mathcal{Z}_{\rm 1d}^{\rm Dec\ (\rho=odd)}(\sigma) &= \vartheta_{10}\left(e^{-2\pi i\omega^{-1}(\sigma_1-\sigma_2)}\middle|q^2\right)\ , \end{aligned} \tag{5.58}$$

where $\vartheta_{00}, \vartheta_{10}$ are the standard theta-function variants with characteristics. It is possible to manipulate the restricted sum in (5.55) for general $k$ and express it in terms of the product of $k-1$ theta functions, but unfortunately we have not uncovered simple expressions like the ones in (5.58) for general $k$.

As in the vortex-loop case, we should mention that more complicated Wilson-loop insertions can be used as the starting point for deconstruction, where the associated representations of the bulk gauge group can be symmetric, antisymmetric or products thereof.

## 5.4 Conclusions and Outlook

In this section we applied the exact-deconstruction procedure, introduced in [2, 3], to exact partition functions of 3d circular-quiver theories that lift to 4d indices. We generalised it to include supersymmetric, codimension-two defects that are associated with vortex- or Wilson-loop insertions at each node of the 3d quiver. In the process of doing so, we made use of some remarkable identities between special functions of hyperbolic and elliptic type. Even though we explicitly compared our post-deconstruction results with the index of superconformal 4d-2d systems, we stress that exact deconstruction more generally produces supersymmetric partition functions on $\mathbb{S}^3 \times \mathbb{S}^1$ for non-conformal setups. We note that we applied our procedure directly at the level of

[72] We remind the reader that a similar $e^{-\pi\sum_b \sigma_b}$ factor had to be cancelled in (5.45) for the case of the round $\mathbb{S}^3$.

[73] This is up to an overall $e^{-\pi\omega^{-1}\rho\sum_b \sigma_b}$ factor, which can be cancelled by the $e^{2\pi i\omega^{-1}\frac{\rho}{k}\sum_b \sigma_b}$ factor proposed in the previous paragraph.

integrands for the 4d/3d and 2d/1d Coulomb-branch parameters. Although we have not done so, the associated integrals can subsequently be performed using the Jeffrey-Kirwan residue prescription [172, 174, 195]. It is also worth pointing out that by employing exact deconstruction we have straightforwardly recovered non-trivial results for 4d-2d indices while completely bypassing the conventional dimensional-deconstruction limit at the level of classical Lagrangians. Regarding the deconstruction of codimension-one defects, we introduced a localised insertion of gauge/matter fields at specific nodes of the 3d circular quiver, which lift to a coupled system of 4d-3d indices/three-sphere partition functions. Obtaining results for this class of defects is particularly simple through our method.

There are various avenues for future research stemming from this work. For example, it would be useful to further examine the prescription of Sec. 5.3 that isolates chiral-surface defect contributions in 4d related to a specific (single-column) Young tableau and, more specifically, contemplate further on its interpretation from the four-dimensional perspective. Moreover, vortex defects in both 4d and 3d can be obtained using certain difference operators that act directly on the 4d/3d index/partition function [140, 189]. These operators satisfy an interesting elliptic algebra and are related by dimensional reduction. It would be interesting to see how exact deconstruction fits into this picture. In the direction of reducing supersymmetry, it would be worth determining whether the surface defects for 4d $\mathcal{N} = 1$ SCFTs recently discussed in [206] can also be studied from three dimensions using exact deconstruction.

Departing from our 3d/4d set-up, an obvious generalisation of our results would involve applying them to the six-dimensional (2,0) theory [2, 23]. One could attempt to deconstruct the (2,0) partition function on $\mathbb{S}^4 \times \mathbb{T}^2$ in the presence of various defects, based on the $\mathbb{S}^4$ (defect) partition functions associated with $\mathcal{N} = 2$ superconformal circular-quiver theories in 4d. Such an approach would make contact with and supplement the results of [207].

In addition, one could remain on the three-sphere to explore 4d non-Lagrangian theories. For example, to see if an orbifold of ABJM theory could reproduce the results of [208] for the index of 4d $\mathcal{N} = 3$ SCFTs [209, 210]. Finally, it would be very interesting to try and extend the principle of deconstruction to non-Lagrangian starting points. This would entail generalising exact deconstruction away from the individual building-block prescription presented here, to an operation at the level of the full partition function.

# Chapter 6

# Conclusions and Outlook

This thesis consisted of two main themes. The first was superconformal representation theory. Specifically, how we can use the superconformal algebras in 5d and 6d to help us in our quest to understand these mysterious higher dimensional theories. The second theme was that of dimensional deconstruction. We explored how one could use information about theories in lower dimensions to construct higher dimensional quantities that we then compared against. In this final chapter we present a short summary of the results along with some concluding remarks about future directions for research.

In Chapter 3 we built on the work of [36] by providing a level-by-level construction of multiplets available in the superconformal algebras in 5d and 6d. Through this study we found various unifying themes that coincided nicely with the lore on SCFTs in $d > 4$. These relied on the recombination rules. Recombination happens when one tunes the conformal dimension to be at a certain threshold $\lim_{\epsilon\to 0} \Delta + \epsilon$, whereupon the long multiplet splits into two short multiplets. This has a wider implication for whether or not a short multiplet is absolutely protected, since a short multiplet that combines into a long multiplet need not necessarily be protected from quantum corrections (if the other short multiplet that it pairs up with is also present). In 4d this $\epsilon$ can be an exactly marginal parameter, though in 5d and 6d these theories are necessarily isolated [87,88], so the recombination rule is simply an algebraic feature.

With this in mind, we have shown that all multiplets in 5d and 6d that contain higher spin currents can never recombine into long multiplets. This implies that there are no exactly marginal deformations of (almost) free theories. Moreover, all multiplets with conserved spin-two currents never recombine, which implies that there are no marginal couplings between two isolated SCFTs, unlike in 4d. Both of these statements are purely algebraic, and are compatible with the isolated nature of 5d and 6d SCFTs.

One can also rule out classes of multiplets in free SCFTs by virtue of the presence of higher spin free multiplets. For example, these include some $\mathcal{B}$ and $\mathcal{C}$ multiplets in

6d (1,0) and (2,0) for $c_1 > 0$; along with some additional $\mathcal{D}$ multiplets in (2,0) where $d_2 = 1$.

On the subject of ruling out multiplets, we included the general superconformal indices for each class of multiplet that we studied following the paper [24]. Specifically in Section 3.4.5 we used a conjectured MacDonald limit of the interacting superconformal index to perform spectroscopy along the lines of [117]. This was a powerful technique that allowed us to probe the spectrum of the (2,0) theory. However, it was unfortunately quite limited. The MacDonald limit is insensitive to a large amount of possible multiplets in the SCA, so we could only make definitive statements about a subsector of the theory.

There are two interesting lines of inquiry that follows this. The first is to try to obtain a closed form for the coefficients of multiplets that appear in the spectral decomposition. This might be interesting from a combinatorics point of view but is still limited in terms of its wider implications for the (2,0) theory spectrum. The second is to move onto the fully refined index. This is quite difficult since the integral expressions for interacting (2,0) indices are very complicated, as they involve sums over the instanton sectors using the Nekrasov functions in App. A. An approach would be to use a series expansion in order to evaluate the integral for low rank to a sufficiently high order to gain meaningful information about the coefficients of the refined indices. However, this is computationally quite an intense procedure, and is not clear to which order in an expansion parameter would be sufficient to get meaningful information. There is the possibility that there exists another limit of the index that allows for exact integration due to a simplification of the Nekrasov partition function. However, such a limit even may not even exist, let alone one that has access to a wider set of multiplets than the Schur limit.

Lastly, Chapter 3 used results that can be obtained using the `python` package detailed in Appendix B. While the work has already been done for dimensions three and above, this package is still useful for two reasons. Firstly, for sixteen supercharge theories, most of the multiplets have been omitted due to their sheer enormity. Thus this package provides a way for the reader to access whichever multiplet they want, and not be at the whim of the author's sensibility of what can or cannot neatly fit onto a page. The other reason is that that there is a large number of defect theories whose superconformal algebra has not been enumerated in this fashion; *cf.* [211–214] which might benefit from having this tool available.

In Chapter 4 we used some of the advances in exact results, such as localisation and the refined topological vertex, to test the efficacy of the dimensional deconstruction proposal of [23] for 6d theories.

We started with the 6d (2,0) theory. This can be deconstructed by starting with a 4d $\mathcal{N} = 2$ circular quiver theory which results in the 6d theory on a two-torus. The

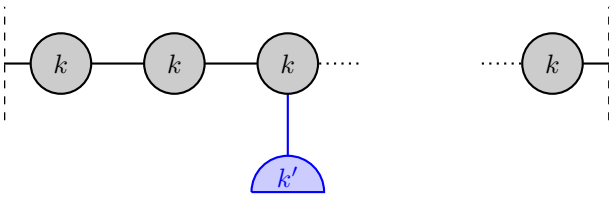


**Figure 13:** A modification of the circular quiver considered in Chapter 4 to include additional field content.

first check was done using a comparison between the Higgs branch Hilbert series and the "half-BPS" limit of the $(2,0)_k$ index. Specifically

$$\lim_{N\to\infty} \mathrm{HS}_k^N = \prod_{m=1}^{k} \frac{1}{1-x^m} = \mathcal{I}^{(2,0)_k}_{\frac{1}{2}\text{-BPS}} \,. \tag{6.1}$$

This was a short calculation that served as a litmus test for the proposal before carrying onto a more refined computation. While this was done for the $\mathrm{A}_{k-1}$ theory in [2], it was later extended to the $\mathrm{D}_k$ case in [215]. The starting quiver was more subtle, and the deconstruction procedure as a whole was more complicated. It would be nice to see if this could be extended to the $\mathrm{E}_k$ series. This could possibly shed some light as to the brane realisation of this theory in M-theory.

The initial computation, while encouraging, can be improved on by including more information. We implemented a prescription for performing dimensional deconstruction at the level of the partition function—a process dubbed as "exact deconstruction". It was shown that, upon integration, we have

$$\int [\mathrm{d}a] \left| \lim_{N\to\infty} Z^{\text{Higgs}}_{\text{4d}} \right|^2 = \int [\mathrm{d}a] \, |Z_{\text{6d}}|^2 = Z_{\mathbb{S}^4_{\epsilon_1,\epsilon_2}\times\mathbb{T}^2} \,. \tag{6.2}$$

While establishing this dictionary is promising, it is not clear whether one can extract novel results using this procedure. For example, while physically motivated, this procedure is simply akin to a $q$-deformation of 4d $\mathcal{N}=2^*$ which will of course give the $(2,0)$ partition function by appealing to 5d MSYM. Extracting correlation functions of chiral operators and Wilson loop expectation values as detailed in Chapter 4 by starting with a 4d $\mathcal{N}=2$ circular quiver might be extraneous when compared to simply starting with 5d MSYM. Perhaps a way to predict new quantities via this method would be more along the lines of the codimension-one defects detailed in [4]. More concretely this would involve having additional field content at, say, one of the nodes and then performing deconstruction as normal as in Fig. 13. This would now have codimension two. This approach would lead to a novel way of generating defects in the (2,0) theory that wrap the $\mathbb{S}^4$, though care would need to be taken in order to ensure the

correct IR behaviour when one takes the deconstruction limit. It would be interesting to investigate this avenue.

In this vein, it could be fruitful to consider the codimension-two defects considered on the $\mathbb{S}^4$ considered in [175,216]. A whole host of defect configurations were considered, including ones where two 2d defects overlap at a point leading to a 0d defect theory on the intersection. They provide a detailed brane system which engineers these defects and meta-defects which could lead to interesting and intricate M2/M5 brane ensembles, alongside the ones considered in [207].

The second thing that we considered in Chapter 4 was to deconstruct Little String Theory. This required a $\mathbb{S}^4$ partition function for a 4d $\mathcal{N}=1$ which, though it should exist in principle, is not currently amenable to any of the known techniques for extracting such information. This was circumvented by [25] by means of an analytic continuation through dimensions. We proposed a refined version of this quantity to be defined on the ellipsoid with squashing parameters $\epsilon_1$ and $\epsilon_2$. The proposed form was

$$\begin{aligned}\mathcal{Z}^{\text{chi}}_{\text{pert}} &= \prod_{\beta\in\mathcal{R}} \frac{\Gamma_3\left(\epsilon_+ + iM + i\langle\beta,\lambda\rangle|\,\epsilon_1,\epsilon_2,\epsilon_+\right)}{\Gamma_3\left(2\epsilon_+ - iM - i\langle\beta,\lambda\rangle|\,\epsilon_1,\epsilon_2,\epsilon_+\right)}\,,\\ \mathcal{Z}^{\text{vec}}_{\text{pert}} &= \prod_{\beta\in\text{Adj}} \frac{\Gamma_3(3\epsilon_+ - i\langle\beta,\lambda\rangle|\epsilon_1,\epsilon_2,\epsilon_+)}{\widehat{\Gamma}_3(i\langle\beta,\lambda\rangle|\epsilon_1,\epsilon_2,\epsilon_+)}\,.\end{aligned} \tag{6.3}$$

These satisfied the preliminary tests that were required of them, and also matched the 6d result in the deconstruction limit. Though a similar problem to the (2,0) case arises: it seems far easier and more robust to simply calculate the partition function of LST through conventional techniques such as the refined topological vertex as in [82, 83]. Moreover, given the subtlety of $\mathcal{N}=1$ partition functions on the $\mathbb{S}^4$ it is not obvious that one could use this deconstruction method to find robust novel things about LST.

An interesting follow up would be to see if one could perform a free-theory calculation for the 4d $\mathcal{N}=1$ multiplets on the ellipsoid. This was performed in [25] on the round sphere where it supported the conjectured partition functions. It would be a nice calculation to put the 4d theory on the ellipsoid *à la* [44] and evaluate its spectrum under the Laplacian via Gaussian elimination.

The last chapter focused on testing some ideas for generalising the "exact deconstruction" procedure. In this section we have already mentioned the idea of extending the discussion to include defects. This was performed in Chapter 5, only in the context of 3d to 4d theories. The reason why was that both sides of the picture are far more tractable with more resources for both. We considered the case of vortex and Wilson loop defects in 3d from [174]. As before, the concrete brane realisation of the 3d theory acted as a robust guiding principle for the implementation of the procedure of dimensional deconstruction. This led to matching the results for (2,2) defects in 4d theories

that were explored in [172]. There were also new results for (4,0) defects which came from the Wilson loops in 3d. These were similar to ones found via affine characters in the context of the superconformal index in [197, 198]. It would be interesting to fully explore the connection between the two approaches.

Moving away from defects but staying in 3d, an extremely interesting line of inquiry would be in exploring the relationship between ABJM and the newly discovered non-Lagrangian 4d $\mathcal{N} = 3$ theories. In [209] it was mentioned that these theories reduce to ABJM at some point in the moduli space. Due to the non-Lagrangian nature of the theory, it is hard to extract information about them. Some approaches for the index have relied on AdS/CFT [217] whereas others have used a so-called discrete gauging [208]. By starting with an orbifold of ABJM on the $\mathbb{S}^3$, one could possibly obtain integral formulas for more refined versions of the mentioned indices for a generic rank of the gauge group.

Exact methods for calculating quantities in quantum field theory are an important and rewarding line of attack. The scope of information that we can extract from them has broadened significantly over the last decade or so. This has happened through obtaining a deeper understanding of these techniques in order to generalise them; or through applying them in interesting and novel ways. This body of work has focused on the latter approach and we hope that it has been successful in inspiring the reader to try some exact methods in unconventional ways.

# Appendix A

# An Exegesis on Special Functions

We use this technical appendix to collect useful formulas and identities that we will use liberally throughout the thesis. This doubles up as a reference for the conventions that will be adhered to. We will build from rational functions, to trigonometric and then to elliptic; as well as any relevant properties. Caution should be paid when using these formulas since they are often defined for specific regions of analyticity.

## A.1 Rational Functions

### Barnes Gamma functions

To start, we define the Barnes $N$-Gamma function as

$$\Gamma_N(x|\omega_1,\ldots,\omega_N) = \exp\left[\frac{\partial}{\partial s}\zeta_N(s,x|\omega_1,\ldots,\omega_N)\big|_{s=0}\right] , \tag{A.1}$$

for $\Re\omega_i > 0$ and the Barnes Zeta function defined as

$$\zeta_N(s,x|\omega_1,\ldots,\omega_N) = \sum_{\ell_1,\ldots,\ell_N\geq 0} \frac{1}{(x+\ell_1\omega_1+\cdots+\ell_N\omega_N)^s} . \tag{A.2}$$

To see the analytic properties it is helpful to write this as

$$\sum_{\boldsymbol{\ell}\in\mathbb{N}^N} \frac{1}{(x+\ell_1\omega_1+\cdots+\ell_N\omega_N)^s} = \frac{1}{\Gamma(s)}\int \frac{dt}{t}t^s \frac{e^{-tx}}{(1-e^{-\omega_1 t})\cdots(1-e^{-\omega_N t})} . \tag{A.3}$$

One requirement for convergence is $\Re\omega_i > 0$ since then $0 < e^{-\omega_i t} < 1$. This is clear because then we can write

$$\frac{1}{\Gamma(s)}\int \frac{dt}{t}t^s \frac{e^{-tx}}{(1-e^{-\omega_1 t})\cdots(1-e^{-\omega_N t})} = \sum_{\boldsymbol{\ell}\in\mathbb{N}^N}\frac{1}{\Gamma(s)}\int\frac{dt}{t}t^s e^{-t(x+\boldsymbol{\ell}\cdot\boldsymbol{\omega})}$$

$$= \sum_{\boldsymbol{\ell}\in\mathbb{N}^N} (x + \boldsymbol{\ell}\cdot\boldsymbol{\omega})^{-s} \ , \tag{A.4}$$

as required. We thus arrive at the product representation

$$\Gamma_N(x|\omega_1,\ldots,\omega_N) \propto \prod_{\boldsymbol{\ell}\in\mathbb{N}^N} \frac{1}{x+\boldsymbol{\ell}\cdot\boldsymbol{\omega}} \ , \tag{A.5}$$

up to a global constant that arises due to the analytic continuation in $s$. We also define the function $\widehat{\Gamma}_N$ which is the same as the above, only the domain of the product is over $\boldsymbol{\ell}\in\mathbb{N}^N\setminus\{\mathbf{0}\}$.

One can combine Barnes Gamma functions to lower the 'rank' using the difference equations

$$\Gamma_{N-1}(x|\boldsymbol{\omega}(i)) = \frac{\Gamma_N(x|\omega_1,\ldots,\omega_N)}{\Gamma_N(x+\omega_i|\omega_1,\ldots,\omega_N)} \ , \tag{A.6}$$

where $\boldsymbol{\omega}(i) = (\omega_1,\ldots,\omega_{i-1},\omega_{i+1},\ldots,\omega_N)$. The Barnes Gamma function satisfies the following nice reflection formula which can be proved through its integral representation:

$$\Gamma_N(-x|\omega_1,\ldots,\omega_N) = \Gamma_N(x+\omega_1+\omega_2+\ldots+\omega_N|\omega_1,\ldots\omega_N)^{(-1)^N} \ . \tag{A.7}$$

Let us now continue the parameter $\omega_1$ such that $\omega_1<0$. Clearly now $e^{-\omega_1 t}>1$ and so the geometric series does not converge. Therefore we need to carefully treat the integral

$$\int \frac{dt}{t} t^s \frac{e^{-tx}}{(1-e^{-\omega_1 t})\cdots(1-e^{-\omega_N t})} = -\int \frac{dt}{t} t^s \frac{e^{-t(x-\omega_1)}}{(1-e^{\omega_1 t})(1-e^{-\omega_2 t})\cdots(1-e^{-\omega_N t})} \ , \tag{A.8}$$

which is now convergent. Thus we can perform the integral to get

$$\int \frac{dt}{t} t^s \frac{e^{-t(x-\omega_1)}}{(1-e^{\omega_1 t})(1-e^{-\omega_2 t})\cdots(1-e^{-\omega_N t})} = \Gamma(s) \sum_{\boldsymbol{\ell}\in\mathbb{N}^N} (x-(\ell_1+1)\omega_1+\hat{\boldsymbol{\ell}}\cdot\hat{\boldsymbol{\omega}})^{-s} \ , \tag{A.9}$$

where we define $\hat{\boldsymbol{\ell}} = (\ell_2,\ldots,\ell_N)$ and $\hat{\boldsymbol{\omega}} = (\omega_2,\ldots,\omega_N)$. Putting everything together we have that the $N$-Gamma function with an analytically continued $\omega_1$ is equal to

$$\Gamma_N(x|\omega_1,\ldots,\omega_N) \propto \prod_{\boldsymbol{\ell}\in\mathbb{N}^N} (x-(\ell_1+1)\omega_1+\hat{\boldsymbol{\ell}}\cdot\hat{\boldsymbol{\omega}}) \ . \tag{A.10}$$

Note that the analytic structure has changed, in particular, instead of poles there are zeros. Moreover, the Gamma function is now well defined at $x=0$.

Through this we can introduce the hyperbolic Gamma function $\Gamma_h(x|\omega_1,\omega_2)$ as defined in [218] which is closely related to the double-gamma function

$$\Gamma_h(x|\omega_1,\omega_2) = \frac{\Gamma_2(x|\omega_1,\omega_2)}{\Gamma_2(-x+\omega_1+\omega_2|\omega_1,\omega_2)} \ . \tag{A.11}$$

This function is actually the rank two specialisation of the so-called multiple sine function defined in [219] as

$$S_N(x|\boldsymbol{\omega}) = \Gamma_N(x|\boldsymbol{\omega})^{-1}\Gamma_N(|\boldsymbol{\omega}|-x|\boldsymbol{\omega})^{(-1)^N} \ , \tag{A.12}$$

where $|\boldsymbol{\omega}| = \omega_1+\ldots+\omega_N$, which satisfies the same difference equation that the multiple gamma function does.

These functions naturally appear in the context of sphere partition functions *cf.* [25, 70, 220]. Another function that we encounter in the context of partition functions, in particular for defects, is

$$\Delta_h(a|\omega,t) \equiv \frac{\Gamma_1(a|\omega)\Gamma_1(\omega-a|\omega)}{\Gamma_1(a+t|\omega)\Gamma_1(\omega-a-t|\omega)} = \frac{\sin(\frac{\pi(a+t)}{\omega})}{\sin(\frac{\pi a}{\omega})} \ . \tag{A.13}$$

### 4d Nekrasov functions

The functions above have all been regularised infinite products. The next set that we consider are finite product formulas associated with partitions of natural numbers $\mu$ such that $\mu_1 \geq \mu_2 \geq \ldots \geq \mu_{l(\mu)}$ where the $\mu_i$ are all non-negative.

An important function that we will encounter in this thesis is the so-called 'Nekrasov' function. It is characterised by two partitions, $\mu$ and $\nu$, and the Omega background parameters $\epsilon_1$ and $\epsilon_2$ [52]. It is defined as

$$\begin{aligned} \mathrm{N}_{\lambda\nu}(x;\epsilon_1,\epsilon_2) = &\prod_{(i,j)\in\lambda} \big(x+\epsilon_1(\lambda_i-j+1)+\epsilon_1(i-\nu_j^t)\big) \\ &\times \prod_{(i,j)\in\nu} \big(x+\epsilon_1(j-\nu_i)+\epsilon_2(\lambda_j^t-i+1)\big) \ , \end{aligned} \tag{A.14}$$

where $\lambda_i$ is the number of boxes in the $i^{th}$ column of the partition $\lambda$. Note that we have $\epsilon_1 > 0$ and $\epsilon_2 < 0$.

These satisfy the following exchange relations [73]

$$\begin{aligned} \mathrm{N}_{\lambda\mu}(m;-\epsilon_2,-\epsilon_1) &= \mathrm{N}_{\mu^t\lambda^t}(m-\epsilon_1-\epsilon_2;\epsilon_1,\epsilon_2), \\ \mathrm{N}_{\lambda\mu}(-m;\epsilon_1,\epsilon_2) &= (-1)^{|\lambda|+|\mu|}\mathrm{N}_{\mu\lambda}(m-\epsilon_1-\epsilon_2;\epsilon_1,\epsilon_2) \ , \\ \mathrm{N}_{\lambda\mu}(m;\epsilon_2,\epsilon_1) &= \mathrm{N}_{\lambda^t\mu^t}(m;\epsilon_1,\epsilon_2) \ , \end{aligned} \tag{A.15}$$

## A.2 Trigonometric and Elliptic Functions

The functions defined above can be generalised to include infinite towers of poles and zeros. A simple way to introduce this is to '$q$-deform' a function. A $q$-number is defined as

$$x \to [x]_q = \frac{1-q^x}{1-q} \ , \tag{A.16}$$

such that $\lim_{q\to 1}[x]_q = x$. This is achieved by writing $q = e^{-\beta}$. In the context of partition functions, this is interpreted as adding Kaluza-Klein modes, with $\beta$ being the radius of the circle. This is seen very easily in the context of $\mathbb{S}^3$ partition functions in 3d and the 4d superconformal index.

A free 3d $\mathcal{N}=2$ chiral multiplet with some r-charge $r$ on a squashed $\mathbb{S}^3$ has the partition function [57, 67]

$$Z_{\text{chi}}(r) = \Gamma_h(r\omega_+|\omega_1,\omega_2) \ , \tag{A.17}$$

with $\omega_+ = \frac{\omega_1+\omega_2}{2}$, where $\omega_1$ and $\omega_2$ are the squashing parameters of the sphere. The superconformal index *à la* [40] of a free 4d $\mathcal{N}=1$ chiral multiplet is simply

$$\mathcal{I}_{\text{chi}}(r) = \prod_{\ell_1,\ell_2\geq 0} \frac{1-(\mathfrak{p}\mathfrak{q})^{-\frac{r}{2}}\mathfrak{p}^{\ell_1+1}\mathfrak{q}^{\ell_2+1}}{1-(\mathfrak{p}\mathfrak{q})^{\frac{r}{2}}\mathfrak{p}^{\ell_1}\mathfrak{q}^{\ell_2}} \ , \tag{A.18}$$

where we have defined $\mathfrak{p} = e^{-\beta\omega_1}$ and $\mathfrak{q} = e^{-\beta\omega_2}$. It is simple to show that

$$\lim_{\beta\to 0}\mathcal{I}_{\text{chi}}(r) = Z_{\text{chi}}(r) \ , \tag{A.19}$$

where the $\beta\to 0$ limit can be seen geometrically as shrinking the circle of the $\mathbb{S}^3\times\mathbb{S}^1_\beta$ partition function. More generally we may define the so-called elliptic gamma function as

$$\Gamma_e(z|\mathfrak{p},\mathfrak{q}) = \prod_{\ell_1,\ell_2\geq 0} \frac{1-z^{-1}\mathfrak{p}^{\ell_1+1}\mathfrak{q}^{\ell_2+1}}{1-z\mathfrak{p}^{\ell_1}\mathfrak{q}^{\ell_2}} \ , \tag{A.20}$$

which is simply the $q$-deformation of the hyperbolic gamma function that we previously defined. It satisfies

$$\Gamma_e(z|\mathfrak{p},\mathfrak{q}) = \Gamma_e\left(\frac{\mathfrak{p}\mathfrak{q}}{z}\middle|\mathfrak{p},\mathfrak{q}\right)^{-1} \ . \tag{A.21}$$

Reducing $\beta\to 0$ takes one from elliptic to hyperbolic, but we can also go in the opposite

direction:

$$\prod_{\alpha=-\infty}^{\infty} \Gamma_h\left(x + i\frac{2\pi\alpha}{\beta}\middle|\omega_1,\omega_2\right) = z^2(\mathfrak{p}\mathfrak{q})^{-\frac{1}{2}}\Gamma_e(z|\mathfrak{p},\mathfrak{q}) \ , \tag{A.22}$$

with $z = e^{-\beta x}$, $\mathfrak{p} = e^{-\beta\omega_1}$ and $\mathfrak{q} = e^{-\beta\omega_2}$. This hinges on the product form of the sin function

$$\sin(\pi x) = \pi x \prod_{\ell=1}^{\infty}\left(1 - \frac{x^2}{\ell^2}\right) \ . \tag{A.23}$$

This can be additionally rephrased through the use of gamma functions

$$\Gamma_1(x|\omega)^{-1}\Gamma_1(\omega - x|\omega)^{-1} = 2\sin\frac{\pi x}{\omega} \ . \tag{A.24}$$

Indeed one can define the trigonometric analogue of the Barnes Gamma function, the multiple $q$-Pochhammer symbol

$$\prod_{\alpha=-\infty}^{\infty} \Gamma_N\left(x + i\frac{2\pi\alpha}{\beta}\middle|\boldsymbol{\omega}\right) \propto \prod_{\boldsymbol{\ell}\in\mathbb{N}^N}\left(1 - z\mathfrak{p}_1^{\ell_1}\cdots\mathfrak{p}_N^{\ell_N}\right)^{-1} = (x;\mathfrak{p}_1,\ldots,\mathfrak{p}_N)^{-1} \ , \tag{A.25}$$

with $\mathfrak{p}_i = e^{-\beta\omega_i}$[74] and $z = e^{-\beta x}$, where we defined

$$(x;\mathfrak{p}_1,\ldots,\mathfrak{p}_N) = \prod_{\ell\in\mathbb{N}^{\mathrm{N}}}(1 - x\mathfrak{p}_1^{\ell_1}\cdots\mathfrak{p}_N^{\ell_N}) \ . \tag{A.26}$$

The exact factor depends on the rank of the gamma function being regularised. This identity can be rephrased as

$$\Gamma_{N+1}\left(x + i\frac{2\pi}{\beta}\middle|\boldsymbol{\omega}, i\frac{2\pi}{\beta}\right)\Gamma_{N+1}\left(x\middle|\boldsymbol{\omega}, -i\frac{2\pi}{\beta}\right) \propto (x;\mathfrak{p}_1,\ldots,\mathfrak{p}_N)^{-1} \ , \tag{A.27}$$

and is core to the process of exact dimensional deconstruction. The analogue of the deconstruction identity for the function $\Delta_h$ is

$$\Delta_e(A|\Omega,T) = \prod_{\alpha=-\infty}^{\infty}\Delta_h\left(a + i\frac{2\pi\alpha}{R}\middle|\omega,t\right) \ , \tag{A.28}$$

where $A = e^{-Ra}$, $\Omega = e^{-R\omega}$, $T = e^{-Rt}$. The function $\Delta_e(A|\Omega,T)$ is the ratio of theta

[74] Note that, when $N = 2$, we will use $\mathfrak{p} = e^{-\beta\omega_1}$ and $\mathfrak{q} = e^{-\beta\omega_2}$ to compare with the superconformal index literature, while we will use $\mathfrak{q} = e^{-\beta\epsilon_1}$ and $\mathfrak{t} = e^{\beta\epsilon_2}$ when comparing to the topological strings literature, after the analytic continuation.

functions

$$\Delta(A|\Omega,T)=\frac{\theta(AT|\Omega)}{\theta(A|\Omega)}\ , \tag{A.29}$$

who explicit form will be defined in the following few lines.

When $N=2$ we have a function similar to the familiar refined MacMahon function

$$(z;\mathfrak{p},\mathfrak{q})=\mathcal{M}(z\mathfrak{q}^{-1};\mathfrak{p},\mathfrak{q})\ . \tag{A.30}$$

The MacMahon function satisfies the reflection formula

$$\mathcal{M}(z^{-1};\mathfrak{p},\mathfrak{q})=\left(-z\sqrt{\frac{\mathfrak{q}}{\mathfrak{t}}}\right)^{\frac{1}{12}}\mathcal{M}\left(z\frac{\mathfrak{t}}{\mathfrak{q}};\mathfrak{p},\mathfrak{q}\right)\ , \tag{A.31}$$

after zeta function regularisation. The elliptic functions used in this thesis are

$$\begin{aligned}\theta(q|y)&=\prod_{\ell=0}^{\infty}(1-yq^{\ell})(1-y^{-1}q^{\ell+1})\ ,\\ \eta(q)&=q^{\frac{1}{24}}\prod_{\ell=0}^{\infty}(1-q^{\ell+1})\ ,\end{aligned} \tag{A.32}$$

alongside

$$\theta_1(q|y)=-iq^{\frac{1}{8}}y^{\frac{1}{2}}\prod_{\ell=0}^{\infty}(1-q^{\ell+1})(1-yq^{\ell+1})(1-y^{-1}q^{\ell})\ , \tag{A.33}$$

where $y=e^{2\pi iz}$ and $q=e^{2\pi i\tau}$ with $\Im\tau>0$.

The modular properties are easier to see when expressing the latter two functions in terms of $\tau$ and $z$. Notably

$$\theta_1(\tau+1;z)=\theta_1(\tau;z)\ ,\qquad \theta_1\left(-\frac{1}{\tau};\frac{z}{\tau}\right)=-i(-i\tau)^{\frac{1}{2}}\exp\left(\frac{i\pi z^2}{\tau}\right)\theta(\tau;z)\ , \tag{A.34}$$

and

$$\eta(\tau+1)=e^{\frac{i\pi}{12}}\eta(\tau)\ ,\qquad \eta\left(-\frac{1}{\tau}\right)=(-i\tau)^{\frac{1}{2}}\eta(\tau)\ . \tag{A.35}$$

However, since we do not exploit any modular properties of these functions in this thesis, we will use the former convention to express the arguments in terms of fugacities rather than chemical potentials.

One can relate the gamma functions to the theta functions through [168]

$$\prod_{\alpha,\hat{\alpha}\in\mathbb{Z}} \Gamma_N(x+\alpha+\hat{\alpha}\tau|\omega_1,\ldots,\omega_N) = \prod_{\boldsymbol{\ell}\in\mathbb{N}^N} \frac{1}{\theta(q|y)} \ , \tag{A.36}$$

with $y = e^{-2\pi i(x+\boldsymbol{\ell}\cdot\boldsymbol{\omega})}$ and $q = e^{2\pi i\tau}$ up to zeta function regularisation.

### 5d Nekrasov Functions

We may also define an analogous set of finite product formulas associated with partitions. The relevant ones for us are defined on the Omega background, $\mathbb{R}^4_{\epsilon_1,\epsilon_2} \times \mathbb{S}^1_\beta$. These functions depend on the exponentiated Omega background parameters

$$\mathfrak{q} = e^{-\beta\epsilon_1} \ , \qquad \mathfrak{t} = e^{\beta\epsilon_2} \ , \tag{A.37}$$

where $\beta$ is the radius of the additional circle. Note that we have $\epsilon_1 > 0$ and $\epsilon_2 < 0$.

These 5d Nekrasov functions come in two forms. First we define

$$\begin{aligned}\mathcal{N}_{\lambda\mu}(Q;\mathfrak{t},\mathfrak{q}) &= \prod_{i,j=1}^{\infty} \frac{1-Q\mathfrak{t}^{i-1-\lambda^t_j}\mathfrak{q}^{j-\mu_i}}{1-Q\mathfrak{t}^{i-1}\mathfrak{q}^j} \\ &= \prod_{(i,j)\in\lambda} (1-Q\mathfrak{q}^{\lambda_i-j+1}\mathfrak{t}^{\mu^t_j-i}) \prod_{(i,j)\in\mu} (1-Q\mathfrak{q}^{-\mu_i+j}\mathfrak{t}^{-\lambda^t_j+i-1}) \ . \end{aligned} \tag{A.38}$$

Since the dependence of $\mathfrak{t}$ and $\mathfrak{q}$ in these functions does not change throughout the thesis, we shall use the shorthand notation $\mathcal{N}_{\lambda\mu}(Q;\mathfrak{t},\mathfrak{q}) = \mathcal{N}_{\lambda\mu}(Q)$ for brevity.

Note that we can build this function with the specialisation of the MacDonald polynomials through

$$\tilde{Z}_\nu(\mathfrak{t},\mathfrak{q})\tilde{Z}_{\nu^t}(\mathfrak{q},\mathfrak{t}) = \left(-\sqrt{\frac{\mathfrak{q}}{\mathfrak{t}}}\right)^{|\nu|} \mathfrak{t}^{-\frac{\|\nu^t\|^2}{2}}\mathfrak{q}^{-\frac{\|\nu\|^2}{2}}\mathcal{N}_{\nu\nu}(1)^{-1} \ , \tag{A.39}$$

with

$$\widetilde{Z}_\nu(\mathfrak{t},\mathfrak{q}) = \mathfrak{t}^{-\frac{\|\nu^t\|^2}{2}} P_\nu(\mathfrak{t}^{-\rho};\mathfrak{q},\mathfrak{t}) = \prod_{(i,j)\in\nu} \left(1-\mathfrak{t}^{\nu^t_j-i+1}\mathfrak{q}^{\nu_i-j}\right)^{-1} \ . \tag{A.40}$$

For special values the $\mathcal{N}_{\lambda\nu}$ function behaves as a delta function. Namely $\mathcal{N}_{\lambda\emptyset}\left(\frac{\mathfrak{t}}{\mathfrak{q}}\right) = \delta_{\lambda\emptyset} = \mathcal{N}_{\emptyset\lambda}(1)$. This form of the Nekrasov functions satisfy the following identities which have been poached from [73]

$$\mathcal{N}_{\lambda\mu}(Q;\mathfrak{q},\mathfrak{t}) = \mathcal{N}_{\mu^t\lambda^t}\left(\frac{\mathfrak{t}}{\mathfrak{q}}Q;\mathfrak{t},\mathfrak{q}\right) \ ,$$

$$\mathcal{N}_{\lambda\mu}(Q^{-1};\mathfrak{t},\mathfrak{q}) = \left(-Q^{-1}\sqrt{\frac{\mathfrak{q}}{\mathfrak{t}}}\right)^{|\lambda|+|\mu|} \mathfrak{t}^{\frac{\|\mu^t\|^2-\|\lambda^t\|^2}{2}} \mathfrak{q}^{\frac{\|\lambda\|^2-\|\mu\|^2}{2}} \mathcal{N}_{\mu\lambda}\left(Q\frac{\mathfrak{t}}{\mathfrak{q}};\mathfrak{t},\mathfrak{q}\right) . \quad (A.41)$$

The other form has somewhat nicer exchange formulas, and is a much simpler generalisation of the 4d case. We may write

$$\mathcal{N}_{\lambda\mu}(Q;\mathfrak{t},\mathfrak{q}) = \left(Q\sqrt{\frac{\mathfrak{q}}{\mathfrak{t}}}\right)^{\frac{|\lambda|+|\mu|}{2}} \mathfrak{t}^{\frac{\|\mu^t\|^2-\|\lambda^t\|^2}{4}} \mathfrak{q}^{\frac{\|\lambda\|^2-\|\mu\|^2}{4}} \mathrm{N}^{\beta}_{\lambda\mu}(x;\epsilon_1,\epsilon_2) , \quad (A.42)$$

for some $Q = e^{-\beta x}$, where

$$\begin{aligned}\mathrm{N}^{\beta}_{\lambda\mu}(x;\epsilon_1,\epsilon_2) = &\prod_{(i,j)\in\lambda} 2\sinh\frac{\beta}{2}\left[x+\epsilon_1(\lambda_i-j+1)+\epsilon_1(i-\mu^t_j)\right] \\ &\times \prod_{(i,j)\in\mu} 2\sinh\frac{\beta}{2}\left[x+\epsilon_1(j-\mu_i)+\epsilon_2(\lambda^t_j-i+1)\right] . \quad (A.43)\end{aligned}$$

These functions behave very simply in the $\beta\to 0$ limit

$$\mathrm{N}^{\beta}_{\lambda\mu} \xrightarrow{\beta\to 0} \beta^{|\mu|+|\lambda|}\mathrm{N}_{\lambda\mu} , \quad (A.44)$$

and satisfy [73]

$$\begin{aligned}\mathrm{N}^{\beta}_{\lambda\mu}(x;\epsilon_2,\epsilon_1) &= \mathrm{N}^{\beta}_{\lambda^t\mu^t}(x;\epsilon_1,\epsilon_2) , \\ \mathrm{N}^{\beta}_{\lambda\mu}(x;-\epsilon_2,-\epsilon_1) &= \mathrm{N}^{\beta}_{\mu^t\lambda^t}(x-\epsilon_1-\epsilon_2;\epsilon_1,\epsilon_2) , \\ \mathrm{N}^{\beta}_{\lambda\mu}(-x;\epsilon_1,\epsilon_2) &= (-1)^{|\mu|+|\lambda|}\mathrm{N}^{\beta}_{\mu\lambda}(x-\epsilon_1-\epsilon_2;\epsilon_1,\epsilon_2) . \quad (A.45)\end{aligned}$$

## A.3 The Plethystic Exponential

A core tool in the combinatorics of operator counting is the Plethystic exponential. It is a way to take all distinct combinations of the "single-particle" set of operators that we might want to count. For example, the grand canonical partition function for an ideal quantum gas of bosons is given by

$$Z = \prod_i \frac{1}{1-x_i^B} , \quad (A.46)$$

and will produce a counting tool to count all possibly combinations of these bosonic states. This admits a simple rewriting as

$$Z = \prod_i \frac{1}{1-x_i^B} = \prod_i \exp(-\log(1-x_i^B)) = \exp\left(\sum_{n=1}^{\infty}\frac{1}{n}\sum_i (x_i^B)^n\right)$$

$$= \text{P.E.}\left[\sum_i x_i^B\right] , \tag{A.47}$$

where the last line has defined the Plethystic exponential. Suppose we now have a gas of multiple species of bosons and fermions, we would simply write

$$Z = \frac{\prod_j (1-x_j^F)}{\prod_i (1-x_i^B)} = \text{P.E.}\left[\sum_i x_i^B - \sum_j x_j^F\right] , \tag{A.48}$$

where the single letter is simple $z_{\text{single}} = \sum_i x_i^B - \sum_j x_j^F$. Since it has this interpretation in terms of operator combinatorics, this operation appears naturally throughout our discussion of exact partition functions.

Indeed, we can rephrase a lot of the trigonometric and elliptic functions that we have previously defined through the Plethystic exponential. The relevant ones are defined through

$$\begin{aligned}
(x;\mathfrak{p}_1,\dots,\mathfrak{p}_N) &= \text{P.E.}\left[\frac{-x}{(1-\mathfrak{p}_1)\cdots(1-\mathfrak{p}_N)}\right] , \\
\eta(q) &= q^{\frac{1}{24}}\,\text{P.E.}\left[\frac{q}{1-q}\right] , \\
\theta(q|y) &= \text{P.E.}\left[-\frac{y}{1-q}-\frac{qy^{-1}}{1-q}\right] , \\
\theta_1(q|y) &= -iq^{\frac{1}{8}}y^{\frac{1}{2}}\,\text{P.E.}\left[-\frac{q}{1-q}-\frac{y}{1-q}-\frac{qy^{-1}}{1-q}\right] , \\
\Gamma_e(z|\mathfrak{p},\mathfrak{q}) &= \text{P.E.}\left[\frac{z-z^{-1}\mathfrak{p}\mathfrak{q}}{(1-\mathfrak{p})(1-\mathfrak{q})}\right] .
\end{aligned} \tag{A.49}$$

Note that, through this definition, we can perform a quick and dirty analytic continuation without having to appeal to the integral representation. For example

$$\begin{aligned}
(x;\mathfrak{p}_1,\dots,\mathfrak{p}_i^{-1},\dots,\mathfrak{p}_N) &= \text{P.E.}\left[\frac{-x}{(1-\mathfrak{p}_1)\cdots(1-\mathfrak{p}_i^{-1})\cdots(1-\mathfrak{p}_N)}\right] \\
&= \text{P.E.}\left[\frac{x\mathfrak{p}_i}{(1-\mathfrak{p}_1)\cdots(1-\mathfrak{p}_N)}\right] \\
&= (x\mathfrak{p}_i;\mathfrak{p}_1,\dots,\mathfrak{p}_N)^{-1} ,
\end{aligned} \tag{A.50}$$

though caution should be taken when doing this, as it can be confusing when dealing with fugacities rather than chemical potentials.

# Appendix B

# The Racah–Speiser Algorithm and Its Implementation

We use this technical appendix to describe how the Racah–Speiser (RS) algorithm used in Chapter 3 works and how to implement it in a `python3` library that was developed by the author. We will also show how the Racah-Speiser algorithm is related to operator constraints through the use of supercharacters in Chapter 3.

## B.1 Racah–Speiser and Operator Constraints

In this section we provide the details needed to carry out the RS algorithm for the 5d $\mathcal{N} = 1$, 6d $(1, 0)$ and 6d $(2, 0)$ SCAs. Fortunately, we need only discuss three different algebras, $\mathfrak{so}(5)$, $\mathfrak{su}(4)$ and $\mathfrak{su}(2)$. We will assume some familiarity with the description of the RS algorithm from App. B of [37], the notation of which we use. First, we describe the Racah–Speiser algorithm.

### B.1.1 The Racah–Speiser Algorithm

The Racah–Speiser algorithm is a prescription for performing Clebsch-Gordan decompositions of tensor products of representations in representation space. A good description for the procedure can be found in [66] and in Appendix B of [37].

The basic principle is that, for a representation to be valid, its Dynkin labels need to be all greater than or equal to zero, *i.e.* it needs to lie in the dominant Weyl chamber in weight space. We denote this by $\mathcal{R}_{\underline{\Lambda}}$ where $\underline{\Lambda} = [\lambda_1, \ldots, \lambda_r]$. The tensor product is performed through

$$\mathcal{R}_{\underline{\Lambda}} \otimes \mathcal{R}_{\underline{\Lambda}'} \simeq \sum_{\lambda \in V_{\underline{\Lambda}'}} \mathcal{R}_{\underline{\Lambda}+\underline{\lambda}} \,, \tag{B.1}$$

where $V_{\underline{\Lambda}'}$ is the set of states in the module parametrised by $\underline{\Lambda}'$. This will generically result in some of the highest weights in the $\underline{\Lambda} + \underline{\lambda}$ becoming negative. When this happens, one reflects the weight until it lands in the dominant Weyl chamber while keeping track of the number of reflections required. Mathematically

$$\mathcal{R}_{\underline{\lambda}} = \text{sign}(\sigma)\mathcal{R}_{\underline{\lambda}^\sigma} \ , \tag{B.2}$$

where $\underline{\lambda}^\sigma = \sigma(\underline{\lambda} + \rho) - \rho$, with $\rho$ being the half-sum of the positive roots, known as the Weyl vector and $\sigma$ an element of the Weyl group.

The Weyl group can be generated by the set of simple reflections corresponding to the simple roots

$$\sigma_i \underline{\lambda} = \underline{\lambda} - 2\frac{\underline{\lambda} \cdot \alpha_i}{\alpha_i^2}\alpha_i \ , \tag{B.3}$$

and $\text{sign}(\sigma) = (-1)^{N_\sigma}$ which is the number of simple reflections. In practice it is often easier to use reflections with respect to all positive roots, since they carry the same sign, and build the Weyl group from there. The signs introduced by the reflections cancel with other representations for typical Lie algebras (these are interpreted as equations of motion and operator constraints in Lie superalgebras, as discussed in the next section).

It is worth noting that, if is a reflection whose length is odd, such that $\underline{\lambda}^\sigma = \underline{\sigma}$ then we have

$$\mathcal{R}_{\underline{\lambda}} = -\mathcal{R}_{\underline{\lambda}} = 0 \ , \tag{B.4}$$

and the vector is said to be on the boundary of the Weyl chamber. Note that all these zeros with respect to the reflections through the positive roots correspond to the zeros of the Weyl dimension formula

$$\mathrm{d}_{\underline{\lambda}} = \prod_{\alpha \in \Delta_+} \frac{(\underline{\lambda} + \rho) \cdot \alpha}{\rho \cdot \alpha} \ . \tag{B.5}$$

As an example let us consider $\mathfrak{so}(5)$. This is the Lorentz Lie algebra for 5d $\mathcal{N} = 1$ and the $R$-symmetry Lie algebra for 6d $(2, 0)$. The highest weight identifications resulting from Weyl reflections ($\sigma$) are given by

$$\begin{aligned}
[d_1, d_2] &= -[-d_1 - 2, 2d_1 + d_2 + 2] \ , \\
&= -[d_1 + d_2 + 1, -d_2 - 2] \ , \\
&= -[-d_1 - d_2 - 3, d_2] \ , \\
&= -[d_1, -4 - 2d_1 - d_2] \ ,
\end{aligned} \tag{B.6}$$

where we have used the shorthand $\mathcal{R}_{\underline{\lambda}} = \underline{\lambda}$ for ease of reading. We see that $\lambda^\sigma = \lambda$ with $\text{sign}(\sigma) = -$ under the following conditions:

$$d_1 = -1 \ , \quad d_2 = -1 \ , \quad 2d_1 + d_2 = -3 \ , \quad d_1 + d_2 = -2 \ . \tag{B.7}$$

Therefore representations which satisfy any one of these conditions are labelled by a highest weight on the boundary of the Weyl chamber, in which case they have zero multiplicity and need to be removed. Notice that the conditions (B.7) correspond to the zeros of the Weyl dimension formula for irreducible representations of $\mathfrak{so}(5)$:

$$\mathrm{d}(d_1, d_2) = \frac{1}{6}(1 + d_1)(1 + d_2)(2 + d_1 + d_2)(3 + 2d_1 + d_2) \ . \tag{B.8}$$

As an example we can consider a tensor product of two representations of $\mathfrak{so}(5)$ given by $[0, 1]$ and $[1, 0]$. The module of states for the $[1, 0]$ representation is

$$V_{[1,0]} = \{[1, 0], [-1, 2], [0, 0], [1, -2], [-1, 0]\} \ , \tag{B.9}$$

So our product is

$$[0, 1] \otimes [1, 0] = [1, 1] \oplus [-1, 2] \oplus [1, 0] \oplus [2, -2] \oplus [0, 0] \ . \tag{B.10}$$

The states with negative Dynkin weights need to be dealt with. $[-1, 2]$ is on the boundary of the Weyl chamber and is therefore deleted, but $[2, -2]$ is reflected to be $-[0, 0]$ using (B.6). Therefore

$$[0, 1] \otimes [1, 0] = [1, 1] \oplus [0, 1] \ , \tag{B.11}$$

which can be verified by looking at the dimensionality of these representations, *i.e.* $4 \times 5 = 16 + 4$. This very simple recipe can be used repeatedly, for example

$$\begin{aligned} [0, 1] \otimes [1, 0] \otimes [1, 0] &= ([1, 1] \otimes [1, 0]) \oplus ([0, 1] \otimes [1, 0]) \\ &= [2, 1] \oplus [0, 3] \oplus 2 \times [1, 1] \oplus 2 \times [0, 1] \ , \end{aligned} \tag{B.12}$$

with $4 \times 5 \times 5 = 40 + 20 + 2 \times 16 + 2 \times 4$.

Next we consider $\mathfrak{su}(4)$, the Lorentz Lie algebra of 6d theories. The highest weight identifications resulting from Weyl reflections are

$$\begin{aligned} [c_1, c_2, c_3] &= -[-c_1 - 2, c_1 + c_2 + 1, c_3] \ , \\ &= -[c_1 + c_2 + 1, -c_2 - 2, c_2 + c_3 + 1] \ , \\ &= -[c_1, c_2 + c_3 + 1, -c_3 - 2] \ , \end{aligned}$$

$$
\begin{aligned}
&= -[-c_2 - 2, -c_1 - 2, c_1 + c_2 + c_3 + 2] \ , \\
&= -[c_1 + c_2 + c_3 + 2, -c_3 - 2, -c_2 - 2] \ , \\
&= -[-c_2 - c_3 - 3, c_2, -c_1 - c_2 - 3] \ . \qquad \text{(B.13)}
\end{aligned}
$$

The representations we delete are the ones where the following conditions are met:

$$
\begin{aligned}
c_1 = -1 \ , \ \ c_2 = -1 \ , \ \ c_3 = -1 \ , \ \ c_1 + c_2 = -2 \ , \\
c_2 + c_3 - 2 \ , \ \ c_1 + c_2 + c_3 = -3 \ . \qquad \text{(B.14)}
\end{aligned}
$$

Again, these correspond to the zeros of the Weyl dimension formula for $\mathfrak{su}(4)$:

$$
\begin{aligned}
&\mathrm{d}(c_1, c_2, c_3) = \\
&\frac{1}{12}(c_1 + 1)(c_2 + 1)(c_3 + 1)(c_1 + c_2 + 2)(c_2 + c_3 + 2)(c_1 + c_2 + c_3 + 3) \ . \qquad \text{(B.15)}
\end{aligned}
$$

Lastly, the $R$-symmetry Lie algebra for the minimally supersymmetric theories is $\mathfrak{su}(2)$, which involves identifying highest weights via the reflection:

$$
[K] = -[-K - 2] \ . \qquad \text{(B.16)}
$$

We therefore see that the representations we delete are the ones where the following condition is met:

$$
K = -1 \ . \qquad \text{(B.17)}
$$

Clearly this corresponds to the zero for the Weyl dimension formula of $\mathfrak{su}(2)$

$$
\mathrm{d}(K) = K + 1 \ . \qquad \text{(B.18)}
$$

We may now simply combine the set of Weyl reflections appropriate for our SCA in order to dictate which states survive when building representations. Our method will involve generating all possible highest weight states, even in cases where the Dynkin labels become negative, and then performing the RS algorithm. This is akin to using the procedure about, but the representations are generated by fermionic operators and thus have a natural termination.

After performing the RS algorithm there can also be negative representations that have not been cancelled. This only occurs in superalgebras and are interpreted as constraints for operators in the multiplet [37].

### B.1.2 Operator Constraints Through Racah–Speiser

We now further explore this concept. Since $R$-symmetry quantum numbers will not play a role in this analysis we will simplify our discussion by denoting all of their quantum numbers by $R$. The only distinction we need to make is between the $\mathfrak{so}(5)$ and $\mathfrak{su}(4)$ Lorentz Lie algebras. It will be instructive to proceed by first providing an example and then the result in full generality.

Consider the Lorentz vector representation in 6d, $[\Delta; 0, 1, 0; R]$, corresponding to an operator $\mathcal{O}_\mu$. In terms of quantum numbers, its components are given by

$$\begin{aligned} \mathcal{O}_1 \sim [0, 1, 0] \ , \ \ \mathcal{O}_2 \sim [1, -1, 1] \ , \ \ \mathcal{O}_3 \sim [-1, 0, 1] \ , \\ \mathcal{O}_4 \sim [1, 0, -1] \ , \ \ \mathcal{O}_5 \sim [-1, 1, -1] \ , \ \ \mathcal{O}_6 \sim [0, -1, 0] \ . \end{aligned} \tag{B.19}$$

One can envisage a conservation-equation state for this object being $-[\Delta+1; 0, 0, 0; R]$, that is we pick components of $P_\mu$ and $\mathcal{O}_\mu$ such that their combination has Lorentz quantum numbers $[0, 0, 0]$. This combination is

$$P_6\mathcal{O}_1 + P_5\mathcal{O}_2 + P_4\mathcal{O}_3 + P_3\mathcal{O}_4 + P_2\mathcal{O}_5 + P_1\mathcal{O}_6 = 0 \ , \tag{B.20}$$

which can be concisely interpreted as the conservation equation[75]

$$\partial^\mu \mathcal{O}_\mu = 0 \ . \tag{B.21}$$

This is precisely what we see e.g. for the $R$-symmetry currents of the $(1, 0)$ and $(2, 0)$ stress-tensor multiplets, $\mathcal{B}[0, 0, 0; 0]$ and $\mathcal{D}[0, 0, 0; 2, 0]$.

More generally, there are only two ways in which operator constraints manifest themselves in 6d using the approach employed in this thesis. These are

$$\begin{aligned} [\Delta; c_1, c_2, c_3; R] &\to -[\Delta + 1; c_1, c_2 - 1, c_3; R] \ , \\ [\Delta; c_1, 0, 0; R] &\to -[\Delta + 1; c_1 - 1, 0, 1; R] + [\Delta + 2; c_1 - 2, 1, 0; R] \\ &\quad - [\Delta + 3, c_1 - 2, 0, 0; R] \ . \end{aligned} \tag{B.22}$$

The first equation is a contraction of a vector index; this is a conservation equation. The other requires that $c_2 = c_3 = 0$. These are the "generalised Dirac equations" or "generalised equations of motion" mentioned in [109]. When $c_1 = 0$ the primary is a scalar $[2; 0, 0, 0; R]$, and the only state that survives the RS algorithm is $-[4; 0, 0, 0; R]$, namely a Klein–Gordon equation. When $c_1 = 1$ the primary is a fermion $[5/2; 1, 0, 0; R]$, with the only state surviving RS being a Dirac equation $-[7/2; 0, 0, 1; R]$. For $c_1 \geq 2$, all states survive RS, leaving a Bianchi identity for a higher $p$-form field; this is usually

[75] One has that $(P_\mu)^\dagger = P^\mu$. Then it can be straightforwardly checked that $P^\mu = P_{7-\mu}$.

endowed with additional constraints, *i.e.* self-duality in the free-tensor case, $c_1 = 2$.

The analogous states in 5d are given by

$$\begin{aligned}[\Delta; d_1, d_2; R] &\to -[\Delta+1; d_1-1, d_2; R]\ , \\ [\Delta; 0, d_2; R] &\to -[\Delta+1; 0, d_2; R] + [\Delta+2; 1, d_2-2; R] \\ &\quad - [\Delta+3, 0, d_2-2; R]\ . \end{aligned} \tag{B.23}$$

Again, the first expression is the contraction of a vector index and the second expression recovers the Klein–Gordon equation ($d_2 = 0$), the Dirac equation ($d_2 = 1$) and the Bianchi identity ($d_2 \geq 2$).

### B.1.3 Relation to Momentum-Null States

The expressions (B.22) and (B.23) can also be understood from a different perspective. When the superconformal primary saturates both a conformal and a superconformal bound, certain components in the multiplet satisfy operator constraints. One is then instructed to remove appropriate $P_\mu$ generators from the auxiliary Verma-module basis [109]. We call the set contained in the resulting module "reduced states".

Following [109], in 5d $\mathcal{N} = 1$ we are instructed to remove $P_5$ for the multiplets $\mathcal{B}[0,0;0]$ and $\mathcal{D}[0,0;2]$. For $\mathcal{D}[0,0;1]$ one removes $P_3$, $P_4$ and $P_5$. In 6d, where $R = K$ for $\mathcal{N} = 1$ and $R = d_1 + d_2$ for $\mathcal{N} = 2$, one removes $P_6$ from $\mathcal{B}[c_1, c_2, 0; R = 0]$, $\mathcal{C}[c_1, 0, 0; R = 1]$ and $\mathcal{D}[0,0,0; R = 2]$. Likewise we remove $P_3$, $P_5$ and $P_6$ from $\mathcal{C}[c_1, 0, 0; R = 0]$ and $\mathcal{D}[0,0,0; R = 1]$.

The connection between the momentum-null states and the negative-multiplicity representations is clear when considering the supercharacter: Taking the character of all states—including the negative-multiplicity representations—produces the same result as doing so for all reduced states with the appropriate $P$s removed from the basis of generators. Hence it is not appropriate to do both. This is reflected in the fact that the following character identity holds in 6d:

$$\hat{\chi}[\Delta; c_1, c_2, c_3; R] \equiv \chi[\Delta; c_1, c_2, c_3; R] - \chi[\Delta+1; c_1, c_2-1, c_3; R]\ , \tag{B.24}$$

where a hat denotes using the $P$-polynomial from (3.198) after having removed $P_6$; the operator constraints that one recovers in this fashion are conservation equations. Likewise when we remove $P_3$, $P_5$ and $P_6$ we obtain:

$$\begin{aligned}\hat{\chi}[\Delta; c_1, 0, 0; R] \equiv \chi[\Delta; c_1, 0, 0; R] - \chi[\Delta+1; c_1-1, 0, 1; R] + \chi[\Delta+2; c_1-2, 1, 0; R] \\ -\chi[\Delta+3; c_1-2, 0, 0; R]\ .\end{aligned} \tag{B.25}$$

The operator constraints recovered in this case are equations of motion.

In 5d one can make the analogous identifications:

$$\hat{\chi}[\Delta; d_1, d_2; R] \equiv \chi[\Delta; d_1, d_2; R] - \chi[\Delta + 1; d_1 - 1, d_2; R] \,, \tag{B.26}$$

where we have removed $P_5$ from $\hat{\chi}$. Likewise, when we remove $P_3$, $P_4$ and $P_5$ we obtain:

$$\begin{aligned}\hat{\chi}[\Delta; 0, d_2; R] \equiv \chi[\Delta; 0, d_2; R] - \chi[\Delta + 1; 0, d_2; R] + \chi[\Delta + 2; 1, d_2 - 2; R] \\ -\chi[\Delta + 3; 0, d_2 - 2; R] \,.\end{aligned} \tag{B.27}$$

This effectively endows us with a choice for how to treat the operator constraints: We can either take the character of all *reduced* states—not including states associated with constraints—with the appropriate $P_\mu$ removed, or we can take the character of all states (including negative-multiplicity representations) without removing any $P_\mu$.

Note that if one has to remove momenta from the basis of generators for a given multiplet then not every component contained within need have an associated operator constraint. The stress-tensor multiplets in 6d $\mathcal{B}[0,0,0;0]$ and $\mathcal{D}[0,0,0;2,0]$ are examples of such superconformal representations: they contain superconformal descendants which do not contain operators satisfying constraints. However, according to the arguments of the previous subsection, we are still instructed to remove $P_6$ in one approach of evaluating the supercharacter. At first glance this is perplexing.

The resolution to this small puzzle is that the associated characters are actually invariant under the removal of $P_6$. Hence such states satisfy

$$\hat{\chi}[\Delta; c_1, c_2, c_3; R] = \chi[\Delta; c_1, c_2, c_3; R] \,, \tag{B.28}$$

in 6d, or in 5d

$$\hat{\chi}[\Delta; d_1, d_2; R] = \chi[\Delta; d_1, d_2; R] \,. \tag{B.29}$$

The method for evaluating characters of conformal UIRs presented in [109] makes no distinction between states that do/do not obey constraints due to the above invariance.

This knowledge is useful when the absent generators of the Verma module are such that the removed $\mathcal{Q}$s anticommute into $P$s; *c.f.* Sec. 3.2.4, Sec. 3.3.4 and Sec. 3.4.4. In that case, one is effectively projecting out the states associated with operator constraints from the very beginning. Therefore what is generated under these circumstances is the spectrum of *reduced* states. It is still possible to reconstruct the full multiplet spectrum using character relations, as e.g. in (B.24). This lets us recover all the negative-multiplicity states.

## B.2 Supersymmetry Module Building in `python3`

We use this section both as an introduction to the `python` group theory package and to see how the results of Chapter 3 were obtained. To begin we need to first put the `reptheory` package in the same directory as the `python3` notebook. It can be found using the following link https://github.com/JHayling/reptheory, and one should ensure that they have the prerequisite libraries in `python3`: `numpy`, `itertools`, `collections` and `functools`.

### B.2.1 Introduction to `reptheory`

This subsection will effectively serve as the documentation for the `reptheory` library. It can be treated as one single `ipython` environment in *e.g.* the terminal. It should be evaluated in order since certain code snippets rely on previously defined objects.

#### Groups

The main object at the heart of library is the group object. These are initialised as

```
>>> import reptheory as rt
>>> A = rt.AGroup
>>> B = rt.BGroup
```

with similar naming conventions for the other groups. Let us focus on $A_2$ and explore some of the methods associated with the group object. These are

```
>>> A(2).simple_roots(basis='orthogonal')
[[1, -1, 0], [0, -1, 1]]
>>> A(2).positive_roots()
[[2, -1], [1, 1], [-1, 2]]
```

Both the `simple_roots()` and `positive_roots()` have an optional argument `basis` which one can assign to either `'orthogonal'`, `'dynkin'` (the default) or `'alpha'`.

The Weyl vector, Cartan matrix and the quadratic form can be obtained via

```
>>> A(2).weyl_vector()
array([1., 1.])
>>> A(2).cartan_matrix()
array([[ 2, -1],
       [-1,  2]])
>>> A(2).quadratic_form()
array([[0.66666667, 0.33333333],
       [0.33333333, 0.66666667]])
```

with the latter being non-integer since it involves irrational numbers in the definition. Using the quadratic form one can compute an inner product in the Dynkin basis through

```
>>> A(2).inner_product([2, 0], [1, 1])
2.0
```

The last method we discuss is `basis_changer()` whose first argument is the vector, with the second and third being one of `'orthogonal'`, `'dynkin'` or `'alpha'` and does what the name suggests. It converts the vector from the second argument to the third:

```
>>> A(2).basis_changer([1, -1, 0], 'orthogonal', 'dynkin')
array([ 2, -1])
```

### Representations

The next object of importance is the representation object. To initialise it one specifies the group and the Dynkin labels. Let us consider the adjoint representation of $A_2$:

```
>>> R = rt.Representation
>>> adj = R(A, [1, 1])
```

Two straightforward methods are `dim()` which gives the dimension or the representation and `dominant_weights()` which returns the set of dominant weights in the representation:

```
>>> adj.dim()
8
>>> adj.dominant_weights()
[[1, 1], [0, 0]]
```

If one simply wants to see the list of weights in a representation and not perform any algebraic manipulations then the method is just `print_weights()`. The other option is to call `weight_system()` with the optional argument `form` which allows for the choice of data structure: `'list'` (default), `'array'` or `'dict'`. The latter returns a dictionary indexed by level, *e.g.* `'Level 2'`.

```
>>> adj.print_weights()
Level 0:  (1, 1)
Level 1:  (-1, 2) (2, -1)
Level 2:  (0, 0) (0, 0)
Level 3:  (-2, 1) (1, -2)
Level 4:  (-1, -1)
>>> adj.weight_system()
[(1, 1), (-1, 2), (2, -1), (0, 0), (0, 0), (-2, 1), (1, -2),
 (-1, -1)]
>>> weights = weight_system(form='dict')
>>> weights['Level 3']
[(-2, 1), (1, -2)]
```

To find the level of a state in a representation we use the method

```
>>> adj.weight_level([-2, 1])
3
```

Note that this needs to be in the Dynkin basis.

Another class that is important in this discussion is the `ProductRep`, which allows us to define representations of products of multiple different representations. For example, let us consider the product representation of the 6d $\mathcal{N} = (1, 0)$ supercharge. It is in the spinor representation of both $\mathfrak{su}(4)$ and $\mathfrak{su}(2)_R$. The full module is then

```
>>> Q = rt.ProductRep((A, [1, 0, 0]), (A, [1]))
>>> Q.build()
array([[ 1,  0,  0,  1],
       [ 1,  0,  0, -1],
       [-1,  1,  0,  1],
       [-1,  1,  0, -1],
       [ 0, -1,  1,  1],
       [ 0, -1,  1, -1],
       [ 0,  0, -1,  1],
       [ 0,  0, -1, -1]])
```

Once the product representation has been established, namely the groups and representations in a specific order, one can start performing advanced operations on these compound vectors. For example, reflecting states that are not in the dominant Weyl chamber of the compound representation space and noting the number of reflections required:

```
>>> Q.product_racah([-1, 0, 2, 1])
[[-1, 0, 2, 1], 'del']
>>> Q.product_racah([-2, 1, 2, 1])
[[0, 0, 2, 1], 1]
>>> Q.product_racah([-2, 1, 2, -2])
[[0, 0, 2, 0], 2]
```

The first item is the reflected vector and the second is either `'del'`, indicating that it is on the boundary and should therefore be deleted, or the number of reflections, and hence the sign of the multiplicity.

### Tensor products

There are two ways to perform tensor products. One is the class `RepTensor` which performs simple tensor products between two representation objects. The other is `ListTensor` which takes a group object and a list of representations that one wants to tensor together. They both have the same method `decompose` with the optional argument `form`. Two options specify the data structure: `'list'` and `'dict'`, which is a dictionary whose keys are the states and values are the multiplicities. The third option is a simple `'print'` option. They are demonstrated below with the examples given in Section B.1.1.

```
>>> r1 = R(B, [0, 1])
>>> r2 = R(B, [1, 0])
>>> T = rt.RepTensor(r1, r2)
>>> T.decompose(form='list')
[(1, 1), (0, 1)]
>>> T.decompose(form='print')
(1, 1) ⊕ (0, 1)
```

and for the `ListTensor`:

```
>>> LT = rt.ListTensor(B, [[0, 1], [1, 0], [1, 0]])
>>> LT.decompose()
{(2, 1): 1, (0, 3): 1, (1, 1): 2, (0, 1): 2}
>>> LT.decompose(form='print')
(2, 1) ⊕ (0, 3) ⊕ 2x(1, 1) ⊕ 2x(0, 1)
```

### B.2.2 Superconformal Module Building

The class core to this section is `SUSYModule`. It is a very effective and simple way of performing implementing the RS algorithm for the multiplets of Chapter 3, and in other references that are similar in spirit [1,35,37].

To construct a multiplet, one first needs to initialise the supercharges. That is, one needs to specify the representations of algebras that the supercharges transform in as `ProductRep` objects. These, and the highest weight state, are needed to instantiate the `SUSYModule` object. As an example let us take an unconstrained 6d $\mathcal{N} = (1,0)$ long multiplet with highest weight $[0,0,0,0]$.

```
>>> Qs = rt.ProductRep((A, [1]), (A, [1, 0, 0]))
>>> sm = rt.SUSYModule([0, 0, 0, 0], Qs)
```

There two methods to generate the module. The first is `build_module()` which returns an iterator data structure. This is preferable if one wants to only access the states that are in the earlier levels of the multiplet, since for theories with sixteen supercharges the number of states grows at a tremendous rate. Note that, since it is an iterator, once one iterates through (either with a `for` loop or a `next(sm)` command) the level, one needs to rebuild the module to access previously seen levels due to how iterators work in `python`.

The second, more user friendly, method is the `return_module()`. This is more intensive since it generates the entire module before it returns anything. Its optional

argument `form` can be either `'print'` (default) which prints the states level by level without returning anything, or `'dict'` which returns a dictionary whose keys are in the form `'Level x'`. The latter is more memory intensive since it stores all the states, but is better for repeated analysis since this method is built on the iterator, hence one does not need to repeatedly generate the module.

```
>>> sm.return_module()
Level 0:  (0, 0, 0, 0)
Level 1:  (1, 1, 0, 0)
Level 2:  (2, 0, 1, 0) ⊕ (0, 2, 0, 0)
Level 3:  (3, 0, 0, 1) ⊕ (1, 1, 1, 0)
Level 4:  (4, 0, 0, 0) ⊕ (2, 1, 0, 1) ⊕ (0, 0, 2, 0)
Level 5:  (3, 1, 0, 0) ⊕ (1, 0, 1, 1)
Level 6:  (2, 0, 1, 0) ⊕ (0, 0, 0, 2)
Level 7:  (1, 0, 0, 1)
Level 8:  (0, 0, 0, 0)
```

Next we can look at a module with level one constraints. Given that we can pick any multiplet of any superconformal algebra, we choose the 4d $\mathcal{N} = 4$ stress tensor multiplet. This also serves to a highlight a subtlety when dealing with theories that have supercharges in different representations of the same algebra. We need to instantiate the module with two sets of supercharges, the ones transforming in the $(\mathbf{4}, \mathbf{2}, \mathbf{1})$ of the $\mathfrak{su}(4)_R \oplus \mathfrak{su}(2)_1 \oplus \mathfrak{su}(2)_2$ subalgebra and the ones transforming in the $(\bar{\mathbf{4}}, \mathbf{1}, \mathbf{2})$. This is done via

```
>>> Qs = rt.ProductRep((A, [1, 0, 0]), (A, [1]), (A, [0]))
>>> QBs = rt.ProductRep((A, [0, 0, 1]), (A, [0]), (A, [1]))
>>> sm = rt.SUSYModule([0, 2, 0, 0, 0], Qs, QBs)
```

The next step is to add the relevant constraints. We use the `add_constraints()` method. The first argument is `level` which is the level at which the constraints are implement, *i.e.* the order or the monomial of the null state. The second argument `nullstates` is the set of combinations of states that are null. According to [37], the null states come from $\mathcal{Q}^{\mathbf{1}}_{\alpha}$, $\mathcal{Q}^{\mathbf{2}}_{\alpha}$, $\widetilde{\mathcal{Q}}_{\mathbf{4}\dot{\alpha}}$ and $\widetilde{\mathcal{Q}}_{\mathbf{3}\dot{\alpha}}$. This is implemented below

```
>>> Q_constraints = [(1, 0, 0, 1, 0), (1, 0, 0, -1, 0),
... (-1, 1, 0, 1, 0), (-1, 1, 0, -1, 0)]
>>> QB_constraints = [(0, 0, 1, 0, 1), (0, 0, 1, 0, -1),
... (0, 1, -1, 0, 1), (0, 1, -1, 0, -1)]
>>> sm.add_constraints(1, Q_constraints)
>>> sm.add_constraints(1, QB_constraints)
>>> sm.return_module(form='print')
Level 0:  (0, 2, 0, 0, 0)
Level 1:  (0, 1, 1, 1, 0) ⊕ (1, 1, 0, 0, 1)
Level 2:  (0, 0, 2, 0, 0) ⊕ (0, 1, 0, 2, 0) ⊕ (1, 0, 1, 1, 1) ⊕
(2, 0, 0, 0, 0) ⊕ (0, 1, 0, 0, 2)
Level 3:  (0, 0, 1, 1, 0) ⊕ (1, 0, 0, 2, 1) ⊕ (1, 0, 0, 0, 1) ⊕
(0, 0, 1, 1, 2)
Level 4:  2x(0, 0, 0, 0, 0) ⊖ (1, 0, 1, 0, 0) ⊕ (0, 0, 0, 2, 2)
Level 5:  ⊖ (1, 0, 0, 1, 0) ⊖ (0, 0, 1, 0, 1)
Level 6:  ⊖ (0, 0, 0, 1, 1)
```

Lastly we consider higher order constraints. The example we consider now is the $\mathcal{D}[0,0,0;0,1]$ multiplet from Section 3.4 in 6d $(2,0)$ theory. Recall that this has the level one constraints that $\mathcal{Q}_{\mathbf{1}a}$ for all $a$ annihilate the primary, but also that $\mathcal{Q}_{\mathbf{2}a}\mathcal{Q}_{\mathbf{2}b}$ annihilate the primary for all $a \neq b$. This is set up through

```
>>> Qs = rt.ProductRep((B, [0, 1]), (A, [1, 0, 0]))
>>> sm = rt.SUSYModule([0, 1, 0, 0, 0], Qs)
>>> L1_constraints = [(0, 1, 1, 0, 0), (0, 1, -1, 1, 0),
... (0, 1, 0, -1, 1), (0, 1, 0, 0, -1)]
>>> sm.add_constraints(1, L1_constraints)
```

One can either manually write out the level two constraints or we can use the `itertools` module.

```
>>> from itertools import combinations
>>> qs = [(1, -1, 1, 0, 0), (1, -1, -1, 1, 0), (1, -1, 0, -1, 1),
...  (1, -1, 0, 0, -1)]
>>> L2_constraints = combinations(qs, 2)
>>> sm.add_constraints(2, L2_constraints)
```

For ease of reading and to demonstrate the dictionary approach:

```
>>> mult_dict = sm.return_module(form='dict')
>>> print(mult_dict['Level 0'])
{(0, 1, 0, 0, 0): 1}
>>> print(mult_dict['Level 1'])
{(1, 0, 1, 0, 0): 1, (0, 0, 1, 0, 0): 1}
>>> print(mult_dict['Level 2'])
{(0, 1, 2, 0, 0): 1}
```

We conclude this appendix with some comments. First is that, as stressed, if one is only interested in the early levels of the multiplet then one should use the iterator approach with the `build_module()` method. The second is that, for higher amounts of supersymmetry and low numbers of level one constraints, these computations can take some time. Therefore it is always preferable to rephrase things using level one constraints if possible.

# Bibliography


[1] M. Buican, J. Hayling, and C. Papageorgakis, *Aspects of Superconformal Multiplets in $D > 4$*, *JHEP* **11** (2016) 091, [arXiv:1606.0081].

[2] J. Hayling, C. Papageorgakis, E. Pomoni, and D. Rodríguez-Gómez, *Exact Deconstruction of the 6D (2,0) Theory*, *JHEP* **06** (2017) 072, [arXiv:1704.0298].

[3] J. Hayling, R. Panerai, and C. Papageorgakis, *Deconstructing Little Strings with $\mathcal{N} = 1$ Gauge Theories on Ellipsoids*, *SciPost Phys.* **4** (2018), no. 6 042, [arXiv:1803.0617].

[4] J. Hayling, V. Niarchos, and C. Papageorgakis, *Deconstructing Defects*, *JHEP* **02** (2019) 067, [arXiv:1809.1048].

[5] W. Taylor and Y.-N. Wang, *The F-theory geometry with most flux vacua*, *JHEP* **12** (2015) 164, [arXiv:1511.0320].

[6] O. Aharony, O. Bergman, D. L. Jafferis, and J. Maldacena, *N=6 superconformal Chern-Simons-matter theories, M2-branes and their gravity duals*, *JHEP* **10** (2008) 091, [arXiv:0806.1218].

[7] A. Strominger, *Open p-branes*, *Phys. Lett.* **B383** (1996) 44–47, [hep-th/9512059]. [,116(1995)].

[8] C. M. Hull and P. K. Townsend, *Unity of superstring dualities*, *Nucl. Phys.* **B438** (1995) 109–137, [hep-th/9410167]. [,236(1994)].

[9] J. Bagger and N. Lambert, *Modeling Multiple M2's*, *Phys. Rev.* **D75** (2007) 045020, [hep-th/0611108].

[10] A. Gustavsson, *Algebraic structures on parallel M2-branes*, *Nucl. Phys.* **B811** (2009) 66–76, [arXiv:0709.1260].

[11] N. Lambert and C. Papageorgakis, *Nonabelian (2,0) Tensor Multiplets and 3-algebras*, *JHEP* **08** (2010) 083, [arXiv:1007.2982].

[12] A. A. Belavin, A. M. Polyakov, and A. B. Zamolodchikov, *Infinite Conformal Symmetry in Two-Dimensional Quantum Field Theory*, *Nucl. Phys.* **B241** (1984) 333–380. [,605(1984)].

[13] S. El-Showk, M. F. Paulos, D. Poland, S. Rychkov, D. Simmons-Duffin, and A. Vichi, *Solving the 3D Ising Model with the Conformal Bootstrap*, *Phys. Rev.* **D86** (2012) 025022, [arXiv:1203.6064].

[14] C. Beem, L. Rastelli, and B. C. van Rees, *The $\mathcal{N} = 4$ Superconformal Bootstrap*, *Phys. Rev. Lett.* **111** (2013) 071601, [arXiv:1304.1803].

[15] C. Beem, M. Lemos, L. Rastelli, and B. C. van Rees, *The (2, 0) superconformal bootstrap*, *Phys. Rev.* **D93** (2016), no. 2 025016, [arXiv:1507.0563].

[16] D. Gaiotto, *N=2 dualities*, *JHEP* **08** (2012) 034, [arXiv:0904.2715].

[17] L. F. Alday, D. Gaiotto, and Y. Tachikawa, *Liouville Correlation Functions from Four-dimensional Gauge Theories*, *Lett. Math. Phys.* **91** (2010) 167–197, [arXiv:0906.3219].

[18] C. Cordova and D. L. Jafferis, *Complex Chern-Simons from M5-branes on the Squashed Three-Sphere*, *JHEP* **11** (2017) 119, [arXiv:1305.2891].

[19] N. Lambert, C. Papageorgakis, and M. Schmidt-Sommerfeld, *M5-Branes, D4-Branes and Quantum 5D super-Yang-Mills*, *JHEP* **1101** (2011) 083, [arXiv:1012.2882].

[20] M. R. Douglas, *On D=5 super Yang-Mills theory and (2,0) theory*, *JHEP* **02** (2011) 011, [arXiv:1012.2880].

[21] H.-C. Kim, S. Kim, E. Koh, K. Lee, and S. Lee, *On instantons as Kaluza-Klein modes of M5-branes*, *JHEP* **12** (2011) 031, [arXiv:1110.2175].

[22] N. Arkani-Hamed, A. G. Cohen, and H. Georgi, *(De)constructing dimensions*, *Phys. Rev. Lett.* **86** (2001) 4757–4761, [hep-th/0104005].

[23] N. Arkani-Hamed, A. G. Cohen, D. B. Kaplan, A. Karch, and L. Motl, *Deconstructing (2,0) and little string theories*, *JHEP* **01** (2003) 083, [hep-th/0110146].

[24] C. Beem, L. Rastelli, and B. C. van Rees, *$\mathcal{W}$ symmetry in six dimensions*, *JHEP* **05** (2015) 017, [arXiv:1404.1079].

[25] A. Gorantis, J. A. Minahan, and U. Naseer, *Analytic continuation of dimensions in supersymmetric localization*, *JHEP* **02** (2018) 070, [arXiv:1711.0566].

[26] D. Simmons-Duffin, *The Conformal Bootstrap*, in *Proceedings, Theoretical Advanced Study Institute in Elementary Particle Physics: New Frontiers in Fields and Strings (TASI 2015): Boulder, CO, USA, June 1-26, 2015*, pp. 1–74, 2017. arXiv:1602.0798.

[27] S. Rychkov, *EPFL Lectures on Conformal Field Theory in D¿= 3 Dimensions*. SpringerBriefs in Physics. 2016.

[28] C. Montonen and D. I. Olive, *Magnetic Monopoles as Gauge Particles?*, *Phys. Lett.* **B72** (1977) 117.

[29] P. Goddard, J. Nuyts, and D. I. Olive, *Gauge Theories and Magnetic Charge*, *Nucl. Phys.* **B125** (1977) 1.

[30] E. Witten and D. I. Olive, *Supersymmetry Algebras That Include Topological Charges*, *Phys. Lett.* **B78** (1978) 97.

[31] N. Seiberg and E. Witten, *Monopoles, duality and chiral symmetry breaking in N=2 supersymmetric QCD*, *Nucl. Phys.* **B431** (1994) 484–550, [hep-th/9408099].

[32] P. C. Argyres and N. Seiberg, *S-duality in N=2 supersymmetric gauge theories*, *JHEP* **12** (2007) 088, [arXiv:0711.0054].

[33] D. Green, Z. Komargodski, N. Seiberg, Y. Tachikawa, and B. Wecht, *Exactly Marginal Deformations and Global Symmetries*, *JHEP* **06** (2010) 106, [arXiv:1005.3546].

[34] W. Nahm, *Supersymmetries and their Representations*, *Nucl. Phys.* **B135** (1978) 149.

[35] C. Cordova, T. T. Dumitrescu, and K. Intriligator, *Multiplets of Superconformal Symmetry in Diverse Dimensions*, *JHEP* **03** (2019) 163, [arXiv:1612.0080].

[36] S. Minwalla, *Restrictions imposed by superconformal invariance on quantum field theories*, *Adv. Theor. Math. Phys.* **2** (1998) 781–846, [hep-th/9712074].

[37] F. A. Dolan and H. Osborn, *On short and semi-short representations for four-dimensional superconformal symmetry*, *Annals Phys.* **307** (2003) 41–89, [hep-th/0209056].

[38] V. K. Dobrev and V. B. Petkova, *All Positive Energy Unitary Irreducible Representations of Extended Conformal Supersymmetry*, *Phys. Lett.* **B162** (1985) 127–132.

[39] J. Kinney, J. M. Maldacena, S. Minwalla, and S. Raju, *An Index for 4 dimensional super conformal theories*, *Commun.Math.Phys.* **275** (2007) 209–254, [hep-th/0510251].

[40] C. Romelsberger, *Counting chiral primaries in N = 1, d=4 superconformal field theories*, *Nucl. Phys.* **B747** (2006) 329–353, [hep-th/0510060].

[41] F. A. Dolan and H. Osborn, *Applications of the Superconformal Index for Protected Operators and q-Hypergeometric Identities to N=1 Dual Theories*, *Nucl. Phys.* **B818** (2009) 137–178, [arXiv:0801.4947].

[42] J. Bhattacharya, S. Bhattacharyya, S. Minwalla, and S. Raju, *Indices for Superconformal Field Theories in 3,5 and 6 Dimensions*, *JHEP* **0802** (2008) 064, [arXiv:0801.1435].

[43] E. Witten, *Constraints on Supersymmetry Breaking*, *Nucl. Phys.* **B202** (1982) 253.

[44] G. Festuccia and N. Seiberg, *Rigid Supersymmetric Theories in Curved Superspace*, *JHEP* **06** (2011) 114, [arXiv:1105.0689].

[45] B. Assel, D. Cassani, and D. Martelli, *Localization on Hopf surfaces*, *JHEP* **08** (2014) 123, [arXiv:1405.5144].

[46] O. Aharony, J. Marsano, S. Minwalla, K. Papadodimas, and M. Van Raamsdonk, *The Hagedorn - deconfinement phase transition in weakly coupled large N gauge theories*, *Adv. Theor. Math. Phys.* **8** (2004) 603–696, [hep-th/0310285]. [,161(2003)].

[47] S. Nawata, *Localization of N=4 Superconformal Field Theory on $S^1$ x $S^3$ and Index*, *JHEP* **11** (2011) 144, [arXiv:1104.4470].

[48] A. Gadde, L. Rastelli, S. S. Razamat, and W. Yan, *Gauge Theories and Macdonald Polynomials*, *Commun. Math. Phys.* **319** (2013) 147–193, [arXiv:1110.3740].

[49] A. Gadde, E. Pomoni, L. Rastelli, and S. S. Razamat, *S-duality and 2d Topological QFT*, *JHEP* **03** (2010) 032, [arXiv:0910.2225].

[50] L. Rastelli and S. S. Razamat, *The supersymmetric index in four dimensions*, *J. Phys.* **A50** (2017), no. 44 443013, [arXiv:1608.0296].

[51] E. Witten, *Topological Quantum Field Theory*, *Commun. Math. Phys.* **117** (1988) 353.

[52] N. A. Nekrasov, *Seiberg-Witten prepotential from instanton counting*, *Adv. Theor. Math. Phys.* **7** (2004) 831–864, [hep-th/0206161].

[53] V. Pestun, *Localization of gauge theory on a four-sphere and supersymmetric Wilson loops*, *Commun. Math. Phys.* **313** (2012) 71–129, [arXiv:0712.2824].

[54] E. Gerchkovitz, J. Gomis, and Z. Komargodski, *Sphere Partition Functions and the Zamolodchikov Metric*, *JHEP* **11** (2014) 001, [arXiv:1405.7271].

[55] A. Kapustin, B. Willett, and I. Yaakov, *Exact Results for Wilson Loops in Superconformal Chern-Simons Theories with Matter*, *JHEP* **03** (2010) 089, [arXiv:0909.4559].

[56] V. Pestun et al., *Localization Techniques in Quantum Field Theories*, arXiv:1608.0295.

[57] N. Hama, K. Hosomichi, and S. Lee, *Notes on SUSY Gauge Theories on Three-Sphere*, *JHEP* **03** (2011) 127, [arXiv:1012.3512].

[58] M. Baggio, V. Niarchos, and K. Papadodimas, *Exact correlation functions in $SU(2)$ $\mathcal{N} = 2$ superconformal QCD*, *Phys. Rev. Lett.* **113** (2014), no. 25 251601, [arXiv:1409.4217].

[59] M. Baggio, V. Niarchos, and K. Papadodimas, *On exact correlation functions in SU(N) $\mathcal{N} = 2$ superconformal QCD*, *JHEP* **11** (2015) 198, [arXiv:1508.0307].

[60] M. Baggio, V. Niarchos, K. Papadodimas, and G. Vos, *Large-N correlation functions in $\mathcal{N} = 2$ superconformal QCD*, arXiv:1610.0761.

[61] D. Rodriguez-Gomez and J. G. Russo, *Large N Correlation Functions in Superconformal Field Theories*, *JHEP* **06** (2016) 109, [arXiv:1604.0741].

[62] A. Pini, D. Rodriguez-Gomez, and J. G. Russo, *Large N correlation functions in $\mathcal{N} = 2$ superconformal quivers*, arXiv:1701.0231.

[63] M. Billo, F. Fucito, A. Lerda, J. F. Morales, Ya. S. Stanev, and C. Wen, *Two-point Correlators in N=2 Gauge Theories*, arXiv:1705.0290.

[64] A. Bourget, D. Rodriguez-Gomez, and J. G. Russo, *A limit for large R-charge correlators in $\mathcal{N} = 2$ theories*, *JHEP* **05** (2018) 074, [arXiv:1803.0058].

[65] A. Bourget, D. Rodriguez-Gomez, and J. G. Russo, *Universality of Toda equation in $\mathcal{N} = 2$ superconformal field theories*, *JHEP* **02** (2019) 011, [arXiv:1810.0084].

[66] J. Fuchs and C. Schweigert, *Symmetries, Lie Algebras and Representations: A Graduate Course for Physicists*. Cambridge Monographs on Mathematical Physics. Cambridge University Press, 2003.

[67] N. Hama, K. Hosomichi, and S. Lee, *SUSY Gauge Theories on Squashed Three-Spheres*, *JHEP* **05** (2011) 014, [arXiv:1102.4716].

[68] A. Iqbal, C. Kozcaz, and C. Vafa, *The Refined topological vertex*, *JHEP* **10** (2009) 069, [hep-th/0701156].

[69] N. Nekrasov and A. Okounkov, *Seiberg-Witten theory and random partitions*, hep-th/0306238.

[70] G. Lockhart and C. Vafa, *Superconformal Partition Functions and Non-perturbative Topological Strings*, arXiv:1210.5909.

[71] B. Haghighat, A. Iqbal, C. Kozçaz, G. Lockhart, and C. Vafa, *M-Strings*, *Commun. Math. Phys.* **334** (2015), no. 2 779–842, [arXiv:1305.6322].

[72] L. Bao, V. Mitev, E. Pomoni, M. Taki, and F. Yagi, *Non-Lagrangian Theories from Brane Junctions*, *JHEP* **01** (2014) 175, [arXiv:1310.3841].

[73] V. Mitev and E. Pomoni, *Toda 3-Point Functions From Topological Strings*, *JHEP* **06** (2015) 049, [arXiv:1409.6313].

[74] V. Mitev, E. Pomoni, M. Taki, and F. Yagi, *Fiber-Base Duality and Global Symmetry Enhancement*, *JHEP* **04** (2015) 052, [arXiv:1411.2450].

[75] H. Hayashi, H.-C. Kim, and T. Nishinaka, *Topological strings and 5d $T_N$ partition functions*, *JHEP* **06** (2014) 014, [arXiv:1310.3854].

[76] H. Hayashi and K. Ohmori, *5d/6d DE instantons from trivalent gluing of web diagrams*, *JHEP* **06** (2017) 078, [arXiv:1702.0726].

[77] S.-S. Kim, M. Taki, and F. Yagi, *Tao Probing the End of the World*, *PTEP* **2015** (2015), no. 8 083B02, [arXiv:1504.0367].

[78] M. Taki, *Refined Topological Vertex and Instanton Counting*, *JHEP* **03** (2008) 048, [arXiv:0710.1776].

[79] L. Bao, E. Pomoni, M. Taki, and F. Yagi, *M5-Branes, Toric Diagrams and Gauge Theory Duality*, *JHEP* **04** (2012) 105, [arXiv:1112.5228].

[80] A. Iqbal and C. Vafa, *BPS Degeneracies and Superconformal Index in Diverse Dimensions*, *Phys. Rev.* **D90** (2014), no. 10 105031, [arXiv:1210.3605].

[81] T. J. Hollowood, A. Iqbal, and C. Vafa, *Matrix models, geometric engineering and elliptic genera*, *JHEP* **03** (2008) 069, [hep-th/0310272].

[82] J. Kim, S. Kim, and K. Lee, *Little strings and T-duality*, *JHEP* **02** (2016) 170, [arXiv:1503.0727].

[83] S. Hohenegger, A. Iqbal, and S.-J. Rey, *Instanton-monopole correspondence from M-branes on $\mathbb{S}^1$ and little string theory*, *Phys. Rev.* **D93** (2016), no. 6 066016, [arXiv:1511.0278].

[84] N. Hama and K. Hosomichi, *Seiberg-Witten Theories on Ellipsoids*, *JHEP* **09** (2012) 033, [arXiv:1206.6359]. [Addendum: JHEP10,051(2012)].

[85] C. Beem, M. Lemos, P. Liendo, W. Peelaers, L. Rastelli, and B. C. van Rees, *Infinite Chiral Symmetry in Four Dimensions*, *Commun. Math. Phys.* **336** (2015), no. 3 1359–1433, [arXiv:1312.5344].

[86] C. Cordova, T. T. Dumitrescu, and K. Intriligator, *Anomalies, Renormalization Group Flows, and the a-Theorem in Six-Dimensional (1,0) Theories*, arXiv:1506.0380.

[87] J. Louis and S. Lüst, *Supersymmetric $AdS_7$ backgrounds in half-maximal supergravity and marginal operators of (1, 0) SCFTs*, *JHEP* **10** (2015) 120, [arXiv:1506.0804].

[88] C. Cordova, T. T. Dumitrescu, and K. Intriligator, *Deformations of Superconformal Theories*, arXiv:1602.0121.

[89] M. Cornagliotto, M. Lemos, and V. Schomerus, *Long Multiplet Bootstrap*, *JHEP* **10** (2017) 119, [arXiv:1702.0510].

[90] V. K. Dobrev and V. B. Petkova, *On the Group Theoretical Approach to Extended Conformal Supersymmetry: Classification of Multiplets*, *Lett. Math. Phys.* **9** (1985) 287–298.

[91] V. K. Dobrev and V. B. Petkova, *Group Theoretical Approach to Extended Conformal Supersymmetry: Function Space Realizations and Invariant Differential Operators*, *Fortsch. Phys.* **35** (1987) 537.

[92] V. K. Dobrev, *Positive energy unitary irreducible representations of $D = 6$ conformal supersymmetry*, *J. Phys.* **A35** (2002) 7079–7100, [hep-th/0201076].

[93] E. Witten, *Some comments on string dynamics*, in *Future perspectives in string theory. Proceedings, Conference, Strings'95, Los Angeles, USA, March 13-18, 1995*, 1995. hep-th/9507121.

[94] N. Seiberg, *Five-dimensional SUSY field theories, nontrivial fixed points and string dynamics*, *Phys. Lett.* **B388** (1996) 753–760, [hep-th/9608111].

[95] D. R. Morrison and N. Seiberg, *Extremal transitions and five-dimensional supersymmetric field theories*, *Nucl. Phys.* **B483** (1997) 229–247, [hep-th/9609070].

[96] M. R. Douglas, S. H. Katz, and C. Vafa, *Small instantons, Del Pezzo surfaces and type I-prime theory*, *Nucl. Phys.* **B497** (1997) 155–172, [hep-th/9609071].

[97] K. A. Intriligator, D. R. Morrison, and N. Seiberg, *Five-dimensional supersymmetric gauge theories and degenerations of Calabi-Yau spaces*, *Nucl. Phys.* **B497** (1997) 56–100, [hep-th/9702198].

[98] J. J. Heckman, D. R. Morrison, T. Rudelius, and C. Vafa, *Atomic Classification of 6D SCFTs*, *Fortsch. Phys.* **63** (2015) 468–530, [arXiv:1502.0540].

[99] L. Bhardwaj, *Classification of 6d $\mathcal{N} = (1, 0)$ gauge theories*, *JHEP* **11** (2015) 002, [arXiv:1502.0659].

[100] C.-M. Chang and Y.-H. Lin, *Carving Out the End of the World or (Superconformal Bootstrap in Six Dimensions)*, *JHEP* **08** (2017) 128, [arXiv:1705.0539].

[101] N. Bobev, E. Lauria, and D. Mazac, *Superconformal Blocks for SCFTs with Eight Supercharges*, *JHEP* **07** (2017) 061, [arXiv:1705.0859].

[102] C. Cordova and K. Diab, *Universal Bounds on Operator Dimensions from the Average Null Energy Condition*, *JHEP* **02** (2018) 131, [arXiv:1712.0108].

[103] C.-M. Chang, M. Fluder, Y.-H. Lin, and Y. Wang, *Spheres, Charges, Instantons, and Bootstrap: A Five-Dimensional Odyssey*, *JHEP* **03** (2018) 123, [arXiv:1710.0841].

[104] X. Zhou, *On Mellin Amplitudes in SCFTs with Eight Supercharges*, *JHEP* **07** (2018) 147, [arXiv:1804.0239].

[105] K. Sen and M. Yamazaki, *Pology of Superconformal Blocks*, arXiv:1810.0126.

[106] A. Passias and P. Richmond, *Perturbing $AdS_6 \times_w S^4$: linearised equations and spin-2 spectrum*, *JHEP* **07** (2018) 058, [arXiv:1804.0972].

[107] M. Gutperle, C. F. Uhlemann, and O. Varela, *Massive spin 2 excitations in $AdS_6 \times S^2$ warped spacetimes*, *JHEP* **07** (2018) 091, [arXiv:1805.1191].

[108] Y. Lozano, N. T. Macpherson, and J. Montero, *$AdS_6$ T-duals and type IIB $AdS_6\times S^2$ geometries with 7-branes*, *JHEP* **01** (2019) 116, [arXiv:1810.0809].

[109] F. A. Dolan, *Character formulae and partition functions in higher dimensional conformal field theory*, *J. Math. Phys.* **47** (2006) 062303, [hep-th/0508031].

[110] J. Penedones, E. Trevisani, and M. Yamazaki, *Recursion Relations for Conformal Blocks*, arXiv:1509.0042.

[111] M. Yamazaki, *Comments on Determinant Formulas for General CFTs*, arXiv:1601.0407.

[112] Y. Oshima and M. Yamazaki, *Determinant Formula for Parabolic Verma Modules of Lie Superalgebras*, arXiv:1603.0670.

[113] M. Bianchi, F. A. Dolan, P. J. Heslop, and H. Osborn, *N=4 superconformal characters and partition functions*, *Nucl. Phys.* **B767** (2007) 163–226, [hep-th/0609179].

[114] H.-C. Kim, S.-S. Kim, and K. Lee, *5-dim Superconformal Index with Enhanced En Global Symmetry*, *JHEP* **1210** (2012) 142, [arXiv:1206.6781].

[115] D. RodrÃguez-GÃ³mez and G. Zafrir, *On the 5d instanton index as a Hilbert series*, *Nucl. Phys.* **B878** (2014) 1–11, [arXiv:1305.5684].

[116] Y. Tachikawa, *Instanton operators and symmetry enhancement in 5d supersymmetric gauge theories*, *PTEP* **2015** (2015), no. 4 043B06, [arXiv:1501.0103].

[117] C. Beem and A. Gadde, *The $N = 1$ superconformal index for class S fixed points*, *JHEP* **04** (2014) 036, [arXiv:1212.1467].

[118] A. Passias and A. Tomasiello, *Spin-2 spectrum of six-dimensional field theories*, arXiv:1604.0428.

[119] S. Benvenuti, G. Bonelli, M. Ronzani, and A. Tanzini, *Symmetry enhancements via 5d instantons, qW -algebrae and (1, 0) superconformal index*, *JHEP* **09** (2016) 053, [arXiv:1606.0303].

[120] P. S. Howe and A. Umerski, *Anomaly Multiplets in Six-Dimensions and Ten-Dimensions*, *Phys. Lett.* **B198** (1987) 57.

[121] S. M. Kuzenko, J. Novak, and I. B. Samsonov, *The Anomalous Current Multiplet in 6D Minimal Supersymmetry*, *JHEP* **02** (2016) 132, [arXiv:1511.0658].

[122] H.-C. Kim, S. Kim, S.-S. Kim, and K. Lee, *The general M5-brane superconformal index*, arXiv:1307.7660.

[123] S. Kim and K. Lee, *Indices for 6 dimensional superconformal field theories*, arXiv:1608.0296.

[124] J. Källén and M. Zabzine, *Twisted supersymmetric 5D Yang-Mills theory and contact geometry*, *JHEP* **05** (2012) 125, [arXiv:1202.1956].

[125] J. Källén, J. Qiu, and M. Zabzine, *The perturbative partition function of supersymmetric 5D Yang-Mills theory with matter on the five-sphere*, *JHEP* **08** (2012) 157, [arXiv:1206.6008].

[126] H.-C. Kim and S. Kim, *M5-branes from gauge theories on the 5-sphere*, *JHEP* **05** (2013) 144, [arXiv:1206.6339].

[127] H.-C. Kim, J. Kim, and S. Kim, *Instantons on the 5-sphere and M5-branes*, arXiv:1211.0144.

[128] J. Källén, J. A. Minahan, A. Nedelin, and M. Zabzine, *$N^3$-behavior from 5D Yang-Mills theory*, *JHEP* **10** (2012) 184, [arXiv:1207.3763].

[129] D. L. Jafferis and S. S. Pufu, *Exact results for five-dimensional superconformal field theories with gravity duals*, *JHEP* **05** (2014) 032, [arXiv:1207.4359].

[130] Z. Bern, J. J. Carrasco, L. J. Dixon, M. R. Douglas, M. von Hippel, and H. Johansson, *D=5 maximally supersymmetric Yang-Mills theory diverges at six loops*, *Phys. Rev.* **D87** (2013), no. 2 025018, [arXiv:1210.7709].

[131] C. Papageorgakis and A. B. Royston, *Revisiting Soliton Contributions to Perturbative Amplitudes*, *JHEP* **09** (2014) 128, [arXiv:1404.0016].

[132] M. Aganagic, A. Klemm, M. Marino, and C. Vafa, *The Topological vertex*, *Commun. Math. Phys.* **254** (2005) 425–478, [hep-th/0305132].

[133] N. Lambert, C. Papageorgakis, and M. Schmidt-Sommerfeld, *Deconstructing (2,0) Proposals*, *Phys. Rev.* **D88** (2013), no. 2 026007, [arXiv:1212.3337].

[134] H. Ooguri and C. Vafa, *Two-dimensional black hole and singularities of CY manifolds*, *Nucl. Phys.* **B463** (1996) 55–72, [hep-th/9511164].

[135] R. Gregory, J. A. Harvey, and G. W. Moore, *Unwinding strings and t duality of Kaluza-Klein and h monopoles*, *Adv. Theor. Math. Phys.* **1** (1997) 283–297, [hep-th/9708086].

[136] D. Tong, *NS5-branes, T duality and world sheet instantons*, *JHEP* **07** (2002) 013, [hep-th/0204186].

[137] E. Witten, *Branes, Instantons, And Taub-NUT Spaces*, *JHEP* **06** (2009) 067, [arXiv:0902.0948].

[138] E. Witten, *Solutions of four-dimensional field theories via M theory*, *Nucl. Phys.* **B500** (1997) 3–42, [hep-th/9703166].

[139] A. Giveon and O. Pelc, *M theory, type IIA string and 4-D N=1 SUSY SU(N(L)) × SU(N(R)) gauge theory*, *Nucl. Phys.* **B512** (1998) 103–147, [hep-th/9708168].

[140] D. Gaiotto, L. Rastelli, and S. S. Razamat, *Bootstrapping the superconformal index with surface defects*, *JHEP* **01** (2013) 022, [arXiv:1207.3577].

[141] S. Bhattacharyya and S. Minwalla, *Supersymmetric states in M5/M2 CFTs*, *JHEP* **12** (2007) 004, [hep-th/0702069].

[142] H.-C. Kim and K. Lee, *Supersymmetric M5 Brane Theories on* $\mathbb{R} \times \mathbb{CP}^2$, *JHEP* **07** (2013) 072, [arXiv:1210.0853].

[143] E. Gerchkovitz, J. Gomis, N. Ishtiaque, A. Karasik, Z. Komargodski, and S. S. Pufu, *Correlation Functions of Coulomb Branch Operators*, arXiv:1602.0597.

[144] S. Benvenuti, B. Feng, A. Hanany, and Y.-H. He, *Counting BPS Operators in Gauge Theories: Quivers, Syzygies and Plethystics*, *JHEP* **11** (2007) 050, [hep-th/0608050].

[145] S. Benvenuti, A. Hanany, and N. Mekareeya, *The Hilbert Series of the One Instanton Moduli Space*, *JHEP* **06** (2010) 100, [arXiv:1005.3026].

[146] D. Gaiotto and S. S. Razamat, *Exceptional Indices*, *JHEP* **05** (2012) 145, [arXiv:1203.5517].

[147] P. C. Argyres, M. R. Plesser, and N. Seiberg, *The Moduli space of vacua of N=2 SUSY QCD and duality in N=1 SUSY QCD*, *Nucl. Phys.* **B471** (1996) 159–194, [hep-th/9603042].

[148] M. R. Douglas and G. W. Moore, *D-branes, Quivers, and ALE Instantons*, hep-th/9603167.

[149] A. Dey, A. Hanany, N. Mekareeya, D. Rodríguez-Gómez, and R.-K. Seong, *Hilbert Series for Moduli Spaces of Instantons on* $C^2/Z_n$, *JHEP* **01** (2014) 182, [arXiv:1309.0812].

[150] J. Kim, S. Kim, K. Lee, and J. Park, *Super-Yang-Mills theories on $S^4 \times \mathbb{R}$*, *JHEP* **08** (2014) 167, [arXiv:1405.2488].

[151] A. Iqbal, *All genus topological string amplitudes and five-brane webs as Feynman diagrams*, hep-th/0207114.

[152] H. Awata and H. Kanno, *Instanton counting, Macdonald functions and the moduli space of D-branes*, *JHEP* **05** (2005) 039, [hep-th/0502061].

[153] F. Nieri, S. Pasquetti, F. Passerini, and A. Torrielli, *5D partition functions, q-Virasoro systems and integrable spin-chains*, *JHEP* **12** (2014) 040, [arXiv:1312.1294].

[154] V. Mitev and E. Pomoni, *Exact effective couplings of four dimensional gauge theories with $\mathcal{N} = 2$ supersymmetry*, *Phys. Rev.* **D92** (2015), no. 12 125034, [arXiv:1406.3629].

[155] B. Fraser, *Higher rank Wilson loops in the $\mathcal{N} = 2 SU(N) \times SU(N)$ conformal quiver*, *J. Phys.* **A49** (2016), no. 2 02LT03, [arXiv:1503.0563].

[156] B. Fiol, E. Gerchkovitz, and Z. Komargodski, *Exact Bremsstrahlung Function in $N = 2$ Superconformal Field Theories*, *Phys. Rev. Lett.* **116** (2016), no. 8 081601, [arXiv:1510.0133].

[157] V. Mitev and E. Pomoni, *Exact Bremsstrahlung and Effective Couplings*, *JHEP* **06** (2016) 078, [arXiv:1511.0221].

[158] J. Bourdier, N. Drukker, and J. Felix, *The $\mathcal{N} = 2$ Schur index from free fermions*, *JHEP* **01** (2016) 167, [arXiv:1510.0704].

[159] E. Pomoni, *Integrability in N=2 superconformal gauge theories*, *Nucl. Phys.* **B893** (2015) 21–53, [arXiv:1310.5709].

[160] R. P. Andrews and N. Dorey, *Spherical deconstruction*, *Phys. Lett.* **B631** (2005) 74–82, [hep-th/0505107].

[161] R. P. Andrews and N. Dorey, *Deconstruction of the Maldacena-Nunez compactification*, *Nucl. Phys.* **B751** (2006) 304–341, [hep-th/0601098].

[162] G. Knodel, J. T. Liu, and L. A. Pando Zayas, *On N=1 partition functions without R-symmetry*, *JHEP* **03** (2015) 132, [arXiv:1412.4804].

[163] J. A. Minahan, *Localizing gauge theories on $S^d$*, *JHEP* **04** (2016) 152, [arXiv:1512.0692].

[164] J. A. Minahan and U. Naseer, *One-loop tests of supersymmetric gauge theories on spheres*, *JHEP* **07** (2017) 074, [arXiv:1703.0743].

[165] F. Benini and A. Zaffaroni, *Supersymmetric partition functions on Riemann surfaces*, *Proc. Symp. Pure Math.* **96** (2017) 13–46, [arXiv:1605.0612].

[166] N. Bobev, H. Elvang, U. Kol, T. Olson, and S. S. Pufu, *Holography for $\mathcal{N} = 1^*$ on $S^4$*, *JHEP* **10** (2016) 095, [arXiv:1605.0065].

[167] D. Gaiotto and S. S. Razamat, *$\mathcal{N} = 1$ theories of class $\mathcal{S}_k$*, *JHEP* **07** (2015) 073, [arXiv:1503.0515].

[168] J. Quine, S. Heydari, and R. Song, *Zeta regularized products*, *Transactions of the American Mathematical Society* **338** (1993), no. 1 213–231.

[169] V. Mitev and E. Pomoni, *2D CFT blocks for the 4D class $\mathcal{S}_k$ theories*, *JHEP* **08** (2017) 009, [arXiv:1703.0073].

[170] T. Bourton and E. Pomoni, *Instanton counting in Class $\mathcal{S}_k$*, arXiv:1712.0128.

[171] D. Gang, E. Koh, and K. Lee, *Superconformal Index with Duality Domain Wall*, *JHEP* **10** (2012) 187, [arXiv:1205.0069].

[172] A. Gadde and S. Gukov, *2d Index and Surface operators*, *JHEP* **03** (2014) 080, [arXiv:1305.0266].

[173] N. Drukker, T. Okuda, and F. Passerini, *Exact results for vortex loop operators in 3d supersymmetric theories*, *JHEP* **07** (2014) 137, [arXiv:1211.3409].

[174] B. Assel and J. Gomis, *Mirror Symmetry And Loop Operators*, *JHEP* **11** (2015) 055, [arXiv:1506.0171].

[175] J. Gomis, B. Le Floch, Y. Pan, and W. Peelaers, *Intersecting Surface Defects and Two-Dimensional CFT*, *Phys. Rev.* **D96** (2017), no. 4 045003, [arXiv:1610.0350].

[176] C. Cordova, D. Gaiotto, and S.-H. Shao, *Surface Defect Indices and 2d-4d BPS States*, *JHEP* **12** (2017) 078, [arXiv:1703.0252].

[177] F. A. H. Dolan, V. P. Spiridonov, and G. S. Vartanov, *From 4d superconformal indices to 3d partition functions*, *Phys. Lett.* **B704** (2011) 234–241, [arXiv:1104.1787].

[178] A. Gadde and W. Yan, *Reducing the 4d Index to the $S^3$ Partition Function*, *JHEP* **12** (2012) 003, [arXiv:1104.2592].

[179] V. Niarchos, *Seiberg dualities and the 3d/4d connection*, *JHEP* **07** (2012) 075, [arXiv:1205.2086].

[180] O. Aharony, S. S. Razamat, N. Seiberg, and B. Willett, *3d dualities from 4d dualities*, *JHEP* **07** (2013) 149, [arXiv:1305.3924].

[181] A. Amariti, D. Orlando, and S. Reffert, *String theory and the 4D/3D reduction of Seiberg duality. A review*, *Phys. Rept.* **705-706** (2017) 1–53, [arXiv:1611.0488].

[182] C. T. Hill, S. Pokorski, and J. Wang, *Gauge Invariant Effective Lagrangian for Kaluza-Klein Modes*, *Phys. Rev.* **D64** (2001) 105005, [hep-th/0104035].

[183] D. B. Kaplan, E. Katz, and M. Unsal, *Supersymmetry on a spatial lattice*, *JHEP* **05** (2003) 037, [hep-lat/0206019].

[184] C. Csaki, J. Erlich, C. Grojean, and G. D. Kribs, *4-D constructions of supersymmetric extra dimensions and gaugino mediation*, *Phys. Rev.* **D65** (2002) 015003, [hep-ph/0106044].

[185] J. de Boer, K. Hori, and Y. Oz, *Dynamics of N=2 supersymmetric gauge theories in three-dimensions*, *Nucl. Phys.* **B500** (1997) 163–191, [hep-th/9703100].

[186] O. Aharony, A. Hanany, K. A. Intriligator, N. Seiberg, and M. J. Strassler, *Aspects of N=2 supersymmetric gauge theories in three-dimensions*, *Nucl. Phys.* **B499** (1997) 67–99, [hep-th/9703110].

[187] D. Gaiotto and E. Witten, *S-Duality of Boundary Conditions In N=4 Super Yang-Mills Theory*, *Adv. Theor. Math. Phys.* **13** (2009), no. 3 721–896, [arXiv:0807.3720].

[188] A. Giveon and D. Kutasov, *Brane dynamics and gauge theory*, *Rev. Mod. Phys.* **71** (1999) 983–1084, [hep-th/9802067].

[189] M. Bullimore, M. Fluder, L. Hollands, and P. Richmond, *The superconformal index and an elliptic algebra of surface defects*, *JHEP* **10** (2014) 062, [arXiv:1401.3379].

[190] C. Closset, T. T. Dumitrescu, G. Festuccia, and Z. Komargodski, *Supersymmetric Field Theories on Three-Manifolds*, *JHEP* **05** (2013) 017, [arXiv:1212.3388].

[191] F. Benini and W. Peelaers, *Higgs branch localization in three dimensions*, *JHEP* **05** (2014) 030, [arXiv:1312.6078].

[192] F. Aprile and V. Niarchos, *$\mathcal{N}$ =2 supersymmetric field theories on 3-manifolds with A-type boundaries*, *JHEP* **07** (2016) 126, [arXiv:1604.0156].

[193] K. Hori, H. Kim, and P. Yi, *Witten Index and Wall Crossing*, *JHEP* **01** (2015) 124, [arXiv:1407.2567].

[194] Y. Ito and Y. Yoshida, *Superconformal index with surface defects for class $\mathcal{S}_k$*, arXiv:1606.0165.

[195] F. Benini, R. Eager, K. Hori, and Y. Tachikawa, *Elliptic Genera of 2d $\mathcal{N}$ = 2 Gauge Theories*, *Commun. Math. Phys.* **333** (2015), no. 3 1241–1286, [arXiv:1308.4896].

[196] F. Benini, R. Eager, K. Hori, and Y. Tachikawa, *Elliptic genera of two-dimensional N=2 gauge theories with rank-one gauge groups*, *Lett. Math. Phys.* **104** (2014) 465–493, [arXiv:1305.0533].

[197] R. Lodin, F. Nieri, and M. Zabzine, *Elliptic modular double and 4d partition functions*, *J. Phys.* **A51** (2018), no. 4 045402, [arXiv:1703.0461].

[198] F. Nieri, *An elliptic Virasoro symmetry in 6d*, *Lett. Math. Phys.* **107** (2017), no. 11 2147–2187, [arXiv:1511.0057].

[199] E. I. Buchbinder, J. Gomis, and F. Passerini, *Holographic gauge theories in background fields and surface operators*, *JHEP* **12** (2007) 101, [arXiv:0710.5170].

[200] J. A. Harvey and A. B. Royston, *Localized modes at a D-brane-O-plane intersection and heterotic Alice strings*, *JHEP* **04** (2008) 018, [arXiv:0709.1482].

[201] J. Gomis and F. Passerini, *Holographic Wilson Loops*, *JHEP* **08** (2006) 074, [hep-th/0604007].

[202] J. Gomis and F. Passerini, *Wilson Loops as D3-Branes*, *JHEP* **01** (2007) 097, [hep-th/0612022].

[203] P. Agarwal, J. Kim, S. Kim, and A. Sciarappa, *Wilson surfaces in M5-branes*, arXiv:1804.0993.

[204] Y. Tachikawa, *On W-algebras and the symmetries of defects of 6d N=(2,0) theory*, *JHEP* **03** (2011) 043, [arXiv:1102.0076].

[205] C. Lawrie, S. Schafer-Nameki, and T. Weigand, *Chiral 2d theories from $N = 4$ SYM with varying coupling*, *JHEP* **04** (2017) 111, [arXiv:1612.0564].

[206] S. S. Razamat, *Flavored surface defects in 4d N=1 SCFTs*, arXiv:1808.0950.

[207] M. Bullimore and H.-C. Kim, *The Superconformal Index of the (2,0) Theory with Defects*, *JHEP* **05** (2015) 048, [arXiv:1412.3872].

[208] T. Bourton, A. Pini, and E. Pomoni, *4d $\mathcal{N} = 3$ indices via discrete gauging*, arXiv:1804.0539.

[209] I. García-Etxebarria and D. Regalado, *$\mathcal{N} = 3$ four dimensional field theories*, *JHEP* **03** (2016) 083, [arXiv:1512.0643].

[210] O. Aharony and Y. Tachikawa, *S-folds and 4d N=3 superconformal field theories*, *JHEP* **06** (2016) 044, [arXiv:1602.0863].

[211] L. Bianchi, L. Griguolo, M. Preti, and D. Seminara, *Wilson lines as superconformal defects in ABJM theory: a formula for the emitted radiation*, *JHEP* **10** (2017) 050, [arXiv:1706.0659].

[212] L. Bianchi, M. Preti, and E. Vescovi, *Exact Bremsstrahlung functions in ABJM theory*, *JHEP* **07** (2018) 060, [arXiv:1802.0772].

[213] L. Bianchi, M. Lemos, and M. Meineri, *Line Defects and Radiation in $\mathcal{N} = 2$ Conformal Theories*, *Phys. Rev. Lett.* **121** (2018), no. 14 141601, [arXiv:1805.0411].

[214] P. Liendo, C. Meneghelli, and V. Mitev, *Bootstrapping the half-BPS line defect*, *JHEP* **10** (2018) 077, [arXiv:1806.0186].

[215] A. Bourget, A. Pini, and D. Rodriguez-Gomez, *Towards Deconstruction of the Type D (2,0) Theory*, *JHEP* **12** (2017) 146, [arXiv:1710.1024].

[216] Y. Pan and W. Peelaers, *Intersecting Surface Defects and Instanton Partition Functions*, *JHEP* **07** (2017) 073, [arXiv:1612.0483].

[217] Y. Imamura and S. Yokoyama, *Superconformal index of $\mathcal{N} = 3$ orientifold theories*, *J. Phys.* **A49** (2016), no. 43 435401, [arXiv:1603.0085].

[218] S. Ruijsenaars, *First order analytic difference equations and integrable quantum systems*, *J. Math. Phys.* **38** (1997) 1069.

[219] M. Jimbo and T. Miwa, *Quantum KZ equation with —q— = 1 and correlation functions of the XXZ model in the gapless regime*, *J. Phys.* **A29** (1996) 2923–2958, [hep-th/9601135].

[220] J. A. Minahan and U. Naseer, *Gauge theories on spheres with 16 supercharges and non-constant couplings*, arXiv:1811.1165.